Characterization of Transgenic Mouse Models of Alzheimer's Disease and Related Dementia

Inaugural dissertation

for the attainment of the title of doctor
in the Faculty of Mathematics and Natural Sciences
at the Heinrich Heine University Düsseldorf

presented by

Luana Cristina Camargo

from Brasília, Brazil

Düsseldorf, August 2021

from the Institut für Physikalische Biologie
at the Heinrich Heine University Düsseldorf

Published by permission of the
Faculty of Mathematics and Natural Sciences at
Heinrich Heine University Düsseldorf

Supervisor: Prof Dr. Dieter Willbold
Co-supervisor: Prof. Dr. Karl-Josef Langen

Date of the oral examination: 26.10.2021

Affidavit

I declare under oath that I have produced my thesis independently and without any undue assistance by third parties under consideration of the ‘Principles for the Safeguarding of Good Scientific Practice at Heinrich Heine University Düsseldorf’.

I also declare that this thesis was not presented to another faculty.

Düsseldorf, 18.08.2021

_____

(Luana Cristina Camargo)

“Our greatest weakness lies in giving up. The most certain way to succeed is always to try just one more time.”

– **Thomas A. Edison**

Acknowledgment

I would like to thank Prof. Dr. Dieter Willbold for the opportunity/support to work my PhD thesis in the Alzheimer's disease field, to attend international conferences and to publish in scientific journals.

I thank Prof. Dr. Karl-Josef Langen for his mentorship and for allowing me to perform most of the experiments in his laboratory.

Many thanks to Dr. Sarah Schemmert, Dr. Janine Kutzsche and Dr. Antje Willuweit for all the scientific discussion, manuscript preparation and support during this time.

I would like to thank all my colleagues from IBI-7 and INM-4 for the help, cakes and get together (before corona). I thank Dominik Honold, Ian Gering, Robert Bauer, Dr. Julia Post, Michael Schöneck, Carina Balduin, Esther Wollert, Markus Tusche and Bettina Kass to all the help and support during the experiments. I also would like to thank Dr. Raphael Eberle and Dr. Monika Coronado for the friendship, scientific discussion and support inside and outside the lab.

Many thanks to the animal caretakers from the Forschungszentrum Jülich and Mrs. Kornadt Beck for the help and taking good care of the mice.

Finally, I thank my partner Raffael, for being by my side, for the patience, the support and to listen to my complains. Many thanks to my Brazilian friends and my family for all the support and for being there for me at the most difficult times.

Table of Contents

Publications and Conferences

List of Publication

2021

Camargo LC, Schöneck M, Sangarapillai N, Honold D, Shah NJ, Langen K-J, Willbold D, Kutzsche J, Schemmert S, Willuweit A. **PEAβ Triggers Cognitive Decline and Amyloid Burden in a Novel Mouse Model of Alzheimer's Disease**. International Journal of Molecular Sciences. 2021; 22(13):7062. https://doi.org/10.3390/ijms22137062

Schemmert S, Camargo LC, Honold D, Gering I, Kutzsche J, Willuweit A, Willbold D. **In Vitro and In Vivo Efficacies of the Linear and the Cyclic Version of an All-D-Enantiomeric Peptide Developed for the Treatment of Alzheimer's Disease**. International Journal of Molecular Sciences. 2021; 22(12):6553. https://doi.org/10.3390/ijms22126553

Camargo LC, Honold D, Bauer R, Shah NJ, Langen K-J, Willbold D, Kutzsche J, Willuweit A, Schemmert S. **Sex-related motor deficits in the Tau-P301L mouse model.** Biomedicines (submitted)

List of Conferences

2021

L. Camargo, D. Honold, R. Bauer, J. Kutzsche, A. Willuweit, D. Willbold, S. Schemmert. **Characterization of the Phenotypic Deficits in a Transgenic Mouse Model of Tauopathy.** AD/PD 2021. The 15th International Conference on Alzheimer and Parkinson's Diseases: Mechanisms, Clinical Strategies and promising Treatments of Neurodegenerative Diseases

2020

Camargo, L.C., Schöneck, M., Sangarapillai, N., Honold, D., Schemmert, S., Langen, K.-J., Kutzsche, J., Willbold, D. and Willuweit, A. **Behavioural characterization of a new Alzheimer's disease mouse model**. Alzheimer's Association International Conference in 2020. AAIC 2020

List of Figures

List of Tables

Abstract

Alzheimer's disease (AD) is a complex neurodegenerative disorder with multiple features. With the help of animal models, the AD physiopathology is starting to be understood. In order to translate the data from animal models to humans, a deep understanding of each model is important. Moreover, the development of new models as well as longitudinal studies play an important role in translational research.

In this context, a new transgenic mouse model called TAPS, was developed to combine the amyloidosis of heterozygous APP/PS1 mice and truncated amyloid-β (Q3-42), which is post-translationally modified to pyroglutamate Amyloid-β (pEAβ) in TBA2.1 mice. Here, the histological and behavioral alterations of TAPS mice were analysed. pEAβ staining showed that pEAβ is present in the core of neuritic plaques in the cortex and hippocampus in the TAPS and APP/PS1 mice. Interestingly, TAPS mice also had pEAβ positive plaques in the striatum. Amyloid-β (Aβ) staining showed progressive plaque formation in the hippocampus, striatum and cortex earlier in TAPS mice. In the SHIRPA, TAPS mice showed a progressive phenotypic alteration compared to wild type (WT) mice starting with 12 months of age. In the open field test, TAPS mice seemed to be faster, travelled more and were more active compared to WT mice. In the novel object recognition test (NOR), WT mice were able to discriminate the novel object from the familiar one. In contrast, TAPS mice spent similar time exploring both objects, indicating deficits in the recognition memory. This was also observed in the T-maze spontaneous alteration, where only WT mice significantly alternated more than the transgenic mice. In the cued and contextual fear conditioning test, only TAPS mice froze less compared to WT mice. In the Morris water maze (MWM), TAPS mice took more time to find the platform than the WT mice on the last day of training. Finally, TAPS mice had an earlier Aβ pathology in the brain, phenotypic alteration and cognitive deficits in different behavioral tests, which underlines their potential as a mouse model for the study of AD physiopathology as well as treatment studies.

To further understand the role of Tau pathology in a mouse model of tauopathy, a longitudinal study was performed to evaluate the sex- dependent phenotypic alterations in the transgenic Tau-P301L mouse model as well as histological alterations. Sex-matched WT and homozygous Tau-P301L mice were tested in different behavioral tests at different ages. At eight months of age, histological analysis of Tau pathology, neuronal loss and gliosis was performed. In the habituation/dishabituation olfactory test, Tau-P301L male mice smelled the new aroma less frequently compared to the WT males at six months of age. In the SHIRPA test, the Tau-P301L male mice had phenotypic alterations starting at four months of age. Motor deficits were observed in the Tau-P301L male mice starting at six months of age in the pole test and as early as two months of age in the open field test. In the NOR, Tau-P301L male

mice were not able to discriminate the novel object from the familiar one starting at six months of age. Interestingly, Tau-P301L female mice did not show any motor alterations, even though they had phenotypic alterations in the SHIRPA test and cognitive deficits in the NOR. Tau pathology was also only observed in Tau-P301L male mice in brainstem, cortex and cerebellum. Neuronal loss was observed in the Tau-P301L male mice's brainstem without gliosis alterations. Summarized, the TauP301L mouse model showed sex-dependent phenotypic alterations as early as two months of age probably due to Tau pathology in the brain.

To evaluate the treatment effect of cRD2D3 in comparison to RD2D3, those peptides' efficacies were evaluated in different *in vitro* assays and in the SwDI mice. Also, in order to generate the best possible study design, an in-house characterization study was conducted where SwDI mice showed deficits in those tests. Both peptides bind to $A\beta_{1-42}$ and Dutch/Iowa (D/I) Aβ, prevent Aβ and D/I Aβ fibril formation and eliminate toxic Aβ and D/I Aβ oligomers. *In vivo*, the treatment did not improve the deficits neither in the nesting behavior nor in the marble burying test. In the open field test, SwDI mice treated with RD2D3 habituated to the arena compared to mice treated with placebo. Mice treated with RD2D3 and cRD2D3 had an improvement in spatial memory in the MWM training trials. No alterations in plaque load, neuronal loss and gliosis were observed. Therefore, both D-enantiomeric peptides were efficient in preventing Aβ and D/I Aβ aggregation *in vitro* and in improving cognitive deficits *in vivo*.

Taken together, different mouse models have been successfully characterized in different behavioral tests. Moreover, pathological alterations were analyzed intensively. Therefore, those models are suitable models for future treatment studies together with the already well-known mouse models. Regarding the treatment study, both RD2D3 and cRD2D3 are also efficient therapeutic drug candidates for AD along with other D-enantiomeric peptides.

Kurzfassung

Die Alzheimersche Krankheit (AD) ist eine komplexe neurodegenerative Erkrankung mit vielfältigen Merkmalen. Mithilfe von Tiermodellen wird versucht die Pathophysiologie dieser Krankheit zu verstehen. Um die so gewonnenen Erkenntnisse von Tiermodellen auf den Menschen zu übertragen, ist ein ausführliches Verständnis des Tiermodelles wichtig. Des Weiteren spielen die Entwicklung neuer Tiermodelle, sowie Längsschnittstudien eine wichtige Rolle in der translationalen Forschung.

In diesem Zusammenhang wurde ein neues transgenes Mausmodell, genannt TAPS, entwickelt, welches die Amyloidose von heterozygoten APP/PS1-Mäusen und das verkürzte Amyloid-β-peptid (Q3-42) von TBA2.1-Mäusen, welches posttranslational zu Pyroglutamat-Amyloid-β (pEAβ) modifiziert wird, kombiniert.

In dieser Arbeit wurden Veränderungen in der Histologie und im Verhalten von TAPS-Mäusen analysiert. Immunohistochemische Färbungen von pEAβ zeigten, dass pEAβ im Kern von senilen Plaques im Kortex und Hippocampus der TAPS- und APP/PS1-Mäuse vorhanden ist. Interessanterweise zeigten die TAPS-Mäuse auch pEAβ-positive Plaques im Striatum. Die Aβ-Färbung zeigte eine progressive Plaquebildung bei TAPS-Mäusen zunächst in Hippocampus, Striatum und im Kortex. Im SHIRPA-Test zeigten TAPS-Mäuse im Vergleich zu Wild Typ (WT)-Mäusen ab einem Alter von 12 Monaten progressive phänotypische Veränderungen. Beim Offenfeldtest schienen TAPS-Mäuse im Vergleich zu WT-Mäusen schneller zu sein, sich mehr zu bewegen und aktiver zu sein, aber dieses Ergebnis erreichte keine Signifikanz. Im „Novel object recognition test“ (NOR) waren WT-Mäuse in der Lage, ein neues Objekt von einem bekannten zu unterscheiden. Im Gegensatz dazu untersuchten TAPS-Mäuse neue und bekannte Objekte auf ähnliche Weise, was auf Defizite im Erkennungsgedächtnis hinweist. Dies wurde auch bei der spontanen Veränderung des T-Labyrinths beobachtet, bei der nur die WT-Mäuse signifikant häufiger die Laufrichtung wechselten als die transgenen Mäuse. Zur Testung von konditionierter und kontextbezogener Angst erstarrten lediglich die TAPS-Mäuse weniger als die WT-Mäuse. Im sogenannten „Morris water maze“ (MWM) benötigten die TAPS-Mäuse am letzten Trainingstag mehr Zeit, um die Plattform zu finden, als die WT-Mäuse. Außerdem wiesen TAPS-Mäuse eine frühere Aβ-Pathologie im Kortex, Hippocampus, sowie im Striatum auf. Des Weiteren zeigten die TAPS-Mäuse auch phänotypische Veränderungen und kognitive Defizite in verschiedenen Verhaltenstests, was ihr Potenzial als Mausmodell für die Untersuchung der Pathophysiologie der Alzheimer-Demenz, sowie für Behandlungsstudien aufzeigt.

Um die Rolle der Tau-Pathologie in einem Mausmodell der Tauopathie besser zu verstehen, wurde eine Längsschnittstudie durchgeführt, um die phänotypischen, sowie die histologischen Veränderungen im transgenen Tau-P301L-Mausmodell zu charakterisieren.

Geschlechtsgleiche WT- und homozygote Tau-P301L-Mäuse wurden in verschiedenen Verhaltenstests zu unterschiedlichen Altersstadien getestet. Im Alter von 8 Monaten wurde eine histologische Analyse der Tau-Pathologie, des Neuronenverlustes und der Gliose durchgeführt. Beim olfaktorischen Habituations-/Dishabituationstest rochen die Tau-P301L-Männchen im Alter von sechs Monaten weniger an dem neuen Geruch als altersgleiche WT-Männchen. Im SHIRPA-Test zeigten die Tau-P301L-Männchen phänotypische Veränderungen ab einem Alter von vier Monaten. Motorische Defizite wurden bei den männlichen Tau-P301L-Mäusen ab dem sechsten Lebensmonat im „Pole-Test“ und bereits im Alter von zwei Monaten im Offenfeldtest beobachtet. Im NOR waren Tau-P301L-Männchen ab einem Alter von sechs Monaten nicht mehr in der Lage, ein neues Objekt von einem bekannten zu unterscheiden. Interessanterweise zeigten weibliche Tau-P301L-Mäuse keine motorischen Veränderungen in diesen Tests, obwohl sie phänotypische Veränderungen im SHIRPA-Test und kognitive Defizite im NOR aufwiesen. Die Tau-Pathologie wurde ebenfalls nur bei männlichen Tau-P301L-Mäusen im Hirnstamm, im Kortex, sowie im Kleinhirn beobachtet. Im Hirnstamm der männlichen Tau-P301L-Mäuse wurde ein Neuronenverlust ohne Veränderungen der Gliose beobachtet. Zusammenfassend lässt sich sagen, dass das TauP301L-Mausmodell bereits im Alter von zwei Monaten geschlechtsabhängige phänotypische Veränderungen aufweist, die wahrscheinlich auf eine Tau-Pathologie im Gehirn zurückzuführen sind.

Um die Behandlungswirkung von cRD2D3 im Vergleich zu RD2D3 zu bewerten, wurde die Wirksamkeit dieser Peptide in verschiedenen *in-vitro*-Tests, sowie in SwDI-Mäusen untersucht. Um das bestmögliche Studiendesign zu erstellen, wurde zunächst eine interne Charakterisierungsstudie durchgeführt, bei der die SwDI-Mäuse Defizite in diesen Tests zeigten. Beide Peptide zeigten Bindung an Aβ(1-42) und Dutch/Iowa (D/I) Aβ, verhinderten die Bildung von Aβ- und D/I Aβ-Fibrillen und eliminierten toxische Aβ- und D/I Aβ-Oligomere. *In vivo* verbesserte die Behandlung weder die Defizite im Nestbauverhalten noch im „Marble-Burying-Test“. Beim Offenfeldtest gewöhnten sich die mit RD2D3 behandelten SwDI-Mäuse besser an die Arena als die mit Placebo behandelten Mäusen. Bei Mäusen, die mit RD2D3 und cRD2D3 behandelt wurden, verbesserte sich das räumliche Gedächtnis bei den MWM-Trainingsversuchen. Bei der Anzahl der zerebralen Plaques, dem neuronalen Verlust und der Gliose wurden jedoch keine Veränderungen beobachtet. Daher kann gesagt werden, dass beide D-enantiomeren-Peptide effizient bei der Verhinderung der Aβ- und D/I-Aβ-Aggregation *in vitro* und bei der Verbesserung der kognitiven Defizite *in vivo* waren.

Insgesamt wurden die unterschiednlichen Mausmodelle in verschiedenen Verhaltenstests erfolgreich charakterisiert. Darüber hinaus wurden die pathologischen Veränderungen intensiv analysiert. Daher sind diese Modelle, zusammen mit den bekannten Mausmodellen, für

künftige Behandlungsstudien geeignet. Was die Behandlungsstudie betrifft, können sowohl RD2D3 als auch cRD2D3, ebenso wie andere D-enantiomere-Peptide als eine wirksame Behandlung für AD betrachtet werden.

1. Introduction

1.1. Alzheimer's disease

The term dementia classifies all the diseases that impair cognitive skills, preventing patients to perform daily tasks. In 2016, around 43 million people were diagnosed with dementia worldwide. Since 1990, the dementia cases more than doubled due to the longer average lifespan of the population. Dementia is the fifth most common cause of death in the world and, in people over 70 years of age, represents the second leading cause of death [1]. As an estimation, the number of people living with dementia will be around 100 million in 2050 [2, 3]. Considering the economic/financial burden, dementia cost around $ 818 million in US in 2015 [4]. Given the fact that dementia has no approved modified disease treatment, this burden will increase in the following years, as will the number of cases [5].

One of the most common forms of dementia is Alzheimer's disease (AD), which accounts for 60% of all dementia cases. First described by Alois Alzheimer in 1906, the classical pathological hallmarks of AD are neuritic plaques, neurofibrillary tangles (NFTs) and neurodegeneration [6] (Figure 1). In AD, Amyloid-β (Aβ) and Tau are constitutes of neuritic plaques and NFTs, respectively [7, 8]. Those pathological structures are proposed to be responsible for the last hallmark, which is the neurodegeneration. Unlike Aβ, misfolded Tau are also present in different dementia. Tauopathy is a class of diseases in which Tau protein occurs as a hallmark [9]. Recent studies have shown that dementias are actually co-pathologies, since most of the patients that are diagnosed with one form of dementia have different types of protein aggregates, as detected in post mortem analysis [10].

In AD patients, MRI images showed an initial atrophy in the hippocampal formation which progressed to the cortical areas and finally nearly all cerebral regions [11]. As patients started to display the first symptoms, the hippocampal atrophy was already prominent, and the brain atrophy progression was correlated to the progression of the symptoms [12].

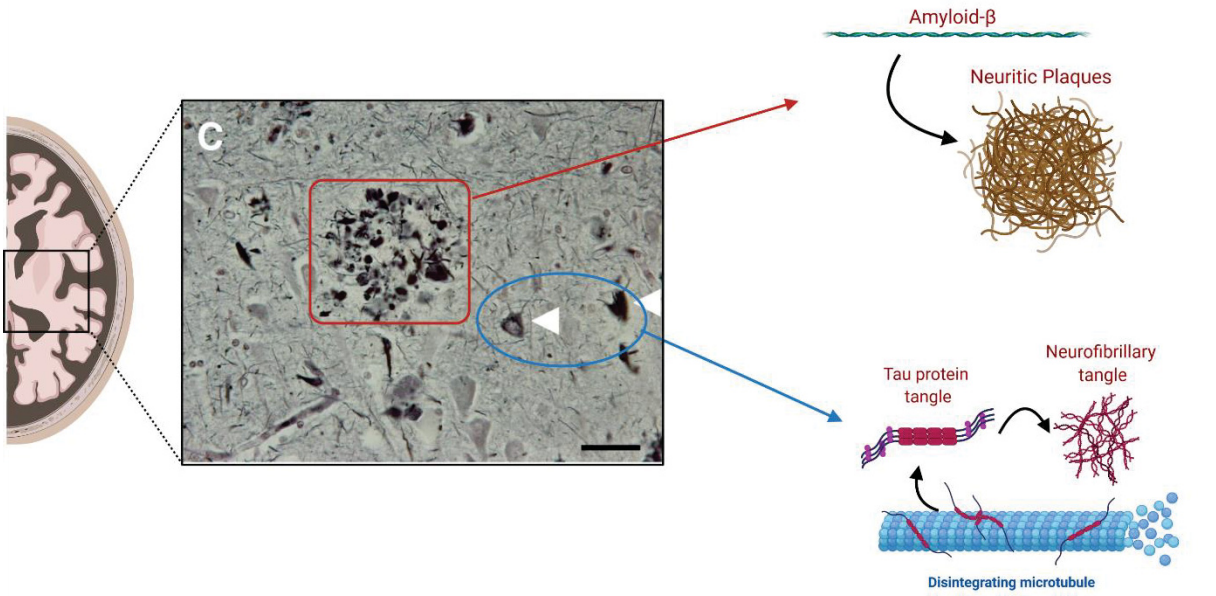

Figure 1: Alzheimer's disease pathology. In Alzheimer's disease, two proteins are neurotoxic and responsible for brain atrophy. Amyloid-β is the main constitute of neuritic plaques. Tau protein aggregates into neurofibrillary tangles. Since Tau protein plays a major role in the microtubule stabilization, the Tau protein loss of function promotes the microtubules disintegration. Created with BioRender.com and adapted from [10].

During this challenging time of the Covid-19 pandemic, patients suffering from dementia have been directly affected not only because they are more vulnerable to die due to the infection, but also because they strongly depend on the health care system and caregivers [13]. It is important to highlight that due to the Covid-19 pandemic, the increase of AD patients deaths was by 16% [14]. Moreover, AD patients are more likely to have the same comorbidities as Covid-19 [13, 15]. This is closely related, since SARS-COV 2 is able to induce neurological alterations that may induce AD at a later time [16, 17]. Besides the diseases itself, the restrictive measures have also affected the AD patients profoundly, aggravating neuropsychiatric problems [18].

1.1.1. Risk factors

Even though the cause of AD and related dementia (ADRD) is still unclear, many factors can increase the possibility of developing it [19]. These factors can be either intrinsic, e.g. genetic mutations, or external, e.g. smoking. The main risk factor is aging, since the prevalence to develop AD in people around 65 years is 10%. Individuals over the age of 80 have a risk of 40% to develop AD [20].

Unlike age, other external risk factors are modifiable [21]. Social interactions and continuing education are known to decrease dementia risk [22-24]. On the other hand, depression and stress are closely related to developing dementia [25, 26]. Some comorbidities are also related to a higher risk of dementia. Diabetes, cardiovascular diseases, obesity and strokes are strong examples of pre-existing diseases that are also commonly occurring in

dementia patients [27-30]. Finally, the way of life can also affect the risk of developing dementia since a sedentary lifestyle, poor diets, smoking, alcohol consumption and sleep disorders may alter our cognitive function chronically [31-34].

Among the intrinsic risk factors, the most common is the apolipoprotein E (APOE) gene mutation on chromosome 17 [35], which is involved in the lipid metabolism and Aβ clearance [36]. APOE4 carriers have an increased risk up to 14% to develop AD [37]. Therefore, the APOE mutation is considered to be partially responsible for the late onset of AD (LOAD) which is the most common onset (95% of patients) [38]. By definition, patients showing deficits before 65 years of age are classified as early onset of AD (EOAD). In those cases, the mutations in the amyloid precursor protein (APP) and in the presenilin (PSEN) genes are the most common detected [39, 40]. However, these cases, so-called familial AD, only make up 10 % of total AD cases. The other 90% of AD cases referred to as sporadic AD of which the exact causes are still unknown, even though the risk factors can already give insights regarding the AD etiology [41].

1.1.2. Diagnosis

In 2011, the National Institute of Aging (NIA) classified AD in three different stages: preclinical, mild cognitive impairment (MCI) and dementia [42-44]. These stages are defined by neuroimaging, cognitive tasks assessment and cerebrospinal fluid (CSF) biomarkers [45]. The preclinical stage occurs before the first cognitive deficits appear [42]. It is estimated that this phase begins 10 to 20 years before the clinical manifestations [45]. Improvements in imaging analysis showed that in the preclinical stage, Aβ is the first protein to aggregate [46]. Moreover, there is a great effort from academics to better identify the pathological alterations in this early stage, especially in the development of new biomarkers detection in cerebrospinal fluid (CSF) and plasma [47] (Figure 2).

Biomarkers are the most recent approach to detect AD in preclinical stages. In the CSF, there is a decrease of Aβ and an increase of Tau and synaptic markers [48-50]. Lately, the improvement of the phosphorylated Tau, neuroinflammation and synaptic markers detection showed that they are increased in the blood of AD patients [51]. So far, the use of biomarkers still needs improvement and great attention has been given to the development of new biomarkers for a more precise diagnosis. One limitation of the diagnostic criteria is that it is not currently possible to differentiate between different forms of dementia since they all result in similar protein detection in the plasma, e.g. Tau in AD and frontotemporal dementia (FTD) [52]. The fact that clinical manifestation of AD occurs years after the pathology begins is a limitation of an efficient diagnosis. More recently, the NIA has developed the A/T/N framework, which A is Aβ, T is Tau and N is neurodegeneration. With this framework it is possible to identify ADRD by the combination of those biomarkers detection via CSF, plasma and imaging [46].

Regarding the brain imaging, magnetic resonance imaging (MRI) is a diagnostic tool which is used to identify the brain atrophy in ADRD and distinguish the different subtypes, based on atrophy patterns in different brain regions [53]. Additionally, different tracers are used to detect either Aβ, Tau or brain metabolism. The Pittsburg compound (PiB) is a tracer for positron emission tomography (PET) developed to detect Aβ in the brain. The alterations in the PiB-PET also happens in earlier stages of AD and correlate inversely with Aβ CSF levels [54-56]. The 2-deoxy-2 (18F) fluoro-D-glucose (FDG-PET) detects the glucose consumption in the brain, which is correlated with brain activity [57, 58]. AD patients have a decrease in the FDG-PET signal due to synaptic dysfunction and neurodegeneration. The ^{18}F-AV1451 and ^{18}F-T807, called nowadays of Flortaucipir, were developed to detect aggregated Tau in the brain via PET, which is related with AD progression [36, 59-62].

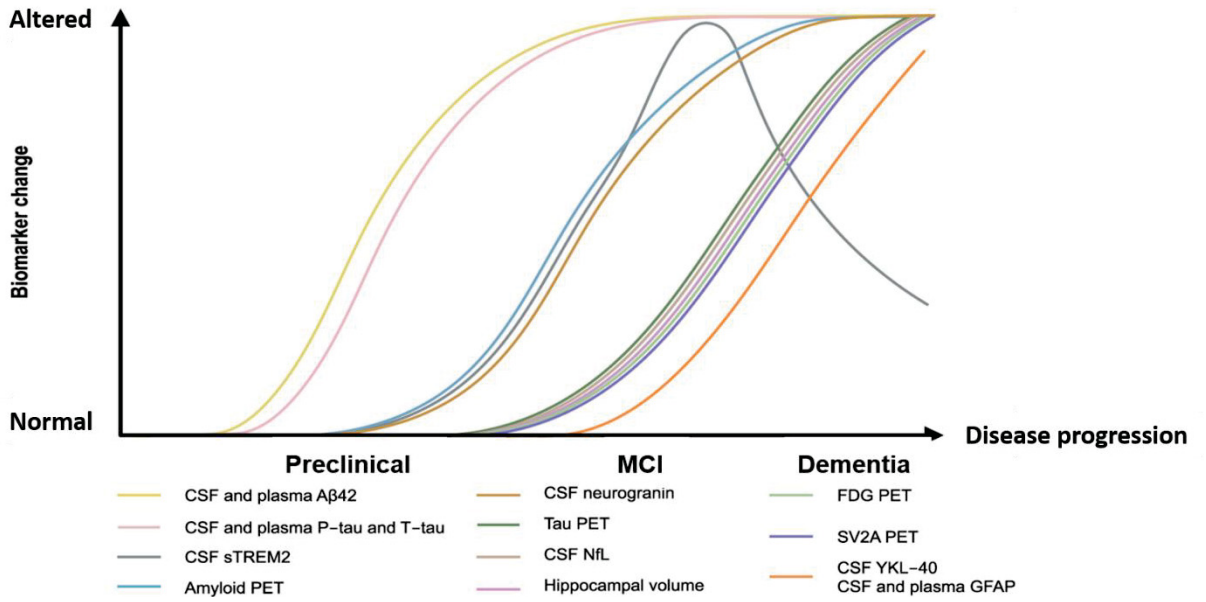

Figure 2: Relationship of biomarkers alterations and Alzheimer's disease progression. In the preclinical stage, Amyloid-β (Aβ42), phosphorylated (p-Tau) and total Tau (T-Tau) in cerebrospinal fluid (CSF) and plasma start being altered. Aβ42 presence in the brain detected by positron emission tomography (Amyloid PET), soluble triggering receptor expressed on myeloid cells 2 (sTREM2) and neurogranin in CSF start to be altered later in the preclinical stage. In mild cognitive impairment (MCI), Tau, synaptic vesicle glycoprotein 2A (SV2A) and glucose metabolism (FDG) in the brain (PET) as well as neurofilament light (NfL), glial fibrillary acidic protein (GFAP) and Chitinase 3-like 1 (YKL-40) in CSF, and hippocampal volume is altered. In dementia, all biomarkers are already altered, except sTREM2. Adapted from [63].

1.1.3. APP processing

Aβ is a peptide fragment from APP, which is a transmembrane protein with a still unclear physiological function. The APP gene is located on the chromosome 21 and has 18 exons that express eight isoforms, the most common being APP695, APP751 and APP770 [64, 65]. Two processes occur during the APP processing: the non-amylogenic and the amylogenic pathway (Figure 3). In the non-amylogenic pathway, α-secretase complexes cleave APP into two peptides, sAPPα and C83, both of which have physiological roles. In the amylogenic pathway, three peptides are formed by first the cleavage of β-secretase (BACE1),

which will produce the sAPPβ and the C99 [66]. The BACE1 catalytic sites are located in between 596/597 and 606/607 amino acid residue position of the APP, which is responsible for the C99 or C89 formation, respectively [67]. The C89 fragment is further cleaved by γ-secretase and produces $A\beta_{11-x}$ peptide fragment in the trans-Golgi network [68, 69].

The C99 fragment is also later cleaved by γ-secretase into γCTF and Aβ peptide fragment in the transmembrane domain. The latter is the main component of neuritic plaques [70]. The γ-secretase protease complex is formed by four different subunits: nicastrin, anterior pharynx defective 1 (APH-1), presenilin enhancer 2 (PEN-2) and presenilin (PS) [71-73]. Little is known regarding the function of the first three subunits, though the PS is known to be the subunit containing the catalytic site of the APP cleavage. The PS domain contains the PS1 and PS2 subunits, which are expressed by the *PSEN1* and *PSEN2* genes, respectively. Different catalytic sites in the C-terminal Aβ fragment can be cleaved by the γ-secretase protease complex [74-77]. The cleavage in those sites produces different Aβ lengths, varying form $A\beta_{x-37}$ to $A\beta_{x-42.}$ Among the different forms of Aβ, $A\beta_{x-42}$ is the most toxic and $A\beta_{x-40}$ is the most abundant [78, 79].

After the cleavage, some fragments of Aβ also suffer posttranslational modification (PTM). The Aβ peptide can be truncated by other proteases and/or aminopeptidades [80]. Those cleavages can expose the glutamate in the 3rd amino acid residue of the Aβ fragment. Pyroglutamate Aβ (pEAβ) is formed by the conversion of the exposed glutamate into pyroglutamate by the glutaminyl cyclase (QC) [80, 81]. This modification provides protease resistance, due to increase of hydrophobicity by change in the Aβ charge. In addition, this Aβ species corresponds to 25% of the neuritic plaques and is mainly located in the core of neuritic plaques [82, 83]. Moreover, pEAβ is more neurotoxic and facilitates Aβ aggregation [84].

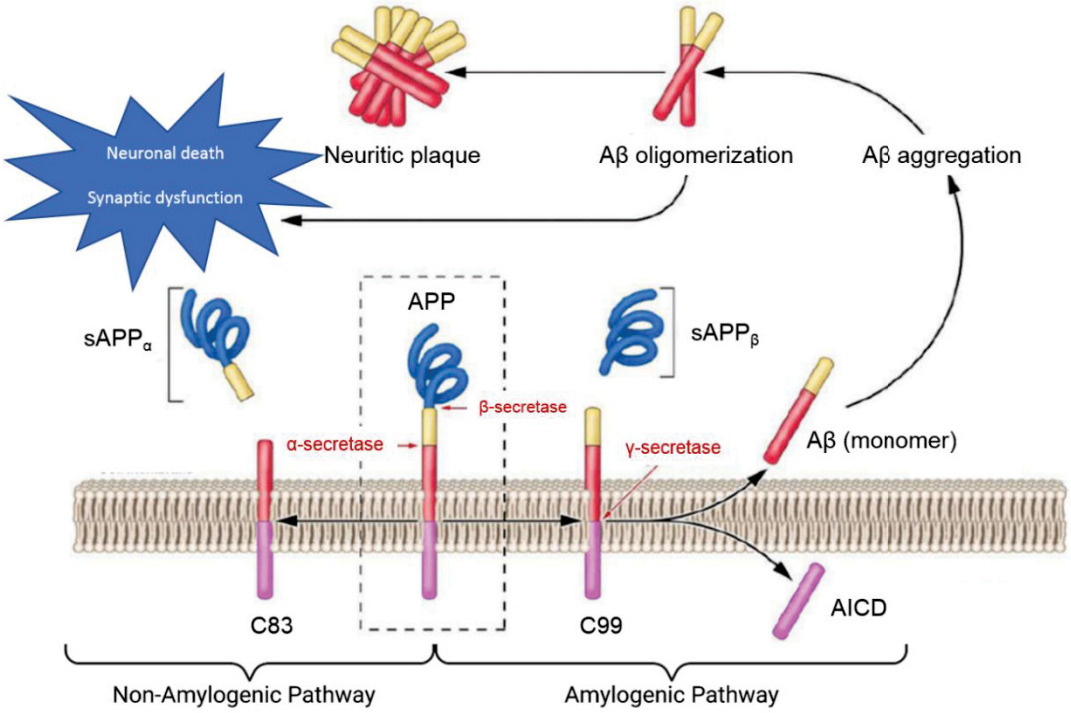

Figure 3: Non-Amylogenic and amylogenic pathway of the APP processing. In the non-amylogenic pathway, amyloid precursor protein (APP) is cleaved by the α-secretase, producing sAPPα and C83. C83 can then be further cleaved by γ-secretase. In the amylogenic pathway, APP is cleaved by the β-secretase, producing sAPPβ and C99. C99 is then further processed by γ-secretase, which produces Amyloid-β (Aβ). The monomeric Aβ peptide formed assembles into oligomers, which then further assembles into fibrils. Those Aβ fibrils are the main component of neuritic plaques. The Aβ oligomers are toxic and responsible for the neuronal death as well as synaptic dysfunction. Adapted from [85]

1.1.4. Amyloid cascade hypothesis

Once Aβ fragments (monomers) are produced from the amylogenic pathway, they assemble into oligomers by forming β-sheets secondary structures, called amyloid. Those amyloid structures then further assemble into fibrils, which are the main structure present in the extracellular plaques (Figure 3) [86, 87]. Together with active microglia, Aβ fibrils forms the neuritic plaques, which are the structure described by Alois Alzheimer [88]. Researchers postulate that Aβ oligomers are the most toxic form, and not the fibrils [89-92]. One reason is that the oligomers have a more flexible structure than fibrils, which facilitates to assemble new interactions and recruits more monomers [93, 94].

The prion-like behavior of Aβ has been widely accepted in the research community lately. By definition, prions can self-propagate; form β-sheets secondary structures; have different species; are resistant to degradation by proteases; spread throughout the brain; and are transmissible [95]. Those characteristics are also shared by Aβ, moreover, Aβ can spread to different areas of the brain when AD brain homogenates are injected in non-human primates brain [96] and in transgenic AD mouse models [97-100].

Once Aβ is produced, it can be cleared in the brain by both APOE4 and microglia. The microglia binds to Aβ through different receptors, e.g. toll-like receptors, which induces inflammation via liberation of proinflammatory cytokines. Under pathological conditions, microglia are unable to provide Aβ clearance and the induced neuroinflammatory process further induce neuronal damage and synaptic loss [101]. These damages can be induced by the production of reactive oxygen species and nitric oxide synthesis. Besides microglia, astrocytes and even neurons induces exacerbated neuroinflammation in response to Aβ [102]. Since astrocytes are responsible for the synaptic maintenance, reactive astrocytes also contribute to synaptic dysfunction [103]. In both, humans and animal models, reactive astrocytes and microglia are located close to Aβ deposits. Moreover, neuroinflammation also plays a role in the activation of β- and γ-secretase as well as the increased production of APP in the membrane [104].

In the brain, Aβ oligomer interacts with different receptors and alters multiple signaling pathways. The Aβ oligomers toxicity at synapses occurs especially due to its ability to interact with the postsynaptic receptors. Among these receptors, the α-amino-3-hydroxy-5-methyl-4-isoxazolepropionate receptor (AMPAr) in the membrane surface is reduced due to ubiquitination by neural precursor cell expressed, developmentally down-regulated 4-1 (Nedd4-1) or facilitation of the N-methyl-D-aspartic acid receptor (NMDAr)-dependent signaling pathway, which are induced by Aβ. Consequently, the dendritic spine density and long-term potentiation (LTP) are affected. Other receptors are also affected by Aβ oligomers inducing synaptic dysfunction and neurotoxicity (for review see: [105, 106]).

As it is postulated in AD, Aβ also affects the pathological formation of NFT. Besides Aβ interactions with synaptic receptors, Aβ also induces the activation of different kinases that phosphorylates Tau [107-110]. Hyperphosphorylated Tau is the initial step in the NFTs formation [111]. Moreover, Aβ activates caspases that produces truncated Tau, which is more prone to aggregates [112]. On the other hand, the formation of hyperphosphorylated Tau facilitates Aβ toxicity in synapses via Src family tyrosine kinase (Fyn) in the dendrites. Initially, it was thought that Aβ pathology was the initial trigger for NFTs formation, which then induces neurodegeneration. Nowadays, it is known that the toxic pathway in AD is more complex and both Aβ and Tau are neurotoxic via similar pathway, e.g. neuroinflammation [113].

1.1.5. APP mutations

Most of the mutations in the APP gene are related to EOAD (Figure 4). The first described mutation was the so called “Swedish mutation”, which was found in a Swedish family with a disease onset around 55 years [114]. This mutation occurs closely to the N-terminal region of the Aβ peptide fragment in the APP, and it facilitates the formation of Aβ by β-secretase. The mutations occur in the position 670 and 671 of APP that substitutes lysine to

asparagine and methionine to leucine, respectively [114]. Lately, the Swedish mutation (APPswe) is the most common transgene in the transgenic models of AD used.

Other APP mutations, like the Dutch and Iowa mutations, occur inside the Aβ fragment in the APP and increase the Aβ toxicity by the loss of negatively charged residues, without increasing the overall Aβ production by the APP processing. Patients harboring the Dutch mutation have the APP mutation in residue 693 substituting the glutamic acid to glutamine. In the brain, it mainly occurs diffuse plaques composed almost exclusively of $A\beta_{42}$. Hence, those patients have been described to develop cerebral hemorrhages due to the cerebral amyloid angiopathy (CAA), which is characterized by Aβ deposition in the brains' vascular system [115-117]. Harboring the Iowa mutation, patients have the APP mutation in the residue 694 that substitute the aspartic acid to asparagine. Unlike the patients carrying the Dutch mutation, both $A\beta_{40}$ and $A\beta_{42}$ are in the deposits [118]; there is also the presence of NFTs and cognitive deficits [119]. In order to study the role of CAA as well as potential treatments, the Dutch and Iowa mutation transgene was also developed in transgenic mouse model.

Mutation in the PSEN 1 gene are also responsible for the EOAD. The deletion of exon 9 in the PSEN1 gene (PS1ΔE9) is known to produces cotton wool plaques, which are mainly composed of $A\beta_{x\text{-}42}$ without the presence of both dense core and dystrophic neurites [120]. In patients, this mutation is also associated with the spastic paraplegia. Mutations in the PSEN1 also induces the increased ratio of $A\beta_{42}/A\beta_{40}$ [120-122]. Combined with the APPswe mutation in transgenic mouse model, the APPswe/PS1ΔE9 has increased pathology compared to only APPswe and PS1ΔE9 parental mouse models [123].

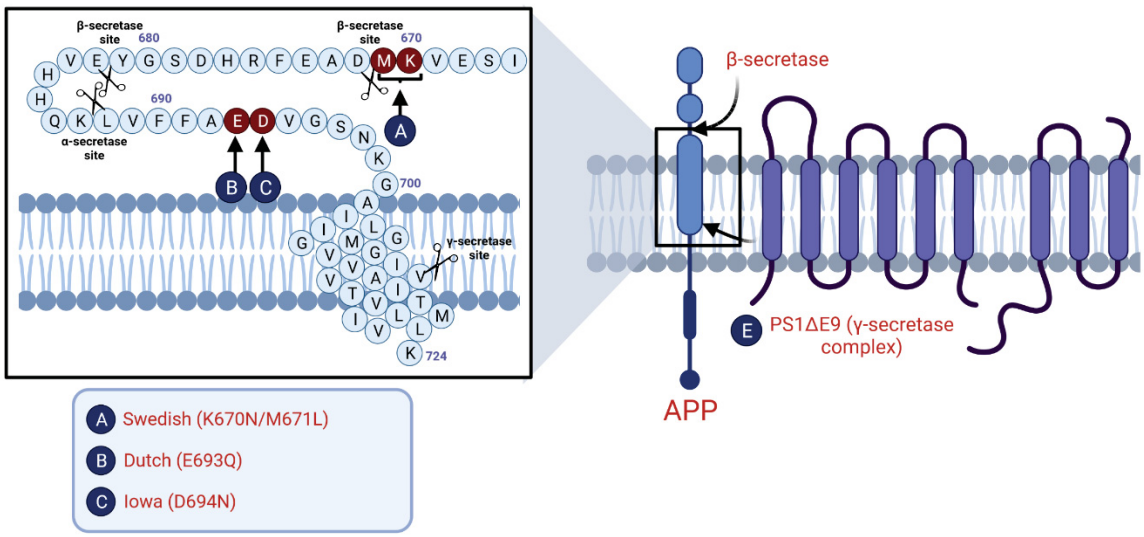

Figure 4: Amylogenic pathway of the APP processing induced by mutations of familial AD. Mutations in the amyloid precursor protein (APP) can occur inside and outside the Amyloid-β (Aβ) fragment. The Swedish mutation (A)

occurs outside and plays a role in facilitating the Aβ production by the β-secretase activity. The Dutch (B) and Iowa (C) mutation occur inside and induces the Aβ aggregation. The mutation in the presenilin subunit (PS1) of the γ-secretase complex (PS1Δe9) (E) facilitates the formation of $Aβ_{42}$. Created with BioRender.com.

1.1.6. Tau protein

Nowadays, some dementias can also be classified as tauopathies, in which the microtubule associated Tau protein is hyperphosphorylated, aggregates intracellularly and finally forms the NFTs. Tauopathies can be divided in primary and secondary [9]. In the secondary tauopathy, e.g. AD, hyperphosphorylated Tau occurs as a second event, probably due to Aβ pathology. The primary tauopathies are diseases in which hyperphosphorylated Tau is the first event, which can be considered frontotemporal lobar degeneration associated with Tau (FTLD-Tau), progressive supranuclear palsy (PSP) and corticobasal degeneration (CBD) [124, 125].

Tau is a microtubule associated heat stable protein which possesses different functions, including preventing the dissociation of microtubules, regulation in synapses, axonal trafficking and the activation of microtubule associated protein (MAP) kinases [126-131]. It is expressed from the microtubule associated protein Tau (MAPT) gene located on chromosome 17 and it can be transcribed in six distinct isoforms by alternative splicing of the 16 exons (Figure 5). The MAPT gene can be divided in two parts: the N-terminal (N); and C-terminal microtubule-binding domain, which can have three or four motifs (3R and 4R) [132, 133]. The shortest isoform is the 0N3R and the longest is 2N4R. In human brain, both the 2N4R and 2N3R are present, but during brain development, 2N3R is the most common [134]. Regarding the microtubule domain, the exon 10 is lack or present in the 3R and 4R, respectively. Considering other isoforms, the lack of exons 2 and 3 in 0N4R and 0N3R isoforms, are present mainly in axons, while 2N4R isoform tau are present mainly in the soma and dendrites [135]. Moreover, PSP and CBD patient mainly have the Tau 4R isoform in the brain, while in Pick's diseases, those are composed of the 3R isoform [136].

The frontotemporal dementia with parkinsonism-17 (FTDP-17) is one of the most common genetic FTD, where mutations in the MAPT have been described. Those mutations affect the ability of Tau to bind to microtubules as well as to promote Tau hyperphosphorylation [137]. The most described mutation is the amino acid residue substitution at position 301 from a proline to leucine [138-140] (Figure 5). This position is in the exon 10, therefore this alteration in the Tau protein sequence can only occurs in the 4R isoform.

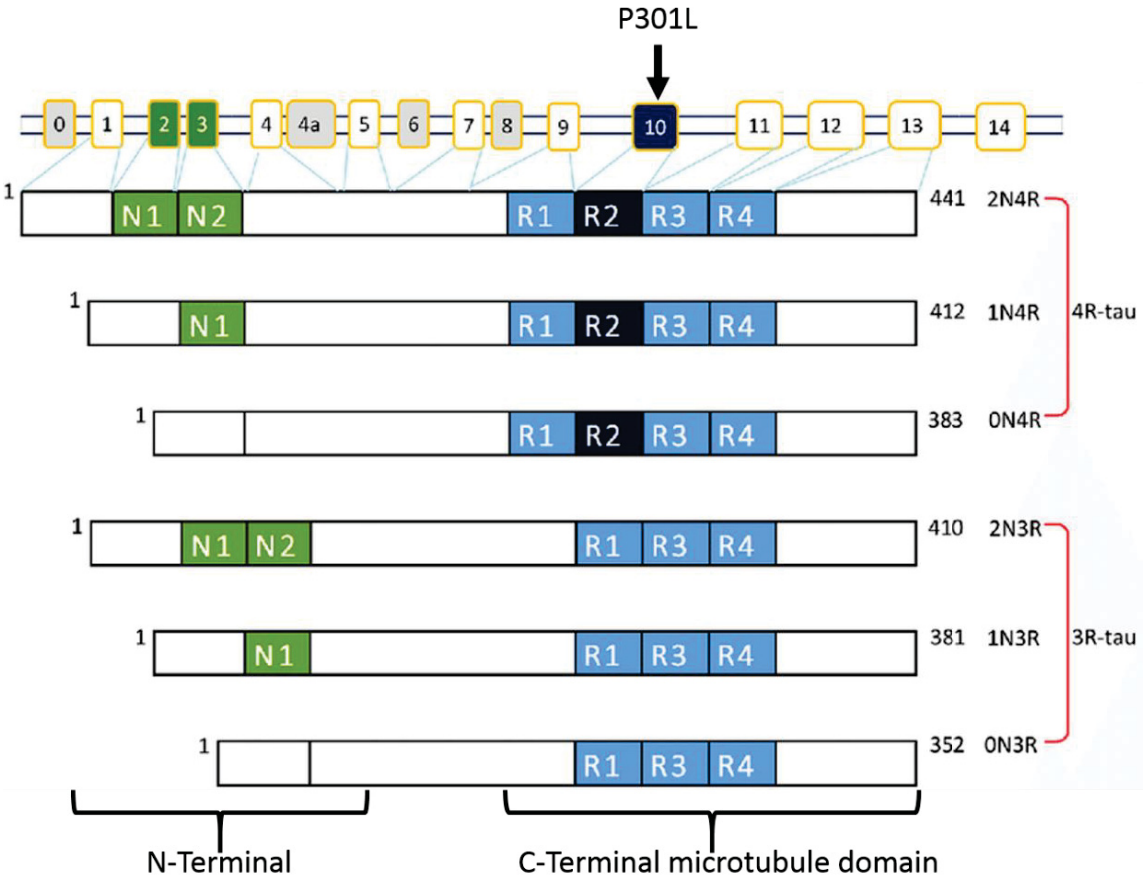

Figure 5: Tau isoforms expressed from the MAPT gene alternative splicing. In the N-terminal (N), three different isoforms can be formed, the 0N, 1N and 2N. In the C-terminal microtubule domain (R), two different isoforms can be expressed, the 3R and 4R. The combination of both regions then produces the six Tau isoforms, 0N3R 1N3R, 2N3R, 0N4R, 1N4R and 2N4R. In the exon 10, P301L mutation is located, which was described in the frontotemporal dementia with parkinsonism-17 (FTDP-17). Adapted from [141].

The Tau protein is also affected by posttranslational modification, such as phosphorylation [142-144]. The phosphorylation of Tau regulates its function and binding to the microtubules. Under pathological conditions, Tau is hyperphosphorylated by kinases, resulting in the loss of function to bind to microtubules and it is misplaced into dendrites, then, the hyperphosphorylated Tau assemble into Tau oligomers, that adopt a β-sheet formation, which further assembles into paired helix filaments (PHF), the main composition of NFTs [145-148], Patterson, Remmers [149]. Those are the intracellular inclusions described by Alois Alzheimer. Braak and Braak (1991) further described that the presence of NFTs in different regions of the brain can be correlated with the cognitive deficits. Nowadays, this technique is called the Braak stages and can be used as a postmortem diagnostic of AD. In the Braak stages I and II, the NFTs positive cells are located initially in the transentorhinal cortex, where the hippocampus is located. In the Braak stages III and IV, the neurodegeneration spreads to the limbic system. In the last Braak stages (V and VI), the neocortex is also affected [150].

Misfolded Tau can also be classified as prion-like since aggregated Tau can induce hyperphosphorylated Tau in mice [151-154]. Moreover, Tau spreads from neuron to neuron

via low-density lipoprotein receptor-related protein 1 (LRP1), which plays a role in the uptake and propagation of Tau [40, 155-157]. Recently, it was demonstrated that different forms of Tau seeds are present in the brain and they seem to determine the severity of dementia in patients [158].

Similar to the neuroinflammatory process induced by Aβ aggregation, misfolded tau also induces microglia and astrocytes activation. One process is induced by the cluster of differentiation 200 (CD200) that is decreased, once the neuronal integrity is compromised, a process that occurs due to the formation of NFTs. This protein inhibits the microglia activation and with its decrease, reactive microglia increase [159]. Moreover, reactive microglia also induce the hyperphosphorylation of Tau and NFT formation, thereby creating a feed forward loop [160].

As Tau helps in the axonal trafficking, it plays an important role in the regulation of synapses, especially by modulating pre- and post-synaptic receptors and mitochondrial transport. Under physiological conditions, Tau also induces AMPAr endocytosis by enhancing its interaction with protein interacting with C Kinase (PICK1). This process provides the long-term depression (LTD) in the CA1 region of the hippocampus. Under pathological conditions, Tau is dislocated to the dendrites and impairs the post-synaptic function. Pathological Tau interacts with Fyn and recruits more Fyn to the postsynaptic site. Fyn then stabilises the interaction of NMDAr and postsynaptic density protein 95 (PSD95), providing an overactivation of NMDAr. Finally, this overactivation results in a known process called glutamatergic excitotoxicity, which induces neuronal death. Besides, Tau deposits activate different Ca^{2+}-dependent enzymes inducing Ca^{2+} dysregulation in the synapses (for review: [106]). Another process that is impaired due to loss of Tau binding to the microtubules is the mitochondrial and receptors transport to the synapses, which decreases adenosine triphosphate (ATP) production in the synapses, inducing synaptic and axonal loss [161].

1.2. Treatment

Despite the research community efforts, dementia has no cure. Fortunately, some drugs are approved to treat the symptoms of AD, especially the cognitive deficits. Those drugs can be divided into two classes: acetylcholinesterase inhibitors (AChEI) and NMDAr blocker [162]. Besides the cognitive deficits, some drugs are also prescribed for the psychic and psychological alterations, e.g. hallucinations and depression, respectively. Moreover, non-medical strategies are also interesting tools to slow the progression or prevent dementia. In the recent years, the use of music and aromatherapy in patients has been increasing [163-166]. In addition, exercise is extensively performed regarding the motor deficits, which demented patients present later in life [167].

The AChEI were developed in the 1990's based on the cholinergic hypothesis. Acetylcholine (ACh) is the most common neurotransmitter in the brain and plays an essential role in memory processing [168]. It was observed that a decrease of ACh in the synaptic cleft affects memory processing and induces cognitive deficits [168, 169]. During the synaptic transmission, ACh in the synaptic cleft is cleared by the AChE by degrading into choline and acetic acid, keeping the system controlled [170]. With a decrease of ACh in the synaptic cleft in AD patients, inhibiting the degradation of ACh improves cognitive deficits [171]. The AChEI increase the ACh in the cleft by preventing ACh degradation thru the inhibition of AChE activity. Nowadays, three AChEI have been approved by the different health organizations: Donepezil, Rivastigmine and Galantamine.

Memantine was developed later based on the glutamatergic excitotoxity theory [172]. As opposed to ACh, glutamate in the synaptic cleft is increased in AD patients [173-175]. This exacerbated amount of glutamate over-activates the NMDA receptor, allowing an increased amount of Ca^{2+} to enter the neuron [176]. The increased Ca^{2+}-uptake impairs the signaling cascade inducing neuronal death [177]. Memantine prevents Ca^{2+} to enter the neurons by blocking the NMDA channel [178]. Even though Memantine was thought to be a neuroprotective drug, dementia still progresses in the patients despite the treatment [179].

Extensive research is being performed in order to find a more effective treatment for AD [180]. Many anti-Aβ drugs have been developed, especially monoclonal antibodies, but almost all of them failed in the clinical trial. One particular antibody, so-called Aducanumab, developed to bind specifically to Aβ oligomers, showed contradicting results in the last clinical trial [181]. Despite these contradictions, the Food and Drugs Administration (FDA) approved it on June 2021 to treat AD patients [182].

1.2.1. D-enantiomeric peptides

Small molecules, including peptides, are promising compounds for treatments in different diseases due to their ability to penetrate membranes and to bind with high specificity to targets. Therefore, peptides have been selected for AD treatment using different techniques [183]. Phage display is a technique in which a library of microphages connected with different peptides is used and selected based on its binding efficiency to the target compound [184, 185]. Originally, this technique was developed for L-peptide selection, but since L-peptides are easily degraded by proteases and are highly immunogenic, those compounds have limited use in treatment studies [186]. Therefore, a modified phage display technique, called Mirror image phage display was developed. The Mirror image phage display consists of a target compound that is synthetize in the D-enantiomeric structure and the library phage is L-enantiomeric. Then, the selected phage is change to D-peptide and should be able to interact with the L-enantiomeric protein target [187]. D-peptides are more resistant to protease degradation and

are less immunogenic, which makes these molecules more suitable for treatments in humans and animal models [188].

In this context, the D-enantiomeric peptide D3, was selected against Aβ monomers or small oligomers. D3 was able to prevent the Aβ aggregation, to eliminate Aβ oligomers and to reduce Aβ toxicity *in vitro* and improve cognitive deficits in different transgenic models [189-192]. Regarding the pharmacokinetics properties, D3 was efficient via intraperitoneal (i.p). and oral application with high bioavailability, high proteolytic stability, high terminal half-life as well as efficiency in brain-blood-barrier (BBB) penetration in mice [190, 191, 193].

In order to improve D3 efficiency, derivative peptides were developed. RD2, also called PRI-002, has a re-arranged but similar amino acid composition like D3. PRI-002 was able to eliminate toxic Aβ oligomers more efficiently than D3 *in vitro* and to improve behavior deficits in different mouse models [194-197]. In mice pharmacokinetics studies, PRI-002 administrated by different routes had high bioavailability properties, high proteolytic stability, high terminal half-life as well as efficiency in BBB penetration [198]. In the clinical phase I trial, PRI-002 also was demonstrated to be safe when administered orally in humans [199]. At the present moment, a clinical phase II trial with PRI-002 is in preparation.

RD2D3 were developed by combining head to tail tandem PRI-002 with D3, respectively, in order to enhance Aβ affinity [192]. Similar to PRI-002, RD2D3 was also able to prevent Aβ aggregation *in vitro* but not *in vivo* when administrated orally [195]. Interestingly, both RD2D3 and D3D3 had similar pharmacokinetics properties, although RD2D3 had higher bioavailability when administrated i.p. [198]. Besides the tandem derivatives, the head-to-tail cyclization of D3 derivatives was evaluated as an approach to improve its binding affinities and efficiency. Cyclic RD2D3 (cRD2D3) reached the highest concentrations in the brain and efficiently cross the BBB compared to other D3 derivatives and its cyclic derivatives [200]. In summary, D-enantiomeric peptides seem to be an advantageous treatment strategy for AD since they show a high proteolytic stability as well as high efficacy to eliminate Aβ oligomers and to improve cognitive deficits in AD mice.

1.3. Animal models

Several animal models can be used in the translational studies of dementia. In aged canines and non-human primates, Aβ aggregation is present but there are some disadvantages like zoonotic transmission and low reproducibility [201-203]. On the other hand, rodent models of dementia depend on induction of the disease, since they do not develop neuritic plaques and NFTs naturally, due to differences from humans to rodents in the protein structure.

There are two types of models that can recall some hallmarks of AD. One is the injection of Aβ (or similar) directly into the brain. These induced models manifest cognitive deficits that

resemble those observed in humans, but lacks Aβ aggregation and neurodegeneration, which are also hallmarks of the disease [204]. Moreover, the reproducibility of these models is limited since fibrils may have different efficiency at each injection. The other type of AD models are the transgenic models. In those models (in general mice), the animals express at least one of the mutated genes described for familial AD (in humans). The transgenic models can be developed by using different promoters as well as genetic backgrounds.

1.3.1. Transgenic APPswe/PS1ΔE9 mice

The APPswe/PS1ΔE9 (APP/PS1) mouse model is a double transgenic line that harbors the abovementioned APPSwe mutation as well as PSEN1 mutation, and is widely used in AD research. The APP/PS1 mouse model was developed by Jankowsky and collaborators (2004) [123]. This mouse model developed an extensive plaque load which progresses with age [205, 206]. APP/PS1 mice had a similar amyloid pathology compared to humans, which makes them a suitable model to study the role of amyloidosis in the brain as well as preclinical studies regarding anti-Aβ drugs. Regarding the behavioral alterations, APP/PS1 mice had spatial memory deficits in the Morris water maze (MWM) and were less anxious compared to non-transgenic mice at 12 months of age [207, 208]. At early ages, impairment in the fear memory was also observed in APP/PS1 mice [209] (Table 1). Even though the behavioral deficits have been widely studied in this line, some differences regarding the onset and severity are still variable from study to study.

The neuritic plaques were present mainly in the cortex and hippocampus starting with six months of age [123] (Table 1). Neuroinflammatory markers were also increased at this age and was located in proximity of plaques [210] (Table 1). This mouse model together with many other APP transgenic mouse lines did not display massive neurodegeneration even in later ages, even though an impairment of transient LTP as early as three months of age and a discrete neuronal death was observed close to the plaques [208, 211]. Interestingly, the APP/PS1 mice had seizures, which is the common cause of premature death [212].

1.3.2. The TBA2.1 line

The TBA2.1 line was developed to understand the role of pEAβ in AD [213]. This model was generated by inserting the cDNA sequence of a murine thyrotropin releasing hormone (TRH) pre-pro-peptide combined with the modified human Aβ polypeptide Aβ(Q3–42) under a neuron specific promotor. The TRH sequence is preferentially processed in the secretory pathway, therefore, after the protein expression of TRH with Aβ(Q3–42), those are further processed in the trans-Golgi network. The peptide is then modified by the QC, forming the pEAβ(3-42). In order to increase the probability of QC processing and pEAβ production, the glutamate in position 3 of the Aβ sequence was replaced by glutamine [214].

Unlike any other AD model, homozygous TBA2.1 mice developed neurodegeneration and severe motor deficits, but they did not develop plaques (only intracellular Aβ deposits) and displayed early death (by five months of age) [213]. Starting with three months old, TBA2.1 mice displayed severe neurodegeneration in the CA1 region of the hippocampus [213]. Neuroinflammation was detected at two months of age reaching a peak with three months of age but decreases at five months due to neurodegeneration [213]. The same pattern was observed with the intracellular Aβ aggregation. Regarding the behavioral deficits, the motor-induced neurotoxicity started as earlier as with two months of age. The cognitive deficits of TBA2.1 mice is still unknown. Moreover, homozygous TBA2.1 showed weight loss starting at four weeks of age [213] (Table 1).

Heterozygous TBA2.1 mice, on the other hand, did not develop a strong phenotypic alteration as late as 18 months of age. At 21 months, heterozygous TBA2.1 displayed phenotypic alterations and a decrease in body weight. At 24 months, the amount of Aβ is increased in the hippocampus and striatum, and seemed to induce neurodegeneration [215].

1.3.3. Transgenic SwDI mice

The APP **Sw**edish (KM670/671NL), **D**utch (E693Q) and **I**owa (D694N) (SwDI) line was first developed by Davis and collaborators (2004) and is the most common transgenic mouse model of CAA [216]. This mouse model starts to accumulate Aβ in the cerebral blood vessels including microvessels at early ages, especially in the thalamus and subiculum areas of the brain. The insoluble Aβ fraction is composed of both Aβ40 and Aβ42 with the mutant Dutch and Iowa substitution. Unlike the APP/PS1 mice, SwDI mice develop diffuse Aβ deposits in the brain parenchyma rather than fibrillary Aβ plaques. The fibrillary Aβ plaques, though, can be found in the vasculatures [216, 217] (Table 1). The homozygous SwDI mice have increased Aβ deposits compared to the heterozygous mice.

Regarding the behavioral alterations, SwDI mice have cognitive deficits in the MWM at six months of age and in Barnes maze starting at three months of age, but no motor deficits have been observed as late as 12 months of age [218, 219]. Interestingly, the spatial memory deficits do not correlate with Aβ plaques but rather with increased neuroinflammation [218, 220] (Table 1).

1.3.4. Transgenic Tau-P301L mice

Models of tauopathy can be induced by expression of Tau human mutations. Those models can be used to understand AD but needs careful interpretation since the mutation of Tau does not exist in AD patients. Therefore, a combination of Tau and APP mutation would be more appropriate for the study of AD. The most common transgenic models of tauopathies are the ones with the P301L mutation [221, 222].

Tau-P301L transgenic mice were developed by Terwel and collaborators (2005) among others [223]. This transgene is expressed under the Thr1 promoter on FVB background and only the full-length Tau (2N4R) is present. Pathological Tau started to appear at six months mainly in the brainstem and cortex of the mice and progresses with age. Due to the presence of pathological Tau in these areas controlling upper airway function, these mice died prematurely due to respiratory problems. Moreover, they developed a severe phenotypic alteration, which was described as a clasping in the limbs, starting at 9 months as well as motor deficits in the beam walk test. Regarding cognitive deficits, Tau-P301L mice on FVB background developed deficits in the passive avoidance and in the novel object recognition test (NOR) at five and nine months of age, respectively [224]. On the other hand, Tau-P301L mice had an improved performance in the NOR that might be related to the enhanced LTP in the hippocampus [225]. Finally, alterations in the open field, elevated plus maze and in the sociability and preference for social novelty (SPSN) were observed at early ages [226] (Table 1).

Table 1: Overview of the transgenic mouse model alterations. The age of onset (in months) for amyloidosis, Tau pathology, neuronal loss, gliosis, synaptic loss and cognitive deficits is given for each model (APP/PS1, TBA2.1, Tau-P301L and SwDI), respectively.

	APP/PS1	**TBA2.1 (homozygous) [213]**	**Tau-P301L**	**SwDI**
Amyloidosis	Six months [123]	Absent (intracellular aggregation at three months)	Absent	Three months: cerebral microvascular fibrillary amyloid [216]
Tau pathology	Absent	Absent	Eight months [223]	Absent
Neuronal loss	Eight months: neuronal death in proximity to the plaques	5 months	No data	No data
Gliosis	Six months [210]	Three months	Seven months	Six months [217]
Synaptic loss	Four months [227]	No data	No data	No data
Cognitive impairment	12 months: Morris water maze [207]	No data	Five months: Passive avoidance test [224] Seven months: novel object recognition test [224]	Three months: Barnes maze task [218]

1.3.5. Limitation of animal models

The transgenic models play an essential role in the translational research, since one isolated hallmark can be studied in-depth in a controlled conditions. A noteworthy drawback, however, is that most models fail to reproduce all of the disease's hallmarks. This limitation may explain the inefficiency of new substances in clinical trials despite positive preliminary results in mouse tests. One solution for this problem may be the development of new mouse models with closer pathological similarities to humans. Lately, a collaboration called MODEL-AD is developing the next generation of animal models in order to have more reliable preclinical studies [228].

Besides the development of new models, in-depth characterization of already existing mouse models, e.g. by longitudinal studies, could also provide more precise information for the treatment study design in contrast to cross-sectional studies. Repeated experiments decrease the anxiety levels of mice since they habituate to handling, the experimental facilities and the tests. The decreased anxiety results in a more reliable result in the behavioral tests, since high levels of anxiety can alter the mice's performance in some (mainly cognitive) tests. On the other hand, some behavioral test are more reliable in cross sectional studies, since habituation would alter the results, e.g. MWM. Moreover, the onset of deficits can be different depending on the disease course, and a longitudinal study can provide more complete data regarding which deficits occur at which time point [229].

2. Objective

More than a century has passed since AD and FTD have been described for the first time. Since then, a lot have been explained regarding its physiopathology and most of the discoveries would not have been possible without animal models. Animal models play an essential role in the translational research since it is possible to isolate a single element of a complex problem and evaluate it in a controlled and reproducible environment. Many transgenic models have been developed to understand the role of Aβ and Tau via the genetic mutations found in patients. Those transgenic models, especially mouse models, have also been used in preclinical trials for years to test new therapeutic options. However, the failure of drugs in subsequent clinical trials have questioned the usefulness of animal models lately. In this context, the research community made efforts, both, to develop new models which are as similar to human diseases as possible, and to further understand the already existing models, in order to increase the translation from preclinical data into the clinic.

Taking together, the aim of this thesis was to characterize different mouse models of dementia to improve their usefulness. The first model is a new transgenic model developed in the Institute of Neuroscience and Medicine (INM-4) at the Forschungszentrum Jülich, called TAPS. The **T**(TBA2.1)**APS**(APP/PS1) line harbours the Aβ production from TBA2.1 combined with both APPswe and PS1ΔE9 transgenes. In the TAPS model, it was expected that the mice develop both the amyloidosis described in the APP/PS1 line as well as the aggressive neurotoxicity induced by the pEAβ [123, 213]. To evaluate the general behavior, SHIRPA and open field test were performed. To assess the cognitive deficits, the NOR, t-maze spontaneous alternation, fear conditioning and MWM were performed. In order to further evaluate the amyloidosis in relation to neuroinflammation, histological analysis was performed.

The second model that was characterized was the Tau-P301L line. This line was developed by Terwel and collaborators (2005) [223]. The initial description though, was restricted to histological analysis of NFT pathology and few behavioral tests. In order to increase the number of longitudinal read-outs for possible therapeutic studies using these mice, the mouse line has been characterized in more detail. Therefore, we have evaluated both sex in an interval of two months starting with two months of age in different behavioral tests. To evaluate the general behavior, the habituation/dishabituation olfactory test, marble burying, nesting behavior, SHIRPA and open field test were performed. To evaluate the motor deficits, the Rotarod and modified pole test were performed. Finally, to assess the cognitive deficits, the NOR, T-maze spontaneous alternation, fear conditioning and MWM were conducted. In order to further evaluate the NFT pathology in relation to neuronal death and neuroinflammation, histological analysis was performed.

Moreover, a proof-of-concept treatment study was performed to demonstrate the importance of an appropriate characterization prior to a treatment study. For this purpose, two D-enantiomeric peptides, the linear RD2D3 and the cyclic derivative cRD2D3, respectively, were chosen. The treatment was performed via i.p. pump implantation in the SwDI transgenic mouse line. Previously, the SwDI had been extensively characterized in the nesting, marble burying, open field and MWM tests. Those behavioral test were then performed after the pump implantation in order to evaluate the treatment efficiency of RD2D3 and cRD2D3.

Overall, the development of a new mouse model as well as the longitudinal study of an existing mouse model provides more suitable models for the study of AD physiopathology and the development of new drugs against AD. Moreover, the RD2D3 and cRD2D3 treatment study would be well design due to the characterization of the SwDI mouse model in advance.

3. Publications

3.1. PEAβ Triggers Cognitive Decline and Amyloid Burden in a Novel Mouse Model of Alzheimer´s Disease

Authors: Luana Cristina Camargo*, Michael Schöneck*, Nivethini Sangarapillai, Dominik Honold, N. Jon Shah, Karl-Josef Langen, Dieter Willbold, Janine Kutzsche, Sarah Schemmert, Antje Willuweit

*contributed equally

Journal: International Journal of Molecular Science (2021), accepted on June 25th, 2021

DOI: 10.3390/ijms22137062

Impact Factor: 5.923 (2020)

Contribution: Performance and analysis of the behavioral tests (open field, novel object recognition, t-maze spontaneous alternation, fear conditioning and Morris water maze).

Analysis of the DAPI staining

Writing of the original draft and the manuscript revision.

International Journal of
Molecular Sciences

MDPI

Article

PEAβ Triggers Cognitive Decline and Amyloid Burden in a Novel Mouse Model of Alzheimer's Disease

Luana Cristina Camargo [1,2,†], Michael Schöneck [3,†], Nivethini Sangarapillai [3,‡], Dominik Honold [1], N. Jon Shah [3,4,5], Karl-Josef Langen [3,6], Dieter Willbold [1,2], Janine Kutzsche [1], Sarah Schemmert [1] and Antje Willuweit [3,*]

1 Institute of Biological Information Processing, Structural Biochemistry (IBI-7), Forschungszentrum Jülich, 52425 Jülich, Germany; l.camargo@fz-juelich.de (L.C.C.); d.honold@fz-juelich.de (D.H.); d.willbold@fz-juelich.de (D.W.); j.kutzsche@fz-juelich.de (J.K.); s.schemmert@fz-juelich.de (S.S.)
2 Institut für Physikalische Biologie, Heinrich-Heine-Universität Düsseldorf, 40225 Düsseldorf, Germany
3 Institute of Neuroscience and Medicine, Medical Imaging Physics (INM-4), Forschungszentrum Jülich, 52425 Jülich, Germany; m.schoeneck@fz-juelich.de (M.S.); nivethini.sangarapillai@uni-marburg.de (N.S.); n.j.shah@fz-juelich.de (N.J.S.); k.j.langen@fz-juelich.de (K.-J.L.)
4 JARA-Brain-Translational Medicine, JARA Institute Molecular Neuroscience and Neuroimaging, 52062 Aachen, Germany
5 Department of Neurology, RWTH Aachen University, 52062 Aachen, Germany
6 Department of Nuclear Medicine, RWTH Aachen University, 52062 Aachen, Germany
* Correspondence: a.willuweit@fz-juelich.de; Tel.: +49-2461-6196358
† Both authors contributed equally to the work.
‡ Present address: Department of Psychology, Philipps-University of Marburg, 35037 Marburg, Germany.

Citation: Camargo, L.C.; Schöneck, M.; Sangarapillai, N.; Honold, D.; Shah, N.J.; Langen, K.-J.; Willbold, D.; Kutzsche, J.; Schemmert, S.; Willuweit, A. PEAβ Triggers Cognitive Decline and Amyloid Burden in a Novel Mouse Model of Alzheimer's Disease. *Int. J. Mol. Sci.* **2021**, *22*, 7062. https://doi.org/10.3390/ijms22137062

Academic Editor: Sónia C. Correia

Received: 31 May 2021
Accepted: 25 June 2021
Published: 30 June 2021

Abstract: Understanding the physiopathology of Alzheimer's disease (AD) has improved substantially based on studies of mouse models mimicking at least one aspect of the disease. Many transgenic lines have been established, leading to amyloidosis but lacking neurodegeneration. The aim of the current study was to generate a novel mouse model that develops neuritic plaques containing the aggressive pyroglutamate modified amyloid-β (pEAβ) species in the brain. The TAPS line was developed by intercrossing of the pEAβ-producing TBA2.1 mice with the plaque-developing line APPswe/PS1ΔE9. The phenotype of the new mouse line was characterized using immunostaining, and different cognitive and general behavioral tests. In comparison to the parental lines, TAPS animals developed an earlier onset of pathology and increased plaque load, including striatal pEAβ-positive neuritic plaques, and enhanced neuroinflammation. In addition to abnormalities in general behavior, locomotion, and exploratory behavior, TAPS mice displayed cognitive deficits in a variety of tests that were most pronounced in the fear conditioning paradigm and in spatial learning in comparison to the parental lines. In conclusion, the combination of a pEAβ- and a plaque-developing mouse model led to an accelerated amyloid pathology and cognitive decline in TAPS mice, qualifying this line as a novel amyloidosis model for future studies.

Keywords: transgenic mice; behavioral tests; amyloid plaques; Alzheimer´s disease; mouse model; amyloidosis; neurodegeneration; neuritic plaques; neuroinflammation; cognitive decline

1. Introduction

Dementia is the most common form of neurodegenerative diseases, leading to a decline in cognitive functions over time. In 2020, an estimated amount of around 27 million people in the world lived with dementia [1–3]. Among the neurodegenerative dementias, Alzheimer's disease (AD) has the highest prevalence with approximately 60% of all dementia cases [4,5]. Besides the cognitive decline, two main pathological hallmarks occur in AD brains, most of which are known as neurofibrillary tangles and neuritic plaques. The latter ones are mainly composed of different aggregated species of the amyloid-β (Aβ) peptide. Aβ aggregation is initiated by the interaction of Aβ monomers, which

assemble into toxic Aβ oligomers. Further aggregation leads to Aβ fibrils that are the main component of the neuritic plaques and can be found extracellularly in human AD brains. Following the amyloidogenic pathway, Aβ monomers are produced by the cleavage of the amyloid precursor protein (APP) [6] through cleavage by the β-secretase, instead of the α-secretase in the non-amyloidogenic pathway, and the consecutive cleavage by the γ-secretase [7]. A minor amount of AD cases are classified as familial AD (fAD), in which different gene mutations have been identified to be the primary cause of AD. Most of the fAD mutations are discovered in the *APP* gene, as well as in an active component of the γ-secretase complex, the presenilin-1 or -2 genes (*PSEN1*, *PSEN2*) [8]. Mutations in these genes lead to increased processing of APP in the amyloidogenic pathway and consecutively to the secretion of Aβ. Taking advantage of this, a number of fAD mutations have been used to generate transgenic animal models developing AD-like amyloidosis in the brain for studying AD pathophysiology and testing of new therapeutic options.

A widely used fAD mutation for transgenic mouse models is the so-called APPswedish mutation (APPswe), which occurs by the change of amino acid residues outside the Aβ domain, facilitating Aβ production [6,9,10]. The combination of an APPswe transgene with a second one, harboring a mutated presenilin transgene, has been shown to additionally increase formation of the Aβ1-42 species, which is highly prone to aggregation and, thus, leads to a progressive amyloidosis phenotype in the brain of double transgenic mice [11]. A double transgenic mouse model commonly used in AD research is the APPswe/PS1ΔE9 (APP/PS1) line, which carries both an APPswe and a mutated presenilin-1 (PS1) transgene. The mice start to develop amyloid plaques and neuroinflammation within six months, which progressively intensifies with age [8,12–14]. Despite the presence of abundant neuritic plaques later in life, the mice do not develop obvious neurodegeneration [14]. Nevertheless, cognitive deficits have been described for this line, although with variable onset [15,16]. One study described a deficit in spatial learning and memory in the so-called Morris water maze (MWM) paradigm with 15 months of age [17]. All in all, this line is a very common mouse model whose amyloidosis seems to be very similar to the human disease, in particular due to the presence of neuritic plaques in both cortex and hippocampus. However, the APP/PS1 line has been shown to be not particularly suited for amyloid imaging with radiotracers routinely used in the clinic, as studies by Stenzel et al. [18] and our research group suggested. A difference in plaque morphology or composition has been discussed as the cause for lower binding of amyloid radiotracers to plaques of this mouse model [19]. In addition, the presence of truncated Aβ species has been proposed to be important for amyloid radiotracer binding and AD-like plaque morphology [20].

A variety of different Aβ species can be detected in amyloid plaques of AD patients. While the main Aβ variants are Aβ1-40 and Aβ1-42, a significant proportion consists also of N-terminally truncated species [21]. Studies identified that N-terminally truncated and pyroglutamate-modified Aβ (pEAβ) represents up to 25% in neuritic plaques in human AD patients´ brains [22–24]. The pEAβ is formed in a post-translational modification of exposed glutamate by the glutaminyl cyclase in both glutamate position 3 (pEAβ3-42) and 11 (pEAβ11-42) of truncated Aβ [25]. These modifications change the overall charge of the Aβ peptide, which increases its hydrophobicity and, thus, facilitates Aβ aggregation and prevention of degradation by proteases [26]. Besides that, pEAβ is more neurotoxic than other Aβ species (for a review, see [27]).

The relevance of pEAβ for AD pathophysiology has also been demonstrated in transgenic mouse models. Firstly described by Alexandru et al. in 2011 [28], the TBA2.1 mouse model was generated to secrete pEAβ3-42 in the brain, which intracellularly forms small Aβ aggregates along with a strong neurodegeneration and severe motor deficits in homozygous mice. However, unlike most of the other amyloidosis mouse lines, the TBA2.1 mice do not develop neuritic plaques but only smaller Aβ particles deposited in the brain [29].

Development of an AD-like amyloidosis phenotype, including neuritic plaques and neuroinflammation, could be shown in a variety of transgenic mouse lines. Additionally, behavioral deficits, in particular cognitive impairment in learning and memory, were

described to be present in most lines (for a review, see [30]). However, neurodegeneration, which is a typical feature of human AD, was only observed in a few transgenic amyloidosis models, including the TBA2.1 line [31]. In an attempt to generate an improved mouse model harboring a combination of AD-relevant hallmarks, i.e., the aggressive phenotype produced by pEAβ, an abundant formation of neuritic plaques and extensive cognitive decline, the novel TAPS mouse line was generated. This line was created by cross-breeding of heterozygous APP/PS1 and TBA2.1 mice and the phenotype of the resulting triple transgenic mice was followed over a period of 20 months in comparison to the parental lines. As a result, we demonstrate that by addition of pEAβ the amyloid pathology is further accelerated, with earlier onset and increased deposition of neuritic plaques in the brain. Furthermore, the TAPS mice displayed a faster and more pronounced cognitive decline in comparison to the parental lines. Due to its stronger phenotype the novel TAPS line has qualified itself as a useful new tool to study AD pathophysiology, and for preclinical studies testing new therapeutic options.

2. Results

2.1. TAPS Mice Accumulate Aβ Aggregates in the Striatum, Hippocampus, and Cortex as Early as 6 Months

TAPS mice were viable and fertile but showed a 14% increased rate of premature death in comparison to wild-type (WT) littermates. For comparison, APP/PS1 mice showed a 3% increased rate of premature death (Table S1). Both, TAPS and APP/PS1 mice, developed an increasing amyloid pathology with neuritic plaques in the brain over time. With an earlier onset, at the age of 6 months, TAPS mice showed plaque formation starting in the cortex, hippocampus, and also lateral striatum. Over time, all mentioned regions underwent a constant increase in plaque density, with the highest amounts in the cortex and slightly less Aβ plaques in the hippocampus. In APP/PS1 mice, visibly less plaque formation could be found at the same age in the cortex and emerged to the hippocampus with 9 months but with nearly no Aβ accumulation in the striatum. Overall, plaque formation in early ages was visibly lower than in the corresponding TAPS mice, and increasing in the cortex and hippocampus to a comparable level in later life. The cerebellum showed only little Aβ accumulation over time and accumulation in the thalamus could be observed in both genotypes. In contrast to the previously mentioned mouse lines, the TBA2.1 mice developed decent amounts of Aβ aggregates in the striatum, already at the age of 6 months and kept those levels until older ages. However, there was nearly no Aβ accumulation visible in brain regions other than the striatum.

To investigate the composition of the Aβ plaques in all mouse lines, a double staining was accomplished with antibodies against truncated pyroglutamate Aβ at position 3 (pE3Aβ) and total Aβ (antibody 6E10) in 24-month-old mice. TAPS and APP/PS1 mice showed an intense staining of plaques in the cerebral cortex for both, Aβ and pE3Aβ, as shown in Figure 1, and comparable results were found also in the hippocampus. It could be seen that compact neuritic plaques, as well as diffuse Aβ, were positively stained with 6E10 in both cases. Albeit the 6E10 signal was stronger, in diffuse Aβ, a minor portion of pE3Aβ could be observed as well, indicating a possibly lower content of those truncated Aβ species than full-length Aβ in diffuse accumulations. In compact plaques, however, pE3Aβ was more prominent in the center core of the plaques than in the surrounding. In principle, the overall plaque morphology and distribution of pE3Aβ in the cortex and hippocampus was comparable between TAPS and APP/PS1 mice. TBA2.1 mice, however, showed no visible Aβ accumulation in the cortex, as well as in the hippocampus, and were not distinguishable from WT mice in those regions. Differences, however, could be seen in the striatum (caudate putamen) of the mouse lines, which are shown in Figure 2.

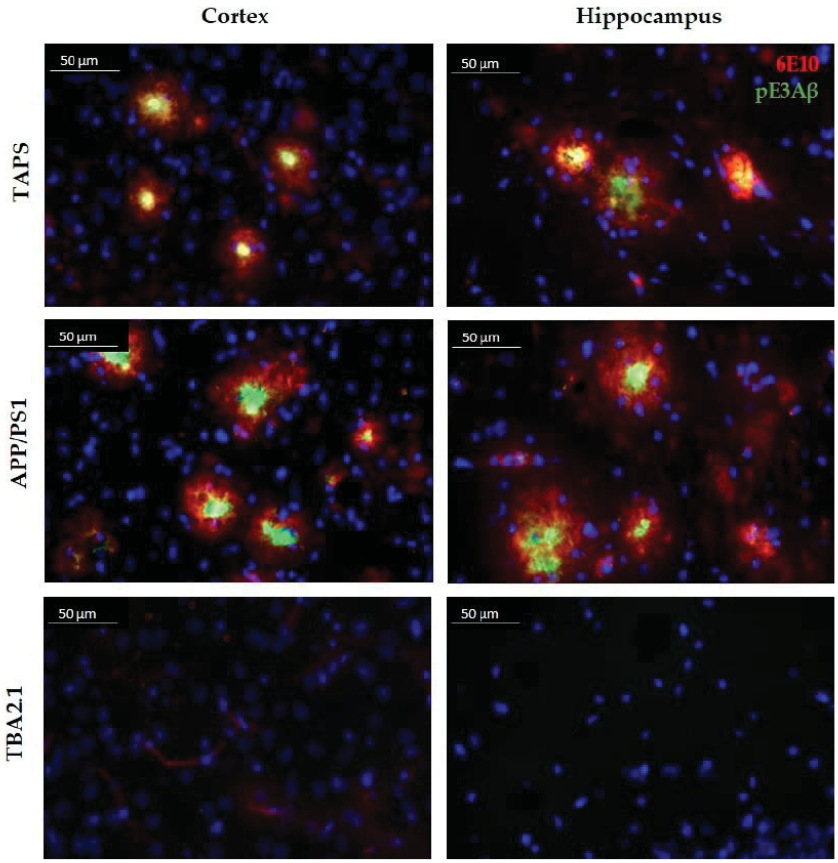

Figure 1. Comparison of the plaque morphology in TAPS, APP/PS1, and TBA2.1 mice. Sagittal slices stained with 6E10 (red) for whole amyloid-β (Aβ), and pE3 antibody (green) for truncated pyroglutamate Aβ (pE3Aβ) species at 400× magnification. Intense labeling of pE3Aβ in the center core of Aβ plaques was visible in the cortex of TAPS and APP/PS1, as well as in the hippocampus (CA3 region). No Aβ accumulation was visible in the cortex and hippocampus of heterozygous TBA2.1 mice. Cell nuclei labeled by DAPI (blue). Images of representative animals are shown; for total animal numbers, see Table 1.

TAPS mice showed a recognizable accumulation of Aβ in the lateral striatum (Figure 2). The signal was almost solely congruent between total Aβ (antibody 6E10) and pE3Aβ (antibody pE3). The TBA2.1 mice accumulated aggregates in the striatum that were positive for pE3Aβ and 6E10, although Aβ aggregates were much smaller compared to TAPS. Delineation of those aggregates in TBA2.1 was also sharper than in TAPS, possibly indicating an intracellular accumulation in this line. APP/PS1 mice, however, showed nearly no accumulation of Aβ species in the corresponding striatal region, compared to TAPS littermates. In summary, TAPS and TBA2.1 mice showed Aβ accumulation in the lateral striatum, in contrast to APP/PS1 mice.

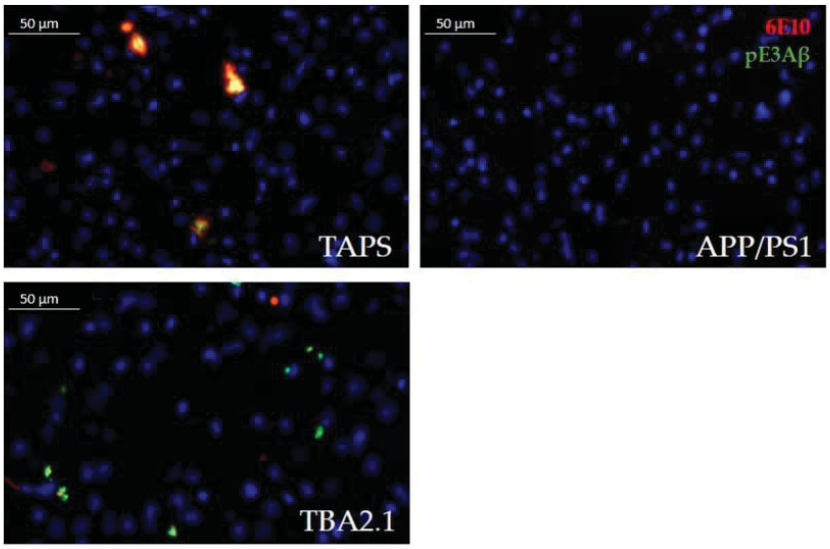

Figure 2. Comparison of Aβ accumulation in the lateral striatum at 400× magnification. TAPS mice accumulated Aβ aggregates in the lateral striatum, positive for total Aβ (red, 6E10) and pE3Aβ (green, pE3). In TBA2.1 mice, Aβ deposits were smaller but also positive for total Aβ and intensively stained for pE3Aβ. APP/PS1 mice in contrast were lacking any Aβ accumulation in this area, showing only cell nuclei, positive for DAPI (blue). Images of representative animals are shown; for total animal numbers, see Table 1.

Looking closer at the cellular response of the brain, a staining against glial fibrillary acidic protein (GFAP) was accomplished. Reactive astrogliosis could be demonstrated in investigated brains between 6 and 18 months. Exemplarily showing the results, comparing 18-month-old brains in Figure 3, the intense staining of Aβ with 6E10 (red) can be shown for the cerebral cortices of TAPS and APP/PS1 mice, as previously mentioned. Acute astrogliosis surrounded the direct vicinity to amyloid plaques, as visible in the cortex images (Figure 3), but Aβ presence also seems to promote general activation of astrocytes throughout the whole brain in TAPS and APP/PS1 mice. Although there was nearly no Aβ in the striatum of the latter, a certain reactive astrogliosis could be observed in this area as well. Overall, this indicates a strong increase in neuroinflammatory processes in both mouse lines and a general activation of astrocytes throughout the brain, also in areas without plaque pathology, e.g., the striatum. TBA2.1 mice also showed a certain degree of astrogliosis for the regions of the lateral striatum, since there were also Aβ aggregates visible. Though, the astrocytes in the rest of the brain were not distinguishable from the WT. Even in WT mice, some GFAP-positive astrocytes could be found, mostly in white matter. The molecular layer of the cerebellum was roughly free from reactive astrocytes in all investigated brains, in concordance with poor Aβ accumulation in this area.

Since neuron loss in the CA1 region of the hippocampus was described for homozygous TBA2.1 mice [28], we analyzed this brain region also in the TAPS line. Quantification of neuronal nuclei in the hippocampus of 24-month-old TAPS and WT mice showed no significant differences in neuronal density in the stratum pyramidale of the CA1. Cell counts were on comparable levels; therefore, no detectable signs of neurodegeneration could be observed in the designated area for TAPS compared to WT mice (Figure S1).

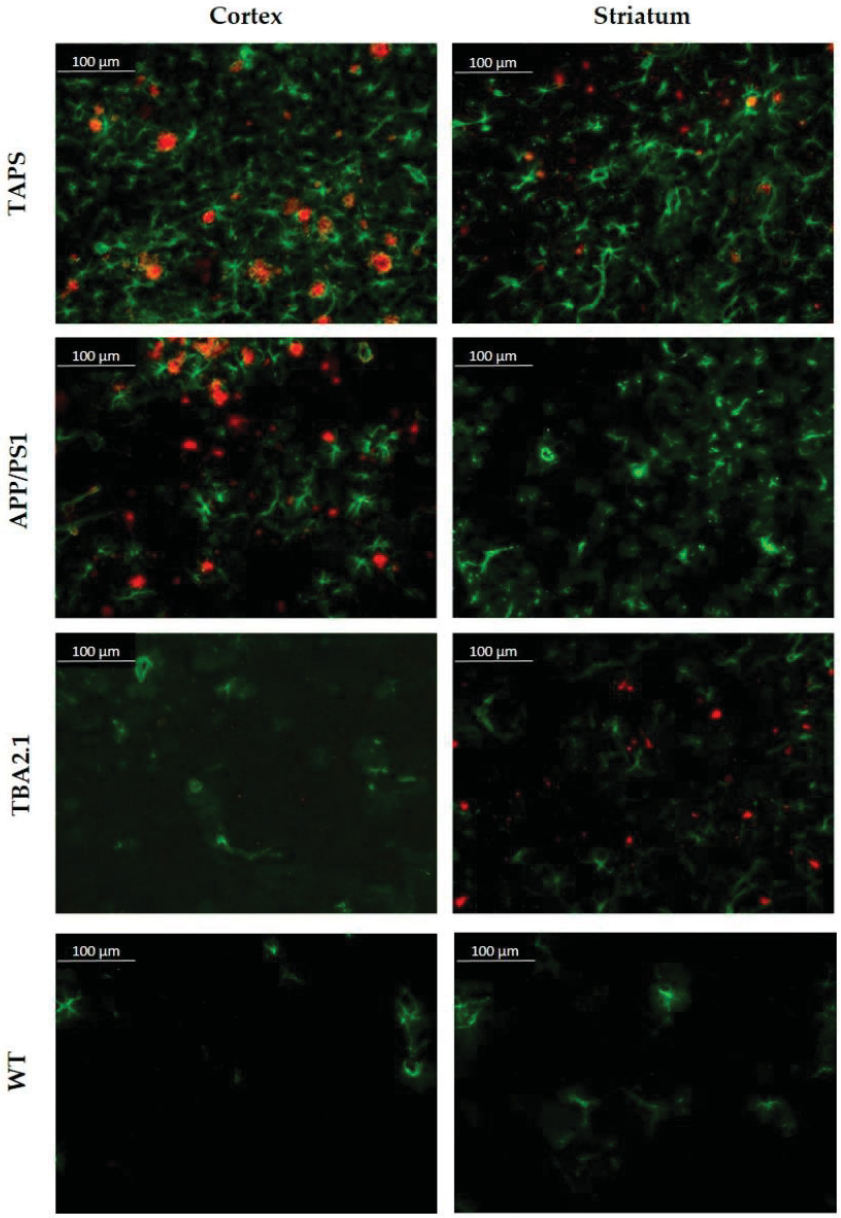

Figure 3. Amyloid-β plaque pattern and reactive astrogliosis in TAPS, APP/PS1, TBA2.1, and wild-type (WT) mice at 200x magnification. Immunofluorescence analysis of Aβ (red, 6E10) and reactive astrocytes (green, GFAP). Both, TAPS and APP/PS1 mice showed abundant plaque load throughout the whole cerebral cortex, accompanied by strong reactive astrogliosis. TBA2.1 mice seemed to lack such aggregation of Aβ in this area. Reactive astrogliosis in the cortex was on comparable low levels, as observed in WT mice. In the striatum, only TAPS and TBA2.1 mice showed higher amounts of Aβ aggregates, which could not be observed in APP/PS1 mice. Images of representative animals are shown; for total animal numbers, see Table 1.

To investigate differences in Aβ load between the mouse lines in more detail, a quantification with ImageJ was accomplished. The number of neuritic plaques and the average size were quantified in the areas of the cortex, striatum, and hippocampus, for TAPS and APP/PS1 (Figure 4). TAPS mice displayed in general a higher number of plaques than APP/PS1 mice, which was significant in all brain regions analyzed (two-way ANOVA; cortex, genotype $p = 0.007$, age $p < 0.001$; hippocampus, genotype $p < 0.001$, age $p < 0.001$; striatum, genotype $p < 0.001$, age $p < 0.001$, genotype x age $p < 0.001$). At the age of 7 months, TAPS mice already had a significantly higher level of Aβ in the cortex, compared to their APP/PS1 counterparts (multiple *t*-test; $p = 0.03$). They built approximately five times more deposits at the same age in the cortex and showed a detectable amount of neuritic plaques in the striatum, as well. At the age of 15 months, both, TAPS and APP/PS1 mice, showed a comparably high plaque load in the cortex but with a higher increase in TAPS after 18 months. The increase in plaque formation of APP/PS1 slowed remarkably down after 15 months in the cortex and hippocampus, trending towards a plateau at this time.

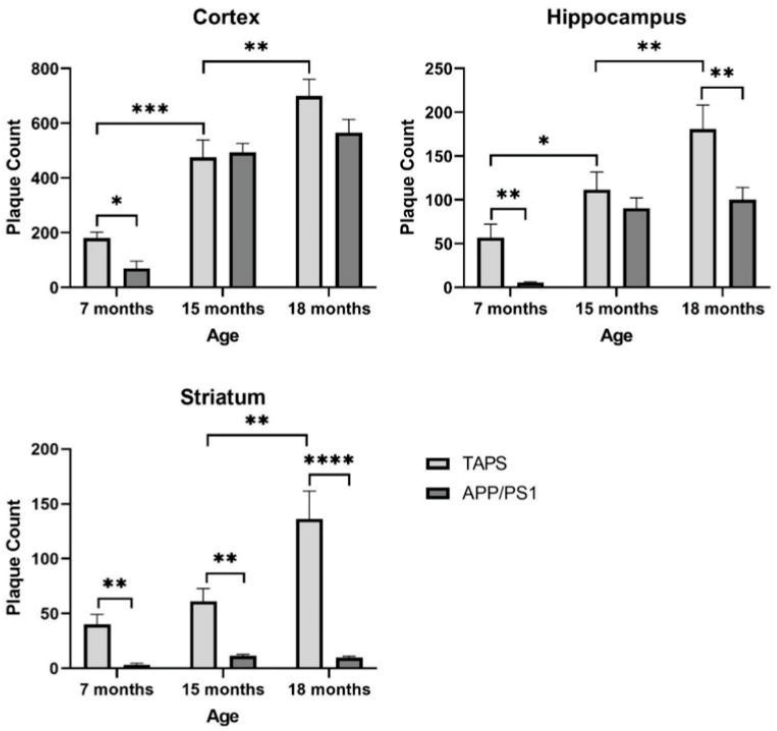

Figure 4. Plaque quantification in the brain of TAPS and APP/PS1 mice. The number of plaques was quantified on brain sections after immunostaining against total Aβ. TAPS mice showed an earlier onset in plaque formation in all investigated areas than APP/PS1 and a stronger progression until the age of 18 months. For statistical analysis, a two-way ANOVA was used to compare the age related, as well as a multiple *t*-test to analyze for genotype-dependent differences. Total number of animals was TAPS ($n = 16$), APP/PS1 ($n = 15$). For exact animal numbers per age, see Table 1. Data are given as mean + SEM; * $p < 0.05$; ** $p < 0.01$; *** $p < 0.001$; **** $p < 0.0001$.

Hippocampal plaque formation could also be observed at a 10 times higher level in 7-month-old TAPS in comparison to APP/PS1 (multiple *t*-test; $p = 0.009$). At the age of 15 months, both, TAPS and APP/PS1 mice, showed a comparably high plaque load in the

hippocampus. With 18 months, TAPS mice, however, displayed a significant increase in hippocampal plaque load (multiple *t*-test; $p = 0.003$), whereas numbers in APP/PS1 mice remained on a relatively constant level.

In the striatum, only TAPS mice developed an amyloid pathology with neuritic Aβ plaques. Differences against APP/PS1 could be demonstrated to be significant at 7 (multiple *t*-test; $p = 0.006$), 15 (multiple *t*-test; $p = 0.009$), and 18 months (multiple *t*-test; $p < 0.000001$). APP/PS1 mice showed only constantly low levels of neuritic plaques in the striatum, even in older individuals.

Analyzing the plaque size at 15 and 18 months of age, it could be shown that TAPS mice tend to have slightly smaller plaques in the cortex (879.3 ± 26.9 μm^2, 15 months; 915.7 ± 52.5 μm^2, 18 months) and hippocampus (994.63 ± 54.0 μm^2, 15 months; 992.8 ± 110.2 μm^2 18 months), compared to the APP/PS1 cortex (922.2 ± 22.6 μm^2, 15 months; 1080.3 ± 21.5 μm^2, 18 months) and hippocampus (1111.1 ± 53.1 μm^2, 15 months; 1083.0 ± 50.1 μm^2, 18 months). Both genotypes showed a constant size of plaques in both areas over the analyzed time. The aggregates in the striatum of TAPS mice, however, were significantly smaller in size, with 588.8 ± 34.3 μm^2 for 15 months, and 586.5 ± 52.4 μm^2 for 18 month-old-mice (two-way ANOVA brain region, $p < 0.001$; Holm-Sidak´s post-hoc, cortex vs. striatum $p = 0.001$, hippocampus vs. striatum $p = 0.001$), compared to those in the cortex and hippocampus.

2.2. TAPS Mice Show Phenotypic Alterations in the SHIRPA and Open Field Tests

In the SmithKline Beecham Pharmaceuticals; Harwell, MRC Mouse Genome Centre and Mammalian Genetics Unit; Imperial College School of Medicine at St Mary's; Royal London Hospital, St Bartholomew's and the Royal London School of Medicine; Phenotype Assessment (SHIRPA) test, TAPS mice were initially compared to their WT littermates for development of a behavioral phenotype with increasing age. TAPS mice showed a consistent increase in scores throughout the whole examination time, as it can be seen in Figure 5. At 4 and 6 months of age, changes were relatively small compared to older animals. At 9 months of age, the average scores increased to 1.6 and further to a score of 3.9 with 12 months. The latter was highly significant compared to the values of the WT littermates (mixed effects analysis, genotype $p < 0.0001$, age $p < 0.0001$, interaction $p < 0.0001$; Sidak's post-hoc test 12 m, $p = 0.0001$). Over time, scores raised to 4.9 at 15 months (Sidak's post-hoc test 15 m, $p = 0.0002$) and finally 6.6 at 18 months of age (Sidak's post-hoc test 18 m, $p = 0.0273$), which both proved to be statistically significant compared to WT. Due to the partly cross-sectional type of this study, not all mice from the initial group endured the full investigation period of 18 months. Male and female animals were pooled for analysis. The most common hallmark of the TAPS phenotype in the SHIRPA test was a reduction in sensory perception, mostly prominent in the pinna reflex, startle response, and the flank pressure. A larger number of animals also showed deficits in the hanging behavior.

Summarizing the results of the WT, the scores remained on a relatively low level throughout the whole examination period. The scores varied on average around 0 and 0.4 for all age groups. Single mice showed minor abnormalities, which were transient and did not exceed a score of one. The most common observation was a slight reduction in movement in the cage and a reduction in the time at the hanging behavior, which could be correlated with a high body weight. Analysis of the bodyweight over time demonstrated that overall, there was no genotype-dependent discrepancy observable for both tested genders (Table S2).

A second cohort of TAPS mice was further tested at the age of 18 months together with their littermates in several behavioral tests. In the open field test, which was done once at 18 months, APP/PS1 and TBA2.1 did not differ significantly from the WT mice. However, TAPS mice seemed to be faster (Figure 6A), to travel more (Figure 6B) and to be more active (Figure 6C) than the WT, indicating that they might display hyperactive behavior. They spent the same amount of time in the center and the border of the open field

(Figure 6D), which indicates that none of the mice had reduced exploration or increased anxiety. Taking these results together, TAPS mice might have alterations in the general spontaneous activity in the open field test.

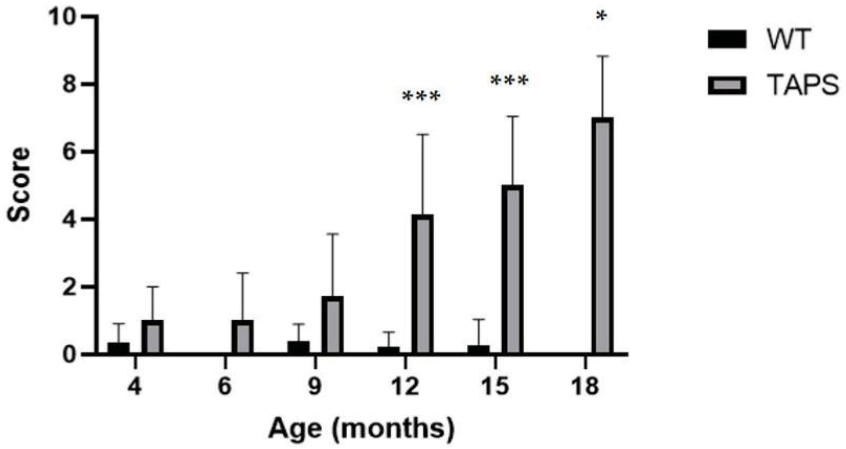

Figure 5. TAPS mice had age-dependent phenotypic alterations in the SHIRPA test. Shown are the mean scores of animals from each age group with SEM for TAPS and wild-type (WT) mice. A significant increase of SHIRPA scores was found for 12- (*** $p = 0.0001$, TAPS $n = 16$, WT $n = 9$), 15- (*** $p = 0.0002$, TAPS $n = 11$, WT $n = 7$), and 18- (* $p = 0.0273$, TAPS $n = 4$, WT $n = 3$)-month-old TAPS compared to their WT littermates. Scores of WT remained widely unchanged over time. For the statistical analysis, mixed effects analysis with Sidak´s post-hoc was used to compare the age and genotype. For all animal numbers per age, see Table 1. Data is given as mean + SEM.

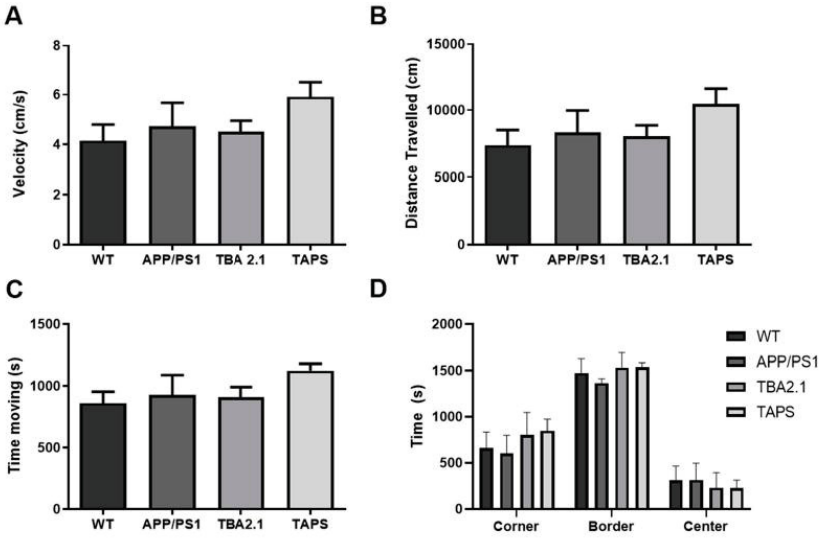

Figure 6. Performance of TAPS mice in the open field test. Wild-type (WT; $n = 8$), APP/PS1 ($n = 5$), and TBA2.1 ($n = 8$) showed similar velocity (**A**), distance traveled (**B**), and activity time (**C**) in the open field test. The TAPS mice ($n = 4$) showed a trend to be faster, traveled more, and were more active compared to the WT. All mice stayed similar time in the border, center, and corner regions of the open field (**D**). Data is given as mean + SEM.

2.3. TAPS Mice Develop Cognitive Deficits in Different Behavioral Tests

Several cognitive behavioral tests were conducted in order to characterize the cognitive abilities of TAPS mice in comparison to their littermates. In the novel object recognition test (NOR), only the WT mice explored significantly more the novel than the familiar object (paired *t*-test, $p = 0.0380$), indicating functional memory for the familiar object. For all other lines, exploration times between the novel and familiar object did not reach statistical significance, although there is some trend for more exploration of the novel object (Figure 7). High variability and low animal numbers, and low overall exploration may be accounted for this in case of the TAPS and APP/PS1 line, respectively. Regarding total exploration time of the objects, TAPS mice showed a tendency towards higher exploration of both objects; however, this did not reach statistical significance.

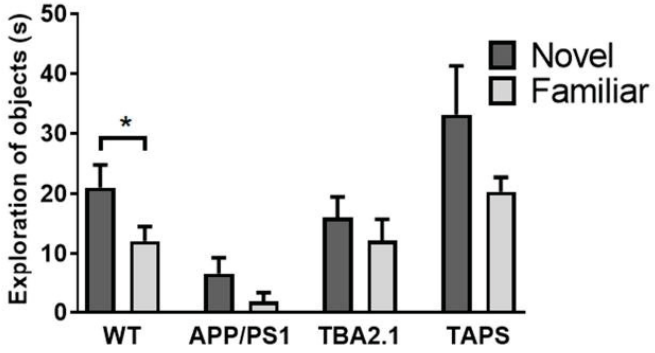

Figure 7. Deficits in the novel object recognition test in TAPS mice. The time animals explored the novel in comparison to a familiar object is given for each mouse line. Only wild-type mice (WT; $n = 8$) were able to discriminate between the novel and the familiar object (* $p = 0.0380$) while APP/PS1 ($n = 5$), TBA2.1 ($n = 8$), and TAPS ($n = 4$) mice showed a cognitive deficit in this task. For statistical analysis, a paired t-test was used to evaluate the difference between the exploration time of the novel and familiar object. Data is given as mean + SEM.

The T-maze spontaneous alternation was measured to assess short-term memory. With 18 months of age, all groups had similar amounts of alternations (Figure S2). However, with 20 months of age, APP/PS1 (one-way ANOVA, $p = 0.0192$; Holm-Sidak's post-hoc test, $p = 0.0349$), TAPS (Holm-Sidak's post-hoc test, $p = 0.0349$) and TBA2.1 (Holm-Sidak's post-hoc test, $p = 0.0145$) mice alternated less than the WT (Figure 8). These results indicated that they were not able to discriminate which arm was visited previously. In comparison, the WT mice were able to discriminate the previous arm, which indicates an intact working memory. Moreover, only WT mice alternated significantly above chance (i.e., >50%) (one sample *t*-test, $p = 0.0001$). Therefore, they were able to choose the new arm instead of entering an arm randomly.

With 18 months of age, the TAPS mice froze less than the WT in the cued fear conditioning paradigm (one-way ANOVA, $p = 0.0015$; Dunnett's post-hoc test, $p = 0.0042$) (Figure 9A). This result indicated that they were not able to associate the sound (cue) with the shock in the habituation phase, implying a deficit in the associative learning process. On the other hand, all groups froze the same amount in the contextual fear conditioning part of the test, meaning they were all able to associate the arena (context) with the shock (Figure 9B). With 20 months of age, the test was repeated with the same cohort of mice. This time the TAPS mice froze less than the WT mice also in the contextual fear conditioning (Figure S3), indicating impairment in the contextual memory at older ages.

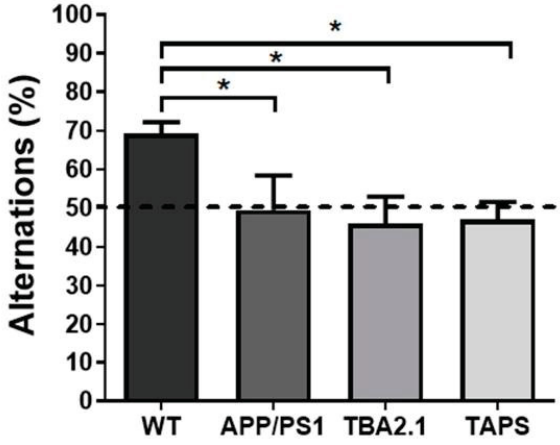

Figure 8. Deficit in spontaneous alternation of TBA2.1, APP/PS1, and TAPS mice in the T-maze. The spontaneous alternation was calculated as the ratio of entries into the correct arm to the amount of total trials in the T maze. With 20 months of age, the APP/PS1 (* $p = 0.0349$; $n = 6$), TAPS (* $p = 0.0349$; $n = 6$), and TBA2.1 (* $p = 0.0145$; $n = 10$) mice alternated significantly less than the wild-type (WT; $n = 10$) mice. Dashed line indicates threshold of chance (50%). For statistical analysis, one-way ANOVA with Holm-Sidak's post-hoc was used to compare the genotypes. Data is given as mean + SEM.

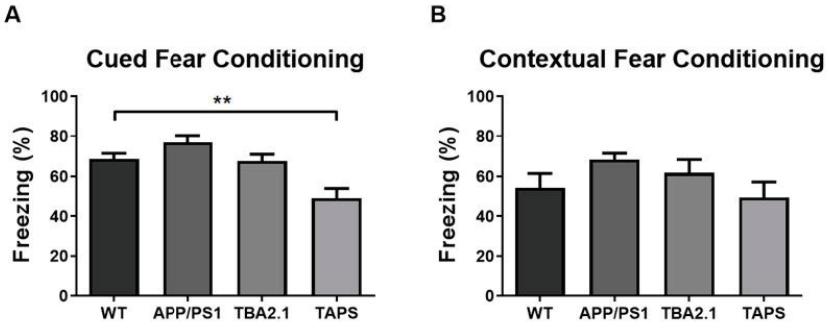

Figure 9. Impaired fear conditioning learning in TAPS mice. The percentage of freezing behavior was measured in the contextual and cued fear conditioning paradigm with 18 months of age. In the cued fear conditioning (**A**), the TAPS mice ($n = 4$) froze less compared to the wild-type (WT; $n = 8$) mice indicating a deficit in fear conditioning learning (** $p = 0.0042$). Both, APP/PS1 ($n = 4$) and TBA2.1 ($n = 8$), showed similar freezing behavior compared to WT mice, indicating intact fear conditioning learning. In the contextual fear conditioning (**B**), all genotypes showed similar freezing behavior. For statistical analysis, one-way ANOVA with Dunnettt´s post-hoc was used to compare the genotypes. Data is given as mean + SEM.

With 20 months of age, the Morris water maze test (MWM) was carried out in order to measure the spatial learning and memory abilities of the mice. During the training session, TAPS mice took longer to find the platform compared to the WT (Figure 10A, mixed effects analysis, genotype $p = 0.0210$, days $p < 0.0001$, interaction $p = 0.5794$; Dunnett´s post-hoc test, $p = 0.0087$). In contrast, APP/PS1 mice were able to find the platform faster along the days of training. Additionally, TBA2.1 mice took longer to find the platform compared to WT only on the fourth day, showing a delay in learning (Dunnett´s post-hoc test, $p = 0.0241$). In conclusion, TAPS mice displayed a learning deficit since they were not able to memorize the platform location in the pool. In the probe trial, both TAPS and APP/PS1 mice had a tendency towards reduced searching time in the target quadrant compared to WT, but this

difference did not reach statistical significance, presumably due to insufficient animal numbers. Interestingly, TBA2.1 mice also had reduced time searching in the target quadrant compared to WT (Figure 10B, one-way ANOVA, $p = 0.0357$; Dunnett's post-hoc test, $p = 0.0319$).

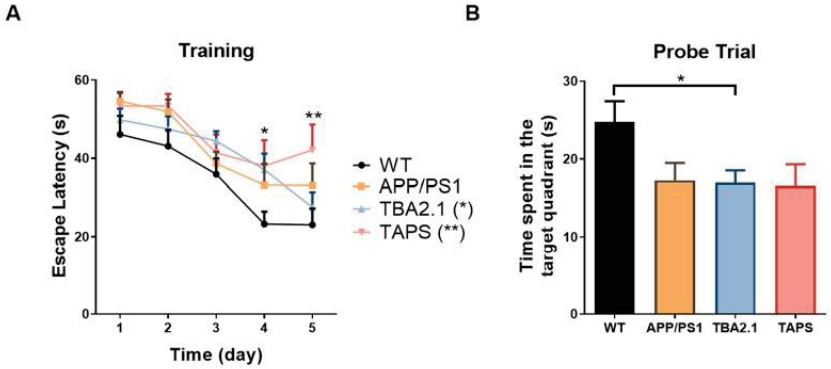

Figure 10. Performance in the Morris water maze with 20 months of age. In the training trials (**A**), the TAPS mice ($n = 6$) took longer to find the hidden platform compared to the wild-type mice (WT; $n = 11$) on the last day (** $p = 0.0087$), as well as TBA2.1 ($n = 12$) on the fourth day (* $p = 0.0241$), indicating a spatial learning deficit. In the probe trial (**B**), the TBA2.1 mice spent significantly less time in the target quadrant compared to WT mice (* $p = 0.0319$), while APP/PS1 ($n = 8$) and TAPS mice showed a non-significant trend towards reduced memory retrieval as they spent less time in the target quadrant than the WT mice. For statistical analysis, two-way and one-way ANOVA with Dunnett´s post-hoc were used to compare the genotypes during the training and in the probe trial, respectively. Data are given as mean + SEM.

3. Discussion

In recent years, a number of drug candidates have been tested in clinical trials to find a new therapeutic option against AD, but almost all failed due to lack of efficacy. Many of the new substances had previously demonstrated efficacy in transgenic mouse models, which is why the mouse models have come under criticism. Although transgenic mouse models have proven to be a valuable tool for studying the pathophysiology of AD, they are incomplete models of the human disease. Most transgenic mouse lines are able to mimic only a few aspects of the disease, i.e., neuritic amyloid plaques, tauopathy, neuroinflammation, cognitive decline, or neurodegeneration [30].

In the current study, we describe the generation of a novel transgenic mouse line as an attempt to generate an improved model harboring a combination of AD-relevant hallmarks, especially the aggressive phenotype produced by pEAβ, an abundant formation of neuritic plaques, and extensive cognitive decline. Thus, the TAPS mice were developed in order to understand the role of pEAβ and its interaction with other Aβ species that are constitute of neuritic plaques. We characterized the progression of cerebral amyloidosis, and the development of general and cognitive behavioral deficits in this novel triple transgenic mouse line.

As expected, TAPS mice developed a more severe phenotype in comparison to its heterozygous parental lines. Like APP/PS1 mice, they developed neuritic plaques throughout the brain, especially in the cortex, thalamus, and hippocampus, and little pathology in the cerebellum. Most striking, and in addition to what can be observed in the APP/PS1 line, TAPS mice also showed Aβ aggregates in the lateral striatum, which appeared larger and more mature than the small Aβ particles present in the striatum of the parental TBA2.1 line. We could confirm data by Alexandru et al. [28] that heterozygous TBA2.1 mice at 21 months had only a low amount of N-terminally truncated and pyroglutamate-modified Aβ in small intracellular aggregates in the striatum, which were, however, not sufficient to induce

motor deficits in this line. The clinical relevance of Aβ aggregates in the striatum are not yet clear, although striatal amyloid plaques have also been found in AD patients. Striatal Aβ depositions have been described mainly in AD patients of advanced stages [31–34] but may also occur in the preclinical stage [35]. A recent study showed that Aβ deposition in the striatum correlates with both, memory deficits and tau pathology [36]. Nearly all amyloid plaques found in TAPS mice stained positive for both total Aβ and pE3Aβ. PE3Aβ was mainly located in the plaque core of compact and neuritic plaques and less in diffuse Aβ deposits. The 6E10 antibody, used in this study to detect total Aβ, has the capability to bind both, full-length Aβ as well as N-terminally truncated species, while the pE3Aβ antibody exclusively binds to truncated pyroglutamate Aβ. Apart from the striatum, neuritic plaques in other brain regions of TAPS mice were also composed of pE3Aβ in addition to other Aβ species. Thus, the TAPS mice had an amyloidosis phenotype combining the distribution patterns from both the APP/PS1 and TBA2.1 mice, but with earlier onset and faster progression. We characterized TAPS mice with a significantly earlier onset of plaque formation in the cortex at the age of 6 to 7 months, whereas APP/PS1 reached comparable Aβ levels later in life. Additionally, deposits in the hippocampus formed at a younger age than in APP/PS1. TAPS showed a constant increase in plaque counts over time, whereas in APP/PS1, progression seemed to slow down towards a plateau after 15 months of age. Taken together, the additional production of the aggregation-prone pE3Aβ species led to both, an accelerated plaque deposition and higher amyloid load at older ages. With regard to plaque size, the TAPS mice developed slightly smaller but more plaques than the APP/PS1 mice at the same age. In a previous study, Frost et al. demonstrated the development of pEAβ-positive plaques in APP/PS1 mice after full-length Aβ deposits formed [24]. This could also be shown in the present study, because, apart from plaque size, old APP/PS1 mice displayed a similar plaque composition than TAPS animals in the cortex and hippocampus. The smaller plaque size of TAPS mice in comparison to the parental APP/PS1 line seemed to be the consequence of early pE3Aβ presence in the brain, possibly facilitating the formation of fibrils and generating smaller plaques through faster aggregation. The specific location of higher pEAβ levels in the center core of compact plaques has also been observed in tissue from human patients and underlines the theory of pEAβ as a seeding spot for other Aβ species or diffuse Aβ in brains [37,38].

Additionally to plaque formation, both APP/PS1 and TAPS mice developed progressive neuroinflammation in the brain, indicated by high numbers of reactive astrocytes around plaques. Neuroinflammation is one of the hallmarks of AD, which contributes to cognitive deficits in human and animals [39]. Reactive astrocytes and microglia exacerbate the Aβ toxicity and neuronal death. Heterozygous TBA2.1 mice, as expected, did not display an overall increase in astrogliosis since they do not develop plaques. Hence, a certain degree of activation could be seen in the striatum, in the vicinity of small Aβ particles. Regarding the neuroinflammatory response, the TAPS mice seemed to develop even higher levels of astrogliosis, compared to APP/PS1 mice. Taken together, the higher activation of astrocytes in the striatum and in other brain regions could have contributed, in conjunction with early production of the highly toxic pE3Aβ species, to more severe cognitive deficits in TAPS mice, compared to the parental lines.

Despite showing a strong reactive astrogliosis and an increased inflammatory milieu in the investigated brain areas, together with a high plaque load, however, neurodegeneration could not be observed in the hippocampus of TAPS mice, compared to WT. The CA1 region of the hippocampus, in particular the stratum pyramidale, showed comparable amounts of neurons throughout the investigated area of TAPS and WT mice. Although neurodegeneration in this brain region was described for homozygous TBA2.1 mice [28], obviously, the heterozygous status of the TBA2.1 transgene was not sufficient to induce neuron loss in TAPS mice. However, this does not exclude the presence of subtle neurodegenerative changes throughout the entire brain, which we might have overlooked.

TAPS mice developed cognitive deficits beginning with 18 months of age mainly in the cued fear conditioning. Later, at 20 months of age, they also displayed a deficit in

T-maze and MWM. Those different behavioral tests evaluated different types of cognitive abilities, which are processed by different areas of the brain. The MWM measures spatial memory [40]. The spatial memory processing occurs primarily in the hippocampus; therefore, lesions in this brain area have been shown to induce cognitive deficits [41,42]. It has been shown before that amyloid pathology in the hippocampus, consisting of plaques and, more importantly, soluble toxic Aβ oligomers, can induce synaptic loss and cognitive deficits [27,43–45], which could also explain the spatial memory deficits in TAPS mice. As seen in histological investigation, TAPS mice showed, in contrast to APP/PS1 mice, a constant increase in hippocampal plaque formation, even at higher ages, possibly facilitating this effect. The spontaneous alternation paradigm in the T-maze is a measure of the spatial working memory, and the NOR is based on working memory and recognition memory, too, which are processed in both the hippocampus and cortex [46–50]. Since Aβ pathology is also abundantly present in the cortex of TAPS mice, deficits in working memory can be explained by toxic Aβ species in the cortex as well. Finally, the cued fear conditioning paradigm is based on fear memory with involvement of the amygdala [49,50], a brain region that was also affected by Aβ pathology in TAPS mice. Deficits in fear memory, particularly in the cued fear conditioning, have also been observed in AD patients [51,52] and other transgenic AD models before [53,54].

Even though TBA2.1 mice do not develop Aβ plaques, they showed clear deficits in both the T-maze and MWM. Cognitive deficits have not been reported for heterozygous mice of this line before, and support the importance of pEAβ for neurotoxicity in the absence of amyloid plaques. A neurotoxic pEAβ-dependent process seemed to be responsible for the working and spatial memory deficits in those mice. Moreover, the APP/PS1 mice developed abundant Aβ plaques in the same brain areas as TAPS mice, without deficits in MWM and fear conditioning tests, unlike TAPS mice at the same age. Therefore, the earlier aggregation of Aβ, most probably induced by pEAβ, and pEAβ´s known neurotoxic potential [55,56], could have accelerated the cognitive decline in TAPS mice.

Besides their cognitive deficits, TAPS mice also developed sensory and motor impairments. In the SHIRPA test, TAPS mice showed phenotypic alterations beginning at 12 months of age compared to both WT and younger TAPS mice. As shown before, TBA2.1 mice developed similar alterations starting at 21 months of age [29]. Therefore, it can be concluded that the combination of pEAβ and full-length Aβ in the brain might be responsible for acceleration of the phenotype in comparison to pEAβ alone. In addition, we observed a trend towards higher velocity, longer distance travelled, and generally more activity in the open field, indicating a hyperactive phenotype of TAPS mice compared to WT and TBA21 mice. One might speculate whether these motoric alterations could be due to the development of Aβ pathology and neuroinflammation in the striatum. The striatum, as a key interface for excitatory and inhibitory neurons, plays a major role in action selection and motor function [57]. Moreover, in other AD mouse models, the observed hyperactivity was correlated with basal ganglia circuitry dysfunction [58–60]; therefore, one might assume that striatal Aβ deposits induce changes in the basal ganglia network. So far, the relevance of a hyperactive phenotype in AD mouse models is not quite clear. Although hyperactivity is also part of the behavioral and psychological symptoms of dementia in patients, its causes are still under discussion and have not been sufficiently investigated yet (for a review, see [61]). Additionally, TAPS mice showed a reduced sensory response in the SHIRPA test. Balsters et al. demonstrated the connectivity of the lateral striatum (caudate putamen) to cortical areas in the motor-cortex (m1) and somatosensory cortex (s1 and s2) in mice [62]. A disturbance in signal transduction in this area could promote the deficits TAPS mice showed in contrast to their parental lines at the same age. It leads to the assumption that the combination of deposits in the striatum with those in the cortex, thalamus, and hippocampus and the elevated response of astroglia in this area could lead to the hyperactivity pattern and sensory deficits seen in these mice. Some studies also demonstrated a hyperactive behavior of APP/PS1 mice in the open field at younger ages (4 to 8 months) [63,64], which was explained by a decrease of endocannabinoids in the

striatum [64]. A similar process can be assumed for TAPS mice, but more studies are needed to prove this connection.

Unlike previous reports, the APP/PS1 mice used in the current study did not develop cognitive deficits in the MWM even at an age of 21 months. One reason for that discrepancy might be the variety of used protocols and differences in the housing conditions [65,66]. However, a non-significant trend towards a deficit could be observed in MWM. This could be due to the relatively small groups of mice included in some of the behavioral tests, whose variability prevented a slight deficit from becoming statistically significant. Concerning heterozygous TBA2.1 mice, little is known about their cognitive abilities, so far. We have described before, that, in contrast to the homozygous animals, the heterozygous TBA2.1 mice did not develop any motor deficits, but a higher score in the SHIRPA test at 21 months of age [29]. Corroborating with this previous study, the TBA2.1 parental line did not show any conspicuities, including activity, exploratory, or anxiety-related behavior, in the open field test at 18 months.

Finally, the new TAPS line is an amyloidosis model that reflects several aspects of the human disease. However, the aspect of tauopathy, which is an important feature of human AD, is missing. Since none of the previously described amyloidosis models show excessive tau phosphorylation and also no neurofibrillary tangles [67], development of tauopathy in TAPS mice was not to be expected. In general, the behavioral deficits of all three mouse lines, and especially the APP/PS1 and TAPS mice, appeared with an advanced age of 18 to 20 months, which might limit their practical use for future studies. On the other hand, mouse models with very aggressive phenotype progression and early behavioral deficits before clear pathological alterations have been criticized because their relevance to the clinical disease has been questioned [67]. In this respect, the new TAPS line joins the ranks of the rather late AD models in which the cognitive deficits clearly develop as a consequence of pathological processes.

In conclusion, we were able to demonstrate an accelerated amyloid pathology in TAPS mice with earlier onset and increased Aβ deposition induced by pE3Aβ. In addition, the TAPS mice developed faster and more pronounced cognitive deficits than the parental lines as measured by several cognitive behavioral tests. Both parental mouse lines, TBA2.1 and APP/PS1, have been successfully used for preclinical therapeutic studies in which new substances were tested during their development as drug candidates against AD [68,69]. The novel TAPS mouse line combines their advantages by increasing the neurotoxic pE3Aβ species and inducing robust cognitive deficits, and thus, qualifies itself as a useful new amyloidosis model for future preclinical studies testing new therapeutic options.

4. Materials and Methods

4.1. Animals

TBA2.1 mice were a generous gift from Probiodrug AG (Halle, Germany) and were bred in house by mating of heterozygous mice. The mice were originally described on a C57BL/6 × DBA1 background and were further crossed to a C57BL/6 background for more than four generations. As described by Alexandru et al. [28], the transgene of the TBA2.1 line was designed for chromosomal integration by addition of cDNA sequences of a pre-pro-peptide of murine thyrotropin releasing hormone (TRH) fused with the modified human Aβ polypeptide Aβ(Q3–42) under a neuron-specific promotor. Aβ(Q3–42) is expressed in neuronal cells and subjected to the secretory pathway, where it is post-translationally modified by the endogenous glutaminyl cyclase into pEAβ3-42. Homozygous TBA2.1 mice develop a motor-neurodegenerative phenotype as a consequence of pEAβ3-42-induced neurotoxicity starting with 2 months and progressing further until the age of 5 months, when the humane endpoint is reached. In addition, an age-related massive neurodegeneration can be observed, especially in the hippocampus, and deposition of small Aβ aggregates in brain regions, such as the hippocampus and striatum, accompanied by neuroinflammation. Heterozygous TBA2.1 mice display a milder phenotype starting with 21 months of age [29].

APPswe/PS1ΔE9 mice were introduced by Jankowsky et al. [8] and express both a chimeric mouse and human Amyloid Precursor Protein (APP695swe) and human presenilin 1 mutated by a deletion of exon 9 (PS1ΔE9) [11] under the control of neuron-specific promotor elements. The mice develop neuritic Aβ plaques and neuroinflammation beginning with 6 months, and cognitive deficits, which are detectable in the Morris water maze test [17]. APPswe/PS1ΔE9 mice on a C57Bl/6 background were received from the Jackson Laboratory (Bar Harbor, MA, USA) and bred in-house by mating of heterozygous and wild-type mice of this line.

T(TBA2.1)APS(APPswe/PS1ΔE9) mice were generated by crossing heterozygous TBA2.1 and heterozygous APPswe/PS1ΔE9 (APP/PS1) mice in the C57BL/6 background. The resulting TAPS mice were heterozygous for both TBA2.1 and APP/PS1 transgenes. For behavioral tests and histological examinations, male and female littermates of these matings were used with the following genotypes: wild-type (WT), APP/PS1, TBA2.1, and TAPS (Table 1). All mice were heterozygous for the respective transgene.

All mice were bred in-house with a 12/12 h light/dark cycle, constant temperature of 22 °C, and 54% humidity. Food and water were available ad libitum. All behavioral experiments were performed in accordance with the German Law on the protection of animals (TierSchG §§ 7–9) and were approved by the local ethics committee before the start of the experiments (Landesamt für Natur, Umwelt und Verbraucherschutz, North Rhine-Westphalia, Germany, numbers 84-02.04.2011.A359, 84-02.04.2014.A362, 81-02.04.2018.A400, 81-02.04.2019.A304 were approved on 09 December 2014, 05 February 2019, 21 February 2019 and 21 January 2019, respectively).

Based on the late behavioral alterations the parental lines displayed in our hands in the past, the cognitive test battery was started at 18 months of age. The first cohort of TAPS and WT littermates was tested in the SHIRPA test battery for initial check of behavioral abnormalities. Then, two more cohorts of 18-month-old littermates were tested repeatedly (at 18 and 20 months of age) in the following behavioral tests to test their cognitive abilities: cohort 2, T-maze (18 and 20 months), MWM (20 months); cohort 3, open field (18 months), novel object recognition (NOR, 18 months), T-maze (18 and 20 months), cued and contextual fear conditioning (18 months), contextual fear conditioning (20 months), and MWM (20 months). Three TAPS, two APP/PS1 mice, one TBA2.1, and one WT mouse died during the longitudinal testing between the age of 18 and 20 months. Three APP/PS1, two TBA2.1, and two WT mice had to be excluded from the T-maze due to inactivity.

Table 1. Number of mice used for each analysis according to genotype and age. MWM, Morris water maze; NOR, novel object recognition test; WT, wild-type.

Analysis	Age	Number of Mice/Genotype			
		WT	TAPS	APP/PS1	TBA 2.1
Histology	6.4 ± 0.3	-	6	5	3
	9.2 ± 0.4	-	1	3	3
	15.1 ± 0.4	-	5	3	-
	18.0 ± 0.4	-	4	4	1
	24.8 ± 1.3	5	6	5	5
SHIRPA	4.1 ± 0.2	3	3	-	-
	5.5 ± 0.4	4	8	-	-
	8.6 ± 0.4	8	18	-	-
	12.5 ± 0.3	9	16	-	-
	14.9 ± 0.2	7	11	-	-
	17.6 ± 0.6	3	4	-	-
Open Field	18.8 ± 0.7	8	4	5	8
NOR	18.8 ± 0.7	8	4	5	8

Table 1. *Cont.*

Analysis		Age	Number of Mice/Genotype			
			WT	TAPS	APP/PS1	TBA 2.1
T-maze		18.4 ± 0.7	13	9	7	13
		20.7 ± 0.7	10	6	6	10
Fear Conditioning	Cued	18.8 ± 0.7	8	4	4	8
	Contextual	18.8 ± 0.7	8	4	4	8
		20.8 ± 0.7	7	2	3	6
MWM		20.7 ± 0.7	11	6	8	12

4.2. Histology

For histological studies, mice from all genotypes were used at different ages from 6 to 24 months (Table 1). Mice were killed by cervical dislocation, and brains were taken and frozen at −80 °C until further processing. Right brain hemispheres were used to generate 20 µm sagittal sections with a cryostat (LEICA Biosystems, Wetzlar, Germany). Immunofluorescence staining was performed in order to evaluate the Aβ-plaque/particle distribution and size with mouse monoclonal antibody anti-Aβ, Clone 6E10 recognizing the N-terminal Aβ strain (1:200; BioLegend, San Diego, CA, USA), as well as neuroinflammation (activated astrocytes) with polyclonal rabbit anti GFAP antibody (1:1000; Dako Omnis, Agilent, Santa Clara, CA, USA). Plaque morphology and composition was analyzed with brains from 24-month-old mice using a double-staining against pE3Aβ with the rabbit anti-Abeta-pE3 antibody (1:500; Synaptic Systems GmbH, Goettingen, Germany) in combination with the 6E10 antibody against whole Aβ.

Briefly, frozen sagittal sections of the brains were fixed in 4% buffered formaldehyde solution. Afterwards, the slides were incubated in 70% formic acid as antigen retrieval and blocked with M.O.M (Mouse on Mouse) blocking reagent (Vector Laboratories Inc., Burlingame, CA, USA) to prevent unspecific binding of the primary antibody. The slides were then incubated overnight with the primary antibody solution in 1% TBS buffer and containing 1% BSA at 4 °C in a humid chamber. The next day, slices were washed in buffer and incubated with the secondary antibodies, diluted in the same solution as the primary ones for 2.5 h at RT: Goat anti-Mouse IgG (H+L) Alexa 568 and Goat anti-Rabbit IgG (H+L) Alexa 488 (1:300; Thermo Fisher Scientific, Waltham, MA, USA). For assessment of the cell nuclei, a DAPI staining (5 µg/mL, Sigma Aldrich, Steinheim, Germany) was performed after washing the slides consecutively to the secondary antibody incubation. Subsequently, slices were mounted with Aqua Poly Mount (Polysciences, Inc., Warrington, Pennsylvania, USA), coverslips and stored at 4 °C until further analysis at the microscopes.

For slice evaluation, overview images were made with a Zeiss Lumar V12 SteREO (Carl Zeiss AG, Oberkochen, Germany) at the corresponding fluorescent channels for the antibodies. In total, 16 animals were used for TAPS (7 months $n = 7$; 15 months $n = 5$; 18 months $n = 4$) and 15 animals for APP/PS1 quantification (7 months $n = 8$; 15 months $n = 3$; 18 months $n = 4$). Nine images per animal were obtained for each channel at a 10× magnification. Those images were used for quantification of plaques with the image analyzer ImageJ v1.48.

For analysis of the plaque pattern and the reactive astrogliosis on a smaller scale, images were obtained by the Leica LMD 6000 Fluorescent Microscope (Leica Microsystems GmbH, Wetzlar, Germany) at a magnification between 100× and 400×. Overlay images were created via the company's software Leica Application Suite v4.5 (LAS). Images obtained with the LMD were used for qualitative measures and for possible discrimination of differences between the investigated genotypes.

For analysis of neuron loss, a subset of six slides per animal was analyzed from 24-month-old TAPS ($n = 5$) and WT mice ($n = 5$). After fixation in 4% buffered formalin, slides were stained for 5 min in 5 µg/mL DAPI solution (4′,6-Diamidin-2-phenylindol, Sigma Aldrich, Steinheim, Germany). Microscope images of the hippocampus were taken

at 50× magnification with the Leica LMD 6000 Fluorescent Microscope. The CA1 region of the hippocampus was evaluated for the number of positive nuclei via Cell Profiler Software (version 2.0.10415, Broad Institute, Cambridge, USA).

4.3. Behavioral Tests

4.3.1. SHIRPA

The SHIRPA test battery was adapted from [70]. This test evaluates the general phenotypic alterations in transgenic mice, especially on their sensoric and locomotoric capacities and has been demonstrated to be very sensitive towards the detection of deficits in different transgenic mouse lines, including the TBA2.1 model [29,71]. The number of mice used in this test are given in Table 1. The test was divided into two parts: (1) Observation in an empty cage and (2) handling. In each part, several criteria were scored compared to WT littermates from 0 (no difference) to 3 (strong difference). For the analysis, each criteria score was summed to a final score per animal. The examined tasks in the SHIRPA consisted of the examination in the cage for abnormalities in posture, gait, alertness, frightening, pain reaction, and the Straub-tail test. For the examination on the hand, the animals were tested for reaction towards handling (gentle pressure on the flank of the animal), pinna reflex, forelimb placing reflex, and the hanging behavior on a thin pole. Additionally, the body weight of the animals was recorded.

4.3.2. Open Field Test

The open field test is used to evaluate the general spontaneous behavior in rodents as well as anxiety. In a cubicle arena (40 cm × 40 cm × 40 cm), mice (for exact numbers, see Table 1) were allowed to explore the arena freely for 30 min. The arena was imaginarily divided into 12 squares to determine the border, center, and corner zones. Mice were observed with a camera driven tracking system (EthoVision XT 15.0.1416, Noldus Information Technology, Wageningen, The Netherlands). The following parameters were evaluated: active time, velocity, distance travelled, time spent in the center, in the border, and in the corner.

4.3.3. Novel Object Recognition Test

In the same arena where the open field was performed, one day later, the mice (Table 1) explored two similar objects (familiar) for 10 min. After 20 min of memory retention interval, mice were placed again in the arena. One familiar object was replaced by a new one (novel) and they were allowed to explore for another 10 min. Exploration time for an object was considered when mouse placed the nose at least within 2 cm distance into the direction of the object. Mice were observed with a camera driven tracking system (EthoVision XT 15.0.1416, Noldus Information Technology, Wageningen, The Netherlands). For the analysis purpose, the time mice spent exploring each object was taken.

4.3.4. T-maze Spontaneous Alternation

The protocol was adapted from Spowart-Manning and Van der Staay [72]. The maze consisted of three arms (31 cm × 10 cm each): the left and right arm can be closed by a gate and the start arm (perpendicular to the left and right) has no gate. In the first trial, mice were forced to enter one goal arm by closing the door of the other arm. Once the mice returned to the start arm, both arms could be freely accessed. After the mice entered one arm, the other one was closed by a door, and it was counted as one trial. This was repeated for a maximum of 14 trials or 15 min. If a mouse did not reach seven trials, it was excluded from the analysis. For analysis, the spontaneous alternation was calculated by the number of correct alternating choices divided by the total amount of trials. For the number of mice included in this test, please refer to Table 1.

4.3.5. Contextual and Cued Fear Conditioning

The protocol for the fear conditioning was adapted from Curzon et al. [73]. First, the mice were placed in the chamber (17 × 17 × 25 cm; Ugo Basile, Gemonio VA, Italy) for 120 s of habituation. Then, a combination of conditioned stimuli [5] and unconditioned stimuli (US) were presented for three times with a 60 s interval. A 3 s CS tone (50%; 2000 Hz) followed, and a US foot shock was given during the last 2 s of the CS (0.35 mA). Before the mice were returned to the cage, they stayed in the arena for an additional 60 s. Then, 24 h later, the mice were placed in the same testing chambers used on day one for 5 min (contextual). After 25 min, the mice were placed in a new environment that could be explored freely for 180 s. Then, the CS tone was played three times for 30 s at 60 s intervals, similar to the habituation phase (cued). All mice (Table 1) were observed with a camera-driven tracking system (EthoVision XT 15.0.1416, Noldus Information Technology, Wageningen, The Netherlands). The following parameters were analyzed in each session: the percentage of freezing behavior as detected by the software.

4.3.6. Morris Water Maze

The protocol for the MWM was modified after Morris [74]. In brief, mice were placed in a circular pool (diameter of 120 cm × 60 cm height) with a hidden platform (diameter of 10 cm × 31. 5 cm height) in a fixed position. In the training, four trials per mouse per day (5 days in total) were performed. The maximum time of each trial was 1 min and the mice started in each trial in a different position. One day after the last training day, the probe trial was performed, where the platform was removed, and mice had to swim for 1 min. All mice (Table 1) were observed with a camera-driven tracking system (EthoVision XT 15.0.1416, Noldus Information Technology, Wageningen, The Netherlands). The time and distance needed for finding the platform in each training section and the time they explored the target quadrant in the probe trial were analyzed.

4.4. Statistics

For the statistical analysis of behavioral tests, GraphPad Prism v8 (GraphPad Software, San Diego, CA, USA) was used. The normality of the data was checked by visualization of the Normal QQ plot. The SHIRPA test was analyzed by mixed effect analysis with Tukey's and Sidak's post-hoc test, to compare age and genotype, respectively. The different parameters of the open field test were analyzed by one-way ANOVA and Dunnett's post-hoc test. The NOR was analyzed with the paired t-test, where the exploration time of the novel object was compared to the exploration time of the familiar object for each mouse. The analysis of the T-maze was calculated via one-way ANOVA and Holm-Sidak's post-hoc test, to be compared to WT mice. One sample t-test was accomplished against the theoretical mean of 50%. For both the cued and the contextual fear conditioning test, a one-way ANOVA and Dunnett's post-hoc test was the chosen statistical analysis. In the MWM training analysis, mixed effect analysis and Dunnett's post-hoc were used. To evaluate the MWM probe trial, the one-way ANOVA and Dunnett's post-hoc test were used. The analysis of plaque quantification was performed with SigmaPlot v12.5 (Systat Software Inc., San Jose, CA, USA) with a two-way ANOVA to calculate for significant differences between genotype and age, and with GraphPad Prism v8 applying multiple *t*-tests for testing within one age group.

Supplementary Materials: The following are available online at https://www.mdpi.com/article/10.3390/ijms22137062/s1, Table S1: Premature death of mice from TAPS and parental lines; Table S2: Means of body weights by gender, genotype and age; Figure S1: Neuronal quantification in the CA1 region of the hippocampus of TAPS and wild-type (WT) mice; Figure S2: Similar performance of all genotypes in the T-maze at 18 months; Figure S3: Impaired fear conditioning learning in TAPS mice.

Author Contributions: Conceptualization, S.S. and A.W.; data curation, L.C.C. and M.S.; formal analysis, L.C.C., M.S. and A.W.; funding acquisition, N.J.S., K.-J.L. and D.W.; investigation, L.C.C.,

M.S., N.S. and D.H.; Supervision, N.J.S., K.-J.L., J.K., S.S. and A.W.; visualization, L.C.C. and M.S.; writing—original draft, L.C.C. and M.S.; writing—review and editing, N.J.S., K.-J.L., D.W., J.K., S.S. and A.W. The planning and organization of the study was done by L.C.C., M.S. and A.W. The behavioral study was planned by L.C.C., S.S. and A.W. Behavioral experiments were done by L.C.C., M.S. and D.H. Histological analysis were done by M.S and N.S. Data were analyzed by L.C.C., M.S. and A.W. All authors have read and agreed to the published version of the manuscript.

Funding: D.W. was supported by grants from the Russian Science Foundation (RSF) (project no. 20-64-46027) and by the Technology Transfer Fund of the Forschungszentrum Jülich. K.-J.L. and D.W. were supported by "Portfolio Drug Research" of the "Impuls und Vernetzungs-Fonds der Helmholtzgemeinschaft".

Institutional Review Board Statement: The study was conducted according to the German Law on the protection of animals (TierSchG §§ 7–9) and was approved by the local ethics committee before start of the experiments (Landesamt für Natur, Umwelt und Verbraucherschutz, North Rhine-Westphalia, Germany, numbers 84-02.04.2011.A359, 84-02.04.2014.A362, 81-02.04.2018.A400, 81-02.04.2019.A304 were approved on 09 December 2014, 05 February 2019, 21 February 2019 and 21 January 2019, respectively).

Data Availability Statement: All data from the study is available in this Manuscript.

Acknowledgments: We thank Probiodrug for providing TBA2.1 animals and the Forschungszentrum Jülich animal facility for their excellent care.

Conflicts of Interest: The authors declare no conflict of interest.

References

1. Prince, M.J. *World Alzheimer Report 2015: The Global Impact of Dementia: An Analysis of Prevalence, Incidence, Cost and Trends*; Alzheimer's Disease International: London, UK, 2015.
2. Wu, Y.-T.; Beiser, A.S.; Breteler, M.M.B.; Fratiglioni, L.; Helmer, C.; Hendrie, H.C.; Honda, H.; Ikram, M.A.; Langa, K.M.; Lobo, A.; et al. The changing prevalence and incidence of dementia over time—Current evidence. *Nat. Rev. Neurol.* **2017**, *13*, 327–339. [CrossRef] [PubMed]
3. Nichols, E.; Szoeke, C.E.I.; Vollset, S.E.; Abbasi, N.; Abd-Allah, F.; Abdela, J.; Aichour, M.T.E.; Akinyemi, R.O.; Alahdab, F.; Asgedom, S.W.; et al. Global, regional, and national burden of Alzheimer's disease and other dementias, 1990–2016: A systematic analysis for the Global Burden of Disease Study 2016. *Lancet Neurol.* **2019**, *18*, 88–106. [CrossRef]
4. Gale, S.A.; Acar, D.; Daffner, K.R. Dementia. *Am. J. Med.* **2018**, *131*, 1161–1169. [CrossRef] [PubMed]
5. Sütterlin, S.; Hoßmann, I.; Klingholz, R. *Demenz-Report: Wie sich die Regionen in Deutschland, Österreich und der Schweiz auf die Alterung der Gesellschaft vorbereiten können*; DEU: Berlin, Germany, 2011.
6. Lannfelt, L.; Bogdanovic, N.; Appelgren, H.; Axelman, K.; Lilius, L.; Hansson, G.; Schenk, D.; Hardy, J.; Winblad, B. Amyloid precursor protein mutation causes Alzheimer's disease in a Swedish family. *Neurosci. Lett.* **1994**, *168*, 254–256. [CrossRef]
7. Heppner, F.L.; Ransohoff, R.M.; Becher, B. Immune attack: The role of inflammation in Alzheimer disease. *Nat. Rev. Neurosci.* **2015**, *16*, 358–372. [CrossRef] [PubMed]
8. Jankowsky, J.L.; Fadale, D.J.; Anderson, J.; Xu, G.M.; Gonzales, V.; Jenkins, N.A.; Copeland, N.G.; Lee, M.K.; Younkin, L.H.; Wagner, S.L.; et al. Mutant presenilins specifically elevate the levels of the 42 residue beta-amyloid peptide in vivo: Evidence for augmentation of a 42-specific gamma secretase. *Hum. Mol. Genet.* **2004**, *13*, 159–170. [CrossRef] [PubMed]
9. Mullan, M.; Crawford, F.; Axelman, K.; Houlden, H.; Lilius, L.; Winblad, B.; Lannfelt, L. A pathogenic mutation for probable Alzheimer's disease in the APP gene at the N–terminus of β–amyloid. *Nat. Genet.* **1992**, *1*, 345–347. [CrossRef] [PubMed]
10. Scheuner, D.; Eckman, C.; Jensen, M.; Song, X.; Citron, M.; Suzuki, N.; Bird, T.D.; Hardy, J.; Hutton, M.; Kukull, W.; et al. Secreted amyloid beta-protein similar to that in the senile plaques of Alzheimer's disease is increased in vivo by the presenilin 1 and 2 and APP mutations linked to familial Alzheimer's disease. *Nat. Med.* **1996**, *2*, 864–870. [CrossRef] [PubMed]
11. Borchelt, D.R.; Thinakaran, G.; Eckman, C.B.; Lee, M.K.; Davenport, F.; Ratovitsky, T.; Prada, C.-M.; Kim, G.; Seekins, S.; Yager, D.; et al. Familial Alzheimer's Disease–Linked Presenilin 1 Variants Elevate Aβ1–42/1–40 Ratio In Vitro and In Vivo. *Neuron* **1996**, *17*, 1005–1013. [CrossRef]
12. Jackson, H.M.; Soto, I.; Graham, L.C.; Carter, G.W.; Howell, G.R. Clustering of transcriptional profiles identifies changes to insulin signaling as an early event in a mouse model of Alzheimer's disease. *BMC Genom.* **2013**, *14*, 831. [CrossRef]
13. Malm, T.M.; Iivonen, H.; Goldsteins, G.; Keksa-Goldsteine, V.; Ahtoniemi, T.; Kanninen, K.; Salminen, A.; Auriola, S.; Van Groen, T.; Tanila, H.; et al. Pyrrolidine dithiocarbamate activates Akt and improves spatial learning in APP/PS1 mice without affecting beta-amyloid burden. *J. Neurosci.* **2007**, *27*, 3712–3721. [CrossRef]
14. Onos, K.D.; Uyar, A.; Keezer, K.J.; Jackson, H.M.; Preuss, C.; Acklin, C.J.; O'Rourke, R.; Buchanan, R.; Cossette, T.L.; Sukoff Rizzo, S.J.; et al. Enhancing face validity of mouse models of Alzheimer's disease with natural genetic variation. *PLoS Genet.* **2019**, *15*, e1008155. [CrossRef]

15. Janus, C.; Flores, A.Y.; Xu, G.; Borchelt, D.R. Behavioral abnormalities in APPSwe/PS1dE9 mouse model of AD-like pathology: Comparative analysis across multiple behavioral domains. *Neurobiol. Aging* **2015**, *36*, 2519–2532. [CrossRef] [PubMed]
16. Huang, H.; Nie, S.; Cao, M.; Marshall, C.; Gao, J.; Xiao, N.; Hu, G.; Xiao, M. Characterization of AD-like phenotype in aged APPSwe/PS1dE9 mice. *Age* **2016**, *38*, 303–322. [CrossRef] [PubMed]
17. Minkeviciene, R.; Ihalainen, J.; Malm, T.; Matilainen, O.; Keksa-Goldsteine, V.; Goldsteins, G.; Iivonen, H.; Leguit, N.; Glennon, J.; Koistinaho, J.; et al. Age-related decrease in stimulated glutamate release and vesicular glutamate transporters in APP/PS1 transgenic and wild-type mice. *J. Neurochem.* **2008**, *105*, 584–594. [CrossRef]
18. Stenzel, J.; Rühlmann, C.; Lindner, T.; Polei, S.; Teipel, S.; Kurth, J.; Rominger, A.; Krause, B.J.; Vollmar, B.; Kuhla, A. [(18)F]-florbetaben PET/CT Imaging in the Alzheimer's Disease Mouse Model APPswe/PS1dE9. *Curr. Alzheimer Res.* **2019**, *16*, 49–55. [CrossRef]
19. Snellman, A.; López-Picón, F.R.; Rokka, J.; Salmona, M.; Forloni, G.; Scheinin, M.; Solin, O.; Rinne, J.O.; Haaparanta-Solin, M. Longitudinal Amyloid Imaging in Mouse Brain with ^{11}C-PIB: Comparison of APP23, Tg2576, and APP$_{swe}$-PS1$_{dE9}$ Mouse Models of Alzheimer Disease. *J. Nucl. Med.* **2013**, *54*, 1434–1441. [CrossRef] [PubMed]
20. Maeda, J.; Ji, B.; Irie, T.; Tomiyama, T.; Maruyama, M.; Okauchi, T.; Staufenbiel, M.; Iwata, N.; Ono, M.; Saido, T.C.; et al. Longitudinal, Quantitative Assessment of Amyloid, Neuroinflammation, and Anti-Amyloid Treatment in a Living Mouse Model of Alzheimer's Disease Enabled by Positron Emission Tomography. *J. Neurosci.* **2007**, *27*, 10957–10968. [CrossRef]
21. Mori, H.; Takio, K.; Ogawara, M.; Selkoe, D.J. Mass spectrometry of purified amyloid beta protein in Alzheimer's disease. *J. Biol. Chem.* **1992**, *267*, 17082–17086. [CrossRef]
22. Harigaya, Y.; Saido, T.C.; Eckman, C.B.; Prada, C.-M.; Shoji, M.; Younkin, S.G. Amyloid β Protein Starting Pyroglutamate at Position 3 Is a Major Component of the Amyloid Deposits in the Alzheimer's Disease Brain. *Biochem. Biophys. Res. Commun.* **2000**, *276*, 422–427. [CrossRef] [PubMed]
23. Güntert, A.; Döbeli, H.; Bohrmann, B. High sensitivity analysis of amyloid-beta peptide composition in amyloid deposits from human and PS2APP mouse brain. *Neuroscience* **2006**, *143*, 461–475. [CrossRef] [PubMed]
24. Frost, J.L.; Le, K.X.; Cynis, H.; Ekpo, E.; Kleinschmidt, M.; Palmour, R.M.; Ervin, F.R.; Snigdha, S.; Cotman, C.W.; Saido, T.C.; et al. Pyroglutamate-3 Amyloid-β Deposition in the Brains of Humans, Non-Human Primates, Canines, and Alzheimer Disease–Like Transgenic Mouse Models. *Am. J. Pathol.* **2013**, *183*, 369–381. [CrossRef] [PubMed]
25. Cynis, H.; Scheel, E.; Saido, T.C.; Schilling, S.; Demuth, H.-U. Amyloidogenic Processing of Amyloid Precursor Protein: Evidence of a Pivotal Role of Glutaminyl Cyclase in Generation of Pyroglutamate-Modified Amyloid-β. *Biochemistry* **2008**, *47*, 7405–7413. [CrossRef] [PubMed]
26. He, W.; Barrow, C.J. The Aβ 3-Pyroglutamyl and 11-Pyroglutamyl Peptides Found in Senile Plaque Have Greater β-Sheet Forming and Aggregation Propensities in Vitro than Full-Length Aβ. *Biochemistry* **1999**, *38*, 10871–10877. [CrossRef] [PubMed]
27. Gunn, A.P.; Masters, C.L.; Cherny, R.A. Pyroglutamate-Aβ: Role in the natural history of Alzheimer's disease. *Int. J. Biochem. Cell Biol.* **2010**, *42*, 1915–1918. [CrossRef]
28. Alexandru, A.; Jagla, W.; Graubner, S.; Becker, A.; Bäuscher, C.; Kohlmann, S.; Sedlmeier, R.; Raber, K.A.; Cynis, H.; Rönicke, R.; et al. Selective hippocampal neurodegeneration in transgenic mice expressing small amounts of truncated Aβ is induced by pyroglutamate-Aβ formation. *J. Neurosci.* **2011**, *31*, 12790–12801. [CrossRef] [PubMed]
29. Dunkelmann, T.; Schemmert, S.; Honold, D.; Teichmann, K.; Butzküven, E.; Demuth, H.-U.; Shah, N.J.; Langen, K.-J.; Kutzsche, J.; Willbold, D.; et al. Comprehensive Characterization of the Pyroglutamate Amyloid-β Induced Motor Neurodegenerative Phenotype of TBA2.1 Mice. *J. Alzheimer's Dis.* **2018**, *63*, 115–130. [CrossRef] [PubMed]
30. Ameen-Ali, K.E.; Wharton, S.B.; Simpson, J.E.; Heath, P.R.; Sharp, P.; Berwick, J. Review: Neuropathology and behavioural features of transgenic murine models of Alzheimer's disease. *Neuropathol. Appl. Neurobiol.* **2017**, *43*, 553–570. [CrossRef] [PubMed]
31. Suenaga, T.; Hirano, A.; Llena, J.F.; Yen, S.H.; Dickson, D.W. Modified Bielschowsky stain and immunohistochemical studies on striatal plaques in Alzheimer's disease. *Acta Neuropathol.* **1990**, *80*, 280–632. [CrossRef]
32. Braak, H.; Braak, E. Alzheimer's Disease: Striatal Amyloid Deposits and Neurofibrillary Changes. *J. Neuropathol. Exp. Neurol.* **1990**, *49*, 215–224. [CrossRef]
33. Gearing, M.; Levey, A.I.; Mirra, S.S. Diffuse Plaques in the Striatum in Alzheimer Disease (AD): Relationship to the Striatal Mosaic and Selected Neuropeptide Markers. *J. Neuropathol. Exp. Neurol.* **1997**, *56*, 1363–1370. [CrossRef]
34. Brilliant, M.J.; Elble, R.J.; Ghobrial, M.; Struble, R.G. The distribution of amyloid β protein deposition in the corpus striatum of patients with Alzheimer's disease. *Neuropathol. Appl. Neurobiol.* **1997**, *23*, 322–325. [CrossRef]
35. Ryan, N.S.; Keihaninejad, S.; Shakespeare, T.J.; Lehmann, M.; Crutch, S.; Malone, I.B.; Thornton, J.; Mancini, L.; Hyare, H.; Yousry, T.; et al. Magnetic resonance imaging evidence for presymptomatic change in thalamus and caudate in familial Alzheimer's disease. *Brain* **2013**, *136*, 1399–1414. [CrossRef]
36. Hanseeuw, B.J.; Lopera, F.; Sperling, R.A.; Norton, D.J.; Guzman-Velez, E.; Baena, A.; Pardilla-Delgado, E.; Schultz, A.P.; Gatchel, J.; Jin, D.; et al. Striatal amyloid is associated with tauopathy and memory decline in familial Alzheimer's disease. *Alzheimer's Res. Ther.* **2019**, *11*, 17. [CrossRef]
37. Sofola-Adesakin, O.; Khericha, M.; Snoeren, I.; Tsuda, L.; Partridge, L. pGluAβ increases accumulation of Aβ in vivo and exacerbates its toxicity. *Acta Neuropathol. Commun.* **2016**, *4*, 109. [CrossRef] [PubMed]
38. Dammers, C.; Schwarten, M.; Buell, A.K.; Willbold, D. Pyroglutamate-modified Aβ(3–42) affects aggregation kinetics of Aβ(1–42) by accelerating primary and secondary pathways. *Chem. Sci.* **2017**, *8*, 4996–5004. [CrossRef]

39. Heneka, M.T.; Carson, M.J.; El Khoury, J.; Landreth, G.E.; Brosseron, F.; Feinstein, D.L.; Jacobs, A.H.; Wyss-Coray, T.; Vitorica, J.; Ransohoff, R.M.; et al. Neuroinflammation in Alzheimer's disease. *Lancet. Neurol.* **2015**, *14*, 388–405. [CrossRef]
40. Tanila, H. Wading pools, fading memories—Place navigation in transgenic mouse models of Alzheimer's disease. *Front. Aging Neurosci.* **2012**, *4*, 11. [CrossRef]
41. Arendash, G.W.; Gordon, M.N.; Diamond, D.M.; Austin, L.A.; Hatcher, J.M.; Jantzen, P.; DiCarlo, G.; Wilcock, D.; Morgan, D. Behavioral Assessment of Alzheimer's Transgenic Mice Following Long-Term Aβ Vaccination: Task Specificity and Correlations between Aβ Deposition and Spatial Memory. *DNA Cell Biol.* **2001**, *20*, 737–744. [CrossRef] [PubMed]
42. Zhu, H.; Yan, H.; Tang, N.; Li, X.; Pang, P.; Li, H.; Chen, W.; Guo, Y.; Shu, S.; Cai, Y.; et al. Impairments of spatial memory in an Alzheimer's disease model via degeneration of hippocampal cholinergic synapses. *Nat. Commun.* **2017**, *8*, 1676. [CrossRef] [PubMed]
43. Chen, G.; Chen, K.S.; Knox, J.; Inglis, J.; Bernard, A.; Martin, S.J.; Justice, A.; McConlogue, L.; Games, D.; Freedman, S.B.; et al. A learning deficit related to age and beta-amyloid plaques in a mouse model of Alzheimer's disease. *Nature* **2000**, *408*, 975–979. [CrossRef] [PubMed]
44. Dineley, K.T.; Kayed, R.; Neugebauer, V.; Fu, Y.; Zhang, W.; Reese, L.C.; Taglialatela, G. Amyloid-beta oligomers impair fear conditioned memory in a calcineurin-dependent fashion in mice. *J. Neurosci. Res.* **2010**, *88*, 2923–2932. [PubMed]
45. Kittelberger, K.A.; Piazza, F.; Tesco, G.; Reijmers, L.G. Natural Amyloid-Beta Oligomers Acutely Impair the Formation of a Contextual Fear Memory in Mice. *PLoS ONE* **2012**, *7*, e29940. [CrossRef] [PubMed]
46. Brown, M.W.; Aggleton, J.P. Recognition memory: What are the roles of the perirhinal cortex and hippocampus? *Nat. Rev. Neurosci.* **2001**, *2*, 51–61. [CrossRef] [PubMed]
47. Deacon, R.M.; Rawlins, J.N. T-maze alternation in the rodent. *Nat. Protoc.* **2006**, *1*, 7–12. [CrossRef] [PubMed]
48. Locchi, F.; Dall'Olio, R.; Gandolfi, O.; Rimondini, R. Water T-maze, an improved method to assess spatial working memory in rats: Pharmacological validation. *Neurosci. Lett.* **2007**, *422*, 213–216. [CrossRef] [PubMed]
49. Izquierdo, I.; Furini, C.R.; Myskiw, J.C. Fear Memory. *Physiol. Rev.* **2016**, *96*, 695–750. [CrossRef]
50. España, J.; Giménez-Llort, L.; Valero, J.; Miñano, A.; Rábano, A.; Rodriguez-Alvarez, J.; LaFerla, F.M.; Saura, C.A. Intraneuronal β-Amyloid Accumulation in the Amygdala Enhances Fear and Anxiety in Alzheimer's Disease Transgenic Mice. *Biol. Psychiatry* **2010**, *67*, 513–521. [CrossRef]
51. Hamann, S.; Monarch, E.S.; Goldstein, F.C. Impaired fear conditioning in Alzheimer's disease. *Neuropsychologia* **2002**, *40*, 1187–1195. [CrossRef]
52. Nasrouei, S.; Rattel, J.A.; Liedlgruber, M.; Marksteiner, J.; Wilhelm, F.H. Fear acquisition and extinction deficits in amnestic mild cognitive impairment and early Alzheimer's disease. *Neurobiol. Aging* **2020**, *87*, 26–34. [CrossRef]
53. Barnes, P.; Good, M. Impaired Pavlovian cued fear conditioning in Tg2576 mice expressing a human mutant amyloid precursor protein gene. *Behav. Brain Res.* **2005**, *157*, 107–117. [CrossRef]
54. Knafo, S.; Venero, C.; Merino-Serrais, P.; Fernaud-Espinosa, I.; Gonzalez-Soriano, J.; Ferrer, I.; Santpere, G.; DeFelipe, J. Morphological alterations to neurons of the amygdala and impaired fear conditioning in a transgenic mouse model of Alzheimer's disease. *J. Pathol.* **2009**, *219*, 41–51. [CrossRef]
55. Nussbaum, J.M.; Schilling, S.; Cynis, H.; Silva, A.; Swanson, E.; Wangsanut, T.; Tayler, K.; Wiltgen, B.; Hatami, A.; Rönicke, R.; et al. Prion-like behaviour and tau-dependent cytotoxicity of pyroglutamylated amyloid-β. *Nature* **2012**, *485*, 651–655. [CrossRef] [PubMed]
56. Wittnam, J.L.; Portelius, E.; Zetterberg, H.; Gustavsson, M.K.; Schilling, S.; Koch, B.; Demuth, H.-U.; Blennow, K.; Wirths, O.; Bayer, T.A. Pyroglutamate amyloid β (Aβ) aggravates behavioral deficits in transgenic amyloid mouse model for Alzheimer disease. *J. Biol. Chem.* **2012**, *287*, 8154–8162. [CrossRef]
57. Nagai, J.; Rajbhandari, A.K.; Gangwani, M.R.; Hachisuka, A.; Coppola, G.; Masmanidis, S.C.; Fanselow, M.S.; Khakh, B.S. Hyperactivity with Disrupted Attention by Activation of an Astrocyte Synaptogenic Cue. *Cell* **2019**, *177*, 1280–1292.e20. [CrossRef] [PubMed]
58. Miyakawa, T.; Yamada, M.; Duttaroy, A.; Wess, J. Hyperactivity and Intact Hippocampus-Dependent Learning in Mice Lacking the M1Muscarinic Acetylcholine Receptor. *J. Neurosci.* **2001**, *21*, 5239–5250. [CrossRef]
59. Unger, E.L.; Eve, D.J.; Perez, X.A.; Reichenbach, D.K.; Xu, Y.; Lee, M.K.; Andrews, A.M. Locomotor hyperactivity and alterations in dopamine neurotransmission are associated with overexpression of A53T mutant human α-synuclein in mice. *Neurobiol. Dis.* **2006**, *21*, 431–443. [CrossRef] [PubMed]
60. Castelli, M.; Federici, M.; Rossi, S.; De Chiara, V.; Napolitano, F.; Studer, V.; Motta, C.; Sacchetti, L.; Romano, R.; Musella, A.; et al. Loss of striatal cannabinoid CB1 receptor function in attention-deficit/hyperactivity disorder mice with point-mutation of the dopamine transporter. *Eur. J. Neurosci.* **2011**, *34*, 1369–1377. [CrossRef]
61. Keszycki, R.M.; Fisher, D.W.; Dong, H. The Hyperactivity–Impulsivity–Irritiability–Disinhibition–Aggression–Agitation Domain in Alzheimer's Disease: Current Management and Future Directions. *Front. Pharmacol.* **2019**, *10*, 1109. [CrossRef] [PubMed]
62. Balsters, J.H.; Zerbi, V.; Sallet, J.; Wenderoth, N.; Mars, R.B. Primate homologs of mouse cortico-striatal circuits. *bioRxiv* **2019**, *9*, 834481.
63. Bonardi, C.; de Pulford, F.; Jennings, D.; Pardon, M.-C. A detailed analysis of the early context extinction deficits seen in APPswe/PS1dE9 female mice and their relevance to preclinical Alzheimer's disease. *Behav. Brain Res.* **2011**, *222*, 89–97. [CrossRef] [PubMed]

64. Maroof, N.; Ravipati, S.; Pardon, M.C.; Barrett, D.A.; Kendall, D.A. Reductions in endocannabinoid levels and enhanced coupling of cannabinoid receptors in the striatum are accompanied by cognitive impairments in the AβPPswe/PS1ΔE9 mouse model of Alzheimer's disease. *J. Alzheimer's Dis.* **2014**, *42*, 227–245. [CrossRef]
65. Egan, K.; Vesterinen, H.; Beglopoulos, V.; Sena, E.; Macleod, M. From a mouse: Systematic analysis reveals limitations of experiments testing interventions in Alzheimer's disease mouse models. *Evid. Based Preclin. Med.* **2016**, *3*, 12–23. [CrossRef] [PubMed]
66. Veening-Griffioen, D.H.; Ferreira, G.S.; van Meer, P.J.K.; Boon, W.P.C.; Gispen-de Wied, C.C.; Moors, E.H.M.; Schellekens, H. Are some animal models more equal than others? A case study on the translational value of animal models of efficacy for Alzheimer's disease. *Eur. J. Pharmacol.* **2019**, *859*, 172524. [CrossRef] [PubMed]
67. Jankowsky, J.L.; Zheng, H. Practical considerations for choosing a mouse model of Alzheimer's disease. *Mol. Neurodegener.* **2017**, *12*, 1–22. [CrossRef]
68. Schemmert, S.; Schartmann, E.; Honold, D.; Zafiu, C.; Ziehm, T.; Langen, K.J.; Shah, N.J.; Kutzsche, J.; Willuweit, A.; Willbold, D. Deceleration of the neurodegenerative phenotype in pyroglutamate-Aβ accumulating transgenic mice by oral treatment with the Aβ oligomer eliminating compound RD2. *Neurobiol. Dis.* **2019**, *124*, 36–45. [CrossRef]
69. Schemmert, S.; Schartmann, E.; Zafiu, C.; Kass, B.; Hartwig, S.; Lehr, S.; Bannach, O.; Langen, K.-J.; Shah, N.J.; Kutzsche, J.; et al. Aβ Oligomer Elimination Restores Cognition in Transgenic Alzheimer's Mice with Full-blown Pathology. *Mol. Neurobiol.* **2019**, *56*, 2211–2223. [CrossRef] [PubMed]
70. Rogers, D.C.; Fisher, E.M.; Brown, S.D.; Peters, J.; Hunter, A.J.; Martin, J.E. Behavioral and functional analysis of mouse phenotype: SHIRPA, a proposed protocol for comprehensive phenotype assessment. *Mamm. Genome Off. J. Int. Mamm. Genome Soc.* **1997**, *8*, 711–713. [CrossRef]
71. Dunkelmann, T.; Teichmann, K.; Ziehm, T.; Schemmert, S.; Frenzel, D.; Tusche, M.; Dammers, C.; Jürgens, D.; Langen, K.J.; Demuth, H.U.; et al. Aβ oligomer eliminating compounds interfere successfully with pEAβ(3–42) induced motor neurodegenerative phenotype in transgenic mice. *Neuropeptides* **2018**, *67*, 27–35. [CrossRef]
72. Spowart-Manning, L.; Van der Staay, F. The T-maze continuous alternation task for assessing the effects of putative cognition enhancers in the mouse. *Behav. Brain Res.* **2004**, *151*, 37–46. [CrossRef]
73. Curzon, P.; Rustay, N.R.; Browman, K.E. Frontiers in Neuroscience Cued and Contextual Fear Conditioning for Rodents. In *Methods of Behavior Analysis in Neuroscience*; Buccafusco, J.J., Ed.; Taylor & Francis Group, LLC.: Boca Raton, FL, USA, 2009.
74. Morris, R. Developments of a water-maze procedure for studying spatial learning in the rat. *J. Neurosci. Methods* **1984**, *11*, 47–60. [CrossRef]

3.2. In Vitro and In Vivo Efficacies of the Linear and the Cyclic Version of an All-D-Enantiomeric Peptide Developed for the Treatment of Alzheimer's Disease

Authors: Sarah Schemmert, Luana Cristina Camargo, Dominik Honold, Ian Gering, Janine Kutzsche, Antje Willuweit, Dieter Willbold

Journal: International Journal of Molecular Science (2021), published on June 18th, 2021

DOI: 10.3390/ijms22126553

Impact Factor: 5.923 (2020)

Contribution: Performance of the *in vivo* treatment (animal handling)

Performance after the treatment of behavioral tests (open field, nesting, marble burying test and Morris water maze).

International Journal of
Molecular Sciences

MDPI

Article

In Vitro and In Vivo Efficacies of the Linear and the Cyclic Version of an All-D-Enantiomeric Peptide Developed for the Treatment of Alzheimer's Disease

Sarah Schemmert [1], Luana Cristina Camargo [1,2], Dominik Honold [1], Ian Gering [1], Janine Kutzsche [1], Antje Willuweit [3] and Dieter Willbold [1,2,*]

[1] Institute of Biological Information Processing, Structural Biochemistry (IBI-7), Forschungszentrum Jülich, 52425 Jülich, Germany; s.schemmert@fz-juelich.de (S.S.); l.camargo@fz-juelich.de (L.C.C.); d.honold@fz-juelich.de (D.H.); i.gering@fz-juelich.de (I.G.); j.kutzsche@fz-juelich.de (J.K.)
[2] Institut für Physikalische Biologie, Heinrich-Heine-Universität Düsseldorf, 40225 Düsseldorf, Germany
[3] Institute of Neuroscience and Medicine, Medical Imaging Physics (INM-4), Forschungszentrum Jülich, 52425 Jülich, Germany; a.willuweit@fz-juelich.de
* Correspondence: d.willbold@fz-juelich.de; Tel.: +49-246-161-2100

Abstract: Multiple sources of evidence suggest that soluble amyloid β (Aβ)-oligomers are responsible for the development and progression of Alzheimer's disease (AD). In order to specifically eliminate these toxic Aβ-oligomers, our group has developed a variety of all-D-peptides over the past years. One of them, RD2, has been intensively studied and showed such convincing in vitro and in vivo properties that it is currently in clinical trials. In order to further optimize the compounds and to elucidate the characteristics of therapeutic D-peptides, several rational drug design approaches have been performed. Two of these D-peptides are the linear tandem (head-to-tail) D-peptide RD2D3 and its cyclized form cRD2D3. Tandemization and cyclization should result in an increased in vitro potency and increase pharmacokinetic properties, especially crossing the blood–brain-barrier. In comparison, cRD2D3 showed a superior pharmacokinetic profile to RD2D3. This fact suggests that higher efficacy can be achieved in vivo at equally administered concentrations. To prove this hypothesis, we first established the in vitro profile of both D-peptides here. Subsequently, we performed an intraperitoneal treatment study. This study failed to provide evidence that cRD2D3 is superior to RD2D3 in vivo as in some tests cRD2D3 failed to show equal or higher efficacy.

Keywords: Alzheimer's disease; D-peptides; treatment; behavior; Tg-SwDI mice; cognition; disassembly; Aβ; oligomers

Citation: Schemmert, S.; Camargo, L.C.; Honold, D.; Gering, I.; Kutzsche, J.; Willuweit, A.; Willbold, D. In Vitro and In Vivo Efficacies of the Linear and the Cyclic Version of an All-D-Enantiomeric Peptide Developed for the Treatment of Alzheimer's Disease. *Int. J. Mol. Sci.* **2021**, *22*, 6553. https://doi.org/10.3390/ijms22126553

Academic Editor: Sónia C. Correia

Received: 21 May 2021
Accepted: 16 June 2021
Published: 18 June 2021

1. Introduction

Our society is aging and, with it, the number of diseases of old age, especially dementias, are increasing [1]. Alzheimer's disease (AD) is a devastating neurodegenerative disorder and the most common form of dementia worldwide. Its clinical symptoms are considered to be disturbances of memory, language, spatial and temporal orientation and cognitive decline. The pathological hallmarks of the disease are characterized by neurodegeneration, intracellular depositions of neurofibrillary tangles and extracellular accumulations of amyloid-β (Aβ) plaques. Aβ is the product of the proteolytic processing of the amyloid precursor protein (APP), which is cleaved by β- and γ-secretases, resulting in Aβ-monomers. Due to unknown reasons, these monomers aggregate into Aβ-oligomers and insoluble Aβ-fibrils, which compact further into senile Aβ-plaques [2,3]. For a long time, it was assumed that Aβ-plaques were responsible for the disease and the cognitive decline of affected patients. Currently, however, the aforementioned soluble Aβ-oligomers are regarded as more than merely an intermediate on their way from monomers to plaques. Instead, they are postulated to be the most toxic species, responsible for synapse deterioration, neuronal death, disrupted Ca^{2+}-homeostasis and dysfunctional plasticity—all in all

leading to the clinical symptoms of AD [4]. In addition, there is increasing evidence that Aβ-oligomers are able to replicate in a prion-like fashion [5]. In our group, we are focused on the development of compounds for a disease modifying or even curative treatment of AD. For this purpose, we designed all-D-enantiomeric peptides to directly destabilize, disassemble and ultimately eliminate toxic Aβ-oligomers via direct disruption, rather than relying on the immune system for their degradation. By use of mirror image phage display against monomeric Aβ, the lead compound D3, a D-enantiomeric peptide consisting of 12 amino acid residues, arose [6]. D-peptides have several advantages as therapeutics compared to their L-enantiomeric equivalents. As shown by our group and others, the proteolytic stability of D-peptides is superior to L-peptides with the same sequence of amino acid residues, because proteases are most often stereoselective for L-amino acid residues [7]. This results also in a reduced immunogenicity and increased bioavailability of D-peptides [8]. In order to optimize the lead structure, with respect to increased stability, affinity to Aβ(1-42), blood–brain-barrier (BBB) penetration, and in vitro potency and in vivo efficacy, rational drug design approaches were conducted. The most promising compound so far, called RD2, is currently under development for the treatment of patients with AD [9]. The suggested mode of action was demonstrated by successful target engagement in vitro and in vivo [10,11]. Furthermore, the in vivo efficacy of RD2 was proven in different AD mouse models, even in old-aged mice with fully developed AD-associated pathology [10–13]. Besides RD2, more D-peptides were developed out of a rational drug design. In order to combine the favorable properties of D3 and RD2, a heteromeric linear head-to-tail version of both D-peptides, called RD2D3, was designed. Compared to RD2 and D3, we have shown increased binding affinity to Aβ(1-42) [14] and a higher potency to eliminate toxic Aβ-oligomers for RD2D3 [12]. In vivo, it was demonstrated that RD2D3 has a favorable pharmacokinetic profile (after intraperitoneal (i.p.) administration), high proteolytic stability and therapeutic efficacy by improving the cognitive abilities of transgenic APP Swedish/Dutch/Iowa (Tg-SwDI) AD mice [14,15]. Besides the development of linear tandem-D-peptides, a further approach for a rational drug design was the cyclization of either homo- or tandem-D-peptides [16,17]. For the cyclized tandem-D-peptide cRD2D3, a remarkably enhanced pharmacokinetic profile was found [17]. Comparing the pharmacokinetic profiles of the linear and cyclic version of the D-peptide RD2D3 (RD2D3 vs. cRD2D3) after intravenous (i.v.). and intraperitoneal (i.p.) administration in C57Bl/6 wild type (WT) mice resulted in a tremendously increased terminal half-life (2.3 vs. 58 h), increased BBB penetration values and brain peptide concentrations of cRD2D3. Furthermore, for cRD2D3 a high oral bioavailability was demonstrated [17]. Both, a long half-life and high oral bioavailability are extremely advantageous for active ingredients used in the therapy of AD and qualify for daily drug administrations. Since it can be assumed that AD therapy will take place over a longer period of time (possibly several years to decades), a therapy regime with once-daily oral drug intake is most convenient for the patient (treatment adherence).

Here, we wanted to investigate whether the more favorable pharmacokinetic profile of the cyclic D-peptide cRD2D3 compared to its linear version RD2D3 results in an increased in vivo efficacy. Before investigating the in vivo efficacy of RD2D3 and cRD2D3 in the Tg-SwDI AD mouse model, we performed an in-depth in vitro characterization of the compounds on the specific Aβ-mutation, which was introduced to the Tg-SwDI AD mouse model in comparison to wild type Aβ(1-42). This Aβ mutation is the so called "Dutch" and "Iowa" mutation (D/I Aβ) and it is described by an exchange of the amino acid glutamate (E) for glutamine (Q) at position 22 and of aspartate (D) for asparagine (N) at position 23 of the Aβ(1-42) sequence.

2. Results

2.1. The Cyclic D-Peptide cRD2D3 Revealed Increased In Vitro Potency Compared to the Linear D-Peptide RD2D3 Without Differences in the Proteolytic Stability

In order to investigate the in vitro potency of the cyclic D-peptide cRD2D3 and its linear form RD2D3, we performed several experiments concerning the binding of the D-peptides to Aβ(1-42) and D/I Aβ. By use of surface plasmon resonance (SPR) mea-

surements, we determined the dissociation constant (K_D) of RD2D3 and cRD2D3 to both Aβ-species, by using Aβ as ligand and the D-peptide as analyte or vice versa. As illustrated in Figure 1, both D-peptides bound with μM concentrations to Aβ(1-42) and to D/I Aβ. By use of Aβ(1-42) or D/I Aβ as an analyte, both D-peptides bound with higher affinity to D/I Aβ (K_D Aβ(1-42): RD2D3 7.01 ± 0.31 μM, cRD2D3 10.41 ± 0.61 μM; D/I Aβ: RD2D3 3.24 ± 0.31 μM, cRD2D3 2.05 ± 0.33, Figure 1). By use of the D-peptides as a ligand, cRD2D3 bound with an almost identical affinity to both Aβ species (K_D Aβ(1-42): 5.63 ± 2.5 μM, K_D D/I Aβ 5.99 ± 0.77 μM, Figure 1). For RD2D3, the picture is different. The D-peptide bound with half the affinity to Aβ(1-42) than to D/I Aβ (K_D Aβ(1-42): 18.4 ± 6.5 μM, K_D D/I Aβ 7.09 ± 1.4 μM, Figure 1).

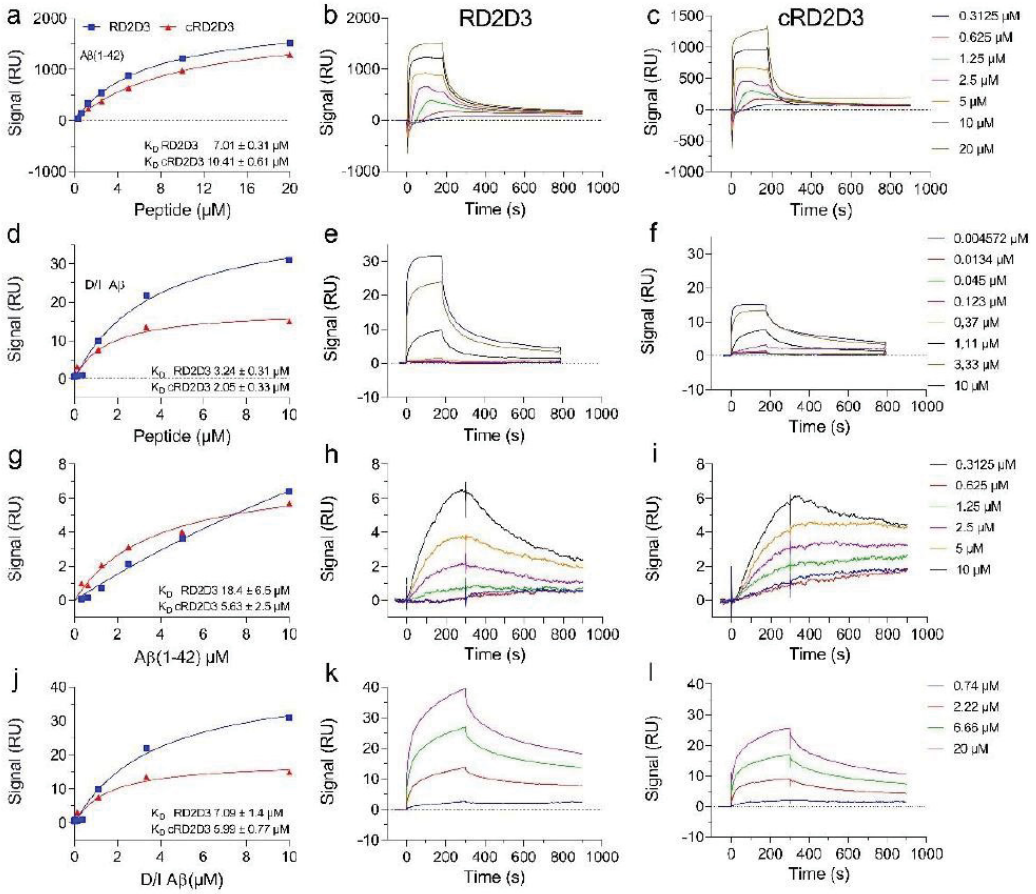

Figure 1. Affinity determination of RD2D3 and cRD2D3 to Aβ(1-42) and D/I Aβ by SPR. By use of the D-peptides as analyte, either Aβ(1-42) or D/I Aβ was immobilized on a CM-5 sensor chip and the binding of different RD2D3 (blue) and cRD2D3 (red) concentrations were analyzed in a multi cycle experiment (**a**–**f**). Real-time surface plasmon resonance (SPR) sensorgrams of different RD2D3 and cRD2D3 concentrations (left). Equilibrium dissociation constants (K_D) were determined by using a Langmuir 1:1 binding model (RD2D3 middle, cRD2D3 right). RD2D3 or cRD2D3 were immobilized on a series S CM-5 sensor chip, and the binding of Aβ(1-42) or D/I Aβ monomers as an analyte at various concentrations was observed (**g**–**l**). For evaluation, the steady-state binding signals were plotted over the concentrations and fitted using a Langmuir 1:1 binding model (**a**,**d**,**g**,**j**).

The ability to inhibit the fibril formation of Aβ is of great importance for substances developed for a treatment of AD. In order to test for interference with fibril formation, we performed a thioflavin T test (ThT). The fluorescence signal of ThT, a benzothiazole dye, increases upon binding to amyloid fibrils. In order to investigate the functional effects of RD2D3 and cRD2D3 on Aβ(1-42) and on D/I Aβ, the D-peptides were incubated with either Aβ(1-42) or D/I Aβ (equimolar concentrations) and 5 µM ThT. ThT fluorescence was monitored every 6 min for 24 h. As demonstrated in Figure 2a,b, both D-peptides were able to inhibit the Aβ(1-42) and D/I Aβ fibril formation. Interestingly, this effect was more pronounced on Aβ(1-42) than on D/I Aβ (Figure 2a,b). Besides the potency of RD2D3 and cRD2D3 to inhibit the Aβ fibril formation, we also investigated the potency of both compounds to eliminate toxic Aβ-oligomers. For this, the so called QIAD (quantitative determination of interference with Aβ aggregate size distribution) assay [18] was conducted with both D-peptides and Aβ(1-42) and D/I Aβ. The outcome of the QIAD assay revealed that both RD2D3 and cRD2D3 were capable to significantly eliminate toxic Aβ(1-42)-oligomers (RD2D3 89%, cRD2D3 80%, Figure 2c, one-way ANOVA, with Bonferroni post hoc analysis, Aβ(1-42) vs. RD2D3 fraction 4 $p = 0.001$, fraction 5, $p = 0.011$, fraction 6 $p = 0.01$, cRD2D3 fraction 4 $p = 0.005$, fraction 5 $p = 0.12$, fraction 6 p = n.s. (0.057)). Furthermore, both D-peptides eliminated toxic D/I Aβ-oligomers with a similar potency (RD2D3 94%, cRD2D3 100%, Figure 2d, not significant for cRD2D3 despite the total elimination of toxic oligomers, one-way ANOVA with Bonferroni post hoc analysis, D/I Aβ vs. RD2D3 fraction 4 p = n.s.(0.062), fraction 5, $p = 0.011$, fraction 6 p = n.s, cRD2D3 fraction 4 p = n.s. (0.094), fraction 5 p = (n.s.) 0.118 and fraction 6 p = n.s.).

In order to verify and extend the proteolytic stability/in vitro ADME (absorption, distribution, metabolism and excretion) of RD2D3 and cRD2D3, previously described for tritium labeled D-peptides (^{3}H) [15,17], we performed different tests to investigate the proteolytic stability in different (simulated) body fluids. In both, simulated gastric (SGF) and intestinal fluid (SIF), RD2D3 and cRD2D3 were remarkably stable (RD2D3: SIF 4 h 100%, 8 h 93.5%, SGF 4 h 100%, 8 h 100%, cRD2D3: SIF 4 h 96%, 8 h 87.2%, SGF 4 h 99.5% and 8 h 99.7% Figure 3a,b). Additionally, we tested the stability of both D-peptides in human plasma and human liver microsomes. In plasma, both D-peptides were stable up to approximately 90% after 48 h (RD2D3: 8 h 84.7%, 24 h 91.9% and 48 h 93.7% and cRD2D3: 8 h 91.8%, 24 h 93.7% and 48 h 92.4%, Figure 3c). In liver microsomes, both D-peptides were slightly metabolized to approximately 25% (RD2D3: 8 h 81.9% and 24 h 78.2% and cRD2D3: 8 h 89.2% and 24 h 73.6%, Figure 3d).

2.2. Tg-SwDI Mice Develop Cognitive Deficits at 12 Months of Age Compared to WT Mice

In all conducted experiments (nesting behavior, marble burying, open field test and Morris water maze (MWM)) Tg-SwDI mice showed an altered behavior compared to WT mice, but there was no significant difference in the body weight of WT compared to Tg-SwDI mice (Figure 4a). Analyses of some basic behavioral characteristics of Tg-SwDI resulted in phenotypic alterations. Compared to WT mice, Tg-SwDI mice formed a less mature nest (unpaired two-tailed t test, $p < 0.001$, Figure 4b). Furthermore, they displayed impaired digging behavior in direct comparison to WT mice of the same age, indicating a less inquisitive behavior (unpaired two-tailed t test, $p < 0.001$, Figure 4c).

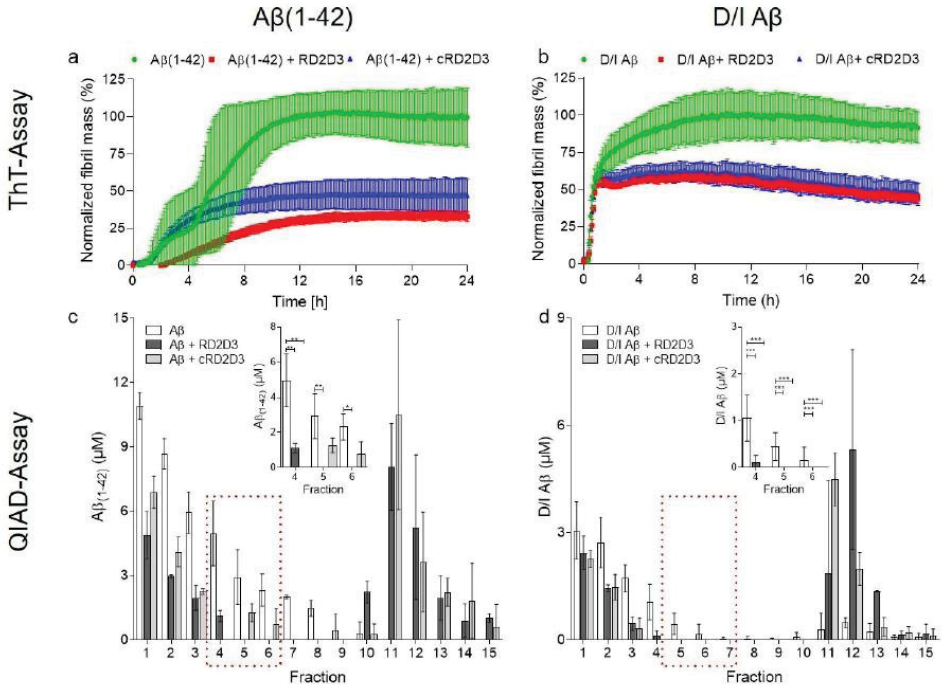

Figure 2. RD2D3 and cRD2D3 inhibited the Aβ(1-42) and D/I Aβ fibril formation and eliminated significantly toxic oligomers. ThT-Assay (upper panel). Both D-peptides, RD2D3 (red) and cRD2D3 (blue), were analyzed according to their ability to inhibit either the Aβ(1-42) (**a**,**left**) or the D/I Aβ (**b**,**right**) fibril formation by use of equimolar concentrations (10 μM). All analyzed D-peptides were able to inhibit either the Aβ(1-42) (**a**) or the D/I Aβ (both green) (**b**) fibril formation. Fibril mass was normalized to the Aβ control. Data are presented as mean ± SD ($N = 3$ out of three independent experiments). QIAD-Assay (lower panel). Aβ(1-42) (**c**,**left**) and D/I Aβ (**d**,**right**) size distribution without (white) or with D-peptide were analyzed by density gradient centrifugation with subsequent measurements of the Aβ concentrations. Aβ-oligomers are located in fractions 4–6. Comparison of 20 μM RD2D3 (dark grey) and 20 μM cRD2D3 (light grey) (**c**) revealed similar Aβ(1-42) (80 μM) oligomer elimination efficacy of both D-peptides. Comparison of 10 μM RD2D3 (dark grey) and 10 μM cRD2D3 (light grey) (**d**) revealed higher potency of RD2D3 to eliminate toxic D/I Aβ (40 μM)-oligomers than cRD2D3 does. Data are presented as mean ± SD ($N = 2$–5) *** $p < 0.001$, ** $p < 0.01$ and * $p < 0.05$.

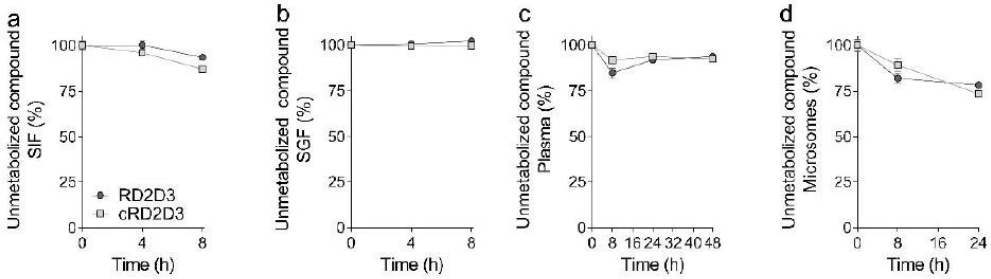

Figure 3. Proteolytic stability of RD2D3 and cRD2D3 in different human (simulated) body fluids. Both D-peptides, RD2D3 and cRD2D3, are remarkably stable in simulated intestinal and gastric fluid (SIF and SGF) (**a**,**b**), and in human plasma (**c**) and human liver microsomes (**d**). Shown are data form three independent experiments (mean ± SD).

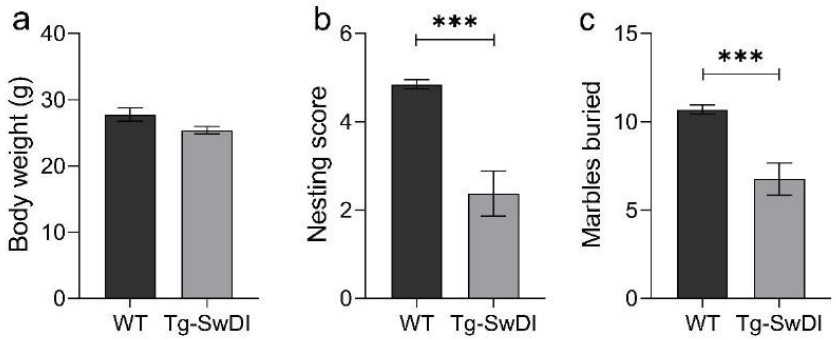

Figure 4. Basic phenotypic analysis of Tg-SwDI mice. No difference in body weight between Wild type (WT) and Tg-SwDI mice (**a**), but significant differences in nesting behavior (**b**) and marble burying (**c**) were found. Tg-SwDI mice formed a less mature nest and buried less marbles. Data are represented as mean ± SEM, all unpaired two-tailed *t* test, *** $p < 0.001$ (WT $N = 13$ and Tg-SwDI $N = 12$).

While performing the open field test, a significant difference was found between the time WT and Tg-SwDI spent in the center and border zone (two-way ANOVA genotypes $p < 0.0001$, Fisher LSD post hoc analysis WT vs. Tg-SwDI center and border $p < 0.0001$, Figure 5a). By analyzing the travelled duration, Tg-SwDI covered an almost two-times longer distance than WT mice (two-tailed t-test, $p < 0.0001$, Figure 5b). Furthermore, Tg-SwDI mice were moving much faster than WT mice (two-tailed t-test, $p < 0.0001$, Figure 5c). Moreover, by analysis of single time slots (each slot 5 min) WT mice showed a clear habituation effect to the arena (Figure 5d). At the beginning of the test period, the center had an aversive effect to the mice, since they tended to avoid open areas. After a while, the WT mice explored the center of the arena more and more. In contrast, Tg-SwDI mice do not show this habituation effect (two-way RM ANOVA, genotype $p = 0.002$, Fisher LSD post hoc analysis, WT vs. Tg-SwDI slot one $p = 0.047$, slot two n.s. ($p = 0.052$), slot three $p = 0.034$, slot four $p < 0.014$ and slot five $p < 0.001$).

In order to analyze spatial memory, we conducted an MWM. On the first day of training, WT and Tg-SwDI mice performed almost equally (Figure 5e,f). Starting at day two, WT mice found the hidden platform significant faster than Tg-SwDI mice (two-way RM ANOVA, genotype $p = 0.001$, Fisher LSD post hoc analysis, WT vs. Tg-SwDI day one n.s. ($p = 0.91$), day two $p = 0.018$, day three $p = 0.091$, day four $p < 0.001$ and day five $p = 0.004$, Figure 5e). A slight learning effect could be seen for both WT and Tg-SwDI mice. However, this effect was much more pronounced in the WT mice. During the probe trial, WT mice spent more time in the platform zone than Tg-SwDI mice, indicating an improved memory retrieval (two-tailed t-test, $p = 0.073$, Figure 5f). Concluding, Tg-SwDI mice developed distinct cognitive deficits as detected by the MWM with 12 months of age.

2.3. RD2D3 Showed Superior Efficacy to Improve Phenotypic Deficits over cRD2D3

All mice, regardless of treatment, showed no changes in their general appearance. Compared to D-peptide treated mice, placebo treated mice displayed a decrease in body weight (before vs. after treatment: placebo 35.1 ± 0.5 g vs. 32.3 ± 0.4 g, RD2D3 33.2 ± 2.6 g vs. 34.3 ± 0.6 g and cRD2D3 35.1 ± 1.4 g vs. 33.2 ± 1.0 g), but not to a significant extent (Figure 6a). There was no difference in the behavior of RD2D3 or cRD2D3 treated mice compared to placebo treated mice, neither in the nesting behavior, nor in the marble burying test. (Figure 6b,c).

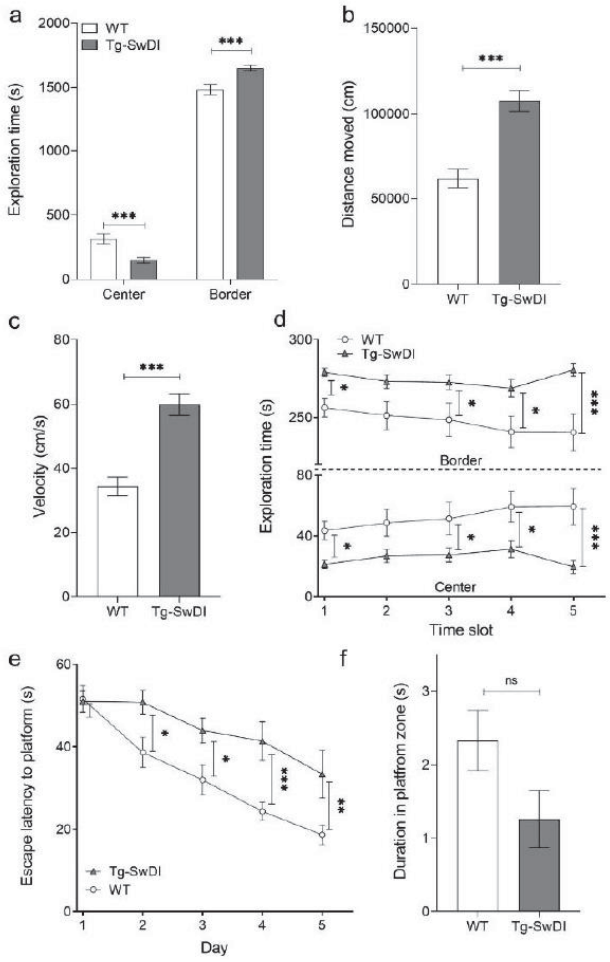

Figure 5. Tg-SwDI mice developed phenotypic deficits in the open field test and showed cognitive spatial impairment in the Morris water maze. In order to analyze some general aspects of the behavior of Tg-SwDI compared to wild type (WT) mice, an open field test was conducted, where mice were allowed to explore a square shaped arena freely for 30 min. The analysis of the test revealed that Tg-SwDI mice explored less the center of the arena (**a**) (two-way ANOVA genotypes $p < 0.0001$, Fisher LSD post hoc analysis WT vs. Tg-SwDI center and border $p < 0.0001$). Furthermore, they showed a reduced covered distance (**b**) and a reduced velocity (**c**) (both two-tailed *t*-test $p = 0.0001$). By analyzing the habituation effect of WT and Tg-SwDI mice to the arena, it was obvious that transgenic mice explored the center of the arena less than WT mice, indicating a reduced habituation effect to the arena (**d**) (two-way RM ANOVA, genotype $p = 0.002$, Fisher LSD post hoc analysis, WT vs. Tg-SwDI slot one $p = 0.047$, slot two n.s. ($p = 0.052$), slot three $p = 0.034$, slot four $p < 0.014$ and slot five $p < 0.001$). In the Morris water maze, a significant difference was detectable in the performance during the training of WT and Tg-SwDI mice starting at day 2, indicating spatial memory deficits (**e**) (two-way RM ANOVA, genotype $p = 0.001$, Fisher LSD post hoc analysis, WT vs. Tg-SwDI day one n.s. ($p = 0.91$), day two $p = 0.018$, day three $p = 0.091$, day four $p < 0.001$ and day five $p = 0.004$)). During the probe trial, WT mice spent more time in the platform zone than Tg-SwDI mice, indicating impairments with memory retrieval (**f**). Data are shown as mean ± SEM, * $p < 0.05$, ** $p < 0.01$ and *** $p < 0.001$ (WT $N = 13$ and Tg-SwDI $N = 12$).

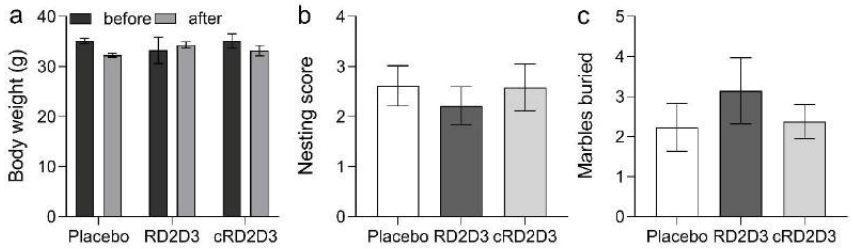

Figure 6. General behavior of RD2D3 and cRD2D3 treated tg-SwDI mice compared to placebo. There were no significant differences in all analyzed groups, neither in the body weight (**a**) nor in the nesting behavior (**b**) or marble burying (**c**). Data are represented as mean ± SEM (placebo $N = 13$, RD2D3 $N = 14$ and cRD2D3 $N = 12$).

During the total open field test duration, no difference between treated or non-treated Tg-SwDI was detectable (Figure 7). Neither in the time the treatment groups spent in the center or border zone (Figure 7a) nor in the covered distance or in the velocity (Figure 7b,c). Taken a closer look, it was also possible to analyze the habituation effect of all mice to the arena. RD2D3 treated mice showed a slight but significant habituation effect to the arena compared to placebo treated mice (two-way RM ANOVA, $p = 0.056$, Fisher LSD post hoc analysis, placebo vs. RD2D3 slot 1 n.s., slot 2 $p = 0.045$, slot 3 n.s., slot 4 n.s. and slot 5 $p = 0.44$), this effect was completely absent in cRD2D3 treated mice. During each analyzed time slot, they spent almost the same time in the center or border, respectively (Figure 7d).

In this study, a MWM was performed to investigate, whether a treatment with RD2D3 or cRD2D3 improves the spatial memory or cognitive abilities of Tg-SwDI mice compared to placebo treated mice. As can be seen from Figure 7e, both compounds were able to improve the performance of Tg-SwDI mice in the MWM during the training phase. For RD2D3, this effect was statistically significant compared to placebo treated mice (two-way RM ANOVA treatment $p = 0.11$, Fisher post-hoc analysis placebo vs. RD2D3 day 1 n.s., day 2 n.n, day 3 $p = 0.004$, day 4 n.s. and day 5 $p = 0.029$). In order to test memory retrieval, a probe trial was conducted. Although not to a significant extent, there was a preference of RD2D3 treated mice spending more time in the platform zone (Figure 7f).

In order to investigate, whether treatment with RD2D3 or cRD2D3 change the pathological characteristics of Tg-SwDI mice, several histological analyses were conducted. As demonstrated in Table 1 and Figure 8, neither RD2D3 nor cRD2D3 were able to reduce the amount of Aβ deposits as shown by 6E10 staining, nor reduce the number of activated astrocytes or microglia, as shown by GFAP or Iba-1 staining, respectively.

Table 1. Immunohistochemical investigations of RD2D3 and cRD2D3 treatment on Aβ deposits and neuroinflammation. Treatment with neither RD2D3, nor cRD2D3 did reveal any increase or decrease in Aβ deposits (6E10), activated astrocytes (GFAP) or microglia (Iba-1). IR: immunoreactivity. Data are represented as mean ± SEM. IR: immunoreactivity (placebo $N = 13$, RD2D3 $N = 14$ and cRD2D3 $N = 12$).

	6E10 IR (%)		GFAP IR (%)		Iba-1 IR (%)	
	Cortex	**Hippocampus**	**Cortex**	**Hippocampus**	**Cortex**	**Hippocampus**
Placebo	1.8 ± 0.7	2.5 ± 0.7	43.8 ± 2.0	39.8 ± 1.0	8.7 ± 1.7	11. 5 ± 1.1
RD2D3	1.0 ± 0.2	2.5 ± 0.5	40.6 ± 2.2	38.0 ± 1.2	8.1 ± 1.6	8.6 ± 1.3
cRD2D3	1.1 ± 0.2	4.2 ± 0.7	43.1 ± 1.8	39.5 ± 1.0	8.1 ± 1.6	10.2 ± 1.8

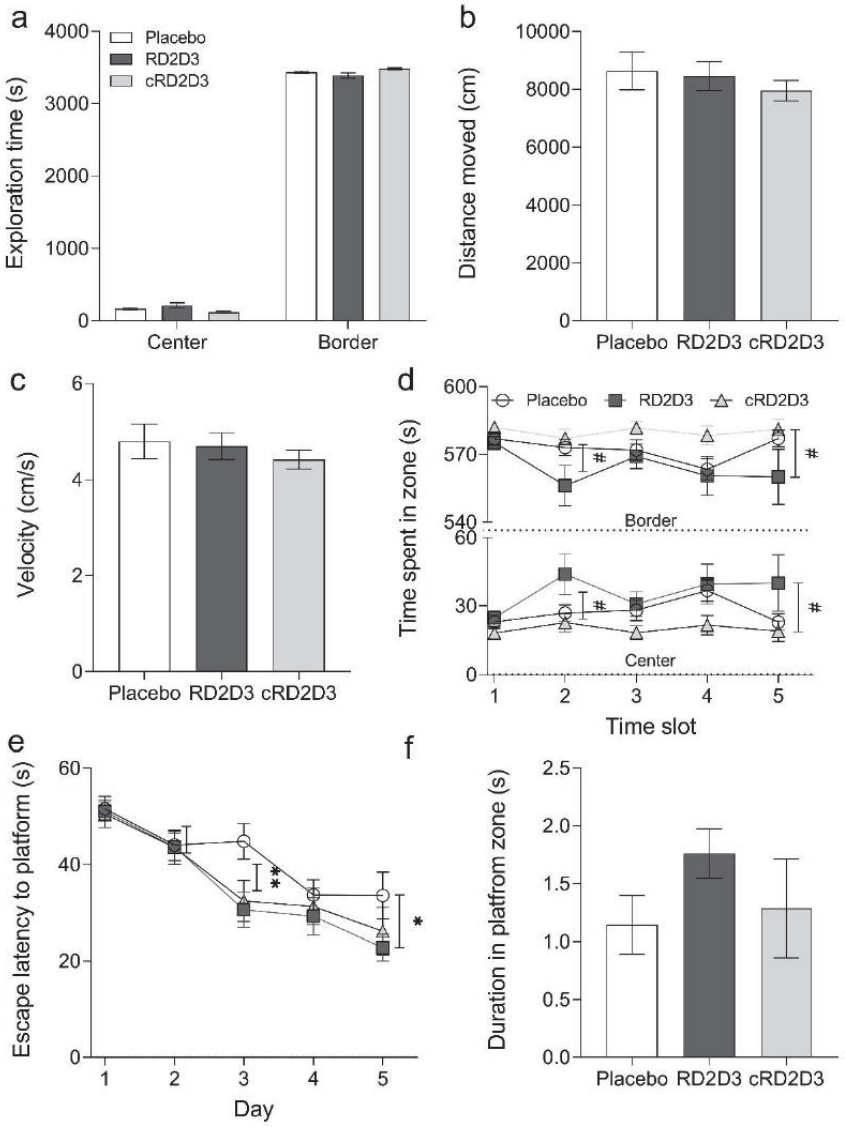

Figure 7. Treatment with RD2D3 significantly improved the phenotype of Tg-SwDI mice compared to placebo and cRD2D3 treated mice. An open field test was conducted to analyze and compare the exploratory and anxiety related behavior of RD2D3 and cRD2D3 treated Tg-SwDI mice compared to placebo treated mice (**a**–**d**). Mice were allowed to freely explore a square shaped arena for 30 min (imaginarily divided into center and border zone (**a**)). While there was no difference in the exploratory behavior or in the traveled distance or velocity, there was a significant habituation effect of RD2D3 treated mice to the arena (**d**). This effect was completely absent in cRD2D3 treated mice (**d**). Additionally, a Morris water maze (MWM) was performed in which mice were trained for 5 days to find a hidden platform (**e**). Both treatment groups (RD2D3 and cRD2D3) found the hidden platform faster than placebo treated mice and spent more time in the platform zone during the probe trial (**f**). Data are shown as mean ± SEM (placebo $N = 13$, RD2D3 $N = 14$ and cRD2D3 $N = 12$). ** $p < 0.01$ and * $p < 0.05$.

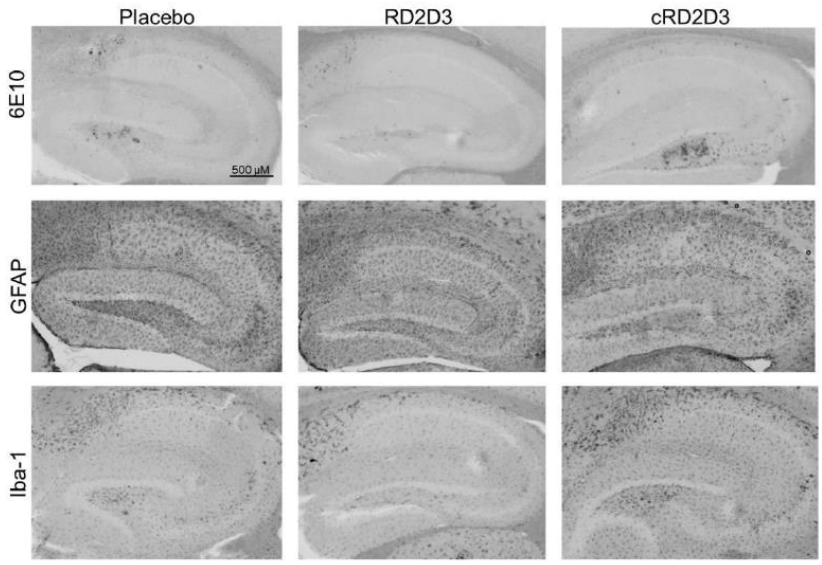

Figure 8. Immunohistochemical analysis of Aβ deposits and neuroinflammation. Representative images of hippocampus of placebo, RD2D3 and cRD2D3 treated mice (placebo $N = 13$, RD2D3 $N = 14$ and cRD2D3 $N = 12$).

3. Discussion

More than 100 years have passed since AD was first described by Alois Alzheimer [19]. Meanwhile, many efforts have been made to find a curative or even disease modifying treatment for this devastating neurodegenerative disease [20]. One of the major pathological hallmarks of the disease are deposits of the so called Aβ-peptide. No toxic properties are attributed to Aβ in its monomeric, native form. Only a soluble intermediate product, the so-called Aβ-oligomers, are considered to be the disease-causing agent [3,18,21]. Our group has focused on the development of compounds, which directly destroy toxic Aβ-oligomers. These therapeutic substances are so-called D-peptides, consisting of 12–24 D-enantiomeric amino acid residues. The most promising compound so far is RD2. In the recent years, RD2 has been studied extensively [10–13]. The efficacy of this compound has been demonstrated in several studies in different mouse models, so RD2 is now in the process of proving its efficacy in humans in clinical trials [9]. Out of several drug optimization approaches, the linear tandem-D-peptide RD2D3 and its cyclic equivalent, cRD2D3, came forth [12,14,15,22]. Tandemization and cyclization of the developed D-enantiomeric peptides were postulated to increase the binding affinity to Aβ(1-42), to increase the efficacy to eliminate toxic Aβ-oligomers and to increase BBB penetration. This last point in particular was demonstrated by Schartmann et al. [22]. After the pharmacokinetic and some in vitro analyses of the D-peptides were conducted recently, we here performed an in-depth comparison of the in vitro potency of both D-peptides on wild type Aβ(1-42) and on the D/I Aβ mutation and a direct comparison of the D-peptide's in vivo efficacy in Tg-SwDI mice.

During the last years, we could demonstrate that our developed D-peptides bound (mostly) to Aβ(1-42) in the micromolar range. This was also already proven for RD2D3 [14]. However, it was never analyzed if these compounds also bind to different Aβ-variants, e.g., the D/I mutation, although there have been several treatment studies conducted with a mouse model harboring this and other mutations [14,16,18,23]. In this study, we analyzed the binding affinity of both RD2D3 and cRD2D3 to Aβ(1-42) for a direct comparison, and the binding affinity of the abovementioned D-peptides to D/I Aβ. The results showed that both D-peptides exhibit similar binding affinities to Aβ(1-42) and D/I Aβ. However, this binding is at least twice as strong to D/I Aβ in comparison to Aβ(1-42).

Taking a closer look into the in vitro functionality of both D-peptides, we performed a ThT and a QIAD assay. Both D-peptides are capable to efficiently inhibit the Aβ(1-42) fibril formation at equimolar concentrations. One might speculate that RD2D3 was slightly more efficient since it also shifted the lag phase of the initial aggregation of Aβ(1-42). By analyzing the ability of both D-peptides to inhibit the D/I Aβ fibril formation, we could not detect a meaningful difference between the potency of both D-peptides. RD2D3 and cRD2D3 inhibit the D/I Aβ fibril formation at equimolar concentrations. Despite the higher binding affinity to D/I Aβ of both D-peptides compared to Aβ(1-42), both D-peptides show a superior potency to inhibit the Aβ(1-42)- than the D/I Aβ-fibril formation. Aβ-oligomer elimination efficacy was already proven for RD2D3 on Aβ(1-42) [12]. Here, we performed an additional QIAD assay to directly compare the Aβ-oligomer elimination efficacy of RD2D3 with cRD2D3. We were able to confirm that RD2D3 and cRD2D3 eliminate Aβ(1-42)-oligomers in vitro especially effective to about 90% or 80%, respectively. For the first time, we also conducted a QIAD assay with an Aβ mutation—D/I Aβ. We could demonstrate that both D-peptides can eliminate (more) efficiently D/I Aβ-oligomers in vitro to about 95% or 100%, respectively.

In order to verify the already demonstrated proteolytic stability of RD2D3 and cRD2D3 with a more sensitive method (HPLC analysis instead of thin layer chromatography with ^{3}H-labeled D-peptide) and to extend the analysis, proteolytic stability tests in different (simulated) human body fluids were done. Analysis of the proteolytic stability of ^{3}H-RD2D3 [15] and ^{3}H-cRD2D3 [22] in human liver microsomes revealed that both D-peptides appeared to be completely stable. In contrast, the D-peptides were metabolized up to 25% after 8 h when analyzed by HPLC. This discrepancy can probably be explained by the fact that analysis by HPLC is many times more sensitive and accurate than analysis by thin-layer chromatography.

In the aforementioned study [22] it was described that cRD2D3 has an extraordinary superior pharmacokinetic profile in C57BL/6 mice compared to its linear equivalent RD2D3 after i.v. and i.p. administration [15,22]. One of the most outstanding properties of the cyclic D-peptide is its enormously long terminal half-life in plasma of more than 2 days (58 h). In comparison, the terminal half-life in plasma of RD2D3 was 2.3 h. Moreover, it was shown that cRD2D3 reached its site of action, the brain as a target organ, with concentrations up to four to five times higher than RD2D3.

After analyzing the in vitro profile of the compounds, we wanted to investigate whether the superior pharmacokinetic profile of cRD2D3 was also reflected in improved efficacy in the Tg-SwDI mouse model. For this purpose, we first performed a small in-house characterization of the mouse model. This served the purpose of confirming that the Tg-SwDI mice also develop the expected (cognitive) deficits in our hands and in our experimental setup. The implemented behavioral experiments (nesting behavior, marble burying, open field test and Morris water maze) gave proof that the Tg-SwDI mouse model develops general and cognitive phenotypic deficits in our hands at 12 months of age. Although development of pathology and especially of cognition impairment is often dependent on breeding cohorts and lab environments, our results are in good accordance with those reported previously [24–27]. After completion of the characterization study, we performed an i.p. treatment study with RD2D3 and cRD2D3 compared to placebo treated mice by use of Alzet osmotic minipumps. Treatment started with 11 months of age and mice were sacrificed after the pump duration of 28 days (at 12 months of age). The treatment start was based on the results of the characterization study, where cognition deficits were detected at 12 months of age. One might speculate that a treatment with an earlier age and a prolonged treatment duration might have also been sufficient. During the last days of treatment, several behavioral tests were conducted. Those tests indicated that RD2D3 had a more pronounced effect on the phenotypic deficits of Tg-SwDI mice than cRD2D3. The analysis of the open field test revealed a clear habituation effect of RD2D3 treated mice to the arena, comparable with the behavior of non-transgenic mice. In contrast, this effect was completely absent in cRD2D3 treated mice. The performed MWM

suggested that both RD2D3 and cRD2D3 treatment improved the cognitive performance of Tg-SwDI mice compared to placebo treated mice. However, this effect reached significance only in the RD2D3 treated Tg-SwDI mice. The use of a larger number of mice would probably have resulted in this effect also being significant in the cRD2D3 treated Tg-SwDI mice. Histological analysis of the brains of all mice revealed no difference between the treatment groups, neither on Aβ-deposits nor on activated astrocytes or microglia. One might speculate that a administering a higher dose of the D-peptide concentration or a longer treatment duration would have resulted in a reduction of AD-associated pathology. Previous pharmacokinetic analyses of RD2D3 and cRD2D3 have shown that both D-peptides do reach the brain [6,7]. Summarized, RD2D3 appears to have a superior efficacy to ameliorate the phenotype of Tg-SwDI than cRD2D3 compared to placebo treated mice.

Referring to the hypothesis that cyclized D-peptides also show improved in vivo efficacy compared to linear D-peptides due to a more favorable pharmacokinetic profile [22] could not be confirmed in this study. In all tests performed, cRD2D3 treated Tg-SwDI mice showed similar or slightly worse behavior than RD2D3 treated mice. In conclusion, the superior pharmacokinetic profile of cRD2D3 was not sufficient to translate into improved in vivo efficacies.

4. Materials and Methods

4.1. Peptides

The D-peptides RD2D3 (ptlhthnrrrrrrprtrlhthrnr) and cRD2D3 (ptlhthnrrrrrrprtrlhthrnr) with amidated C-terminus were purchased as lyophilized powder with >95% purity from peptides&elephants (Henningsdorf, Germany) and Cambridge peptides (UK), respectively.

Synthetic Aβ(1-42) and (Gln^{22}, Asn^{23})-Amyloid β-Protein (1-40) (D/I Aβ) with >95% purity were purchased as lyophilized powder from Bachem (Bubendorf, Switzerland). Lyophilized Aβ-species were dissolved overnight in HFIP (1,1,1,3,3,3-hexafluoro-2-propanol, Sigma-Aldrich, Darmstadt, Germany). Aliquots were stored at −20 °C until further processing. Before usage, Aβ was lyophilized and dissolved in 10 mM sodium phosphate buffer, pH 7.4.

4.2. In Vitro Potency

4.2.1. Binding Affinity

The dissociation constant (K_D) of RD2D3 and cRD2D3 binding to Aβ(1-42) and D/I Aβ was determined by SPR spectroscopy using a Biacore T200 instrument (Biacore, GE Healthcare, Uppsala, Sweden). Aβ(1-42) or D/I Aβ was used as the ligand, while RD2D3 and cRD2D3 were used as the analyte or vice versa.

By using Aβ(1-42) or D/I Aβ as a ligand, it was immobilized onto a series S CM-5 sensor chip (GE Healthcare, Uppsala, Sweden) by amine coupling. In short, the flow cells were activated by a mixture of 50 mM N-hydroxysuccinimide (NHS) and 16.1 mM N-Ethyl-N′-(dimethylaminopropyl)carbodiimide (EDC) (XanTec, Düsseldorf, Germany) for 7 min. Aβ(1-42) or D/I Aβ were dissolved to a final concentration of 50 µg/mL in 10 mM sodium acetate pH 5 (AppliChem, Darmstadt, Germany) and injected over one of the activated flow cells to a final signal of 1700 RU. After the immobilization, the ligand and reference flow cells were quenched by injecting 1 M ethanolamine pH 8.5 (XanTec, Düsseldorf, Germany) for 7 min. For the determination of the K_D, multicycle kinetic experiments were performed with 10 mM HEPES + 50 mM NaCl (AppliChem, Darmstadt, Germany) pH 7.4 as the running buffer at 25 °C and at a flow rate of 30 µL/min. The peptides were diluted in the running buffer to the following concentrations: 20 µM, 10 µM, 5 µM, 2.5 µM, 1.25 µM and 0.625 µM. All samples were injected over the flow cells for 180 s, followed by a dissociation step of 600 s with running buffer. Regeneration of the sensor chip was accomplished by a 45 s injection of 2 M of guanidinium hydrochloride (AppliChem, Darmstadt, Germany). The reference flow cell and buffer injections (c = 0 nM) were used for double referencing

of the sensorgrams. For data evaluation, the sensorgrams were fitted by the steady-state affinity model implemented in the Biacore T200 Evaluation Software 3.2.

By using the compounds (RD2D3 and cRD2D3) as ligands, they were immobilized on two separate channels on a series S CM-5 sensor chip (Cytiva, GE Healthcare, Uppsala, Sweden) by amine coupling. Both flow cells on each channel were activated with a mixture of 50 mM N-hydroxysuccinimide (NHS) and 16.1 mM N-ethyl-N'-(dimethylaminopropyl)carbodiimide (EDC) (XanTec, Düsseldorf, Germany) for 7 min. The peptides were diluted to 50 µg/mL in 10 mM maleic acid pH 6 (AppliChem, Darmstadt, Germany) and injected over flow cell two of each channel to a final signal between 600 and 900 RU. After the peptides were immobilized, the ligand and reference flow cells of each channel were quenched by injecting 1 M ethanolamine pH 8.5 (XanTec, Düsseldorf, Germany) for 7 min. For the determination of the K_D multicycle kinetic experiments were performed with 10 mM HEPES + 50 mM NaCl (AppliChem, Darmstadt, Germany) pH 7.4 as the running buffer at 25 °C and at a flow rate of 30 µL/min. Aβ(1-42) or D/I Aβ were diluted in the running buffer to the following concentrations: 10 µM, 3.3 µM, 1.1 µM, 0.37 µM, 0.12 µM, 0.045 µM, 0.014 µM and 0.0045 µM. All samples were injected over the flow cells for 180 s, followed by a dissociation step of 600 s with running buffer. Regeneration of the sensor chip was accomplished by a 45 s injection of 2 M guanidinium hydrochloride (AppliChem, Darmstadt, Germany). The reference flow cell of each channel and the buffer injections (c = 0 nM) were used for double referencing of the sensorgrams. For data evaluation, the sensorgrams were fitted by the steady-state affinity model implemented in the Biacore Insight Evaluation Software version 3.0.

4.2.2. Thioflavin-T Assay

Using the ThT assay, the potency of RD2D3 and cRD2D3 to inhibit the fibril formation of Aβ(1-42) and D/I Aβ was analyzed. For this purpose, 10 µM Aβ(1-42) or D/I Aβ were incubated with 10 µM of the corresponding D-peptide and 5 µM ThT. ThT fluorescence was monitored over 24 h every 6 min at λex = 440 nm and λem = 490 nm in a fluorescence plate reader (Clariostar, BMG Labtech, Ortenberg, Germany) at RT. Correction was done using all supplements without Aβ and D-peptide (blank).

4.2.3. QIAD Assay

According to Brener et al., a QIAD assay was performed in order to evaluate the Aβ(1-42) or D/I Aβ oligomer elimination efficacies of RD2D3 and cRD2D3 [18]. In short, 80 µM lyophilized Aβ(1-42) or 40 µM D/I Aβ was preincubated for 2 h or 15 min, respectively, to enrich Aβ-oligomers. Afterwards, either 20 µM RD2D3 or cRD2D3 for Aβ(1-42) or 10 µM RD2D3 or cRD2D3 for D/I Aβ were added to the preincubated solution and coincubated for additional 30 min. Subsequently, the samples were loaded on the top of a density gradient (5–50% (w/v) iodixanol (OptiPrep, Sigma-Aldrich, Darmstadt, Germany)) followed by an ultracentrifugation step (3 h at 4 °C and 259000× g (Optima TL-100, Beckman Coulter, Brea, CA, USA)). Following the ultracentrifugation, 14 fractions (140 µL each) were harvested by upward displacement. Fraction 15 contains the dissolved pellet in 6 M guanidine hydrochloride solution. Top fractions 1–2 contained Aβ-monomers, fractions 4–6 contained the Aβ-oligomers, which are of special interest, and the bottom fractions 11–14 contained high molecular weight (co-)precipitates or aggregated Aβ. Aβ(1-42) or D/I Aβ concentrations of each fraction were determined via analytical RP-HPLC and UV absorbance detection at 214 nm.

4.2.4. Proteolytic Stability

Both compounds have already been extensively studied with respect to their in vivo pharmacokinetic profiles [15,22]. Here, we performed some additional test to investigate the proteolytic stability of the compounds in simulated gastric (SGF) and intestinal fluid (SIF) and human plasma and human liver microsomes. The experiments were performed as described previously [28]. According to the guidelines of the European Pharmacopoeia

7.0, SGF and SIF were prepared. Plasma was purchased from Biotrend with K3-EDTA as an anticoagulant (Biotrend, Köln, Germany). Human liver microsomes were pooled from different donors and purchased from Sekisui XenoTech (Kansas City, KS, USA).

In order to determine whether the compounds RD2D3 and cRD2D3 are stable or would be metabolized, 150 µM of each compound was incubated in triplicate for defined time points slightly shaking at 37 °C in the media described above (SGF and SIF: 4 and 8 h, plasma: 8, 24 and 48 h and microsomes: 8 and 24 h). Incubation was stopped by precipitating the proteins. For this, 3% trichloroacetic acid (*w*/*v*) was added to the respective sample under vortexing followed by a centrifugation step (14,000× *g* at 4 °C for 5 min). For analysis, supernatants containing the compounds were collected. The precipitated media without compound was used as a control and as reference for the quantification served each medium with compound where the reaction was stopped immediately by precipitating the proteins. All samples were analyzed by RP-HPLC as previously described [28].

4.3. In Vivo Efficacy

4.3.1. Animals

In this study, the Tg-SwDI AD mouse model was used. Tg-SwDI were first described by Davis et al. in 2004 and carried the human APP gene (isoform 770) with the Swedish (K670N/M671L), Dutch (E693Q) and Iowa (D694N) mutations under the control of the mouse Thy1 promoter [24]. Aβ-depositions can be found starting with three months of age and cognition deficits can be detected as early as three months of age in the Barnes maze [24,26]. Tg-SwDI mice are known to show distinct AD-associated pathology. This includes Aβ-deposition in various areas of the brain (particularly in the cortex and hippocampus) and associated gliosis. Gliosis is characterized by the presence of activated microglia and astrocytes, especially in those regions where Aβ-deposits are also found. In addition to Aβ-deposits in the tissue, this mouse model is particularly characterized by a so-called cerebral amyloid angiopathy (CAA). This means that Tg-SwDI mice show increased Aβ-deposits in cerebral vessels.

Tg-SwDI mice were ordered by the Jackson Laboratory (C57BL/6-Tg(Thy1-APPSwDutIowa)BWevn/Mmjax, Jackson Laboratory, Bar Harbor, ME, USA) and bred in-house in a controlled environment on a light/dark cycle (12/12 h), with 54% humidity and a temperature of 22 °C. Food and water were available ad libitum.

4.3.2. Ethical Approval

All animal experiments were done in accordance with the German Law on the protection of animals and approved by the Landesamt für Natur, Umwelt und Verbraucherschutz (LANUV) North-Rhine-Westphalia, Germany (AZ84-02.04.2016.A523).

4.3.3. Characterization

In order to perform a short in-house characterization of the Tg-SwDI mouse model, we used 12 months old female homozygous (n = 12) and corresponding wild type (n = 13) mice to verify cognition deficits at the same age at which the treatment study should be performed. Mice were tested in several behavioral tests to identify differences between Tg-SwDI and WT mice.

4.3.4. Nesting Behavior

Building a nest is a core behavior of mice, not just for maternal nesting. It is crucial for mice for shelter from the environment and protection against predators. Here, a protocol after Deacon was used. In brief, 1 h before the dark phase of the animal house, mice were single placed in a new cage with a fresh nestlet (Sniff, Soest, Germany). The next morning, built nests were scored from 1 to 5, whereby 1 represents no nest and 5 represents a perfect nest [29].

4.3.5. Marble Burying

Digging and burrowing is a fundamental behavior of mice to find and hide food and to build a nest. Several drugs or genetic modifications may alter the digging behavior of mice. For analysis of digging behavior, the marble burying test was performed after Deacon. Mice were single placed in a new cage with approximately 5 cm deep wood chip bedding. On the bedding, 12 glass marbles (diameter: 1.6 cm and weight: 5.3 g) were laid down in a predefined pattern. After 30 min, the number of marbles buried was counted [30].

4.3.6. Open Field Test

Analysis of explorative and anxiety related behavior of mice can be done by use of the so-called open field test [31]. Following a 30 min habituation phase in the experiment's room, the mice were placed in a square-shaped arena (45 cm × 45 cm × 45 cm) for an additional 30 min, imaginarily divided into two zones: center and border zone (center: 19 cm × 19 cm and border: space around the center zone). During the 30 min exploration, mice were recorded with a camera driven tracking system (Ethovision 15, Noldus, Wageningen, The Netherlands). For analysis, the duration the mice stayed in each zone was evaluated. Moreover, several time slots (1: 0–5 min, 2: 5–10 min, 3: 10–15 min, 4: 15–20 min and 5: 20–25 min) were analyzed independently to determine habituation behavior of the mice.

4.3.7. Morris Water Maze

Investigation of spatial learning can be conducted by the use of the MWM. The MWM is one of the most widely used tests to investigate cognitive impairments, especially spatial memory, in neuroscience [32]. The water maze we have used consists of a circular white pool (120 cm in diameter and 60 cm in height). Rendering of the water was ensured by adding a non-toxic white coloring solution. To conduct the test, the pool is imaginarily subdivided into four quadrants (north-east, south-east, south-west and north-west). In the middle of the target quadrant, an invisible round platform was placed 1 cm below the surface. The used protocol was modified after the original one from Morris et al. [33]. During the training period, mice were allowed to swim for 60 s or until they found the hidden platform. If they did not find the hidden platform, they were set on the platform for 10 s to orient themselves before they were returned to their cages. On each of the five training days, the mice had to swim four trials, each trial starting from a different quadrant, with the order changing each day. To avoid a decrease of body temperature of the mice, they were placed under a heating lamp for 60 s between each trial. On the sixth day, the mice had to swim freely without a hidden platform (probe trial). During each trial, the mice were recorded with a video driven tracking system (Ethovision 15, Noldus, Wageningen, The Netherlands). The following parameters were analyzed: escape latency to find the hidden platform during the training phase or duration in platform zone during the probe trial.

4.4. Treatment

Eleven months old Tg-SwDI were treated for 28 d i.p. by use of an osmotic minipump (Alzet osmotic pumps, Modell 1004, Charles River, Wilmington, MS, USA) with a daily dosage of 8 mg/kg peptide (RD2D3 (n = 14) or cRD2D3 (n = 12)) in PBS (pH 7.4) or vehicle (Placebo (n = 13), PBS, pH 7.4). The minipumps and the i.p. application route have been used to achieve continuous application of the study drug. After surgery, mice were monitored daily the following three days and twice each week until the end of the treatment. A loss of body weight and severe conspicuities were defined as exclusion criteria. No mouse was affected by these exclusion criteria. During the last one and a half weeks of treatment, different behavioral tests (nesting behavior, marble burying, open field test and MWM) were conducted with all mice.

Since RD2D3 did not show any efficacy in vivo after oral administration [12], but after i.p. administration [14], we decided to perform an i.p. treatment study for the direct comparison of the linear and cyclic D-peptide.

4.5. Histology

After the treatment duration was finished, the mice were anesthetized (intraperitoneal injection of 100 mg/kg ketamine (bela-pharm, Vechta, Germany) and 0.3 mg/kg medetomidine (Dormilan, alfavet, Neumünster, Germany) and transcardially perfused with ice-cold PBS. Subsequently, brains were removed and one hemisphere was frozen. The other hemisphere was fixed overnight in 4% paraformaldehyde, followed by a post-fixation and cryoprotection in 30% sucrose for an additional day. For histological analysis, 40 µm free floating sections were prepared on a cryostat. In total, eight series of six sections each were cut sagittally through the brain. One series of each brain was used for the following stainings: 6E10 (Biolegend, San Diego, CA, USA) for Aβ-deposits, GFAP (Agilent, Santa Clara, CA, USA) for reactive astrocytes and Iba-1 (Fujifilm, Neuss, Germany) for activated microglia. In brief, sections were washed in TBST (TBS with 1% Triton X-100), followed by an overnight incubation with the primary antibody (6E10 1 µg/mL, GFAP 1 µg/mL and Iba-1 0.5 µg/mL). The very next day, sections were washed in TBST, followed by the incubation with the secondary antibody (6E10 goat anti-Mouse IgG (H + L) secondary antibody 1.3 µg/mL, GFAP and Iba-1 goat anti-rabbit IgG (H + L) secondary antibody, 1.5 µg/mL, all Thermo Fisher, Germany) for 2 h at RT. After an additional washing step in TBST, stainings were visualized with the use of 3,3′ diaminobenzidine (DAB) enhanced with saturated nickel ammonium sulphate solution. Afterwards, sections were mounted with DPX Mountant (Sigma-Aldrich, Darmstadt, Germany).

To avoid any irregularities in the staining results, all stainings were performed in one batch and in one microscopy session. Zeiss SteREO Lumar V12 microscope and the according software (Zeiss AxioVision 6.4 RE) was used for visualization. Quantification was done with ImageJ (NIH, USA) and CellProfiler (Broad Institute, Cambridge, MA, USA).

4.6. Statistics

All statistical analyses were performed using GraphPad Prism 8 (GraphPad Software, Inc., San Diego, CA, USA) or SigmaPlot Version 11 (Systat Software, Düsseldorf, Germany). In vitro data are represented as mean ± SD and in vivo data as mean ± SEM. Normal distributed data were analyzed by use of an unpaired one- or two-tailed *t*-test or one-way analysis of variance (ANOVA) with Tukey post hoc analysis. Not normal distributed data were analyzed by use of the Kruskal–Wallis test with Dunn's multiple comparison test. The MWM and open field test were analyzed by a repeated measure ANOVA with Fisher or Bonferroni post hoc analysis. Data with $p < 0.05$ were stated as significant.

5. Conclusions

In this study, we analyzed the in vitro potency of two of our developed D-enantiomeric D-peptides on an artificial contribution of two familial mutations within the Aβ sequence, namely the Dutch and Iowa mutations, for the first time. The analysis of the in vitro profile revealed that RD2D3 and cRD2D3 have a similar potency on both analyzed Aβ-species, regarding the potency to inhibit the Aβ-fibril formation and the potency to eliminate toxic Aβ-oligomers. Referring to the hypothesis that a cyclization of our D-peptides might show superior in vivo efficacy could not be confirmed in this study. Compared to linear RD2D3, cyclic cRD2D3 failed to show superior efficacy.

Author Contributions: The overall study was planned by S.S. and D.W. In vivo study was planned by S.S., D.W., J.K., and A.W. In vitro experiments were carried out by I.G. and S.S. In vivo experiments were done by D.H. and L.C.C. Histological analysis were done by D.H. and S.S. Data were analyzed by S.S. All authors contributed to writing. All authors have read and agreed to the published version of the manuscript.

Funding: D.W. was supported by grants from the Russian Science Foundation (RSF) (project no. 20-64-46027), by the Technology Transfer Fund of the Forschungszentrum Jülich and was supported by "Portfolio Drug Research" of the "Impuls und Vernetzungs-Fonds der Helmholtzgemeinschaft.

Institutional Review Board Statement: All animal experiments were performed in accordance with the German Law on the protection of animals (TierSchG §§ 7–9) and were approved by a local ethics committee (LANUV, North-Rhine-Westphalia, Germany, reference number: Az: 84-02.04.2016.A523).

Data Availability Statement: The data presented in this study are available in this article.

Conflicts of Interest: D.W. declares to be the coinventor of patent applications describing the compounds used in the study. D.W. declares to be the cofounder and co-owner of the company Priavoid GmbH. This had no influence on the interpretation of the data. All other authors declare no conflict of interest.

References

1. Grande, G.; Qiu, C.; Fratiglioni, L. Prevention of dementia in an ageing world: Evidence and biological rationale. *Ageing Res. Rev.* **2020**, *64*, 101045. [CrossRef]
2. Hardy, J.; Selkoe, D.J. The amyloid hypothesis of Alzheimer's disease: Progress and problems on the road to therapeutics. *Science* **2002**, *297*, 353–356. [CrossRef] [PubMed]
3. Selkoe, D.J.; Hardy, J. The amyloid hypothesis of Alzheimer's disease at 25 years. *EMBO Mol. Med.* **2016**, *8*, 595–608. [CrossRef] [PubMed]
4. Cline, E.N.; Bicca, M.A.; Viola, K.L.; Klein, W.L. The Amyloid-β Oligomer Hypothesis: Beginning of the Third Decade. *J. Alzheimer's Dis.* **2018**, *64*, S567–S610. [CrossRef] [PubMed]
5. Willbold, D.; Kutzsche, J. Do We Need Anti-Prion Compounds to Treat Alzheimer's Disease? *Molecules* **2019**, *24*, 2237. [CrossRef]
6. van Groen, T.; Wiesehan, K.; Funke, S.A.; Kadish, I.; Nagel-Steger, L.; Willbold, D. Reduction of Alzheimer's disease amyloid plaque load in transgenic mice by D3, A D-enantiomeric peptide identified by mirror image phage display. *ChemMedChem* **2008**, *3*, 1848–1852. [CrossRef] [PubMed]
7. Van Regenmortel, M.H.; Muller, S. D-peptides as immunogens and diagnostic reagents. *Curr. Opin. Biotechnol.* **1998**, *9*, 377–382. [CrossRef]
8. Dintzis, H.M.; Symer, D.E.; Dintzis, R.Z.; Zawadzke, L.E.; Berg, J.M. A comparison of the immunogenicity of a pair of enantiomeric proteins. *Proteins Struct. Funct. Bioinform.* **1993**, *16*, 306–308. [CrossRef]
9. Kutzsche, J.; Jürgens, D.; Willuweit, A.; Adermann, K.; Fuchs, C.; Simons, S.; Windisch, M.; Hümpel, M.; Rossberg, W.; Wolzt, M.; et al. Safety and pharmacokinetics of the orally available antiprionic compound PRI-002: A single and multiple ascending dose phase I study. *Alzheimer Dement. Transl. Res. Clin. Interv.* **2020**, *6*, e12001. [CrossRef]
10. van Groen, T.; Schemmert, S.; Brener, O.; Gremer, L.; Ziehm, T.; Tusche, M.; Nagel-Steger, L.; Kadish, I.; Schartmann, E.; Elfgen, A.; et al. The Abeta oligomer eliminating D-enantiomeric peptide RD2 improves cognition without changing plaque pathology. *Sci. Rep.* **2017**, *7*, 16275. [CrossRef]
11. Schemmert, S.; Schartmann, E.; Zafiu, C.; Kass, B.; Hartwig, S.; Lehr, S.; Bannach, O.; Langen, K.; Shah, N.J.; Kutzsche, J.; et al. Abeta Oligomer Elimination Restores Cognition in Transgenic Alzheimer's Mice with Full-blown Pathology. *Mol. Neurobiol.* **2019**, *56*, 2211–2223. [CrossRef]
12. Kutzsche, J.; Schemmert, S.; Tusche, M.; Neddens, J.; Rabl, R.; Jürgens, D.; Brener, O.; Willuweit, A.; Hutter-Paier, B.; Willbold, D. Large-Scale Oral Treatment Study with the Four Most Promising D3-Derivatives for the Treatment of Alzheimer's Disease. *Molecules* **2017**, *22*, 1693. [CrossRef]
13. Schemmert, S.; Schartmann, E.; Honold, D.; Zafiu, C.; Ziehm, T.; Langen, K.-J.; Shah, N.J.; Kutzsche, J.; Willuweit, A.; Willbold, D. Deceleration of the neurodegenerative phenotype in pyroglutamate-Abeta accumulating transgenic mice by oral treatment with the Abeta oligomer eliminating compound RD2. *Neurobiol. Dis.* **2019**, *124*, 36–45. [CrossRef] [PubMed]
14. Cavini, I.A.; Munte, C.E.; Erlach, M.B.; van Groen, T.; Kadish, I.; Zhang, T.; Ziehm, T.; Nagel-Steger, L.; Kutzsche, J.; Kremer, W.; et al. Inhibition of amyloid Aβ aggregation by high pressures or specific d-enantiomeric peptides. *Chem. Commun.* **2018**, *54*, 3294–3297. [CrossRef] [PubMed]
15. Leithold, L.H.E.; Jiang, N.; Post, J.; Niemietz, N.; Schartmann, E.; Ziehm, T.; Kutzsche, J.; Shah, N.J.; Breitkreutz, J.; Langen, K.-J.; et al. Pharmacokinetic properties of tandem d-peptides designed for treatment of Alzheimer's disease. *Eur. J. Pharm. Sci.* **2016**, *89*, 31–38. [CrossRef] [PubMed]
16. Ziehm, T.; Brener, O.; Van Groen, T.; Kadish, I.; Frenzel, D.; Tusche, M.; Kutzsche, J.; Reiß, K.; Gremer, L.; Nagel-Steger, L.; et al. Increase of Positive Net Charge and Conformational Rigidity Enhances the Efficacy of d-Enantiomeric Peptides Designed to Eliminate Cytotoxic Aβ Species. *ACS Chem. Neurosci.* **2016**, *7*, 1088–1096. [CrossRef]
17. Schartmann, E.; Schemmert, S.; Niemietz, N.; Honold, D.; Ziehm, T.; Tusche, M.; Elfgen, A.; Gering, I.; Brener, O.; Shah, N.J.; et al. In Vitro Potency and Preclinical Pharmacokinetic Comparison of All-D-Enantiomeric Peptides Developed for the Treatment of Alzheimer's Disease. *J. Alzheimer Dis.* **2018**, *64*, 859–873. [CrossRef]

18. Brener, O.; Dunkelmann, T.; Gremer, L.; Van Groen, T.; Mirecka, E.A.; Kadish, I.; Willuweit, A.; Kutzsche, J.; Jürgens, D.; Rudolph, S.; et al. QIAD assay for quantitating a compound's efficacy in elimination of toxic Aβ oligomers. *Sci. Rep.* **2015**, *5*, 13222. [CrossRef]
19. Alzheimer, A. Concerning unsual medical cases in old age. *Z. Gesamte Neurol. Psychiatr.* **1911**, *4*, 356–385. [CrossRef]
20. Scheltens, P.P.; De Strooper, B.; Kivipelto, M.; Holstege, H.; Chételat, G.; Teunissen, C.E.; Cummings, J. Alzheimer's disease. *Lancet* **2021**, *397*, 1577–1590. [CrossRef]
21. Li, S.; Selkoe, D.J. A mechanistic hypothesis for the impairment of synaptic plasticity by soluble Aβ oligomers from Alzheimer's brain. *J. Neurochem.* **2020**, *154*, 583–597. [CrossRef]
22. Schartmann, E.; Schemmert, S.; Ziehm, T.; Leithold, L.H.E.; Jiang, N.; Tusche, M.; Shah, N.J.; Langen, K.-J.; Kutzsche, J.; Willbold, D.; et al. Comparison of blood-brain barrier penetration efficiencies between linear and cyclic all-d-enantiomeric peptides developed for the treatment of Alzheimer's disease. *Eur. J. Pharm. Sci.* **2018**, *114*, 93–102. [CrossRef]
23. Klein, A.N.; Ziehm, T.; van Groen, T.; Kadish, I.; Elfgen, A.; Tusche, M.; Thomaier, M.; Reiss, K.; Brener, O.; Gremer, L.; et al. Optimization of d-Peptides for Abeta Monomer Binding Specificity Enhances Their Potential to Eliminate Toxic Abeta Oligomers. *ACS Chem. Neurosci.* **2017**, *8*, 1889–1900. [CrossRef]
24. Davis, J.; Xu, F.; Deane, R.; Romanov, G.; Previti, M.L.; Zeigler, K.; Zlokovic, B.V.; van Nostrand, W.E. Early-onset and robust cerebral microvascular accumulation of amyloid beta-protein in transgenic mice expressing low levels of a vasculotropic Dutch/Iowa mutant form of amyloid beta-protein precursor. *J. Biol. Chem.* **2004**, *279*, 20296–20306. [CrossRef] [PubMed]
25. Miao, J.; Xu, F.; Davis, J.; Otte-Höller, I.; Verbeek, M.M.; van Nostrand, W.E. Cerebral microvascular amyloid beta protein deposition induces vascular degeneration and neuroinflammation in transgenic mice expressing human vasculotropic mutant amyloid beta precursor protein. *Am. J. Pathol.* **2005**, *167*, 505–515. [CrossRef]
26. Xu, F.; Grande, A.M.; Robinson, J.K.; Previti, M.L.; Vasek, M.; Davis, J.; van Nostrand, W.E. Early-onset subicular microvascular amyloid and neuroinflammation correlate with behavioral deficits in vasculotropic mutant amyloid beta-protein precursor transgenic mice. *Neuroscience* **2007**, *146*, 98–107. [CrossRef] [PubMed]
27. Robison, L.S.; Francis, N.; Popescu, D.L.; Anderson, M.E.; Hatfield, J.; Xu, F.; Anderson, B.J.; Van Nostrand, W.E.; Robinson, J.K. Environmental Enrichment: Disentangling the Influence of Novelty, Social, and Physical Activity on Cerebral Amyloid Angiopathy in a Transgenic Mouse Model. *Int. J. Mol. Sci.* **2020**, *21*, 843. [CrossRef] [PubMed]
28. Elfgen, A.; Santiago-Schübel, B.; Gremer, L.; Kutzsche, J.; Willbold, D. Surprisingly high stability of the Aβ oligomer eliminating all-d-enantiomeric peptide D3 in media simulating the route of orally administered drugs. *Eur. J. Pharm. Sci.* **2017**, *107*, 203–207. [CrossRef]
29. Deacon, R.M.J. Assessing nest building in mice. *Nat. Protoc.* **2006**, *1*, 1117–1119. [CrossRef] [PubMed]
30. Deacon, R.M.J. Digging and marble burying in mice: Simple methods for in vivo identification of biological impacts. *Nat. Protoc.* **2006**, *1*, 122–124. [CrossRef]
31. Archer, J. Tests for emotionality in rats and mice: A review. *Anim. Behav.* **1973**, *21*, 205–235. [CrossRef]
32. Paulson, J.B.; Ramsden, M.; Forster, C.; Sherman, M.A.; McGowan, E.; Ashe, K.H. Amyloid plaque and neurofibrillary tangle pathology in a regulatable mouse model of Alzheimer's disease. *Am. J. Pathol.* **2008**, *173*, 762–772. [CrossRef] [PubMed]
33. Morris, R.G.M.; Garrud, P.; Rawlins, J.N.P.; O'Keefe, J. Place navigation impaired in rats with hippocampal lesions. *Nature* **1982**, *297*, 681–683. [CrossRef] [PubMed]

3.3. **Sex-related motor deficits in the Tau-P301L mouse model**

Authors: Luana Cristina Camargo, Dominik Honold, Robert Bauer, N. Jon Shah, Karl-Josef Langen, Dieter Willbold, Janine Kutzsche, Antje Willuweit, Sarah Schemmert

Journal: Biomedicines, submitted on July 29th, 2021

DOI:

Impact Factor: 6.081 (2020)

Contribution: Performance and analysis of the behavioral tests;
Performance and analysis of histological experiments;
Writing of the original draft and the manuscript revision.

biomedicines

MDPI

Article

Sex-related motor deficits in the Tau-P301L mouse model

Luana Cristina Camargo[1,2], Dominik Honold[1], Robert Bauer[1], N. Jon Shah[3,4,5], Karl-Josef Langen[3,6], Dieter Willbold[1,2], Janine Kutzsche[1], Antje Willuweit[3], Sarah Schemmert[1,*]

[1] Institute of Biological Information Processing, Structural Biochemistry (IBI-7), Forschungszentrum Jülich, 52425 Jülich, Germany; l.camargo@fz-juelich.de (L.C.C.); d.honold@fz-juelich.de (D.H.); d.willbold@fz-juelich.de (D.W.); j.kutzsche@fz-juelich.de (J.K.); s.schemmert@fz-juelich.de (S.S.); Robert.Bauer@hhu.de

[2] Institut für Physikalische Biologie, Heinrich-Heine-Universität Düsseldorf, 40225 Düsseldorf, Germany

[3] Institute of Neuroscience and Medicine, Medical Imaging Physics (INM-4), Forschungszentrum Jülich, 52425 Jülich, Germany; a.willuweit@fz-juelich.de

[4] JARA-Brain-Translational Medicine, JARA Institute Molecular neuroscience and neuroimaging, 52062 Aachen, Germany

[5] Department of Neurology, RWTH Aachen University, 52062 Aachen, Germany; n.j.shah@fz-juelich.de (N.J.S.);

[6] Department of Nuclear Medicine, RWTH Aachen University, 52062 Aachen, Germany; k.j.langen@fz-juelich.de (K.-J.L.)

* Correspondence: s.schemmert@fz-juelich.de; Tel.: +49-2461-619447

Abstract: The contribution of mouse models for basic and translational research at different levels is important to understand neurodegenerative diseases, including tauopathies, by studying the alterations in the corresponding mouse models in detail. Moreover, several studies demonstrated that pathological as well as behavioral changes are influenced by the sex. For this purpose, we performed an in-depth characterization of the behavioral alterations in the transgenic Tau-P301L mouse model. Sex-matched wild type and homozygous Tau-P301L mice were tested in a battery of behavioral tests at different ages. Tau-P301L male mice showed olfactory and motor deficits as well as increased Tau pathology, which was not observed in Tau-P301L female mice. Both Tau-P301L male and female mice had phenotypic alterations in the SHIRPA test battery and cognitive deficits in the novel object recognition test. This study demonstrated that Tau-P301L mice have phenotypic alterations, which are in line with the histological changes and with a sex-dependent performance in those tests. Summarized, the Tau-P301L mouse model shows phenotypic alterations due to the presence of neurofibrillary tangles in the brain.

Keywords: tauopathy; Tau-P301L mouse models; behavior; phosphorylated Tau, motor deficits, cognitive deficits, sex-related deficits.

Citation: Lastname, F.; Lastname, F.; Lastname, F. Title. *Biomedicines* **2021**, *9*, x. https://doi.org/10.3390/xxxxx

Academic Editor: Firstname Lastname

Received: date
Accepted: date
Published: date

1. Introduction

Tau protein is a microtubule associated protein, located in the axons, which plays a major role in the stabilization of microtubules [1] and trafficking [2-4]. It is expressed by the microtubule associated protein Tau (*MAPT*) gene located on the chromosome 17. In total, six isoforms can be produced by the presence/absence of exon 2, 3 (N-terminal) and 10 (microtubule-binding domain). Therefore, the isoform expression varies from 0N3R, which is the shortest form, to 2N4R, which is the longest form. In humans, the 3R is more frequent during the development, while both, 3R and 4R, are present in similar amount in the adult brain [5, 6]. Phosphorylation of the Tau protein can occur at different sites by different kinases, a process that assists in Tau physiological function. Under pathological conditions, the Tau binding site to the microtubules is hyperphosphorylated and results

in loss of its function. Hyperphosphorylated Tau then assembles into paired helical filament (PHF) forming the neurofibrillary tangles (NFTs) in the dendrites [7, 6]. Pathological Tau is present in different neurodegenerative diseases called tauopathies.

Tauopathies in turn are a heterogeneous class of diseases that can be classified as primary and secondary tauopathies. In secondary tauopathies, the presence of NFTs occurs as a second event probably due to the toxicity downstream of another event, e.g. aggregation of amyloid-β (Aβ) into neuritic plaques in Alzheimer's disease (AD). In primary tauopathies, the presence of NFTs occurs first and is mainly responsible for the arising neurodegeneration, e.g. in frontotemporal dementia (FTD)[8]. In those dementias, the formation of NFTs in a specific region is correlated with progression of the disease and brain atrophy [9, 10]. Considering that brain atrophy and cognitive deficits are a consequence of neurodegeneration and synaptic dystrophy, it is postulated that the presence of NFTs induce synaptic deficits and neurodegeneration [11, 12]. Besides in dementias, pathological Tau can also be found in patients with epilepsy, chronic traumatic encephalopathy and other neurological disorders [13]. Similar to AD, most of the FTDs and other tauopathies are sporadic and, unlike AD, different mutations can cause the familial FTDs. The mutations in the *MAPT* gene are genetic causes of FTDs with parkinsonism linked to chromosome 17 (FTDP-17) [14, 15]. Those mutations prevent Tau from binding to microtubules due to the hyperphosphorylation [16].

Many transgenic mouse models have been developed with different Tau mutations. Those models provide a more detailed understanding of how hyperphosphorylated Tau and NFTs affect the pathophysiology, depending on the type of mutation and the isoform. The most common transgenic models of tauopathy are constructed with the human Tau-P301L mutation [17], [18]. The Tau-P301L mouse models only include the 4R Tau isoform, since this mutation is located in the exon 10. Terwel and collaborators [19] developed a transgenic mouse model expressing human Tau-P301L (homozygous) under the regulation of a *thy1* gene promoter at moderate levels. This mouse model did not develop severe motor deficits, but a strong paralysis in the limbs, starting at nine months of age. They died before the age of 12 months due to respiratory problems [19, 20]. Moreover, Tau-P301L mice showed NFTs at nine months of age in the brainstem and cortex [19]. The presence of NFTs in different areas of the brainstem was postulated to be the cause of the respiratory deficits and the strong moribund conditions [20]. At earlier ages, this mouse model also showed increased long-term potentiation (LTP) in the dentate gyrus (DG) [21].

Nowadays, mouse models are considered a method to represent human disease and to test newly developed substances to treat it. Mouse models, especially for neurodegenerative diseases, are coming under criticism, in part because many clinical trials failed even though the compounds did previously show promising results in animal models. Very often in these cases, however, treatment studies in mice often had an insufficient study design, which does not mimic the human situation very well. It is essential to know your animal model as good as possible, especially concerning the selection of behavioral tests and to characterize them in longitudinal studies, instead of just analyzing deficits at one certain age, and to do this also in a sex-specific manner. The objective of this study was to carry out a longitudinal and sex-related characterization of the Tau-P301L model to clarify the onset of the disease with a broader behavioral test battery and to have an in-depth understanding about the deficits of the model. As described before, the Tau-P301L model was evaluated in few behavior experiments (beam walk, rotarod and novel object recognition) and some studies were cross-sectional. A longitudinal study is advantageous since the onset of each behavior deficit occur at different time points; therefore, the cross-sectional studies have limited information regarding the course of the disease. Thus, the present study focused on the characterization of general, motor and cognitive alterations

induced by the pathological Tau in the Tau-P301L mouse model at different ages and sexes.

2. Materials and Methods

2.1. Animals

Tau-P301L mice were first described by Terwel et al [19] and were backcrossed from a FVB to a C57BL/6J background. Mice were maintained in a homozygous colony. In this study, we compared homozygous Tau-P301L mice with age and sex-matched wild type (WT) mice from a parallel breeding.

Mice were bred in-house with a 12/12 h light/dark cycle. In each cage, 3 to 5 mice were housed and food and water were available *ad libitum*. All behavioral experiments were approved by the responsible authorities (*Landesamt für Natur, Umwelt und Verbraucherschutz (LANUV)*, North Rhine-Westphalia, Germany, number 84-02.04.2014.A362, 81-02.04.2018.A400, 81-02.04.2019.A304 approval was received on 05/02/2019, 21/02/2019 and 21/01/2019, respectively) and were performed longitudinal at different ages (2, 4, 6 and 8 months). For all behavioral tests, seven female and 12 male mice of both genotypes were included.

2.2. Behavioral tests

2.2.1. Habituation/dishabituation olfactory test

Olfactory deficits from Tau-P301L mice were evaluated by performing the habituation/dishabituation olfactory test [22]. Three different aromas (bacon, cheesecake and hazelnut) (Perfumer's Apprentice, Scotts Valley, USA) were sprayed on a cotton pad which was placed into an embedding cassette. The bacon aroma was placed in the cage for 24 h before the test for habituation. Later, the bacon aroma was presented again to the mice for six times for 30 s each. Next, the bacon aroma was replaced by cheesecake and hazelnut aroma once (30 s each). The time that the mice sniffed the embedding cassette was taken for analysis.

2.2.2. Nesting behavior test

Nesting behavior was performed as previously described [23]. One hour before the dark cycle of the animal facility, the mice were single caged with new nesting material. On the next morning, the built nest was scored from 1 to 5, whereby 1 was no nest and 5 was a complete built nest.

2.2.3. Marble burying test

In the marble burying test [24], mice were placed in a cage with 5 cm of bedding material with 12 equally distant marbles for 30 min, which were placed on the top of the bedding material. Later, the mice were placed back in the habituation cage and the number of marbles each mouse had buried was counted for analysis.

2.2.4. SHIRPA test battery

To evaluate the phenotypic alterations of Tau-P301L mice in comparison to the WT mice, the SmithKline Beecham Pharmaceuticals; Harwell, MRC Mouse Genome Centre and Mammalian Genetics Unit; Imperial College School of Medicine at St Mary's; Royal London Hospital, St Bartholomew's and the Royal London School of Medicine; Phenotype

Assessment (SHIRPA)-test battery was performed (protocol adapted from [25]). In this test, the different parameters described in table 1 were evaluated in a scoring system from 0 to 3 (0 = no alteration; 1 = slightly altered; 2 = altered; 3 = strongly altered).

Table 1: Evaluated Parameter on the SHIRPA test.

Parameters	Description
Restlessness	Difficulty staying in one body position for an extended period of time
Apathy	Motionless and lowered head
Stereotyped behaviour	
Convulsion	
Abnormal body carriage	Body posture
Alertness	Response to object proximity
Abnormal gait	Uncommon walk, e.g. paddling, waddling, running
Startle response	Response to an acoustic signal
Loss of righting reflex	Time when the mouse return to standing position when turned on its back
Touch response	
Pinna reflex	
Cornea reflex	
Forelimb placing reflex	Response to stretch their front paws when hanged in proximity to the surface
Hanging behaviour	Mouse stay on the rod or fall
Pain response	Response to tail pinch
Grooming	Overall fur condition

2.2.5. Open field test

In the open field test, mice were placed in a cubicle arena (40 cm) for 30 min. During this time, mice were allowed to freely explore the arena, imaginarily divided into different zones (border, center, corner). For evaluation, a tracking software was used (EthoVision XT15, Noldus Information Technology, Wageningen, The Netherlands). The following parameters were analyzed: velocity, locomotion, exploration time, time spent in center, border and corner zone.

2.2.6. Accelerating Rotarod

The accelerating Rotarod (Ugo Basile, Gemonio, Italy) test consisted of 4 trials. In the first trial, the mice were placed onto the rod and should stay there for at least 60 s at 10 rpm (habituation to the apparatus). If they fell, the trial was repeated. In the last three trials, the mice should stay on the rod for 300 s at 4 to 40 rpm. For evaluation, the latency time to fall was noted and the mice were placed back into their home cages. Three sessions in each trial with an interval of 15 min were performed [26].

2.2.7. Modified pole test

In order to gain a deeper understanding of the developed motor deficits, a modified version of the so-called pole test was performed [27]. For this, mice were placed facing down on the top of a pole and the way they walk down was scored three times. The scoring system was: 0 = running, 1 = partly running, 2 = slipped and 3 = fallen. This procedure was repeated three times with an interval of 15 min between each trial. For the final evaluation, the sum of the three scores was calculated.

2.2.8. Novel object recognition test

For the novel object recognition test (NOR), two identical objects (familiar object) were presented to the mice during 10 min in the same arena used for the open field test. In the intertrial interval of 20 min, the mice were placed back in their home cages. Afterwards, the mice were placed back into the arena where one familiar object was replaced by a new object (novel object). The time of exploration was evaluated as the time the mouse spent with the nose at least 2 cm from the object. This was analysed by EthoVision XT15 (Noldus Information Technology, Wageningen, The Netherlands).

For evaluation, the discrimination index was calculated by the following formula: $\frac{Tnovel-Tfamiliar}{Tnovel+Tfamiliar}$, which *Tnovel* was the time the mice explored the novel object and *Tfamiliar* the time the mice explore the familiar object.

2.2.9. T-maze spontaneous alternation

In the T- maze spontaneous alternation [28], the mice were placed in the start arm in an arena with three arms (start, left and right arm) (31 cm x 10 cm) in a "T" format. In the first trial, only the left or right arm was free to be explored and the opposite one was closed by a gate. Once the mice came back to the start arm, both arms were free to be explored and the second trial started. The same procedure was performed for 14 trials or a maximum of 15 min. If the mouse did not reach seven trials, it was excluded from the experiment.

The spontaneous alternation was calculated by the following formula: $\frac{number\ of\ correct\ choices}{total\ of\ trials}$. Correct choices are considered as the alternations from the opposite arm which the mouse previously entered.

2.2.10. Fear conditioning test

In order to evaluate the associative memory deficits, the cued and contextual fear conditioning was performed [29] starting with 4 months of age. On the habituation day, mice were placed in the apparatus (Ugo Basile, Gemonio, Italy) for 120 s of habituation. Afterwards, a sound (50%; 2000 Hz) was presented for 30 s and during the last 2 s, a mild shock (0.35 mA) was also given. The mice stayed in the cage for additional 60 s before returning to their home cage.

On the next day, the contextual fear conditioning was evaluated. The mice were placed in the same cage for 5 min and neither the shock nor the sound were presented. After 25 min, the cued fear conditioning was evaluated. The walls and floor of the cage were changed and only the sound was presented three times to the mice. The freezing (%) was analyzed with a tracking software (EthoVision XT15, Noldus Information Technology, Wageningen, The Netherlands).

2.2.11. Morris water maze

The performance of the Morris water maze (MWM) [30] was divided into three stages: training, probe and reversal test. For the MWM training, the mice were placed in a pool (diameter of 120 cm x 60 cm height) filled with water divided into four quadrants (NE, NW, SE, SW) with a hidden platform (diameter of 10 cm x 31.5 cm height). An opaque non-toxic liquid was added into the water to prevent the mice from seeing the platform. For a maximum of 60 s, the mice had to find the hidden platform. In case the mice did not find it, they were placed onto the platform for 10 s for acquisition (to orientate themselves). This trial was then repeated four times per mouse. Also, at each trial, the mice were placed in a different start position. Those trials were performed for four consecutive days. On the fifth day, the platform was removed and the probe trial was performed. Moreover, the reversal test was also performed, similar to the training, for three consecutive days and the platform was placed in a different position (opposite position). Similar to the previous cognitive tests, the evaluation and tracking was analyzed by a tracking software (EthoVision XT15, Noldus Information Technology, Wageningen, The Netherlands). In the training and reversal test, the time the mice needed to find the hidden platform (escape latency) was analyzed. In the probe trial, the time spent in the platform zone was analyzed. The MWM was performed only at 8 months of age. One female mouse developed a forelimb paralysis and was therefore excluded from the MWM experiment.

2.3. Histology

After the performance of the last behavioral tests (MWM), mice were deeply anesthetized for tissue collection. The brains were snap frozen and one hemisphere was cut into 20 µm sagittal sections using a Cryotome (Leica Biosystems Nussloch GmbH, Wetzlar, Germany). Before the staining procedure, the brain slices were placed in 4% formalin and washed three times with TBS for 5 min. Antigen retrieval was performed in citrate buffer, pH 6 at 85 °C for 30 min and slides were washed three times with TBS for 5 min. In order to remove the endogenous peroxidases, the sections were incubated in 0.6% H_2O_2 in methanol for 15 min and washed once with deionized water and two times with TBS for 5 min. Then, the sections were blocked in 10% horse serum for 1 h and incubated overnight with the primary antibody (AT8 (1:500; MN1020, Thermo Fisher scientific, Waltham, MA, USA) or AT100 (1:500; MN1060, Thermo Fisher scientific, Waltham, MA, USA) in 1% horse serum in TBS at 4 °C. At the subsequent day, the sections were washed and incubated with the secondary antibody (biotinylated goat anti-mouse, 1:1000; Extra2, Sigma-Aldrich, Darmstadt, Germany) for 2 h. Afterwards, slides were again washed and incubated with ExtrAvidin® (1:1000; Extra2, Sigma-Aldrich, Darmstadt, Germany) for additional 2 h, followed by a washing step. Finally, the sections were colored with DAB and saturated nickel ammonium sulphate solution, washed, dehydrated in an ascending alcohol series and covered with DPX (Sigma-Aldrich, Darmstadt, Germany).

To evaluate neurodegeneration and neuroinflammation, the following staining procedure was done. The brain slides were placed in 4% formalin and washed three times with TBS-T (1% triton) for 5 min. Antigen retrieval was performed in 70% formic acid and slides were washed. In order to remove the endogenous peroxidases, the sections were incubated in 3% H_2O_2 in methanol solution for 15 min and washed. Then, the sections were incubated overnight with the primary antibody (NeuN (1:1000; Merck, Darmstadt, Germany) and GFAP (1:1000; MN1060, Thermo Fisher scientific, Waltham, MA, USA) in 3% BSA in TBS-T at 4 °C. On the next day, the sections were washed and incubated with the secondary antibody (biotinylated goat anti-rabbit, 1:1000; Thermo Fisher scientific, Dreieich, Germany) for 2 h. Afterwards, the same procedure was performed as described above. For the detection of reactive microglia (CD11b, 1:2000, Abcam, Berlin, Germany), the staining procedure was the same as previously described although the primary antibody was incubated in 1% normal goat serum (NGS) and 1% bovine serum albumin (BSA)

described to be present in most lines (for a review, see [30]). However, neurodegeneration, which is a typical feature of human AD, was only observed in a few transgenic amyloidosis models, including the TBA2.1 line [31]. In an attempt to generate an improved mouse model harboring a combination of AD-relevant hallmarks, i.e., the aggressive phenotype produced by pEAβ, an abundant formation of neuritic plaques and extensive cognitive decline, the novel TAPS mouse line was generated. This line was created by cross-breeding of heterozygous APP/PS1 and TBA2.1 mice and the phenotype of the resulting triple transgenic mice was followed over a period of 20 months in comparison to the parental lines. As a result, we demonstrate that by addition of pEAβ the amyloid pathology is further accelerated, with earlier onset and increased deposition of neuritic plaques in the brain. Furthermore, the TAPS mice displayed a faster and more pronounced cognitive decline in comparison to the parental lines. Due to its stronger phenotype the novel TAPS line has qualified itself as a useful new tool to study AD pathophysiology, and for preclinical studies testing new therapeutic options.

2. Results

2.1. TAPS Mice Accumulate Aβ Aggregates in the Striatum, Hippocampus, and Cortex as Early as 6 Months

TAPS mice were viable and fertile but showed a 14% increased rate of premature death in comparison to wild-type (WT) littermates. For comparison, APP/PS1 mice showed a 3% increased rate of premature death (Table S1). Both, TAPS and APP/PS1 mice, developed an increasing amyloid pathology with neuritic plaques in the brain over time. With an earlier onset, at the age of 6 months, TAPS mice showed plaque formation starting in the cortex, hippocampus, and also lateral striatum. Over time, all mentioned regions underwent a constant increase in plaque density, with the highest amounts in the cortex and slightly less Aβ plaques in the hippocampus. In APP/PS1 mice, visibly less plaque formation could be found at the same age in the cortex and emerged to the hippocampus with 9 months but with nearly no Aβ accumulation in the striatum. Overall, plaque formation in early ages was visibly lower than in the corresponding TAPS mice, and increasing in the cortex and hippocampus to a comparable level in later life. The cerebellum showed only little Aβ accumulation over time and accumulation in the thalamus could be observed in both genotypes. In contrast to the previously mentioned mouse lines, the TBA2.1 mice developed decent amounts of Aβ aggregates in the striatum, already at the age of 6 months and kept those levels until older ages. However, there was nearly no Aβ accumulation visible in brain regions other than the striatum.

To investigate the composition of the Aβ plaques in all mouse lines, a double staining was accomplished with antibodies against truncated pyroglutamate Aβ at position 3 (pE3Aβ) and total Aβ (antibody 6E10) in 24-month-old mice. TAPS and APP/PS1 mice showed an intense staining of plaques in the cerebral cortex for both, Aβ and pE3Aβ, as shown in Figure 1, and comparable results were found also in the hippocampus. It could be seen that compact neuritic plaques, as well as diffuse Aβ, were positively stained with 6E10 in both cases. Albeit the 6E10 signal was stronger, in diffuse Aβ, a minor portion of pE3Aβ could be observed as well, indicating a possibly lower content of those truncated Aβ species than full-length Aβ in diffuse accumulations. In compact plaques, however, pE3Aβ was more prominent in the center core of the plaques than in the surrounding. In principle, the overall plaque morphology and distribution of pE3Aβ in the cortex and hippocampus was comparable between TAPS and APP/PS1 mice. TBA2.1 mice, however, showed no visible Aβ accumulation in the cortex, as well as in the hippocampus, and were not distinguishable from WT mice in those regions. Differences, however, could be seen in the striatum (caudate putamen) of the mouse lines, which are shown in Figure 2.

p = 0.0139, respectively). Tau-P301L male mice were not able to discriminate the cheesecake and hazelnut from the bacon aroma. At 6 months of age, unlike Tau-P301L male mice, the Tau-P301L female mice did not show any olfactory deficits (Fig 1).

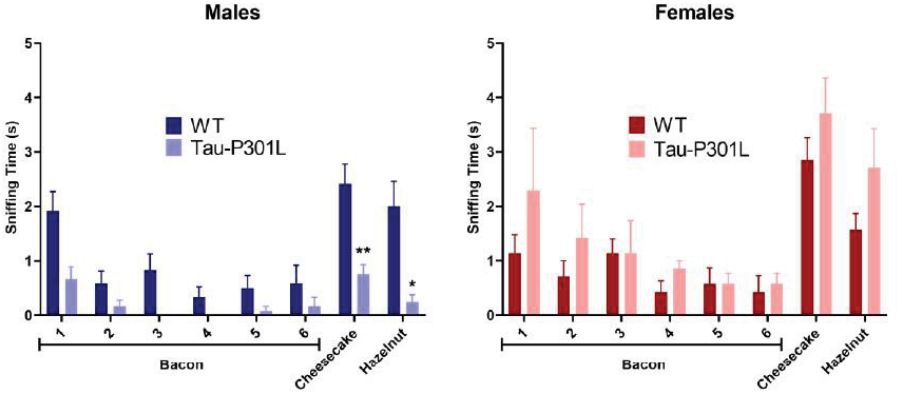

Figure 1: Tau-P301L mice develop olfactory deficits in the habituation/dishabituation olfactory test at 6 months of age. The bacon aroma was presented six times to the mice, the cheesecake and hazelnut aroma were presented afterwards. The sniffing (exploration) time was evaluated as the time the mouse placed the nose on the box with aroma sprayed cotton. Tau-P301L male mice (n = 12) smelled less the new aroma (cheesecake and hazelnut) compared to the age-matched WT male mice (n = 12) but this was not observed in the females (n = 7). The Two-way ANOVA was used as statistical analysis. *; $p < 0.05$ and **; $p < 0.01$ compared to the age-matched WT. Data given as mean ± SEM.

In the SHIRPA test battery, Tau-P301L male mice had phenotypic alterations compared to the WT male mice starting at 4 months of age. Those were especially observed in parameters related to motor alterations (Table 2). Tau-P301L mice showed abnormal gait as demonstrated by a waddling walk. Moreover, they appeared less agile; they were slower than WT mice at 8 months of age. Furthermore, Tau-P301L mice showed an abnormal body carriage (hunched back) compared to WT male mice starting with 4 months of age. When elevated by the tail, Tau-P301L mice presented clasping of all limbs, especially with increasing age, that can be described as slight paralysis starting with 6 months of age. This paralysis increased dramatically with age. Those findings are in correspondence with those published by Terwel et al [19]. When placed hanging at a rod, Tau-P301L mice were not able to hold nor hang with both forelimbs starting with 4 months of age, but some WT mice showed similar impairments with 6 months of age. Finally, some Tau-P301L mice showed a mild loss of postural reflex when placed on their back (Table 2) starting with 4 months of age. Tau-P301L mice had higher SHIRPA scores compared to WT mice from 4 months onward (Fig 2) (two-way ANOVA; 4 months: $p = 0.0008$, 6 months: $p = 0.0009$, 8 months: $p < 0.0001$). Moreover, an age-dependent deterioration of the phenotype was observed starting with 2 months of age (two-way ANOVA; 2 vs. 4: $p < 0.0001$; 2 vs. 6: $p = 0.0003$; 2 vs. 8: $p = 0.0204$). Tau-P301L female mice had a higher score compared to WT female mice at 4 months (two-way ANOVA; $p = 0.0022$) as well as an increased score compared to 2 and 6 months (two-way ANOVA; 2 vs. 6: $p = 0.0002$; 6 vs. 8: $p = 0.0030$). Interestingly, Tau-P301L female mice did not showed any of those alterations

Table 2: Tau-P301L male mice showed phenotypic alterations in different evaluated parameters in the SHIRPA test starting at 4 months of age

Parameters	Phenotypic Alterations
Restlessness	No alterations
Apathy	No alterations
Stereotyped behavior	No alterations
Convulsion	No alterations
Abnormal body carriage	Hunchback
Alertness	No alterations
Abnormal gait	Waddling walk and slower compared to WT
Startle response	No alterations
Loss of righting reflex	Some Tau-P301L mice have light loss of righting reflex
Touch response	Less responsive to touch than WT
Pinna reflex	No alterations
Cornea reflex	No alterations
Forelimb placing reflex	Paralysis ("Clasping") of the limbs
Hanging behavior	Tau-P301L male mice fall faster from the rod than WT male mice
Pain response	No alterations
Grooming	The Tau-P301L male mice have very good fur condition compared to WT

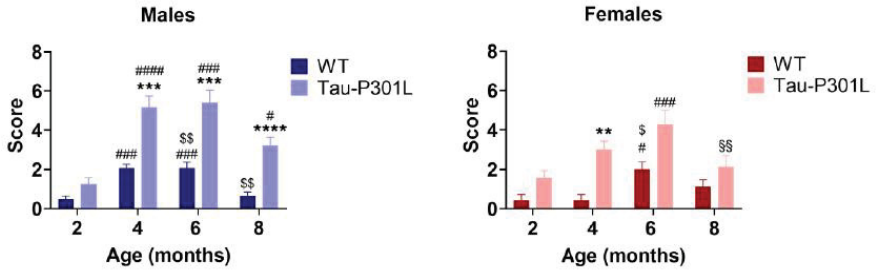

Figure 2: Tau-P301L male mice show phenotypic alteration in the SHIRPA test battery. Both, Tau-P301L mice and WT were evaluated at 2, 4, 6 and 8 months of age. At 4, 6 and 8 months of age, Tau-P301L male mice (n = 12) had a higher score compared to the age-matched WT male mice (n = 12). Only at 4 months of age, Tau-P301L female mice (n = 7) had a higher score compared to the age-matched WT female mice (n = 7). Two-way ANOVA was performed. **: $p < 0.01$, ***: $p < 0.001$ and ****: $p < 0.0001$ compared to the age-matched WT. #: $p < 0.05$, ###: $p < 0.001$ and ####: $p < 0.0001$

compared to 2 months genotype-matched. $: $p < 0.05$ and $$: $p < 0.01$ compared to 4 months genotype-matched. §§: $p < 0.01$ compared to 6 months genotype-matched. Data given as mean ± SEM.

3.2. Tau-P301L male mice display early motor deficits

In the open field test, Tau-P301L male mice had motor deficits from to 2 months of age, since they were slower (Two-way ANOVA; 2 months: $p = 0.0068$; 4 months: $p = 0.0059$; 6 months: $p = 0.0015$; 8 months: $p = 0.0298$) (Fig 3A) and travelled less (Two-way ANOVA; 2 months: $p = 0.0073$; 4 months: $p = 0.0060$; 6 months: $p = 0.0020$; 8 months: $p = 0.0296$) (Fig 3B). This deficit persisted until 8 months of age and progressed throughout aging (Two-way ANOVA; 2 vs. 6: $p = 0.0003$; 2 vs. 8: $p = 0.0003$; 4 vs. 8: $p = 0.0031$). Regarding the exploratory behavior, Tau-P301L male mice also spent less time exploring the arena compared to WT male mice beginning with 2 months of age (Two-way ANOVA; 2 months: $p = 0.0216$; 4 months: $p = 0.0198$; 6 months: $p = 0.0011$; 8 months: $p = 0,.0454$) (Fig. 3C). Mice of both genotypes spent the same amount of time in the corner, border and center zone of the arena, demonstrating that Tau-P301L mice do not have increased anxiety levels compared to WT (Fig S4). Similar to the previous data, Tau-P301L female mice did not show any differences compared to the WT female mice (Fig 3D, E and F).

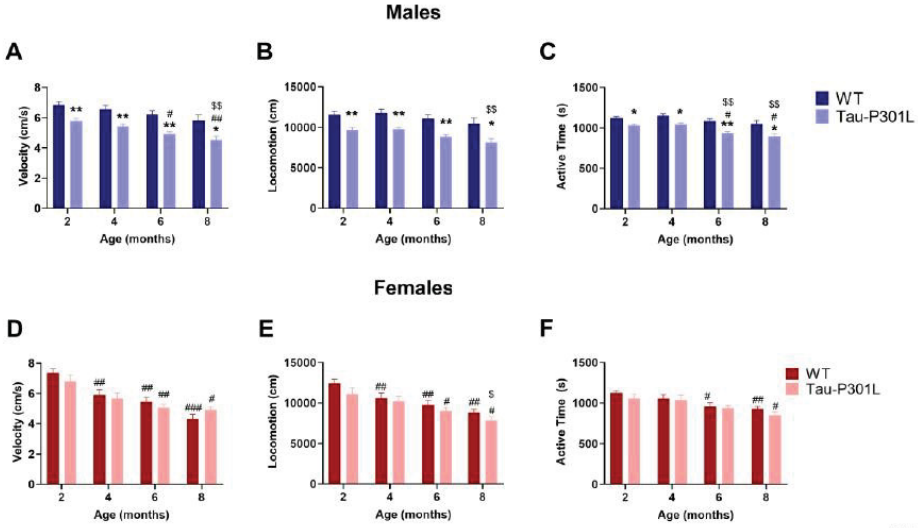

Figure 3: Tau-P301L male mice develop motor deficits in the open field test. Both, Tau-P301L mice and WT were evaluated at 2, 4, 6 and 8 months of age. At all ages, Tau-P301L male mice (n = 12) were slower (A), travelled less (B) and were less active (C) compared to the age-matched WT males (n = 12). Tau-P301L female mice (n = 7) had similar velocity (D), locomotion (E) and active time (F) compared to the age-matched WT females (n = 7). Two-way ANOVA was performed. *: $p < 0.05$ and **: $p < 0.01$ compared to the age-matched WT. #: $p < 0.05$, ##: $p < 0.01$ and ###: $p < 0.001$ compared to 2 months genotype-matched. $: $p < 0.05$ and $$: $p < 0.01$ compared to 4 months genotype-matched. Data given as mean ± SEM.

Analysis of the modified pole test revealed that Tau-P301L male mice had higher scores compared to the WT male mice starting by 6 months of age (Fig 5) (Two-way ANOVA; 6 months: $p = 0.0365$ and 8 months: $p = 0.0040$). This indicates that Tau-P301L mice developed motor deficits in this test and the deficits progressed throughout aging (Two-way ANOVA; 2 vs. 8: $p = 0.0003$; 4 vs. 8: $p = 0.0031$) (Fig 4). Tau-P301L female mice had similar performance as the WT female mice, indicating no motor deficits in this test.

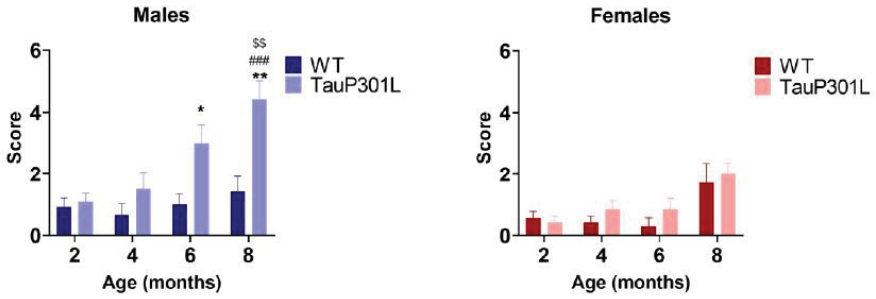

Figure 4: Tau-P301L male mice display motor deficits in the modified pole test. Both, Tau-P301L mice and WT mice were evaluated at 2, 4, 6 and 8 months of age. The test was performed three times with a 15 min intertrial interval and the sum of the three trials was used for analysis. At 6 and 8 months of age, Tau-P301L male mice (n = 12) had a higher score compared to the age-matched WT male mice (n = 12) but this was not observed in the females (n = 7). Two-way ANOVA was performed. *: $p < 0.05$ and **: $p < 0.01$ compared to the age-matched WT. ###: $p < 0.001$ compared to 2 months genotype-matched. $$: $p < 0.01$ compared to 4 months genotype-matched. Data given as mean ± SEM.

Analysis of the Rotarod performance of both, Tau-P301L male and female mice did not show any motor alteration in the acceleration Rotarod (Fig S3). Similar to the before described paralysis, those results are in correspondence with those published by Terwel et al [19].

3.3. Tau-P301L show mild cognitive deficits in the NOR

In order to analyze the development of possible cognitive deficits, several behavioral tests were performed. In the NOR, Tau-P301L mice were not able to discriminate between the novel and familiar object beginning with 6 months of age (Fig 5) (One sample t-test against 0%, 2 months: $p = 0.0001$; 4 months: $p = 0.0045$; 6 months: $p = 0.2078$ and 8 months: $p = 0.1365$). WT male mice were able to discriminate significantly the novel from the familiar object at all analyzed ages (One sample t-test against 0%, 2 months: $p = 0.0001$; 4 months: $p < 0.0001$; 6 months: $p = 0.0157$ and 8 months: $p = 0.0153$). Tau-P301L female mice did not discriminate the novel from the familiar object with 4 months of age (Fig 6) (One sample t-test against, 2 months: $p = 0.0266$; 4 months: $p = 0.1221$; 6 months: $p = 0.1945$ and 8 months: $p = 0.1293$) unlike the WT female mice (One sample t-test against, 2 months: $p = 0.0037$; 4 months: $p = 0.0009$; 6 months: $p = 0.0562$ and 8 months: $p = 0.0187$). In summary, since Tau-P301L mice did not significantly explore more the novel object, they had deficits in the recognition memory beginning with 6 (males) and 4 (females) months of age.

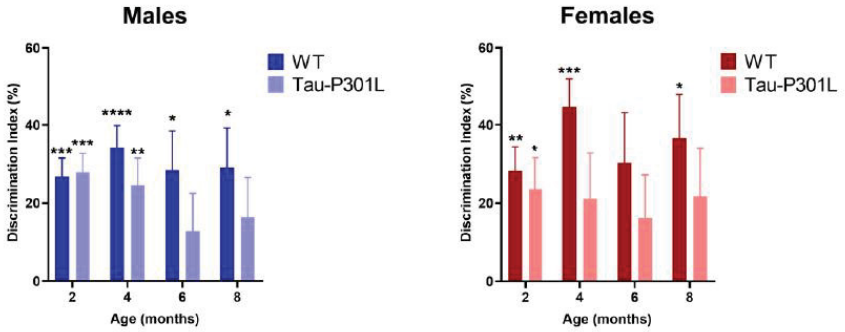

Figure 5: Deficits in recognition memory in Tau-P301L mice in the novel object recognition test (NOR)._Both, Tau-P301L mice and WT were evaluated at 2, 4, 6 and 8 months of age. Tau-P301L male mice (n = 12) were not able to discriminate the novel from the familiar object by 6 months of age and Tau-P301L female mice (n = 7) by 4 months of age. Both WT male (n = 12) and female mice (n = 7) were able to discriminate the novel object. The One sample t-test against 0% was used to evaluate the missing discrimination from the novel object. *: $p < 0.05$, **: $p < 0.01$, ***: $p < 0.001$ and ****: $p < 0.0001$. Data is given as mean ± SEM.

No cognitive deficits were detectable, neither in the T-maze spontaneous alternation (Fig S5), nor in the contextual and cued fear conditioning within the here analyzed ages (Fig S6.). Furthermore, no differences could be detected between Tau-P301L and WT mice in the MWM. During the four days of training, all tested mice showed similar escape latencies (Fig 6). In the probe trial, all genotypes spent similar amount of time in the target quadrant (NW). Moreover, no difference was detectable between Tau-P301L mice neither between males, nor between females. During the reversal trial, Tau-P301L mice and non-transgenic mice spent similar amount of time to find the platform. Overall, Tau-P301L mice did not have any cognitive deficits in the MWM at the age of 8 months.

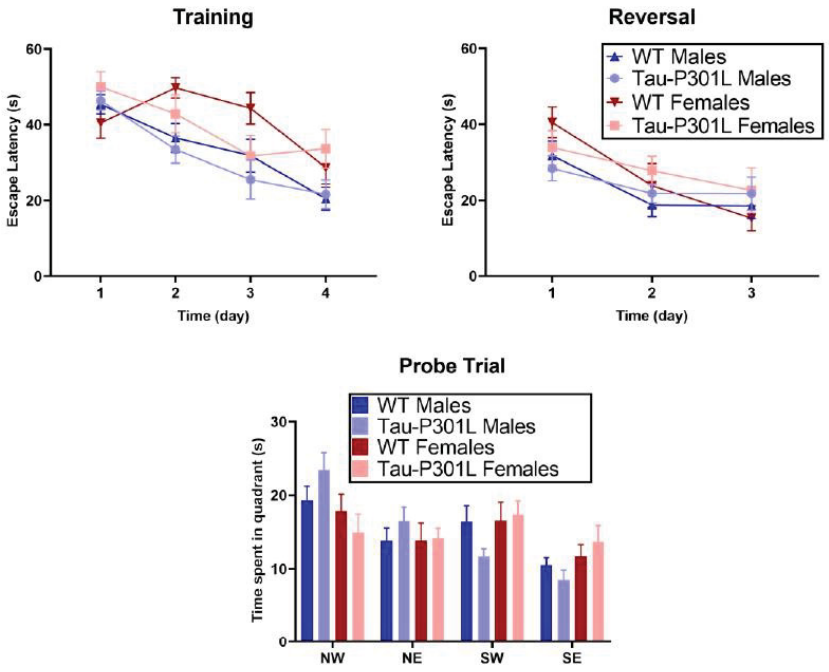

Figure 6: Tau-P301L mice did not have any deficits in the Morris Water Maze (MWM). Tau-P301L and WT mice were evaluated at 8 months of age. In the training and reversal test, both Tau-P301L mice (males: n = 12; females: n = 7) and WT mice (males: n = 12; females: n = 7) spent similar amount of time to find the platform throughout the days. In the probe trial, both Tau-P301L mice and WT male mice explored similarly the target quadrant (NW). Mixed effect and two-way ANOVA were used for analysis, respectively. Data given as mean ± SEM.

3.3 Tau-P301L showed distinct Tau pathology in the brain at 8 months of age

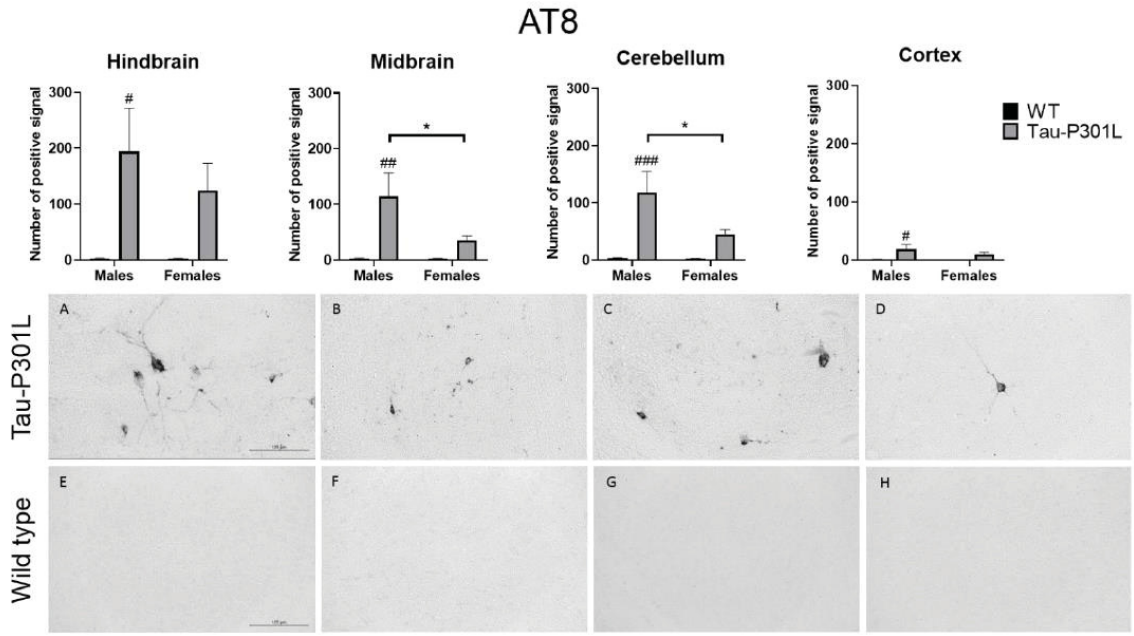

Figure 7: Tau-P301L mice show pathological Tau in different areas of the brain at 8 months of age. The phosphorylated Tau was detected by AT8 antibody. The hindbrain (A and E), cortex (D and H), midbrain (B and F), and cerebellum (C and G) from Tau-P301L (A, B, C and D) and Wild type (WT) male mice (E, F, G and H) were analyzed. The positive signal was counted at different regions of the brain using the ImageJ software. Two-way ANOVA was used for analysis. *: $p < 0.05$; #: $p < 0.05$, ##: $p < 0.01$ and ###: $p < 0.001$ compared to sex-matched WT. Scale bar of 125 μm.

After performance of the MWM, the brains from all mice were collected. Regarding the histopathology, AT8 positive signal was found in a significant higher number in the brains of Tau-P301L male mice compared to WT male mice. AT8 antibody binds to pSer202 and pThr204 and the phosphorylation of this site increases with age [19]. Therefore, those phosphorylated sites occur mainly in PHF [31, 32]. In Tau-P301L male mice, more pathological Tau is found compared to WT male mice in the hindbrain (Two-way ANOVA; males: $p = 0.0131$), the midbrain (Two-way ANOVA; males: $p = 0.0032$), the cortex (Two-way ANOVA; males: $p = 0.0318$) and the cerebellum (Two-way ANOVA; males: $p = 0.0009$) (Fig 7). Moreover, Tau-P301L male mice ($n = 8$) had more AT-8 positive signal than Tau-P30L female mice ($n = 7$) in the midbrain (Two-way ANOVA; $p = 0.0452$) and the cerebellum (Two-way ANOVA; $p = 0.0412$). Finally, Tau-P301L female mice did not have more pathological Tau compared to WT male mice in any analyzed brain region.

Using the AT100 antibody that recognizes pSer214 and pThr212, which are only present in PHF **[33]** (Fig 8), it was found that Tau-P301L male mice had increased AT100 positive signal in the midbrain (Two-way ANOVA; males: $p = 0.0004$), the hindbrain (Two-way ANOVA; males: $p = 0.0449$) and the cerebellum (Two-way ANOVA; males: $p = 0.0024$) compared to WT male mice. However, in the cortex, the number of positive signal was not significantly different from WT male mice. Regarding the sex, Tau-P301L male mice had an increased amount of AT100 positive signal only in the midbrain compared to Tau-P301L female mice (Two-way ANOVA; $p = 0.0083$). Taken together, those regions

with both AT100 and AT8 positive signal are mainly responsible for the motor coordination response and this could be an explanation for the motor deficits observed in the Tau-P301L male mice and not in the female mice.

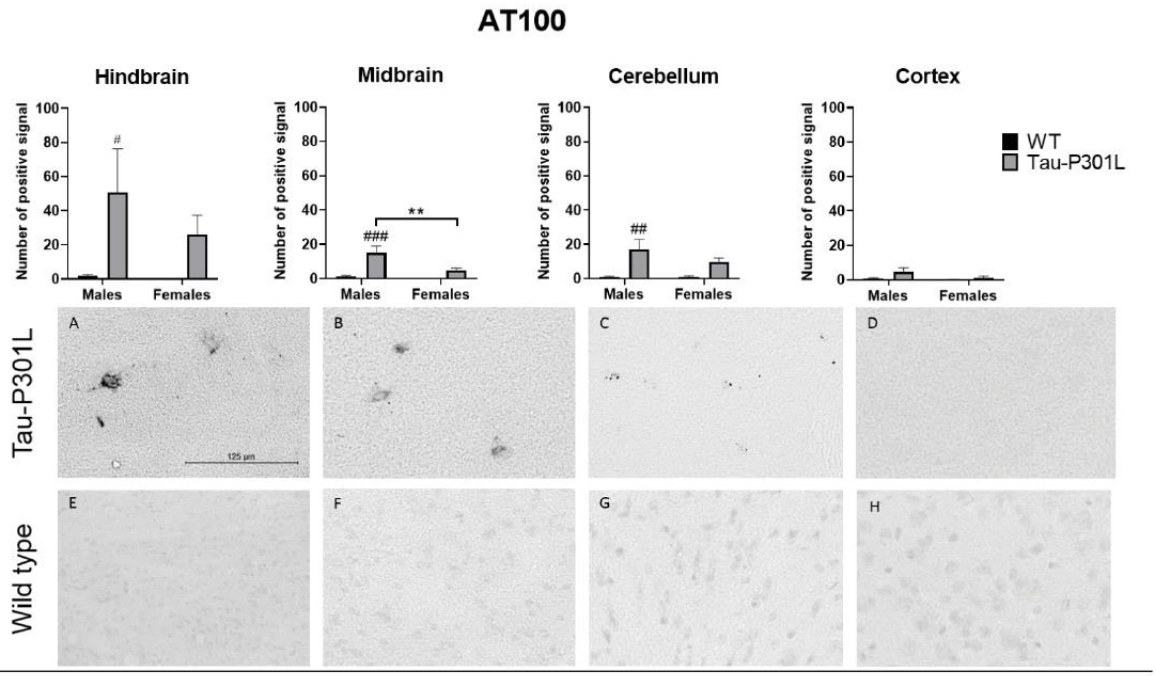

Figure 8: Tau-P301L mice had phosphorylated Tau in different areas of the brain at 8 months. The phosphorylated Tau was detected by AT100 antibody. The hindbrain (A and E), cortex (D and H), midbrain (B and F), and cerebellum (C and G) from Tau-P301L male (A, B, C and D) and wild type (WT) male mice (E, F, G and H) were analyzed. The positive signal was counted in different regions of the brain using the ImageJ software. Two-way ANOVA and Multiple t-test were used for analysis. *: $p < 0.05$; #: $p < 0.05$, ##: $p < 0.01$ and ###: $p < 0.001$ compared to sex-matched WT. Scale bar of 125µm.

More specifically, pathological Tau is present throughout different nuclei in the hindbrain specially in the locus coeruleus (LC), pontine reticular nuclei, vestibular nucleus (medial and spinal) and reticular nuclei (parvicellular and intermediate). In the midbrain, the nuclei with Tau pathology were found in the vestibular tegmental area, substantia nigra reticular, periaqueductal gray (PAG), midbrain reticular nuclei and superior colliculus. In the cerebellum, the main region where pathological Tau is present is the interposed nucleus. The pathological Tau observed in those regions were AT8 and AT100-positive, but as expected, more AT8 signal was observed compared to AT100. In the striatum, olfactory bulb and hippocampus, neither AT8 nor AT100 signal was detected, therefore, there is no pathological Tau in those regions.

Table 3: Neuronal loss and gliosis in Tau-P301L mice in different brain regions. Quantification of activated astrocytes (GFAP), reactive microglia (CD11b) and neuronal nuclei (NeuN) of 8 months old Tau-P301L (Tau-P301L) and wild type (WT) mice. The spot count analysis per selected area analysis was done in different brain regions (cortex, cerebellum, midbrain and hindbrain), resulting in a significant decrease of neurons in the Tau-P301L males' hindbrain. Analysis of gliosis, evaluated as stained area, revealed no differences between groups in different regions. Not statistically significant is represented by n.s.

Staining	Brain region	WT		Tau-P301L		Significance
		Males	Females	Males	Females	
NeuN (Spot Count)	Hindbrain	1434.7 ± 111.3	1307.6 ± 208.9	817.1 ± 181.7	1286.0 ± 246.4	WT males vs. Tau-P301L males ($p = 0.012$)
	Midbrain	1376.8 ± 184.5	1487.8 ± 108.9	1191.9± 139.9	1474.3 ± 237.6	n.s
	Cortex	3545.1 ± 197.0	2879.1 ± 262.8	4141.1 ± 210.7	3651.3 ± 285.7	n.s
	Cerebellum	1834.0 ± 83.6	1259.0 ± 123.5	2060.1 ± 158.2	1461.1 ± 187.0	n.s
GFAP (Stained Area)	Hindbrain	27.0 ± 1.0	29.3 ± 1.5	31.5 ± 3.6	33.4 ± 1.1	n.s
	Midbrain	18.6 ± 2.8	21.0 ± 3.3	19.9 ± 2.8	31.2 ± 2.1	n.s
	Cortex	15.7 ± 2.7	23.4 ± 3.1	21.7 ± 4.4	31.8 ± 1.7	n.s
	Cerebellum	8.5 ± 1.3	11.0 ± 1.8	11.8 ± 1.6	15.4 ± 1.0	n.s
CD11b (Stained Area)	Hindbrain	6.7 ± 0.9	5.6 ± 0.4	6.5 ± 0.6	5.7 ± 0.8	n.s
	Midbrain	6.0 ± 0.4	5.2 ± 0.6	5.5 ± 0.7	5.1 ± 0.5	n.s
	Cortex	6.0 ± 0.5	5.9 ± 0.6	6.9 ± 0.9	6.0 ± 0.7	n.s
	Cerebellum	6.5 ± 0.4	4.9 ± 0.7	6.6 ± 0.3	5.8 ± 0.3	n.s

Regarding neuronal loss, Tau-P301L male mice had less neurons in the hindbrain compared to WT (Table 3). The neurodegeneration was detected in the same region where the presence of AT8 positive signal but not of AT100 positive signal was abundant. One could speculate that, since NFTs are present mainly intracellular, the neuronal death in the hindbrain is inversely correlated with AT100 positive signal. Therefore, the increase of neuronal death would explain the low amount of AT100 positive signal in the hindbrain. No decrease of neurons was observed in Tau-P301L female mice in any region. In contrast, the reactive astrocytes and microglia were not increased in any brain region of Tau-P301L mice.

4. Discussion

Translational research is essential to understand the mechanisms of diseases and mouse models play an important role in this context. Even though mouse models have several limitations, they are still the most complete option to be used in basic and preclinical research of neurodegenerative diseases [34]. For this reason, it is essential to characterize different mouse models down to the smallest details in order to obtain the most accurate translation and correlation to the corresponding human disease. In most characterization studies, only a few aspects of the phenotype are investigated and often only single ages are analyzed, e.g. until first phenotypic differences are detectable, which might give limited information regarding the model. In this study, we focused on a longitudinal characterization study of the Tau-P301L mouse model, which was first described by Terwel and colleagues [19].

In summary, we showed that Tau-P301L mice had behavioral alterations in different behavioral tests probably due to the presence of pathological Tau in different brain regions. In the habituation/dishabituation olfactory test, Tau-P301L male mice spent less time smelling the newly presented aromas compared to WT male mice at 6 months of age. In the SHIRPA test, Tau-P301L mice had phenotypic alterations starting at 4 months of age. Moreover, the males had more prominent deficits compared to the females, especially regarding the motor alterations. In the modified pole test, Tau-P301L male mice had motor deficits demonstrated by a higher score compared to WT mice starting at 6 months of age. In the open field test, Tau-P301L male mice also had motor deficits since they were slower, travelled less distance and explored less in an age-dependent manner compared to WT mice starting at 2 months of age. The Tau-P301L female mice did not show any of those alterations, therefore, one can assume they did not develop any motor deficits. Regarding the cognitive deficits, Tau-P301L male mice were not able to discriminate the novel from the familiar object in the NOR from 6 months of age. Moreover, Tau-P301L female mice did not discriminate the novel object from the familiar object at 4 months of age. Therefore, the Tau-P301L mouse model also displayed cognitive deficits. Those alterations can be explained by the presence of pathological Tau (AT8 and AT100 positive signal) in the hindbrain, cerebellum and midbrain, in which the latter ones are more pronounced in the Tau-P301L male mice than in female mice. The presence of pathological Tau induced neurodegeneration in the hindbrain in Tau-P301L male mice. Interestingly, the decrease of neurons seems to occur after the increase of AT8 positive signaling the hindbrain, but an increase of AT100 positive signal was not observed. Since AT100 antibody detects later stages of pathological Tau, one might speculate that the lack of increase of AT100 positive signal in the hindbrain might be due to the neuronal death of those neurons, which had pathological Tau. Finally, no increased neuroinflammation was observed in this study, therefore, pathological Tau does not seem to induce the activation of astrocytes and microglia in Tau-P301L mice brain.

In the present study, Tau-P301L mice did not show alterations on the rotarod at any analyzed ages, similar to the results published in previous studies [19, 35]. In one study [35] it was described that Tau-P301L male mice on a C57BL/6J background showed phenotypic alterations at early ages (2 to 5 months of age) in some behavioral tests. Corroborating to the present study, Tau-P301L male mice did not develop any deficit with 4 months of age in the nesting and marble burying test. Moreover, we were able to demonstrate that Tau-P301L mice do not develop any deficits as late as 8 months of age in those tests. In the open field test, Tau-P301L mice travelled less as early as with 2 months of age. This effect can be observed up to the age of 8 months. Again, these results agree with the one published by Samaey et al [35]. In contrast to the study published by Samaey et al [35], we were not able to observe any difference between Tau-P301L and WT mice in the amount of time they explore the different zones (border, center and corner).

Described for the first time, Tau-P301L male mice had phenotypic alterations in the SHIRPA test battery. Starting at 4 months of age, Tau-P301L mice developed postural changes described by a hunched back, mild deficits in the hanging behavior and some mice developed a loss of the postural reflex. Then, beginning with 6 months of age, Tau-P301L mice started to display clasping of the limbs, which can be considered as paralysis, as well as abnormal gait described as a waddling walk. Those alterations progressed throughout the aging. This result contrasts with those shown by other groups, analyzing other mouse models of tauopathy, since they did not describe any differences in the SHIRPA compared to the WT [36, 37]. Only one study described a similar result regarding the hanging behavior. In this study, it was shown that the motor skills of Tau58-2/B mice (Tau-P301L mutation) were so limited regarding this specific subtest that the mice could not perform the test adequately [38]. In the present study, we also conducted a modified pole test. We were able to show that the mice exhibit deficits in this test that become more pronounced with increasing age. The motor deficits in the modified pole test were also described for another mouse model of tauopathy, called SJLB mouse model [39]. Moreover, Tau-P301L mice had olfactory deficits in the habituation/dishabituation olfactory test at 6 months of age. This deficit was also observed in another Tau-P301L mouse model [40]. Regarding the histopathology, neither AT8 nor AT100 positive signal were detected in the olfactory bulb/cortex. Therefore, another pathophysiological mechanism might play a role in the olfactory deficits observed in this study. Another explanation for this alteration is that the olfactory deficits bear on cognitive deficits, so one might speculate that Tau-P301L male mice were not able to recognize the new aroma.

The pathology described for this Tau-P301L mouse model is similar to the same and others mouse models with this specific mutation [19-21] [41, 42]. Therefore, the strain background and the used promoter do not seem to have any influence on the appearance of NFTs in the brains. Though, the presence of NFTs can occur in different brain regions since the pR5 mouse model also shows tauopathy in the hippocampus [41], which is not observed in the mouse model from this study. The Tau pathology in Tau-P301L mice mainly occurs in the brainstem and it might be an explanation for the behavioral deficits. The presence of pathological Tau in the brainstem, especially in SNr [43-47] and superior colliculus [48, 49] can be related to motor deficits in Tau-P301L male mice. Moreover, the lack of NFTs in Tau-P301L female mice in those regions can be also related to the lack of motor deficits. Sex dimorphism is observed in other transgenic mouse models but the results are contradictory [50]. Therefore, more experiments are needed in order to understand this sex-differences more precise.

Regarding the cognitive deficits, both Tau-P301L female and male mice developed deficits in the NOR that are in line with the Tau aggregation in the LC since it also plays a role in cognition, and NFTs in this region induce cognitive deficits [51, 52]. Tau-P301L mice did not have any deficits in the MWM, T-Maze and contextual fear conditioning probably due to the lack of NFTs in the hippocampus, which play a main role in processing of the spatial memory [53]. Tau-P301L mice also did not show cognitive deficits in the cued fear conditioning, probably also due to the lack of NFTs in the amygdala, which is the region that processes fear memory [54].

Sex differences in neurodegenerative diseases are observed in both, animals and humans. In humans, women have a higher probability to develop AD than men as well as developing a more severe pathology [55, 56]. In AD mice, Aβ levels are also higher and cognitive deficits are more prominent in females. Regarding Tau pathology, not much information is available about transgenic models. In the present study, Tau-P301L male mice had motor deficits compared to females even though both sexes had cognitive deficits. Another study also demonstrated motor deficits in the Tau-P301S males and later cognitive deficits compared to females, but a similar tau pathology in the brain [57]. In a

triple transgenic mouse model, which develops both Aβ plaques and NFTs, 3xTg-AD females had a higher amount of Tau pathology and cognitive deficits compared to males. This discrepancy might be due to the age of the tested mice, since AD mice develop the alterations later than Tau mice [58]. Additionally, female reproductive senescence is reached at 12 months of age, when estrogen levels are decreased [59]. Estrogen is known to have neuroprotective effects and its decrease might explain the severity of tau pathology in the 3xTg-AD females [60-63]. In this study, reproductive active females were evaluated and the estrogen levels might explain the milder Tau pathology in females. Although, it is important to highlight that the comparison of different models must be done with caution since each model has different behavioral and physiopathological outcomes. Moreover, more studies are needed to further explain the remarkable sex differences in the Tau-P301L mouse model as observed in this study.

Taking together, this longitudinal study demonstrates that Tau-P301L mice have alterations due to the presence of pathological Tau in the brain that are in agreement with age and are sex-dependent. Tau-P301L male mice had olfactory deficits, motor deficits and increased Tau pathology in the brain. None of those alterations were observed in Tau-P310L female mice. Both sexes, though, had phenotypic alterations in the SHIRPA test battery and cognitive deficits in the NOR. It is possible to determine that the disease onset in the males occurs as early as 2 months of age regarding the motor deficits and 6 months of age regarding the cognitive deficits.

Supplementary Materials: The following are available online at www.mdpi.com/xxx/s1, Figure S1: Tau-P301L mice had similar weight compared to WT mice.; Figure S2: Tau-P301L mice had similar performance in the nesting and marble burying test compared to WT mice.; Figure S3: Tau-P301L mice had similar performance in the Rotarod test compared to WT mice.; Figure S4: Tau-P301L mice spent similar amount of time in the border and center of the open field compared to WT mice.; Figure S5: Tau-P301L mice had similar performance in the T-maze spontaneous alternation compared to WT mice.; Figure S6: Tau-P301L mice froze similarly compared to WT mice in the cued and contextual fear conditioning.

Author Contributions: Conceptualization, S.S, L.C.C. and A.W.; experiments, L.C.C., D.H. and R.B.; data analysis, L.C.C., D.H. and S.S.; writing—original draft preparation, L.C.C.; writing—review and editing, S.S, J.K, A.W, K-.J.L, N.J.S. and D.W.; funding acquisition, D.W and K-.J.L.. All authors have read and agreed to the published version of the manuscript.

Funding: D.W. was supported by grants from the Russian Science Foundation (RSF) (project no. 20-64-46027) and by the Technology Transfer Fund of the Forschungszentrum Jülich. K.-J.L. and D.W. were supported by "Portfolio Drug Research" of the "Impuls und Vernetzungs-Fonds der Helmholtzgemeinschaft".

Institutional Review Board Statement: The study was conducted according to the German Law on the protection of animals (TierSchG §§ 7–9) and was approved by the local ethics committee before start of the experiments (Landesamt für Natur, Umwelt und Verbraucherschutz, North Rhine-Westphalia, Germany, numbers 84-02.04.2011.A359, 84-02.04.2014.A362, 81-02.04.2018.A400, 81-02.04.2019.A304 were approved on 09 December 2014, 05 February 2019, 21 February 2019 and 21 January 2019, respectively).

Data Availability Statement: All data from the study is available in this Manuscript.

Conflicts of Interest: The authors declare no conflict of interest.

References

1. Jean, D.C.; Baas, P.W. *It cuts two ways: microtubule loss during Alzheimer disease.* EMBO J 2013, 32, 2900-2902, doi:10.1038/emboj.2013.219.

2. Dixit, R.; Ross, J.L.; Goldman, Y.E.; Holzbaur, E.L.F. *Differential regulation of dynein and kinesin motor proteins by tau.* Science 2008, 319, 1086-1089, doi:10.1126/science.1152993.

3. Combs, B.; Mueller, R.L.; Morfini, G.; Brady, S.T.; Kanaan, N.M. *Tau and Axonal Transport Misregulation in Tauopathies.* Advances in experimental medicine and biology 2019, 1184, 81-95, doi:10.1007/978-981-32-9358-8_7.

4. Barbier, P.; Zejneli, O.; Martinho, M.; Lasorsa, A.; Belle, V.; Smet-Nocca, C.; Tsvetkov, P.O.; Devred, F.; Landrieu, I. *Role of Tau as a Microtubule-Associated Protein: Structural and Functional Aspects.* Frontiers in Aging Neuroscience 2019, 11, doi:10.3389/fnagi.2019.00204.

5. Tapia-Rojas, C.; Cabezas-Opazo, F.; Deaton, C.A.; Vergara, E.H.; Johnson, G.V.W.; Quintanilla, R.A. *It's all about tau.* Prog Neurobiol 2019, 175, 54-76, doi:10.1016/j.pneurobio.2018.12.005.

6. Fischer, I.; Baas, P.W. *Resurrecting the Mysteries of Big Tau.* Trends Neurosci 2020, 43, 493-504, doi:10.1016/j.tins.2020.04.007.

7. Mandelkow, E.M.; Biernat, J.; Drewes, G.; Gustke, N.; Trinczek, B.; Mandelkow, E. *Tau domains, phosphorylation, and interactions with microtubules.* Neurobiology of Aging 1995, 16, 355-362, doi:https://doi.org/10.1016/0197-4580(95)00025-A.

8. Götz, J.; Halliday, G.; Nisbet, R.M. *Molecular Pathogenesis of the Tauopathies.* Annual Review of Pathology: Mechanisms of Disease 2019, 14, 239-261, doi:10.1146/annurev-pathmechdis-012418-012936.

9. Quintas-Neves, M.; Teylan, M.A.; Besser, L.; Soares-Fernandes, J.; Mock, C.N.; Kukull, W.A.; Crary, J.F.; Oliveira, T.G. *Magnetic resonance imaging brain atrophy assessment in primary age-related tauopathy (PART).* Acta neuropathologica communications 2019, 7, 204-204, doi:10.1186/s40478-019-0842-z.

10. Braak, H.; Alafuzoff, I.; Arzberger, T.; Kretzschmar, H.; Del Tredici, K. *Staging of Alzheimer disease-associated neurofibrillary pathology using paraffin sections and immunocytochemistry.* Acta neuropathologica 2006, 112, 389-404, doi:10.1007/s00401-006-0127-z.

11. Liao, D.; Miller, E.C.; Teravskis, P.J. *Tau acts as a mediator for Alzheimer's disease-related synaptic deficits.* Eur J Neurosci 2014, 39, 1202-1213, doi:10.1111/ejn.12504.

12. Jadhav, S.; Cubinkova, V.; Zimova, I.; Brezovakova, V.; Madari, A.; Cigankova, V.; Zilka, N. *Tau-mediated synaptic damage in Alzheimer's disease.* Transl Neurosci 2015, 6, 214-226, doi:10.1515/tnsci-2015-0023.

13. Puvenna, V.; Engeler, M.; Banjara, M.; Brennan, C.; Schreiber, P.; Dadas, A.; Bahrami, A.; Solanki, J.; Bandyopadhyay, A.; Morris, J.K.; et al. *Is phosphorylated tau unique to chronic traumatic encephalopathy? Phosphorylated tau in epileptic brain and chronic traumatic encephalopathy.* Brain research 2016, 1630, 225-240, doi:10.1016/j.brainres.2015.11.007.

14. Poorkaj, P.; Grossman, M.; Steinbart, E.; Payami, H.; Sadovnick, A.; Nochlin, D.; Tabira, T.; Trojanowski, J.Q.; Borson, S.; Galasko, D.; et al. *Frequency of tau gene mutations in familial and sporadic cases of non-Alzheimer dementia.* Arch Neurol 2001, 58, 383-387, doi:10.1001/archneur.58.3.383.

15. Forrest, S.L.; Kril, J.J.; Stevens, C.H.; Kwok, J.B.; Hallupp, M.; Kim, W.S.; Huang, Y.; McGinley, C.V.; Werka, H.; Kiernan, M.C.; et al. *Retiring the term FTDP-17 as MAPT mutations are genetic forms of sporadic frontotemporal tauopathies.* Brain 2017, 141, 521-534, doi:10.1093/brain/awx328.

16. Hasegawa, M.; Smith, M.J.; Goedert, M. *Tau proteins with FTDP-17 mutations have a reduced ability to promote microtubule assembly.* FEBS Letters 1998, 437, 207-210, doi:https://doi.org/10.1016/S0014-5793(98)01217-4.

17. Roberson, E.D. *Mouse models of frontotemporal dementia.* Annals of neurology 2012, 72, 837-849, doi:10.1002/ana.23722.

18. Kitazawa, M.; Medeiros, R.; Laferla, F.M. *Transgenic mouse models of Alzheimer disease: developing a better model as a tool for therapeutic interventions.* Curr Pharm Des 2012, 18, 1131-1147, doi:10.2174/138161212799315786.

19. Terwel, D.; Lasrado, R.; Snauwaert, J.; Vandeweert, E.; Van Haesendonck, C.; Borghgraef, P.; Van Leuven, F. *Changed Conformation of Mutant Tau-P301L Underlies the Moribund Tauopathy, Absent in Progressive, Nonlethal Axonopathy of Tau-4R/2N Transgenic Mice**. Journal of Biological Chemistry 2005, 280, 3963-3973, doi:https://doi.org/10.1074/jbc.M409876200.

20. Dutschmann, M.; Menuet, C.; Stettner, G.M.; Gestreau, C.; Borghgraef, P.; Devijver, H.; Gielis, L.; Hilaire, G.; Van Leuven, F. *Upper airway dysfunction of Tau-P301L mice correlates with tauopathy in midbrain and ponto-medullary brainstem nuclei*. J Neurosci 2010, 30, 1810-1821, doi:10.1523/jneurosci.5261-09.2010.

21. Boekhoorn, K.; Terwel, D.; Biemans, B.; Borghgraef, P.; Wiegert, O.; Ramakers, G.J.; de Vos, K.; Krugers, H.; Tomiyama, T.; Mori, H.; et al. *Improved long-term potentiation and memory in young tau-P301L transgenic mice before onset of hyperphosphorylation and tauopathy*. J Neurosci 2006, 26, 3514-3523, doi:10.1523/jneurosci.5425-05.2006.

22. Lehmkuhl, A.M.; Dirr, E.R.; Fleming, S.M. *Olfactory assays for mouse models of neurodegenerative disease.* Journal of visualized experiments : JoVE 2014, e51804-e51804, doi:10.3791/51804.

23. Deacon, R. *Assessing burrowing, nest construction, and hoarding in mice.* Journal of visualized experiments : JoVE 2012, e2607, doi:10.3791/2607.

24. Deacon, R.M. *Digging and marble burying in mice: simple methods for in vivo identification of biological impacts*. Nature protocols 2006, 1, 122-124, doi:10.1038/nprot.2006.20.

25. Rogers, D.C.; Fisher, E.M.; Brown, S.D.; Peters, J.; Hunter, A.J.; Martin, J.E. *Behavioral and functional analysis of mouse phenotype: SHIRPA, a proposed protocol for comprehensive phenotype assessment.* Mammalian genome : official journal of the International Mammalian Genome Society 1997, 8, 711-713, doi:10.1007/s003359900551.

26. Alexandru, A.; Jagla, W.; Graubner, S.; Becker, A.; Bäuscher, C.; Kohlmann, S.; Sedlmeier, R.; Raber, K.A.; Cynis, H.; Rönicke, R.; et al. *Selective hippocampal neurodegeneration in transgenic mice expressing small amounts of truncated Aβ is induced by pyroglutamate-Aβ formation.* J Neurosci 2011, 31, 12790-12801, doi:10.1523/JNEUROSCI.1794-11.2011.

27. Dunkelmann, T.; Schemmert, S.; Honold, D.; Teichmann, K.; Butzküven, E.; Demuth, H.-U.; Shah, N.J.; Langen, K.-J.; Kutzsche, J.; Willbold, D.; et al. *Comprehensive Characterization of the Pyroglutamate Amyloid-β Induced Motor Neurodegenerative Phenotype of TBA2.1 Mice*. Journal of Alzheimer's Disease 2018, 63, 115-130, doi:10.3233/JAD-170775.

28. Spowart-Manning, L.; Van der Staay, F. *The T-maze continuous alternation task for assessing the effects of putative cognition enhancers in the mouse.* Behavioural brain research 2004, 151, 37-46.

29. Curzon, P.; Rustay, N.R.; Browman, K.E. Frontiers in Neuroscience. *Cued and Contextual Fear Conditioning for Rodents*. In Methods of Behavior Analysis in Neuroscience, Buccafusco, J.J., Ed.; CRC Press/Taylor & Francis. Copyright © 2009, Taylor & Francis Group, LLC.: Boca Raton (FL), 2009.

30. Morris, R. *Developments of a water-maze procedure for studying spatial learning in the rat.* Journal of neuroscience methods 1984, 11, 47-60, doi:10.1016/0165-0270(84)90007-4.

31. Augustinack, J.C.; Schneider, A.; Mandelkow, E.-M.; Hyman, B.T. *Specific tau phosphorylation sites correlate with severity of neuronal cytopathology in Alzheimer's disease*. Acta neuropathologica 2002, 103, 26-35.

32. Goedert, M.; Jakes, R.; Vanmechelen, E. *Monoclonal antibody AT8 recognises tau protein phosphorylated at both serine 202 and threonine 205.* Neuroscience Letters 1995, 189, 167-170, doi:https://doi.org/10.1016/0304-3940(95)11484-E.

33. Zheng-Fischhöfer, Q.; Biernat, J.; Mandelkow, E.-M.; Illenberger, S.; Godemann, R.; Mandelkow, E. *Sequential phosphorylation of Tau by glycogen synthase kinase-3β and protein kinase A at Thr212 and Ser214 generates the Alzheimer-specific epitope of antibody AT100 and requires a paired-helical-filament-like conformation*. European Journal of Biochemistry 1998, 252, 542-552, doi:https://doi.org/10.1046/j.1432-1327.1998.2520542.x.

34. Scearce-Levie, K.; Sanchez, P.E.; Lewcock, J.W. *Leveraging preclinical models for the development of Alzheimer disease therapeutics.* Nature reviews. Drug discovery 2020, 19, 447-462, doi:10.1038/s41573-020-0065-9.

35. Samaey, C.; Schreurs, A.; Stroobants, S.; Balschun, D. *Early Cognitive and Behavioral Deficits in Mouse Models for Tauopathy and Alzheimer's Disease.* Front Aging Neurosci 2019, 11, 335, doi:10.3389/fnagi.2019.00335.

36. Polydoro, M.; Acker, C.M.; Duff, K.; Castillo, P.E.; Davies, P. *Age-Dependent Impairment of Cognitive and Synaptic Function in the htau Mouse Model of Tau Pathology*. The Journal of Neuroscience 2009, 29, 10741-10749, doi:10.1523/jneurosci.1065-09.2009.

37. Bodea, L.-G.; Evans, H.T.; Van der Jeugd, A.; Ittner, L.M.; Delerue, F.; Kril, J.; Halliday, G.; Hodges, J.; Kiernan, M.C.; Götz, J. *Accelerated aging exacerbates a pre-existing pathology in a tau transgenic mouse model.* Aging Cell 2017, 16, 377-386, doi:10.1111/acel.12565.

38. Van der Jeugd, A.; Vermaercke, B.; Halliday, G.M.; Staufenbiel, M.; Götz, J. *Impulsivity, decreased social exploration, and executive dysfunction in a mouse model of frontotemporal dementia.* Neurobiology of Learning and Memory 2016, 130, 34-43, doi:https://doi.org/10.1016/j.nlm.2016.01.007.

39. Takenokuchi, M.; Kadoyama, K.; Chiba, S.; Sumida, M.; Matsuyama, S.; Saigo, K.; Taniguchi, T. *SJLB mice develop tauopathy-induced parkinsonism.* Neuroscience Letters 2010, 473, 182-185, doi:https://doi.org/10.1016/j.neulet.2010.02.032.

40. Hu, Y.; Ding, W.; Zhu, X.; Chen, R.; Wang, X. *Olfactory Dysfunctions and Decreased Nitric Oxide Production in the Brain of Human P301L Tau Transgenic Mice.* Neurochemical research 2016, 41, 722-730, doi:10.1007/s11064-015-1741-8.

41. Lewis, J.; McGowan, E.; Rockwood, J.; Melrose, H.; Nacharaju, P.; Van Slegtenhorst, M.; Gwinn-Hardy, K.; Murphy, M.P.; Baker, M.; Yu, X.; et al. *Neurofibrillary tangles, amyotrophy and progressive motor disturbance in mice expressing mutant (P301L) tau protein.* Nature Genetics 2000, 25, 402-405, doi:10.1038/78078.

42. Götz, J.; Chen, F.; Barmettler, R.; Nitsch, R.M. *Tau Filament Formation in Transgenic Mice Expressing P301L Tau**. Journal of Biological Chemistry 2001, 276, 529-534, doi:https://doi.org/10.1074/jbc.M006531200.

43. You, Y.; Botros, M.B.; Enoo, A.A.V.; Bockmiller, A.; Herron, S.; Delpech, J.C.; Ikezu, T. *Cre-inducible Adeno Associated Virus-mediated Expression of P301L Mutant Tau Causes Motor Deficits and Neuronal Degeneration in the Substantia Nigra.* Neuroscience 2019, 422, 65-74, doi:10.1016/j.neuroscience.2019.10.001.

44. Mirra, S.S.; Murrell, J.R.; Gearing, M.; Spillantini, M.G.; Goedert, M.; Crowther, R.A.; Levey, A.I.; Jones, R.; Green, J.; Shoffner, J.M.; et al. *Tau Pathology in a Family with Dementia and a P301L Mutation in Tau.* Journal of Neuropathology & Experimental Neurology 1999, 58, 335-345, doi:10.1097/00005072-199904000-00004.

45. Klein, R.L.; Dayton, R.D.; Lin, W.L.; Dickson, D.W. *Tau gene transfer, but not alpha-synuclein, induces both progressive dopamine neuron degeneration and rotational behavior in the rat.* Neurobiology of disease 2005, 20, 64-73, doi:10.1016/j.nbd.2005.02.001.

46. Kovacs, G.G. *Invited review: Neuropathology of tauopathies: principles and practice*. Neuropathology and Applied Neurobiology 2015, 41, 3-23, doi:https://doi.org/10.1111/nan.12208.

47. Dickson, D.W.; Ahmed, Z.; Algom, A.A.; Tsuboi, Y.; Josephs, K.A. *Neuropathology of variants of progressive supranuclear palsy*. Current Opinion in Neurology 2010, 23, 394-400, doi:10.1097/WCO.0b013e32833be924.

48. Armstrong, R.A.; McKee, A.C.; Cairns, N.J. *Pathology of the Superior Colliculus in Chronic Traumatic Encephalopathy*. Optometry and vision science : official publication of the American Academy of Optometry 2017, 94, 33-42, doi:10.1097/opx.0000000000000911.

49. Dugger, B.N.; Tu, M.; Murray, M.E.; Dickson, D.W. *Disease specificity and pathologic progression of tau pathology in brainstem nuclei of Alzheimer's disease and progressive supranuclear palsy.* Neuroscience letters 2011, 491, 122-126, doi:10.1016/j.neulet.2011.01.020.

50. Dennison, J.L.; Ricciardi, N.R.; Lohse, I.; Volmar, C.-H.; Wahlestedt, C. *Sexual Dimorphism in the 3xTg-AD Mouse Model and Its Impact on Pre-Clinical Research*. Journal of Alzheimer's Disease 2021, 80, 41-52, doi:10.3233/JAD-201014.

51. Grudzien, A.; Shaw, P.; Weintraub, S.; Bigio, E.; Mash, D.C.; Mesulam, M.M. *Locus coeruleus neurofibrillary degeneration in aging, mild cognitive impairment and early Alzheimer's disease.* Neurobiol Aging 2007, 28, 327-335, doi:10.1016/j.neurobiolaging.2006.02.007.

52. Kelly, S.C.; He, B.; Perez, S.E.; Ginsberg, S.D.; Mufson, E.J.; Counts, S.E. *Locus coeruleus cellular and molecular pathology during the progression of Alzheimer's disease.* Acta Neuropathol Commun 2017, 5, 8, doi:10.1186/s40478-017-0411-2.

53. Tanila, H. *Wading pools, fading memories—place navigation in transgenic mouse models of Alzheimer's disease.* Frontiers in Aging Neuroscience 2012, 4, doi:10.3389/fnagi.2012.00011.

54. Izquierdo, I.; Furini, C.R.; Myskiw, J.C. *Fear Memory.* Physiological reviews 2016, 96, 695-750, doi:10.1152/physrev.00018.2015.

55. Dye, R.V.; Miller, K.J.; Singer, E.J.; Levine, A.J. *Hormone replacement therapy and risk for neurodegenerative diseases.* Int J Alzheimers Dis 2012, 2012, 258454, doi:10.1155/2012/258454.

56. Phung, T.K.; Waltoft, B.L.; Laursen, T.M.; Settnes, A.; Kessing, L.V.; Mortensen, P.B.; Waldemar, G. *Hysterectomy, oophorectomy and risk of dementia: a nationwide historical cohort study.* Dement Geriatr Cogn Disord 2010, 30, 43-50, doi:10.1159/000314681.

57. Sun, Y.; Guo, Y.; Feng, X.; Jia, M.; Ai, N.; Dong, Y.; Zheng, Y.; Fu, L.; Yu, B.; Zhang, H.; et al. *The behavioural and neuropathologic sexual dimorphism and absence of MIP-3α in tau P301S mouse model of Alzheimer's disease.* J Neuroinflammation 2020, 17, 72, doi:10.1186/s12974-020-01749-w.

58. Yang, J.-T.; Wang, Z.-J.; Cai, H.-Y.; Yuan, L.; Hu, M.-M.; Wu, M.-N.; Qi, J.-S. *Sex Differences in Neuropathology and Cognitive Behavior in APP/PS1/tau Triple-Transgenic Mouse Model of Alzheimer's Disease.* Neuroscience Bulletin 2018, 34, 736-746, doi:10.1007/s12264-018-0268-9.

59. Clinton, L.K.; Billings, L.M.; Green, K.N.; Caccamo, A.; Ngo, J.; Oddo, S.; McGaugh, J.L.; LaFerla, F.M. *Age-dependent sexual dimorphism in cognition and stress response in the 3xTg-AD mice.* Neurobiology of disease 2007, 28, 76-82, doi:10.1016/j.nbd.2007.06.013.

60. Goodman, Y.; Bruce, A.J.; Cheng, B.; Mattson, M.P. *Estrogens attenuate and corticosterone exacerbates excitotoxicity, oxidative injury, and amyloid beta-peptide toxicity in hippocampal neurons.* J Neurochem 1996, 66, 1836-1844, doi:10.1046/j.1471-4159.1996.66051836.x.

61. Luine, V.N. *Estradiol increases choline acetyltransferase activity in specific basal forebrain nuclei and projection areas of female rats.* Exp Neurol 1985, 89, 484-490, doi:10.1016/0014-4886(85)90108-6.

62. Behl, C.; Widmann, M.; Trapp, T.; Holsboer, *F. 17-beta estradiol protects neurons from oxidative stress-induced cell death in vitro.* Biochem Biophys Res Commun 1995, 216, 473-482, doi:10.1006/bbrc.1995.2647.

63. Bruce-Keller, A.J.; Keeling, J.L.; Keller, J.N.; Huang, F.F.; Camondola, S.; Mattson, M.P. *Antiinflammatory effects of estrogen on microglial activation.* Endocrinology 2000, 141, 3646-3656, doi:10.1210/endo.141.10.7693.

4. Discussion

The translational research is an important field to understand the underlying mechanisms of AD, and animal models play an essential role in this field. The advantage of animal models is that it is possible to study in depth one particularity of the disease under controlled conditions. However, the disadvantage is that no animal model can recreate all aspects of AD. In case of transgenic mouse models, different approaches can be implemented in order to overcome this limitation. Considering AD, the development of new models that develop not only plaques and tangles, but also neurodegeneration, is desired. Moreover, in order to design a more precise treatment strategy, a profound understanding of the mouse model is necessary. Therefore, longitudinal studies with mouse models including animals of both sexes should be performed for the determination of disease onset, progression and sex-dependent alterations.

The first part of the work presented here describes the characterization of the so-called TAPS mouse model of amyloidosis. Another approach in this study was to characterize an already described Tau-P301L mouse model of tauopathy, evaluating the sex-differences and disease progression in a longitudinal behavioral test battery starting at two months of age. Besides, the SwDI mouse model was also further characterized in the previous years by other researchers in our institute, in order to investigate whether the mouse model also develops the deficits described in the literature in our hands and to ensure the best possible point in time to start a treatment study. After this initial characterization, the treatment study was performed to evaluate the treatment efficacy of cRD2D3 in comparison to RD2D3 in SwDI.

4.1. Phenotype of used mouse models

In order to have an AD mouse model that developed an extensive amyloidosis combined with strong phenotypic alterations induced by pEAβ, the TAPS mouse line were created by crossing heterozygous APP/PS1 mice with heterozygous TBA2.1 mice on a C57/B6J background. At a high age, APP/PS1 mice show an extensive amyloid plaque formation as well as cognitive deficits [123]. Homozygous TBA2.1 mice, which express the truncated Aβ (Q3-42) and develop a pEAβ accumulation in the brain show neurodegeneration and striatal amyloid aggregation at an early age [213]. Heterozygous TBA2.1 mice do not develop any of the abovementioned features [213, 215]. Therefore, TAPS mice expressed the APPSwe, PS1ΔE9 mutation combined with the truncated Aβ(Q3-42) which should provide a model with stronger amyloidosis and pathological alterations.

The TAPS mice developed plaques in the cortex, striatum and hippocampus starting at six months of age and progressing with age, which is an earlier onset compared to the parental APP/PS1 line. Moreover, the plaques were composed of both Aβ and pEAβ. Regarding the behavioral deficits, TAPS mice had higher average scores in the SHIRPA test, increasing with age. More specifically, they showed deficits in hanging behavior and decreased reflexes

starting at 12 months of age. In the open field test, TAPS mice had a non-significant tendency to move faster, travel more and behave more actively overall. In the NOR, T-maze, cued and contextual fear conditioning and MWM, TAPS mice had cognitive deficits starting at 18 months of age [230] (Table 2).

The Tau-P301L mice developed NFTs in the brainstem, motor deficits in the beam walk at nine months of age and cognitive deficits at seven months of age [223, 224]. In this study, Tau-P301L mice of both sexes were compared to wild type (WT) mice. Tau-P301L male mice were slower, travelled less and were less active starting at two months of age in the open field test. Later, starting at four months of age, Tau-P301L female and male mice had higher scores in the SHIRPA test. More specifically, they developed a waddling walk and a hunchback. Tau-P310L female mice also developed cognitive deficits in the NOR at this age. Starting at six months of age, Tau-P301L male mice developed motor deficits in the pole test, clasping of limbs and hanging behavioral deficits in the SHIRPA as well as cognitive deficits in the NOR (Figure 6). No behavior alterations were observed in the marble burying, nesting behavior, cued and contextual fear conditioning and in the T-maze spontaneous alternation tests. Regarding the histopathology, Tau-P301L mice had NFTs in the brainstem area (hind and midbrain) and cerebellum, which was also previously described , and neurodegeneration in the hindbrain [223] (Table 2).

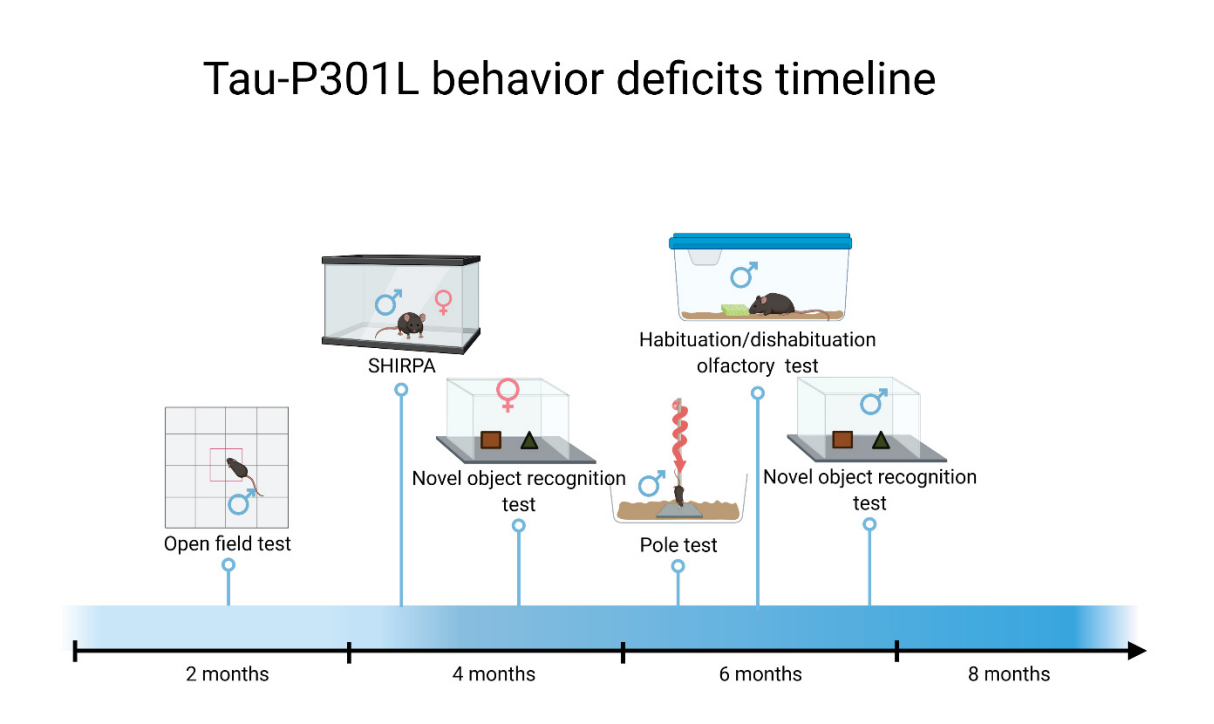

Figure 6: Timeline of Tau-P301L phenotypic alterations. From two months of age, Tau-P301L male mice had motor deficits in the open field test. From four months of age, Tau-P301L mice had phenotypic alterations in the SHIRPA test and Tau-P301L female mice had cognitive deficits in the novel object recognition test. From six months of age, Tau-P301L male mice had motor deficits in the modified pole test. Created with BioRender.com.

The SwDI had increased Aβ levels and Aβ accumulation in the brain as early as three months and cognitive deficits at 12 months of age [216, 218]. In the present study, the SwDI mouse model was characterized beforehand in order to have a more precise treatment study. This served the purpose of investigating whether the mouse model also develops the deficits described in literature in our hands, and to detemine the best possible time to start a treatment study. Hence, the SwDI mice had deficits in the nesting behavior and marble burying. Moreover, SwDI mice explored the center of the open field arena less during the total time of the test, which indicated that they were unable to habituate to the arena. Moreover, they were faster and travelled more in the arena compared to WT mice. Regarding the cognitive test, SwDI mice took longer to find the platform on average during the training days in the MWM, and explored the target quadrant less in the probe trial [231] (Table 2).

4.2. Behavioral alterations of transgenic mouse models of dementia

4.2.1. Cognitive deficits

Behavioral tests are a way to measure brain function and to understand how pathological changes in the brain can alter the physiology. Hence, it is a valuable asset in the field of neuroscience [232]. Neuritic plaques and diffuse Aβ aggregates in the cortex and hippocampus are known to be neurotoxic and result in cognitive deficits in different behavioral assessments [54, 233]. The cortex is the region where the executive memory is processed, including the recognition memory [234, 235]. This type of memory is evaluated by the NOR and T-maze spontaneous alternation test. The NOR evaluates the ability of rodents to recognize objects. As rodents have a natural behavior of exploring new environments, once two objects are presented to them, one of which was already presented previously (familiar), mice would naturally explore the new object more [236-238]. A similar paradigm occurs in the T-maze spontaneous alteration, where mice can choose to enter the left or right arm, and they naturally tend to choose the new arm instead of the previously visited one [239, 240].

The hippocampus is the main region in which memory processing occurs, more specifically, the spatial memory [234, 240, 241]. Spatial memory can be evaluated in the MWM and contextual fear conditioning [242, 243]. In the MWM, mice are placed in a pool filled with opaque water and a hidden, so-called “escape” platform [244]. To find the platform, the mice must use visual cues in the room to associate with the position of the platform, therefore, during the training trial, mice learn to associate and find the platform’s location faster. Afterwards, in the probe trial, the platform is removed to confirm the learning of the platform location. Also, the reversal trial can be performed to evaluate the re-learning ability of mice to find the platform when it is placed in a different location. The contextual fear conditioning also uses the same behavioral paradigm. In the fear conditioning, mice receive an unconditioned stimulus, normally an electric shock, together with a conditioned stimulus (light or sound). Due to this

aversive stimulus, they tend to associate the conditioned stimulus with the unconditioned stimulus when presented repeatedly. Moreover, they also associated the aversive stimulus with the arena where it is given, therefore, once they are placed in the same arena, mice would expect the shock [245]. The normal fear response of rodents is to freeze.

Both amyloid plaques in the cortex and impaired recognition memory were observed in the TAPS mice, therefore, Aβ and pEAβ in the cortex might be inducing the TAPS mice's cognitive deficits observed in NOR and T-maze spontaneous alternation [230]. Since TBA2.1 and APP/PS1 parental lines also had deficits in those test, it is not possible to distinguish the role of either Aβ or pEAβ in the recognition memory. Finally, cognitive deficits in the fear conditioning are associated with impairment in the amygdala network [246-249]. TAPS mice had deficits in this behavioral test, which can be explained by the Aβ aggregates in the amygdala [230]. Tau-P301L mice had deficits in the NOR, even though no pathological Tau was observed in the cortex. Despite the lack of pathological Tau in the cortex, pathological alterations might still occur in this region. Besides, one region in the brainstem, called locus coeruleus, has also been shown to play a role in the memory processing [250, 251]. Interestingly, pathological Tau is present in this region, which might explain the cognitive deficit observed in the Tau-P301L.

4.2.2. General behavior

The general behavior of mice can also be explored when studying new mouse models. The ability to build nests is a natural behavior for mice since it helps to control the housing temperature and to secure littermates. This behavior is processed in different regions of the brain, including the hippocampus. The role of the hippocampus in the nest-building behavior is related to the conceptual knowledge, also known as semantic memory [252]. Interestingly, SwDI were not able to build a nest compared to WT, which might also be due to the diffuse Aβ aggregates in the hippocampus [231]. The Tau-P301L mice, on the other hand, could build nests similarly to WT. The lack of alteration in this behavior might occur due to the lack of pathological Tau in the hippocampus. The burrowing behavior was also observed in rodents and impairment in this behavior can be induced by hippocampal lesions [253]. Similar to the observations in the nesting behavior, SwDI also had impairments in the marble burying test, probably also due to the diffuse Aβ aggregates in the hippocampus [231, 253, 254].

The SHIRPA phenotypic assessment was developed to evaluate the general differences in transgenic mouse models compared to non-transgenic mice [255]. In this test, different parameters can be evaluated using a scoring system. The parameters are divided into three sections: mouse behavior in the home cage, in the arena and during handling. In each section, different behaviors can be evaluated, ranging from social interactions in the home cage to some basic physiological features, e.g. pinna and cornea reflexes. TAPS mice had alterations

in the SHIRPA test starting at 12 months of age, more specifically regarding the reflexes and the hanging behavior [230]. Those alterations progressed until 18 months of age. WT mice also showed increased scores when they age, especially in the hanging behavior, but this might be due to the increase of body weight, which is similar to the TAPS mice [230]. Tau-P301L mice also had alterations in the SHIRPA test. In this case, Tau-P301L male mice showed alterations in their body carriage and gait, which progressed to paralysis in the limbs and slower walking, probably due to the Tau pathology present in the brainstem.

4.2.3. Motor deficits

The basal ganglia circuitry plays a major role in the motor assessment of mice and occurs in different regions of the brain. This circuitry is highly regulated; therefore, changes in this network induce motor deficit as observed in Parkinson's disease and other motor related neurodegenerative diseases [256, 257]. To evaluate the motor deficits associated with this circuitry, the modified pole test was performed. The pole test was designed to evaluate the alteration in the striatal dopaminergic neurons in an induced model of 6-hydroxydopamine. It consists of a pole on which the mice are placed on top facing upwards, and the time they take to go down the pole is recorded [258]. In our institute, a modified version of the protocol was developed since some mouse lines are severely motor impaired [215]. In the homozygous TBA2.1, motor deficits, as well as intracellular Aβ aggregates in the basal ganglia network were observed [215]. These aggregates might induce alterations in the dopaminergic circuitry. In our study, Tau-P301L male mice also had motor deficits in the modified pole test. Interestingly, no pathological Tau was observed in the striatum but in the substantia nigra. The substantia nigra also has dopaminergic neurons and receives input/output in the basal ganglia circuitry. Therefore, the pole test might also be able to evaluate the alterations in other areas involved in the basal ganglia network.

TAPS mice seemed to be hyperactive in the open field and this might be due to the fact that these mice developed amyloid plaques in the striatum [259-265]. Tau-P301L male mice, on the other hand, had motor deficits in the open field despite not displaying pathological Tau in the striatum. Alterations in the open field can also be attributed in a certain level to alterations in the basal ganglia network, though, since those are more complex behavior experiments, pathological Tau in the cerebellum and brainstem might also explain the deficits observed there. Another parameter that can be evaluated in the open field is the arena habituation. During the test time, mice habituated to the arena and therefore explored the center area more over time [266, 267]. The SwDI mice showed an impairment in habituating to the arena, since they explored the center of the arena less [231]. This can indicates that SwDI mice had an increased anxiety compared to WT.

It is important to note that the relation to brain pathology and behavioral deficits is not always clear since more than one region can be involved in the same behavioral outcome and the brain network is complex and highly regulated in rodents. Another important observation is that, in the characterization of TAPS mice, the number of animals used was not ideal. Since the TAPS and APP/PS1 mortality rate was 17% and 9% respectively, more than one cohort was necessary and a longitudinal study was not possible [230]. Moreover, in the behavioral experiments, it seems that the alteration existed but it did not reach significance probably due to the low number of mice.

4.3. Histological alterations in transgenic mouse model

Aβ plaques are an important hallmark of AD. In fact, the latest recommendation for specifically diagnosing AD is the detection of altered Aβ levels in the brain [43, 44]. In transgenic mice harboring the APP transgene, Aβ plaques are also present. The TAPS mice also developed plaques at earlier ages compared to APP/PS1, moreover, TAPS mice also had more plaques compared to APP/PS1 in different areas of the brain at different ages. Therefore, the combination of APP and PS1 mutations as well as truncated Aβ seemed to induce a more prominent amyloidosis. In order to evaluate the role of pEAβ in the TAPS mice, an antibody which specifically detects truncated pyroglutamate Aβ in position 3 was used. It was shown that pEAβ was present in the core of the amyloid plaques while unmodified Aβ, which was detected by the widely used antibody6E10, was more prominent in the surrounding area. No differences were observed compared the TAPS mice with the APP/PS1, probably, since this analysis was done in older mice (24 months of age) [230] (Table 2).

In Tau-P301L mice, pathological Tau was evaluated by the detection of hyperphosphorylated Tau. The hyperphosphorylation of Tau at different sites is postulated to occur at different stages of the NFTs [268]. Once the NFTs are formed intracellularly, the serine 214 and threonine 212 (AT100 epitope) are phosphorylated mainly by mitogen-activated protein kinase (MAPK), but also by glycogen synthase kinase 3β (GSK-3 β) and cAMP-dependent protein kinase (PKA). At this stage, filamentous aggregates are present, the cell nucleus is displaced and phosphorylated Tau is misplaced in the dendrites at proximal axons. At later stages, extracellular NFTs can be found. The serine 202 and threonine 205 are phosphorylated (AT8 epitope) by the MAPK, GSK-3 β and cyclin-dependent protein kinase 5 (CDK5) [269]. Two antibodies can recognize those phosphorylated sites: AT8 and AT100. Those antibodies have been widely used in research since these phosphorylation sites can be associated with the formation of NFTs at later stages detected by silver staining. AT8 positive cells and AT100 positive cells were detected in the brainstem (midbrain and hindbrain) and cerebellum of Tau-P301L mice but not in WT mice. Therefore, Tau-P301L mutation induced

hyperphosphorylation of Tau in the transgenic mouse model, as described previously [223] (Table 2).

Neurodegeneration, synaptic loss and neuroinflammation are also relevant hallmarks of neurodegenerative diseases. Most of the transgenic mouse models do not develop neurodegeneration even though they do develop behavioral deficits. Therefore, it has lately been in discussion that synaptic loss correlates more closely to behavioral deficits than neuronal loss [270-272]. Moreover, synaptic markers in the CSF have been studied since they tend to occur in higher concentrations in those fluids in demented patients [273-275]. In TAPS mice, no neuronal loss was observed in the CA1 region of the hippocampus, therefore, similar to observations in humans and other mouse models, synaptic loss might be inducing behavioral alterations [231]. On the other hand, Tau-P301L mice had neurodegeneration in the hindbrain at eight months of age. Even though these results seem to be in contradiction with the TAPS result, it is important to highlight that the neurodegeneration in Tau-P301L mice was evaluated at eight months and the first behavioral alterations started at two months of age, therefore, the neuronal dysfunction might have progressed with age. Finally, an increased number of reactive astrocytes was observed in TAPS mice as well as APP/PS1 mice. Those astrocytes were found in the surroundings of amyloid plaques. The role of astrocytes has already been described in AD in both humans and mice [101-103, 276]. In Tau-P301L mice, no increase of reactive astrocytes or microglia was detected; therefore, pathological Tau did not seem to be sufficient to induce neuroinflammation (Table 2).

Table 2: Overview of the mouse models alterations. The histological hallmarks, cognitive, motor and general deficits for each transgenic mouse model are described.

Mouse model	Histological hallmarks	Cognitive deficits	Motor deficits	General deficits
TAPS mice	+ Aβ + pEAβ + Reactive astrocytes	MWM T-Maze NOR Fear Conditioning	Open field (hyperactivity)	SHIRPA
SwDI	+Aβ	MWM Open field	--	Nesting Marble burying
Tau-P301L	+ Tau + Neuronal loss	NOR	Open field Pole test	SHIRPA Olfactory test

4.4. Treatment with RD2D3 and cRD2D3

D-enantiomeric peptides, developed for the treatment of AD, have proven their efficacy in various AD mouse models [190, 191, 194, 196, 197, 277, 278]. Moreover, these D-peptides are resistant to degradation and penetrate the BBB efficiently [193, 198, 200]. One of these D-peptides, named RD2D3, was developed as a combination of D3 and RD2, in order to increase the *in vitro* and *in vivo* potency [192]. RD2D3 was able to eliminate Aβ oligomers and had a high binding affinity for Aβ42 [195]. In order to improve the pharmacokinetic properties of RD2D3, a cyclized tandem-D-peptide was developed, named cRD2D3 [200]. The pharmacokinetic properties of cRD2D3 were increased compared to the linear peptide, especially its terminal half-life and bioavailability in the brain [200]. In this context, both RD2D3 and cRD2D3 were compared as a potential treatment for AD against Aβ42, Aβ with two amino acid substitutions of glutamate for glutamine at position 22 (Dutch mutation) and of aspartate for asparagine at position 23 (Iowa mutation) (*D/I* Aβ) *in vitro* and *in vivo.* Regarding the binding affinity of both peptides to Aβ42 and *D/I* Aβ, cRD2D3 bound similarly to both Aβ species. RD2D3, though, bound more effectively to *D/I* Aβ than to Aβ as shown by surface plasmon resonance (SPR) analysis. Both peptides were able to prevent Aβ and D/I Aβ fibril formation in the Thioflavin T (ThT) assay and to eliminate oligomers of both Aβ-species in the quantitative determination of interference with Aβ aggregate size distribution (QIAD) assay. Moreover, both peptides were also stable in different simulated body fluids [231].

After treatment of SwDI mice, neither peptide was able to improve the nesting score nor the amount of buried marbles compared to the placebo treated mice in an i.p. treatment study. In the open field test, RD2D3 treatment improved the habituation effect to the arena compared to placebo treatment. In the MWM, RD2D3 and cRD2D3 treatment improved the time the mice needed to find the hidden platform in the training trial, although only RD2D3 treated mice reached statistical significance. Altogether, both peptides were able to improve cognitive deficits in SwDI mice. All in all, no changes were observed in the plaque load and neuroinflammation in the AD mice's brains treated with either peptide compared to placebo [231]. Therefore, the cognitive improvement did not seem to be due to the decrease of plaque load, but rather the elimination of Aβ oligomers which is in line with the hypothesis that Aβ oligomers are more toxic that fibrils [93].

5. Conclusion

Summarized, in this study, the behavioral and pathology of different (AD) mouse models was evaluated. All three mouse lines, TAPS, Tau-P301L and SwDI, are promising mouse models to be used in future treatment studies. The newly developed TAPS mice had an earlier and more pronounced phenotype induced by the aggregation of pEAβ. In this mouse line, amyloid plaques are present in the cortex, hippocampus and striatum as early as six months of age and they displayed robust behavioral deficits. Another model, the Tau-P301L mice had sex-dependent deficits induced by pathological Tau in different brain regions starting at two months of age in the longitudinal studies. Tau-P301L male mice had olfactory deficits, phenotypic alterations, cognitive deficits and motor deficits in different tests at different ages. On the other hand, Tau-P301L female mice did not display any motor deficits and this result might be explained by the lack of pathological Tau in the brain.

The SwDI line was also characterized beforehand in order to improve the treatment design. SwDI mice treated with RD2D3 and cRD2D3 displayed a cognitive improvement compared to placebo. Both peptides also showed efficacy in binding to Aβ and D/I Aβ *in vitro.* Finally, RD2D3 and cRD2D3 are both potential new treatment options for AD, since the peptides proved their efficiency against Aβ and D/I Aβ *in vitro* and *in vivo*.

List of Abbreviations

Ach	Acetylcholine
AchEI	Acetylcholinesterase inhibitors
AD	Alzheimer's diseaase
ADRD	Alzheimer's disease and related dementias
AMPAr	α-amino-3-hydroxy-5-methyl-4-isoxazolepropionate receptor
APH-1	Anterior pharynx defective 1
APOE	Apolipoprotein E
APP	Amyloid precursor protein
APP/PS1	APPswe/PS1dE9
APPSwDI	APP Swedish (KM670/671NL) Dutch (E693Q) and Iowa (D694N)
APPSwe	Swedish mutation
ATP	Adenosine triphosphate
Aβ	Amyloid-β
BACE1	B-secretase
BBB	Blood-brain-barrier
CAA	Cerebral amyloid angiopathy
CBD	Corticobasal degeneration
CDK5	Cyclin-dependent protein kinase 5
CSF	Cephalospinal fluid
EOAD	Early onset Alzheimer's disease
FDA	Food and drugs administration
FDG	2-deoxy-2 (18F) Fluoro-D-glucose
FTD	Frontotemporal dementia
FTDP-17	frontotemporal dementia with parkinsonism-17
FTLD-Tau	Frontotemporal lobar degeneration associated with Tau
Fyn	Src family Tyrosine kinase
GFAP	Glial fibrillary acidic protein
GSK-3β	Glycogen synthase kinase-3
LOAD	Late onset Alzheimer's disease
LRP1	Low-density lipoprotein receptor-related protein 1
LTD	Long-term depression
LTP	Long-term potentiation
MAP	Microtubule associated protein
MAPK	Mitogen-activated protein kinase
MAPT	Microtubule associated protein Tau
MCI	Mild cognitive impairment
MRI	Magnetic resonance imaging
MWM	Morris water maze
Nedd4-1	neural precursor cell expressed, developmentally down-regulated 4-1
NfL	Neurofilament light
NFTs	Neurofibrilary tangles
NIA	National institute of aging
NMDAr	N-methyl-D-aspartic acid receptor
NOR	Novel object recognition test
pEAβ	Pyroglutamate Aβ
PEN-2	Presenilin enhancer 2
PET	Positron emission tomography
PHF	Paired helix filaments
PiB	Pittsburg Compound
PICK1	Protein interacting with C Kinase
PKA	cAMP-dependent protein kinase

PS	Presenilin
PS1ΔE9	Deletion of exon 9 in the PSEN1 gene
PSD95	Postsynaptic density protein 95
PSEN	Presenilin genes
PSP	Progressive supranuclear palsy
p-Tau	Phosphorylated Tau
PTM	Posttranslational modification
QIAD	Quantitative determination of interference with Aβ aggregate size distribution
SHIRPA	SmithKline Beecham Pharmaceuticals; Harwell, MRC Mouse Genome Centre and Mammalian Genetics Unit; Imperial College School of Medicine at St Mary's; Royal London Hospital, St Bartholomew's and the Royal London School of Medicine Assessment
SPR	Surface plasmon resonance
SPSN	Sociability and preference for social novelty
sTREM2	Soluble triggering receptor expressed on myeloid cells 2
ThT	Thioflavin T
TRH	Thyrotropin releasing hormone
WT	Wild type
YKL-40	Chitinase 3-like 1

References

1. Nichols, E., C.E. Szoeke, S.E. Vollset, N. Abbasi, F. Abd-Allah, J. Abdela, M.T.E. Aichour, R.O. Akinyemi, F. Alahdab, and S.W. Asgedom, *Global, regional, and national burden of Alzheimer's disease and other dementias, 1990–2016: a systematic analysis for the Global Burden of Disease Study 2016.* The Lancet Neurology, 2019. **18**(1): p. 88-106.
2. Brookmeyer, R., E. Johnson, K. Ziegler-Graham, and H.M. Arrighi, *Forecasting the global burden of Alzheimer's disease.* Alzheimers Dement, 2007. **3**(3): p. 186-91.
3. Patterson, C., *World alzheimer report 2018.* 2018.
4. Wimo, A., M. Guerchet, G.C. Ali, Y.T. Wu, A.M. Prina, B. Winblad, L. Jönsson, Z. Liu, and M. Prince, *The worldwide costs of dementia 2015 and comparisons with 2010.* Alzheimers Dement, 2017. **13**(1): p. 1-7.
5. Prince, M., A. Comas-Herrera, M. Knapp, M. Guerchet, and M. Karagiannidou, *World Alzheimer report 2016: improving healthcare for people living with dementia: coverage, quality and costs now and in the future.* 2016.
6. Alzheimer, A., *Über eigenartige Krankheitsfälle des späteren Alters.* Zeitschrift für die gesamte Neurologie und Psychiatrie, 1911. **4**(1): p. 356.
7. Kosik, K.S., C.L. Joachim, and D.J. Selkoe, *Microtubule-associated protein tau (tau) is a major antigenic component of paired helical filaments in Alzheimer disease.* Proc Natl Acad Sci U S A, 1986. **83**(11): p. 4044-8.
8. Tanzi, R.E., J.F. Gusella, P.C. Watkins, G.A. Bruns, P. St George-Hyslop, M.L. Van Keuren, D. Patterson, S. Pagan, D.M. Kurnit, and R.L. Neve, *Amyloid beta protein gene: cDNA, mRNA distribution, and genetic linkage near the Alzheimer locus.* Science, 1987. **235**(4791): p. 880-4.
9. Irwin, D.J., *Tauopathies as clinicopathological entities.* Parkinsonism Relat Disord, 2016. **22 Suppl 1**(0 1): p. S29-33.
10. DeTure, M.A. and D.W. Dickson, *The neuropathological diagnosis of Alzheimer's disease.* Molecular neurodegeneration, 2019. **14**(1): p. 1-18.
11. Henneman, W.J.P., J.D. Sluimer, J. Barnes, W.M. van der Flier, I.C. Sluimer, N.C. Fox, P. Scheltens, H. Vrenken, and F. Barkhof, *Hippocampal atrophy rates in Alzheimer disease: added value over whole brain volume measures.* Neurology, 2009. **72**(11): p. 999-1007.
12. Vemuri, P. and C.R. Jack, *Role of structural MRI in Alzheimer's disease.* Alzheimer's Research & Therapy, 2010. **2**(4): p. 23.
13. Brown, E.E., S. Kumar, T.K. Rajji, B.G. Pollock, and B.H. Mulsant, *Anticipating and Mitigating the Impact of the COVID-19 Pandemic on Alzheimer's Disease and Related Dementias.* Am J Geriatr Psychiatry, 2020. **28**(7): p. 712-721.
14. Association, A.s., *2021 Alzheimer's Disease Facts and Figures.* Alzheimer's Dementia, 2021 **17**(3).
15. Bauer, K., L. Schwarzkopf, E. Graessel, and R. Holle, *A claims data-based comparison of comorbidity in individuals with and without dementia.* BMC geriatrics, 2014. **14**: p. 10.
16. Mao, L., H. Jin, M. Wang, Y. Hu, S. Chen, Q. He, J. Chang, C. Hong, Y. Zhou, D. Wang, X. Miao, Y. Li, and B. Hu, *Neurologic Manifestations of Hospitalized Patients With Coronavirus Disease 2019 in Wuhan, China.* JAMA neurology, 2020. **77**(6): p. 683-690.
17. Xia, X., Y. Wang, and J. Zheng, *COVID-19 and Alzheimer's disease: how one crisis worsens the other.* Translational Neurodegeneration, 2021. **10**(1): p. 15.
18. Lara, B., A. Carnes, F. Dakterzada, I. Benitez, and G. Piñol-Ripoll, *Neuropsychiatric symptoms and quality of life in Spanish patients with Alzheimer's disease during the COVID-19 lockdown.* European Journal of Neurology, 2020. **27**(9): p. 1744-1747.

19. Andrews, S.J., B. Fulton-Howard, P. O'Reilly, E. Marcora, and A.M. Goate, *Causal Associations Between Modifiable Risk Factors and the Alzheimer's Phenome.* Ann Neurol, 2021. **89**(1): p. 54-65.
20. Prince, M.J., *World Alzheimer Report 2015: the global impact of dementia: an analysis of prevalence, incidence, cost and trends*. 2015: Alzheimer's Disease International.
21. Organization, W.H., *Risk reduction of cognitive decline and dementia: WHO guidelines.* 2019.
22. Wada, M., Y. Noda, S. Shinagawa, J.K. Chung, K. Sawada, K. Ogyu, R. Tarumi, S. Tsugawa, T. Miyazaki, B. Yamagata, A. Graff-Guerrero, M. Mimura, and S. Nakajima, *Effect of Education on Alzheimer's Disease-Related Neuroimaging Biomarkers in Healthy Controls, and Participants with Mild Cognitive Impairment and Alzheimer's Disease: A Cross-Sectional Study.* J Alzheimers Dis, 2018. **63**(2): p. 861-869.
23. Sommerlad, A., S. Sabia, A. Singh-Manoux, G. Lewis, and G. Livingston, *Association of social contact with dementia and cognition: 28-year follow-up of the Whitehall II cohort study.* PLoS Med, 2019. **16**(8): p. e1002862.
24. Fancourt, D., A. Steptoe, and D. Cadar, *Community engagement and dementia risk: time-to-event analyses from a national cohort study*. Journal of epidemiology and community health, 2020. **74**(1): p. 71-77.
25. Diniz, B.S., M.A. Butters, S.M. Albert, M.A. Dew, and C.F. Reynolds, 3rd, *Late-life depression and risk of vascular dementia and Alzheimer's disease: systematic review and meta-analysis of community-based cohort studies.* Br J Psychiatry, 2013. **202**(5): p. 329-35.
26. Sindi, S., G. Hagman, K. Håkansson, J. Kulmala, C. Nilsen, I. Kåreholt, H. Soininen, A. Solomon, and M. Kivipelto, *Midlife Work-Related Stress Increases Dementia Risk in Later Life: The CAIDE 30-Year Study.* J Gerontol B Psychol Sci Soc Sci, 2017. **72**(6): p. 1044-1053.
27. Xue, M., W. Xu, Y.N. Ou, X.P. Cao, M.S. Tan, L. Tan, and J.T. Yu, *Diabetes mellitus and risks of cognitive impairment and dementia: A systematic review and meta-analysis of 144 prospective studies.* Ageing Res Rev, 2019. **55**: p. 100944.
28. McGrath, E.R., A.S. Beiser, C. DeCarli, K.L. Plourde, R.S. Vasan, S.M. Greenberg, and S. Seshadri, *Blood pressure from mid- to late life and risk of incident dementia.* Neurology, 2017. **89**(24): p. 2447-2454.
29. Tolppanen, A.M., T. Ngandu, I. Kåreholt, T. Laatikainen, M. Rusanen, H. Soininen, and M. Kivipelto, *Midlife and late-life body mass index and late-life dementia: results from a prospective population-based cohort.* J Alzheimers Dis, 2014. **38**(1): p. 201-9.
30. Zhou, J., J.T. Yu, H.F. Wang, X.F. Meng, C.C. Tan, J. Wang, C. Wang, and L. Tan, *Association between stroke and Alzheimer's disease: systematic review and meta-analysis.* J Alzheimers Dis, 2015. **43**(2): p. 479-89.
31. Xu, W., L. Tan, B.-J. Su, H. Yu, Y.-L. Bi, X.-F. Yue, Q. Dong, and J.-T. Yu, *Sleep characteristics and cerebrospinal fluid biomarkers of Alzheimer's disease pathology in cognitively intact older adults: The CABLE study.* Alzheimer's & Dementia, 2020. **16**(8): p. 1146-1152.
32. Zhong, G., Y. Wang, Y. Zhang, J.J. Guo, and Y. Zhao, *Smoking is associated with an increased risk of dementia: a meta-analysis of prospective cohort studies with investigation of potential effect modifiers.* PLoS One, 2015. **10**(3): p. e0118333.
33. Xu, W., H. Wang, Y. Wan, C. Tan, J. Li, L. Tan, and J.T. Yu, *Alcohol consumption and dementia risk: a dose-response meta-analysis of prospective studies.* Eur J Epidemiol, 2017. **32**(1): p. 31-42.
34. Chen, X., B. Maguire, H. Brodaty, and F. O'Leary, *Dietary Patterns and Cognitive Health in Older Adults: A Systematic Review.* J Alzheimers Dis, 2019. **67**(2): p. 583-619.
35. Corder, E.H., A.M. Saunders, W.J. Strittmatter, D.E. Schmechel, P.C. Gaskell, G.W. Small, A.D. Roses, J.L. Haines, and M.A. Pericak-Vance, *Gene dose of apolipoprotein*

E type 4 allele and the risk of Alzheimer's disease in late onset families. Science, 1993. **261**(5123): p. 921-3.
36. Xia, C.F., J. Arteaga, G. Chen, U. Gangadharmath, L.F. Gomez, D. Kasi, C. Lam, Q. Liang, C. Liu, V.P. Mocharla, F. Mu, A. Sinha, H. Su, A.K. Szardenings, J.C. Walsh, E. Wang, C. Yu, W. Zhang, T. Zhao, and H.C. Kolb, *[(18)F]T807, a novel tau positron emission tomography imaging agent for Alzheimer's disease.* Alzheimers Dement, 2013. **9**(6): p. 666-76.
37. Strittmatter, W.J., A.M. Saunders, D. Schmechel, M. Pericak-Vance, J. Enghild, G.S. Salvesen, and A.D. Roses, *Apolipoprotein E: high-avidity binding to beta-amyloid and increased frequency of type 4 allele in late-onset familial Alzheimer disease.* Proc Natl Acad Sci U S A, 1993. **90**(5): p. 1977-81.
38. Jeong, W., H. Lee, S. Cho, and J. Seo, *ApoE4-Induced Cholesterol Dysregulation and Its Brain Cell Type-Specific Implications in the Pathogenesis of Alzheimer's Disease.* Mol Cells, 2019. **42**(11): p. 739-746.
39. Janssen, J.C., J.A. Beck, T.A. Campbell, A. Dickinson, N.C. Fox, R.J. Harvey, H. Houlden, M.N. Rossor, and J. Collinge, *Early onset familial Alzheimer's disease.* Mutation frequency in 31 families, 2003. **60**(2): p. 235-239.
40. Wu, L., P. Rosa-Neto, G.Y. Hsiung, A.D. Sadovnick, M. Masellis, S.E. Black, J. Jia, and S. Gauthier, *Early-onset familial Alzheimer's disease (EOFAD).* Can J Neurol Sci, 2012. **39**(4): p. 436-45.
41. Bali, J., A.H. Gheinani, S. Zurbriggen, and L. Rajendran, *Role of genes linked to sporadic Alzheimer's disease risk in the production of β-amyloid peptides.* Proceedings of the National Academy of Sciences, 2012. **109**(38): p. 15307-15311.
42. Sperling, R.A., P.S. Aisen, L.A. Beckett, D.A. Bennett, S. Craft, A.M. Fagan, T. Iwatsubo, C.R. Jack Jr, J. Kaye, and T.J. Montine, *Toward defining the preclinical stages of Alzheimer's disease: recommendations from the National Institute on Aging-Alzheimer's Association workgroups on diagnostic guidelines for Alzheimer's disease.* Alzheimer's & dementia, 2011. **7**(3): p. 280-292.
43. McKhann, G.M., D.S. Knopman, H. Chertkow, B.T. Hyman, C.R. Jack Jr, C.H. Kawas, W.E. Klunk, W.J. Koroshetz, J.J. Manly, and R. Mayeux, *The diagnosis of dementia due to Alzheimer's disease: recommendations from the National Institute on Aging-Alzheimer's Association workgroups on diagnostic guidelines for Alzheimer's disease.* Alzheimer's & dementia, 2011. **7**(3): p. 263-269.
44. Albert, M.S., S.T. DeKosky, D. Dickson, B. Dubois, H.H. Feldman, N.C. Fox, A. Gamst, D.M. Holtzman, W.J. Jagust, R.C. Petersen, P.J. Snyder, M.C. Carrillo, B. Thies, and C.H. Phelps, *The diagnosis of mild cognitive impairment due to Alzheimer's disease: Recommendations from the National Institute on Aging-Alzheimer's Association workgroups on diagnostic guidelines for Alzheimer's disease.* Alzheimer's & Dementia, 2011. **7**(3): p. 270-279.
45. Jack Jr, C.R., M.S. Albert, D.S. Knopman, G.M. McKhann, R.A. Sperling, M.C. Carrillo, B. Thies, and C.H. Phelps, *Introduction to the recommendations from the National Institute on Aging-Alzheimer's Association workgroups on diagnostic guidelines for Alzheimer's disease.* Alzheimer's & dementia, 2011. **7**(3): p. 257-262.
46. Jack, C.R., Jr., D.A. Bennett, K. Blennow, M.C. Carrillo, B. Dunn, S.B. Haeberlein, D.M. Holtzman, W. Jagust, F. Jessen, J. Karlawish, E. Liu, J.L. Molinuevo, T. Montine, C. Phelps, K.P. Rankin, C.C. Rowe, P. Scheltens, E. Siemers, H.M. Snyder, and R. Sperling, *NIA-AA Research Framework: Toward a biological definition of Alzheimer's disease.* Alzheimers Dement, 2018. **14**(4): p. 535-562.
47. Blennow, K. and H. Zetterberg, *Biomarkers for Alzheimer's disease: current status and prospects for the future.* Journal of Internal Medicine, 2018. **284**(6): p. 643-663.
48. Andreasen, N., C. Hesse, P. Davidsson, L. Minthon, A. Wallin, B. Winblad, H. Vanderstichele, E. Vanmechelen, and K. Blennow, *Cerebrospinal fluid β-amyloid (1-42) in Alzheimer disease: differences between early-and late-onset Alzheimer disease*

and stability during the course of disease. Archives of neurology, 1999. **56**(6): p. 673-680.
49. Vanmechelen, E., H. Vanderstichele, P. Davidsson, E. Van Kerschaver, B. Van Der Perre, M. Sjögren, N. Andreasen, and K. Blennow, *Quantification of tau phosphorylated at threonine 181 in human cerebrospinal fluid: a sandwich ELISA with a synthetic phosphopeptide for standardization.* Neuroscience letters, 2000. **285**(1): p. 49-52.
50. Meredith Jr, J.E., S. Sankaranarayanan, V. Guss, A.J. Lanzetti, F. Berisha, R.J. Neely, J.R. Slemmon, E. Portelius, H. Zetterberg, K. Blennow, H. Soares, M. Ahlijanian, and C.F. Albright, *Characterization of Novel CSF Tau and ptau Biomarkers for Alzheimer's Disease.* PLOS ONE, 2013. **8**(10): p. e76523.
51. Karikari, T.K., T.A. Pascoal, N.J. Ashton, S. Janelidze, A.L. Benedet, J.L. Rodriguez, M. Chamoun, M. Savard, M.S. Kang, J. Therriault, M. Schöll, G. Massarweh, J.P. Soucy, K. Höglund, G. Brinkmalm, N. Mattsson, S. Palmqvist, S. Gauthier, E. Stomrud, H. Zetterberg, O. Hansson, P. Rosa-Neto, and K. Blennow, *Blood phosphorylated tau 181 as a biomarker for Alzheimer's disease: a diagnostic performance and prediction modelling study using data from four prospective cohorts.* Lancet Neurol, 2020. **19**(5): p. 422-433.
52. Lloret, A., D. Esteve, M.-A. Lloret, A. Cervera-Ferri, B. Lopez, M. Nepomuceno, and P. Monllor, *When Does Alzheimer's Disease Really Start? The Role of Biomarkers.* International journal of molecular sciences, 2019. **20**(22): p. 5536.
53. Ferreira, D., C. Verhagen, J.A. Hernández-Cabrera, L. Cavallin, C.-J. Guo, U. Ekman, J.S. Muehlboeck, A. Simmons, J. Barroso, L.-O. Wahlund, and E. Westman, *Distinct subtypes of Alzheimer's disease based on patterns of brain atrophy: longitudinal trajectories and clinical applications.* Scientific Reports, 2017. **7**(1): p. 46263.
54. Klunk, W.E., H. Engler, A. Nordberg, Y. Wang, G. Blomqvist, D.P. Holt, M. Bergström, I. Savitcheva, G.F. Huang, S. Estrada, B. Ausén, M.L. Debnath, J. Barletta, J.C. Price, J. Sandell, B.J. Lopresti, A. Wall, P. Koivisto, G. Antoni, C.A. Mathis, and B. Långström, *Imaging brain amyloid in Alzheimer's disease with Pittsburgh Compound-B.* Ann Neurol, 2004. **55**(3): p. 306-19.
55. Lopresti, B.J., W.E. Klunk, C.A. Mathis, J.A. Hoge, S.K. Ziolko, X. Lu, C.C. Meltzer, K. Schimmel, N.D. Tsopelas, S.T. DeKosky, and J.C. Price, *Simplified quantification of Pittsburgh Compound B amyloid imaging PET studies: a comparative analysis.* J Nucl Med, 2005. **46**(12): p. 1959-72.
56. Zhang, S., N. Smailagic, C. Hyde, A.H. Noel-Storr, Y. Takwoingi, R. McShane, and J. Feng, *(11)C-PIB-PET for the early diagnosis of Alzheimer's disease dementia and other dementias in people with mild cognitive impairment (MCI).* Cochrane Database Syst Rev, 2014. **2014**(7): p. Cd010386.
57. Mosconi, L., W.H. Tsui, A. Pupi, S. De Santi, A. Drzezga, S. Minoshima, and M.J. de Leon, *(18)F-FDG PET database of longitudinally confirmed healthy elderly individuals improves detection of mild cognitive impairment and Alzheimer's disease.* J Nucl Med, 2007. **48**(7): p. 1129-34.
58. Ou, Y.-N., W. Xu, J.-Q. Li, Y. Guo, M. Cui, K.-L. Chen, Y.-Y. Huang, Q. Dong, L. Tan, J.-T. Yu, and I. on behalf of Alzheimer's Disease Neuroimaging, *FDG-PET as an independent biomarker for Alzheimer's biological diagnosis: a longitudinal study.* Alzheimer's Research & Therapy, 2019. **11**(1): p. 57.
59. Chien, D.T., S. Bahri, A.K. Szardenings, J.C. Walsh, F. Mu, M.Y. Su, W.R. Shankle, A. Elizarov, and H.C. Kolb, *Early clinical PET imaging results with the novel PHF-tau radioligand [F-18]-T807.* J Alzheimers Dis, 2013. **34**(2): p. 457-68.
60. Marquié, M., M.D. Normandin, C.R. Vanderburg, I.M. Costantino, E.A. Bien, L.G. Rycyna, W.E. Klunk, C.A. Mathis, M.D. Ikonomovic, M.L. Debnath, N. Vasdev, B.C. Dickerson, S.N. Gomperts, J.H. Growdon, K.A. Johnson, M.P. Frosch, B.T. Hyman, and T. Gómez-Isla, *Validating novel tau positron emission tomography tracer [F-18]-AV-1451 (T807) on postmortem brain tissue.* Ann Neurol, 2015. **78**(5): p. 787-800.

61. Ossenkoppele, R., D.R. Schonhaut, M. Schöll, S.N. Lockhart, N. Ayakta, S.L. Baker, J.P. O'Neil, M. Janabi, A. Lazaris, A. Cantwell, J. Vogel, M. Santos, Z.A. Miller, B.M. Bettcher, K.A. Vossel, J.H. Kramer, M.L. Gorno-Tempini, B.L. Miller, W.J. Jagust, and G.D. Rabinovici, *Tau PET patterns mirror clinical and neuroanatomical variability in Alzheimer's disease.* Brain : a journal of neurology, 2016. **139**(Pt 5): p. 1551-1567.
62. Johnson, K.A., A. Schultz, R.A. Betensky, J.A. Becker, J. Sepulcre, D. Rentz, E. Mormino, J. Chhatwal, R. Amariglio, K. Papp, G. Marshall, M. Albers, S. Mauro, L. Pepin, J. Alverio, K. Judge, M. Philiossaint, T. Shoup, D. Yokell, B. Dickerson, T. Gomez-Isla, B. Hyman, N. Vasdev, and R. Sperling, *Tau positron emission tomographic imaging in aging and early Alzheimer disease.* Ann Neurol, 2016. **79**(1): p. 110-9.
63. Zetterberg, H. and B.B. Bendlin, *Biomarkers for Alzheimer's disease—preparing for a new era of disease-modifying therapies.* Molecular Psychiatry, 2021. **26**(1): p. 296-308.
64. Bayer, T.A., R. Cappai, C.L. Masters, K. Beyreuther, and G. Multhaup, *It all sticks together--the APP-related family of proteins and Alzheimer's disease.* Mol Psychiatry, 1999. **4**(6): p. 524-8.
65. Karch, C.M. and A.M. Goate, *Alzheimer's disease risk genes and mechanisms of disease pathogenesis.* Biological psychiatry, 2015. **77**(1): p. 43-51.
66. Cai, H., Y. Wang, D. McCarthy, H. Wen, D.R. Borchelt, D.L. Price, and P.C. Wong, *BACE1 is the major beta-secretase for generation of Abeta peptides by neurons.* Nat Neurosci, 2001. **4**(3): p. 233-4.
67. Zhang, S., Z. Wang, F. Cai, M. Zhang, Y. Wu, J. Zhang, and W. Song, *BACE1 Cleavage Site Selection Critical for Amyloidogenesis and Alzheimer's Pathogenesis.* J Neurosci, 2017. **37**(29): p. 6915-6925.
68. Huse, J.T., K. Liu, D.S. Pijak, D. Carlin, V.M.Y. Lee, and R.W. Doms, *β-Secretase Processing in the Trans-Golgi Network Preferentially Generates Truncated Amyloid Species That Accumulate in Alzheimer’s Disease Brain *.* Journal of Biological Chemistry, 2002. **277**(18): p. 16278-16284.
69. Deng, Y., Z. Wang, R. Wang, X. Zhang, S. Zhang, Y. Wu, M. Staufenbiel, F. Cai, and W. Song, *Amyloid-β protein (Aβ) Glu11 is the major β-secretase site of β-site amyloid-β precursor protein-cleaving enzyme 1(BACE1), and shifting the cleavage site to Aβ Asp1 contributes to Alzheimer pathogenesis.* European Journal of Neuroscience, 2013. **37**(12): p. 1962-1969.
70. Selkoe, D.J., *Alzheimer disease: mechanistic understanding predicts novel therapies.* Ann Intern Med, 2004. **140**(8): p. 627-38.
71. De Strooper, B., *Aph-1, Pen-2, and Nicastrin with Presenilin generate an active gamma-Secretase complex.* Neuron, 2003. **38**(1): p. 9-12.
72. Kimberly, W.T., M.J. LaVoie, B.L. Ostaszewski, W. Ye, M.S. Wolfe, and D.J. Selkoe, *Gamma-secretase is a membrane protein complex comprised of presenilin, nicastrin, Aph-1, and Pen-2.* Proc Natl Acad Sci U S A, 2003. **100**(11): p. 6382-7.
73. Iwatsubo, T., *The gamma-secretase complex: machinery for intramembrane proteolysis.* Curr Opin Neurobiol, 2004. **14**(3): p. 379-83.
74. Takami, M., Y. Nagashima, Y. Sano, S. Ishihara, M. Morishima-Kawashima, S. Funamoto, and Y. Ihara, *γ-Secretase: successive tripeptide and tetrapeptide release from the transmembrane domain of β-carboxyl terminal fragment.* Journal of Neuroscience, 2009. **29**(41): p. 13042-13052.
75. Qi-Takahara, Y., M. Morishima-Kawashima, Y. Tanimura, G. Dolios, N. Hirotani, Y. Horikoshi, F. Kametani, M. Maeda, T.C. Saido, R. Wang, and Y. Ihara, *Longer forms of amyloid beta protein: implications for the mechanism of intramembrane cleavage by gamma-secretase.* The Journal of neuroscience : the official journal of the Society for Neuroscience, 2005. **25**(2): p. 436-445.
76. Fernandez, M.A., J.A. Klutkowski, T. Freret, and M.S. Wolfe, *Alzheimer presenilin-1 mutations dramatically reduce trimming of long amyloid β-peptides (Aβ) by γ-secretase*

to increase 42-to-40-residue Aβ. The Journal of biological chemistry, 2014. **289**(45): p. 31043-31052.
77. Bolduc, D.M., D.R. Montagna, M.C. Seghers, M.S. Wolfe, and D.J. Selkoe, *The amyloid-beta forming tripeptide cleavage mechanism of γ-secretase.* Elife, 2016. **5**: p. e17578.
78. Iwatsubo, T., A. Odaka, N. Suzuki, H. Mizusawa, N. Nukina, and Y. Ihara, *Visualization of A beta 42(43) and A beta 40 in senile plaques with end-specific A beta monoclonals: evidence that an initially deposited species is A beta 42(43).* Neuron, 1994. **13**(1): p. 45-53.
79. McGowan, E., F. Pickford, J. Kim, L. Onstead, J. Eriksen, C. Yu, L. Skipper, M.P. Murphy, J. Beard, P. Das, K. Jansen, M. DeLucia, W.L. Lin, G. Dolios, R. Wang, C.B. Eckman, D.W. Dickson, M. Hutton, J. Hardy, and T. Golde, *Abeta42 is essential for parenchymal and vascular amyloid deposition in mice.* Neuron, 2005. **47**(2): p. 191-199.
80. Gunn, A.P., C.L. Masters, and R.A. Cherny, *Pyroglutamate-Aβ: Role in the natural history of Alzheimer's disease.* The International Journal of Biochemistry & Cell Biology, 2010. **42**(12): p. 1915-1918.
81. Cynis, H., E. Scheel, T.C. Saido, S. Schilling, and H.-U. Demuth, *Amyloidogenic Processing of Amyloid Precursor Protein: Evidence of a Pivotal Role of Glutaminyl Cyclase in Generation of Pyroglutamate-Modified Amyloid-β.* Biochemistry, 2008. **47**(28): p. 7405-7413.
82. Harigaya, Y., T.C. Saido, C.B. Eckman, C.-M. Prada, M. Shoji, and S.G. Younkin, *Amyloid β Protein Starting Pyroglutamate at Position 3 Is a Major Component of the Amyloid Deposits in the Alzheimer's Disease Brain.* Biochemical and Biophysical Research Communications, 2000. **276**(2): p. 422-427.
83. Frost, J.L., K.X. Le, H. Cynis, E. Ekpo, M. Kleinschmidt, R.M. Palmour, F.R. Ervin, S. Snigdha, C.W. Cotman, T.C. Saido, R.J. Vassar, P.S. George-Hyslop, T. Ikezu, S. Schilling, H.-U. Demuth, and C.A. Lemere, *Pyroglutamate-3 Amyloid-β Deposition in the Brains of Humans, Non-Human Primates, Canines, and Alzheimer Disease–Like Transgenic Mouse Models.* The American Journal of Pathology, 2013. **183**(2): p. 369-381.
84. He, W. and C.J. Barrow, *The Aβ 3-Pyroglutamyl and 11-Pyroglutamyl Peptides Found in Senile Plaque Have Greater β-Sheet Forming and Aggregation Propensities in Vitro than Full-Length Aβ.* Biochemistry, 1999. **38**(33): p. 10871-10877.
85. Spies, P., M. Verbeek, T. Groen, and J. Claassen, *Reviewing reasons for the decreased CSF Abeta42 concentration in Alzheimer disease.* Frontiers in bioscience : a journal and virtual library, 2012. **17**: p. 2024-34.
86. Chen, G.-f., T.-h. Xu, Y. Yan, Y.-r. Zhou, Y. Jiang, K. Melcher, and H.E. Xu, *Amyloid beta: structure, biology and structure-based therapeutic development.* Acta Pharmacologica Sinica, 2017. **38**(9): p. 1205-1235.
87. Stroud, J.C., C. Liu, P.K. Teng, and D. Eisenberg, *Toxic fibrillar oligomers of amyloid-β have cross-β structure.* Proceedings of the National Academy of Sciences, 2012. **109**(20): p. 7717-7722.
88. Hardy, J. and G. Higgins, *Alzheimer's disease: the amyloid cascade hypothesis.* Science, 1992. **256**(5054): p. 184-185.
89. McLean, C.A., R.A. Cherny, F.W. Fraser, S.J. Fuller, M.J. Smith, K. Beyreuther, A.I. Bush, and C.L. Masters, *Soluble pool of Abeta amyloid as a determinant of severity of neurodegeneration in Alzheimer's disease.* Ann Neurol, 1999. **46**(6): p. 860-6.
90. Haass, C. and D.J. Selkoe, *Soluble protein oligomers in neurodegeneration: lessons from the Alzheimer's amyloid beta-peptide.* Nat Rev Mol Cell Biol, 2007. **8**(2): p. 101-12.
91. Yang, T., S. Li, H. Xu, D.M. Walsh, and D.J. Selkoe, *Large Soluble Oligomers of Amyloid β-Protein from Alzheimer Brain Are Far Less Neuroactive Than the Smaller*

Oligomers to Which They Dissociate. The Journal of Neuroscience, 2017. **37**(1): p. 152-163.
92. Shea, D., C.-C. Hsu, T.M. Bi, N. Paranjapye, M.C. Childers, J. Cochran, C.P. Tomberlin, L. Wang, D. Paris, J. Zonderman, G. Varani, C.D. Link, M. Mullan, and V. Daggett, *α-Sheet secondary structure in amyloid β-peptide drives aggregation and toxicity in Alzheimer's disease.* Proceedings of the National Academy of Sciences, 2019. **116**(18): p. 8895-8900.
93. Hardy, J. and D.J. Selkoe, *The amyloid hypothesis of Alzheimer's disease: progress and problems on the road to therapeutics.* Science, 2002. **297**(5580): p. 353-6.
94. Selkoe, D.J. and J. Hardy, *The amyloid hypothesis of Alzheimer's disease at 25 years.* EMBO molecular medicine, 2016. **8**(6): p. 595-608.
95. Walker, L.C., *Prion-like mechanisms in Alzheimer disease.* Handb Clin Neurol, 2018. **153**: p. 303-319.
96. Baker, H.F., R.M. Ridley, L.W. Duchen, T.J. Crow, and C.J. Bruton, *Induction of beta (A4)-amyloid in primates by injection of Alzheimer's disease brain homogenate. Comparison with transmission of spongiform encephalopathy.* Mol Neurobiol, 1994. **8**(1): p. 25-39.
97. Kane, S.J., T.K. Farley, E.O. Gordon, J. Estep, H.R. Bender, J.A. Moreno, J. Bartz, G.C. Telling, M.C. Pickering, and M.D. Zabel, *Complement Regulatory Protein Factor H Is a Soluble Prion Receptor That Potentiates Peripheral Prion Pathogenesis.* The Journal of Immunology, 2017. **199**(11): p. 3821-3827.
98. Walker, L.C., M.J. Callahan, F. Bian, R.A. Durham, A.E. Roher, and W.J. Lipinski, *Exogenous induction of cerebral β-amyloidosis in βAPP-transgenic mice.* Peptides, 2002. **23**(7): p. 1241-1247.
99. Meyer-Luehmann, M., J. Coomaraswamy, T. Bolmont, S. Kaeser, C. Schaefer, E. Kilger, A. Neuenschwander, D. Abramowski, P. Frey, A.L. Jaton, J.M. Vigouret, P. Paganetti, D.M. Walsh, P.M. Mathews, J. Ghiso, M. Staufenbiel, L.C. Walker, and M. Jucker, *Exogenous induction of cerebral beta-amyloidogenesis is governed by agent and host.* Science, 2006. **313**(5794): p. 1781-4.
100. Aoyagi, A., C. Condello, J. Stöhr, W. Yue, B.M. Rivera, J.C. Lee, A.L. Woerman, G. Halliday, S. van Duinen, M. Ingelsson, L. Lannfelt, C. Graff, T.D. Bird, C.D. Keene, W.W. Seeley, W.F. DeGrado, and S.B. Prusiner, *Aβ and tau prion-like activities decline with longevity in the Alzheimer's disease human brain.* Sci Transl Med, 2019. **11**(490).
101. Heneka, M.T., M.J. Carson, J. El Khoury, G.E. Landreth, F. Brosseron, D.L. Feinstein, A.H. Jacobs, T. Wyss-Coray, J. Vitorica, R.M. Ransohoff, K. Herrup, S.A. Frautschy, B. Finsen, G.C. Brown, A. Verkhratsky, K. Yamanaka, J. Koistinaho, E. Latz, A. Halle, G.C. Petzold, T. Town, D. Morgan, M.L. Shinohara, V.H. Perry, C. Holmes, N.G. Bazan, D.J. Brooks, S. Hunot, B. Joseph, N. Deigendesch, O. Garaschuk, E. Boddeke, C.A. Dinarello, J.C. Breitner, G.M. Cole, D.T. Golenbock, and M.P. Kummer, *Neuroinflammation in Alzheimer's disease.* Lancet Neurol, 2015. **14**(4): p. 388-405.
102. Vehmas, A.K., C.H. Kawas, W.F. Stewart, and J.C. Troncoso, *Immune reactive cells in senile plaques and cognitive decline in Alzheimer's disease.* Neurobiol Aging, 2003. **24**(2): p. 321-31.
103. Liddelow, S.A., K.A. Guttenplan, L.E. Clarke, F.C. Bennett, C.J. Bohlen, L. Schirmer, M.L. Bennett, A.E. Münch, W.S. Chung, T.C. Peterson, D.K. Wilton, A. Frouin, B.A. Napier, N. Panicker, M. Kumar, M.S. Buckwalter, D.H. Rowitch, V.L. Dawson, T.M. Dawson, B. Stevens, and B.A. Barres, *Neurotoxic reactive astrocytes are induced by activated microglia.* Nature, 2017. **541**(7638): p. 481-487.
104. Sastre, M., J. Walter, and S.M. Gentleman, *Interactions between APP secretases and inflammatory mediators.* Journal of neuroinflammation, 2008. **5**: p. 25-25.
105. Tu, S., S.-i. Okamoto, S.A. Lipton, and H. Xu, *Oligomeric Aβ-induced synaptic dysfunction in Alzheimer's disease.* Molecular neurodegeneration, 2014. **9**: p. 48-48.

106. Forner, S., D. Baglietto-Vargas, A.C. Martini, L. Trujillo-Estrada, and F.M. LaFerla, *Synaptic Impairment in Alzheimer's Disease: A Dysregulated Symphony.* Trends Neurosci, 2017. **40**(6): p. 347-357.
107. Hernandez, P., G. Lee, M. Sjoberg, and R.B. Maccioni, *Tau phosphorylation by cdk5 and Fyn in response to amyloid peptide Abeta (25-35): involvement of lipid rafts.* J Alzheimers Dis, 2009. **16**(1): p. 149-56.
108. Terwel, D., D. Muyllaert, I. Dewachter, P. Borghgraef, S. Croes, H. Devijver, and F. Van Leuven, *Amyloid activates GSK-3beta to aggravate neuronal tauopathy in bigenic mice.* Am J Pathol, 2008. **172**(3): p. 786-98.
109. Iijima, K., A. Gatt, and K. Iijima-Ando, *Tau Ser262 phosphorylation is critical for Abeta42-induced tau toxicity in a transgenic Drosophila model of Alzheimer's disease.* Hum Mol Genet, 2010. **19**(15): p. 2947-57.
110. Singh, T.J., N. Haque, I. Grundke-Iqbal, and K. Iqbal, *Rapid Alzheimer-like phosphorylation of tau by the synergistic actions of non-proline-dependent protein kinases and GSK-3.* FEBS Lett, 1995. **358**(3): p. 267-72.
111. Lee, S., G.F. Hall, and T.B. Shea, *Potentiation of tau aggregation by cdk5 and GSK3β.* J Alzheimers Dis, 2011. **26**(2): p. 355-64.
112. Gamblin, T.C., F. Chen, A. Zambrano, A. Abraha, S. Lagalwar, A.L. Guillozet, M. Lu, Y. Fu, F. Garcia-Sierra, N. LaPointe, R. Miller, R.W. Berry, L.I. Binder, and V.L. Cryns, *Caspase cleavage of tau: linking amyloid and neurofibrillary tangles in Alzheimer's disease.* Proc Natl Acad Sci U S A, 2003. **100**(17): p. 10032-7.
113. Zhang, H., W. Wei, M. Zhao, L. Ma, X. Jiang, H. Pei, Y. Cao, and H. Li, *Interaction between Aβ and Tau in the Pathogenesis of Alzheimer's Disease.* International journal of biological sciences, 2021. **17**(9): p. 2181-2192.
114. Mullan, M., F. Crawford, K. Axelman, H. Houlden, L. Lilius, B. Winblad, and L. Lannfelt, *A pathogenic mutation for probable Alzheimer's disease in the APP gene at the N–terminus of β–amyloid.* Nature genetics, 1992. **1**(5): p. 345-347.
115. Levy, E., M.D. Carman, I.J. Fernandez-Madrid, M.D. Power, I. Lieberburg, S.G. van Duinen, G.T. Bots, W. Luyendijk, and B. Frangione, *Mutation of the Alzheimer's disease amyloid gene in hereditary cerebral hemorrhage, Dutch type.* Science, 1990. **248**(4959): p. 1124-6.
116. Van Broeckhoven, C., J. Haan, E. Bakker, J.A. Hardy, W. Van Hul, A. Wehnert, M. Vegter-Van der Vlis, and R.A. Roos, *Amyloid beta protein precursor gene and hereditary cerebral hemorrhage with amyloidosis (Dutch).* Science, 1990. **248**(4959): p. 1120-2.
117. Fernandez-Madrid, I., E. Levy, K. Marder, and B. Frangione, *Codon 618 variant of Alzheimer amyloid gene associated with inherited cerebral hemorrhage.* Ann Neurol, 1991. **30**(5): p. 730-3.
118. Grabowski, T.J., H.S. Cho, J.P. Vonsattel, G.W. Rebeck, and S.M. Greenberg, *Novel amyloid precursor protein mutation in an Iowa family with dementia and severe cerebral amyloid angiopathy.* Ann Neurol, 2001. **49**(6): p. 697-705.
119. Tomidokoro, Y., A. Rostagno, T.A. Neubert, Y. Lu, G.W. Rebeck, B. Frangione, S.M. Greenberg, and J. Ghiso, *Iowa variant of familial Alzheimer's disease: accumulation of posttranslationally modified AbetaD23N in parenchymal and cerebrovascular amyloid deposits.* Am J Pathol, 2010. **176**(4): p. 1841-54.
120. Dumanchin, C., I. Tournier, C. Martin, M. Didic, S. Belliard, B. Carlander, F. Rouhart, C. Duyckaerts, J.-F. Pellissier, J.B. Latouche, D. Hannequin, T. Frebourg, M. Tosi, and D. Campion, *Biological effects of four PSEN1 gene mutations causing Alzheimer disease with spastic paraparesis and cotton wool plaques.* Human Mutation, 2006. **27**(10): p. 1063-1063.
121. Borchelt, D.R., G. Thinakaran, C.B. Eckman, M.K. Lee, F. Davenport, T. Ratovitsky, C.-M. Prada, G. Kim, S. Seekins, D. Yager, H.H. Slunt, R. Wang, M. Seeger, A.I. Levey, S.E. Gandy, N.G. Copeland, N.A. Jenkins, D.L. Price, S.G. Younkin, and S.S. Sisodia,

Familial Alzheimer's Disease–Linked Presenilin 1 Variants Elevate Aβ1–42/1–40 Ratio In Vitro and In Vivo. Neuron, 1996. **17**(5): p. 1005-1013.
122. Shen, J. and R.J. Kelleher, 3rd, *The presenilin hypothesis of Alzheimer's disease: evidence for a loss-of-function pathogenic mechanism.* Proc Natl Acad Sci U S A, 2007. **104**(2): p. 403-9.
123. Jankowsky, J.L., D.J. Fadale, J. Anderson, G.M. Xu, V. Gonzales, N.A. Jenkins, N.G. Copeland, M.K. Lee, L.H. Younkin, S.L. Wagner, S.G. Younkin, and D.R. Borchelt, *Mutant presenilins specifically elevate the levels of the 42 residue beta-amyloid peptide in vivo: evidence for augmentation of a 42-specific gamma secretase.* Hum Mol Genet, 2004. **13**(2): p. 159-70.
124. Crary, J.F., J.Q. Trojanowski, J.A. Schneider, J.F. Abisambra, E.L. Abner, I. Alafuzoff, S.E. Arnold, J. Attems, T.G. Beach, E.H. Bigio, N.J. Cairns, D.W. Dickson, M. Gearing, L.T. Grinberg, P.R. Hof, B.T. Hyman, K. Jellinger, G.A. Jicha, G.G. Kovacs, D.S. Knopman, J. Kofler, W.A. Kukull, I.R. Mackenzie, E. Masliah, A. McKee, T.J. Montine, M.E. Murray, J.H. Neltner, I. Santa-Maria, W.W. Seeley, A. Serrano-Pozo, M.L. Shelanski, T. Stein, M. Takao, D.R. Thal, J.B. Toledo, J.C. Troncoso, J.P. Vonsattel, C.L. White, 3rd, T. Wisniewski, R.L. Woltjer, M. Yamada, and P.T. Nelson, *Primary age-related tauopathy (PART): a common pathology associated with human aging.* Acta Neuropathol, 2014. **128**(6): p. 755-66.
125. Mackenzie, I.R., M. Neumann, E.H. Bigio, N.J. Cairns, I. Alafuzoff, J. Kril, G.G. Kovacs, B. Ghetti, G. Halliday, I.E. Holm, P.G. Ince, W. Kamphorst, T. Revesz, A.J. Rozemuller, S. Kumar-Singh, H. Akiyama, A. Baborie, S. Spina, D.W. Dickson, J.Q. Trojanowski, and D.M. Mann, *Nomenclature and nosology for neuropathologic subtypes of frontotemporal lobar degeneration: an update.* Acta Neuropathol, 2010. **119**(1): p. 1-4.
126. Leugers, C.J., J.Y. Koh, W. Hong, and G. Lee, *Tau in MAPK activation.* Frontiers in neurology, 2013. **4**: p. 161-161.
127. Weingarten, M.D., A.H. Lockwood, S.-Y. Hwo, and M.W. Kirschner, *A protein factor essential for microtubule assembly.* Proceedings of the National Academy of Sciences, 1975. **72**(5): p. 1858-1862.
128. Jean, D.C. and P.W. Baas, *It cuts two ways: microtubule loss during Alzheimer disease.* The EMBO journal, 2013. **32**(22): p. 2900-2902.
129. Kimura, T., D.J. Whitcomb, J. Jo, P. Regan, T. Piers, S. Heo, C. Brown, T. Hashikawa, M. Murayama, H. Seok, I. Sotiropoulos, E. Kim, G.L. Collingridge, A. Takashima, and K. Cho, *Microtubule-associated protein tau is essential for long-term depression in the hippocampus.* Philos Trans R Soc Lond B Biol Sci, 2014. **369**(1633): p. 20130144.
130. Pooler, A.M., W. Noble, and D.P. Hanger, *A role for tau at the synapse in Alzheimer's disease pathogenesis.* Neuropharmacology, 2014. **76 Pt A**: p. 1-8.
131. Dixit, R., J.L. Ross, Y.E. Goldman, and E.L.F. Holzbaur, *Differential regulation of dynein and kinesin motor proteins by tau.* Science (New York, N.Y.), 2008. **319**(5866): p. 1086-1089.
132. Goedert, M., M.G. Spillantini, R. Jakes, D. Rutherford, and R.A. Crowther, *Multiple isoforms of human microtubule-associated protein tau: sequences and localization in neurofibrillary tangles of Alzheimer's disease.* Neuron, 1989. **3**(4): p. 519-26.
133. Himmler, A., D. Drechsel, M.W. Kirschner, and D.W. Martin, Jr., *Tau consists of a set of proteins with repeated C-terminal microtubule-binding domains and variable N-terminal domains.* Mol Cell Biol, 1989. **9**(4): p. 1381-8.
134. Kosik, K.S., L.D. Orecchio, S. Bakalis, and R.L. Neve, *Developmentally regulated expression of specific tau sequences.* Neuron, 1989. **2**(4): p. 1389-97.
135. Zempel, H., F.J.A. Dennissen, Y. Kumar, J. Luedtke, J. Biernat, E.-M. Mandelkow, and E. Mandelkow, *Axodendritic sorting and pathological missorting of Tau are isoform-specific and determined by axon initial segment architecture.* The Journal of biological chemistry, 2017. **292**(29): p. 12192-12207.
136. Dickson, D.W., *Sporadic tauopathies: Pick's disease, corticobasal degeneration, progressive supranuclear palsy and argyrophilic grain disease*, in *The Neuropathology*

of Dementia, J.Q. Trojanowski, M.M. Esiri, and V.M.Y. Lee, Editors. 2004, Cambridge University Press: Cambridge. p. 227-256.
137. Spillantini, M.G., T.D. Bird, and B. Ghetti, *Frontotemporal Dementia and Parkinsonism Linked to Chromosome 17: A New Group of Tauopathies.* Brain Pathology, 1998. **8**(2): p. 387-402.
138. Dumanchin, C., A. Camuzat, D. Campion, P. Verpillat, D. Hannequin, B. Dubois, P. Saugier-Veber, C. Martin, C. Penet, F. Charbonnier, Y. Agid, T. Frebourg, and A. Brice, *Segregation of a missense mutation in the microtubule-associated protein tau gene with familial frontotemporal dementia and parkinsonism.* Hum Mol Genet, 1998. **7**(11): p. 1825-9.
139. Hutton, M., C.L. Lendon, P. Rizzu, M. Baker, S. Froelich, H. Houlden, S. Pickering-Brown, S. Chakraverty, A. Isaacs, A. Grover, J. Hackett, J. Adamson, S. Lincoln, D. Dickson, P. Davies, R.C. Petersen, M. Stevens, E. de Graaff, E. Wauters, J. van Baren, M. Hillebrand, M. Joosse, J.M. Kwon, P. Nowotny, L.K. Che, J. Norton, J.C. Morris, L.A. Reed, J. Trojanowski, H. Basun, L. Lannfelt, M. Neystat, S. Fahn, F. Dark, T. Tannenberg, P.R. Dodd, N. Hayward, J.B. Kwok, P.R. Schofield, A. Andreadis, J. Snowden, D. Craufurd, D. Neary, F. Owen, B.A. Oostra, J. Hardy, A. Goate, J. van Swieten, D. Mann, T. Lynch, and P. Heutink, *Association of missense and 5'-splice-site mutations in tau with the inherited dementia FTDP-17.* Nature, 1998. **393**(6686): p. 702-5.
140. Clark, L.N., P. Poorkaj, Z. Wszolek, D.H. Geschwind, Z.S. Nasreddine, B. Miller, D. Li, H. Payami, F. Awert, K. Markopoulou, A. Andreadis, I. D'Souza, V.M. Lee, L. Reed, J.Q. Trojanowski, V. Zhukareva, T. Bird, G. Schellenberg, and K.C. Wilhelmsen, *Pathogenic implications of mutations in the tau gene in pallido-ponto-nigral degeneration and related neurodegenerative disorders linked to chromosome 17.* Proc Natl Acad Sci U S A, 1998. **95**(22): p. 13103-7.
141. Wu, X., J. Piña-Crespo, Y. Zhang, X. Chen, and H. Xu, *Tau-mediated Neurodegeneration and Potential Implications in Diagnosis and Treatment of Alzheimer's Disease.* Chinese medical journal, 2017. **130**.
142. Liu, F., K. Iqbal, I. Grundke-Iqbal, G.W. Hart, and C.X. Gong, *O-GlcNAcylation regulates phosphorylation of tau: a mechanism involved in Alzheimer's disease.* Proc Natl Acad Sci U S A, 2004. **101**(29): p. 10804-9.
143. Cohen, R.M., K. Rezai-Zadeh, T.M. Weitz, A. Rentsendorj, D. Gate, I. Spivak, Y. Bholat, V. Vasilevko, C.G. Glabe, J.J. Breunig, P. Rakic, H. Davtyan, M.G. Agadjanyan, V. Kepe, J.R. Barrio, S. Bannykh, C.A. Szekely, R.N. Pechnick, and T. Town, *A transgenic Alzheimer rat with plaques, tau pathology, behavioral impairment, oligomeric aβ, and frank neuronal loss.* J Neurosci, 2013. **33**(15): p. 6245-56.
144. Martin, L., X. Latypova, and F. Terro, *Post-translational modifications of tau protein: implications for Alzheimer's disease.* Neurochem Int, 2011. **58**(4): p. 458-71.
145. Chirita, C.N., E.E. Congdon, H. Yin, and J. Kuret, *Triggers of full-length tau aggregation: a role for partially folded intermediates.* Biochemistry, 2005. **44**(15): p. 5862-72.
146. Sahara, N., S. Maeda, Y. Yoshiike, T. Mizoroki, S. Yamashita, M. Murayama, J.M. Park, Y. Saito, S. Murayama, and A. Takashima, *Molecular chaperone-mediated tau protein metabolism counteracts the formation of granular tau oligomers in human brain.* J Neurosci Res, 2007. **85**(14): p. 3098-108.
147. Mondragón-Rodríguez, S., G. Basurto-Islas, I. Santa-Maria, R. Mena, L.I. Binder, J. Avila, M.A. Smith, G. Perry, and F. García-Sierra, *Cleavage and conformational changes of tau protein follow phosphorylation during Alzheimer's disease.* Int J Exp Pathol, 2008. **89**(2): p. 81-90.
148. Lasagna-Reeves, C.A., D.L. Castillo-Carranza, M.J. Guerrero-Muoz, G.R. Jackson, and R. Kayed, *Preparation and characterization of neurotoxic tau oligomers.* Biochemistry, 2010. **49**(47): p. 10039-41.

149. Patterson, K.R., C. Remmers, Y. Fu, S. Brooker, N.M. Kanaan, L. Vana, S. Ward, J.F. Reyes, K. Philibert, M.J. Glucksman, and L.I. Binder, *Characterization of prefibrillar Tau oligomers in vitro and in Alzheimer disease.* J Biol Chem, 2011. **286**(26): p. 23063-76.
150. Braak, H. and E. Braak, *Neuropathological stageing of Alzheimer-related changes.* Acta Neuropathologica, 1991. **82**(4): p. 239-259.
151. Clavaguera, F., T. Bolmont, R.A. Crowther, D. Abramowski, S. Frank, A. Probst, G. Fraser, A.K. Stalder, M. Beibel, M. Staufenbiel, M. Jucker, M. Goedert, and M. Tolnay, *Transmission and spreading of tauopathy in transgenic mouse brain.* Nat Cell Biol, 2009. **11**(7): p. 909-13.
152. Guo, J.L. and V.M. Lee, *Seeding of normal Tau by pathological Tau conformers drives pathogenesis of Alzheimer-like tangles.* J Biol Chem, 2011. **286**(17): p. 15317-31.
153. Holmes, B.B. and M.I. Diamond, *Prion-like Properties of Tau Protein: The Importance of Extracellular Tau as a Therapeutic Target *.* Journal of Biological Chemistry, 2014. **289**(29): p. 19855-19861.
154. Polanco, J.C., B.J. Scicluna, A.F. Hill, and J. Götz, *Extracellular Vesicles Isolated from the Brains of rTg4510 Mice Seed Tau Protein Aggregation in a Threshold-dependent Manner.* J Biol Chem, 2016. **291**(24): p. 12445-12466.
155. Frost, B. and M.I. Diamond, *Prion-like mechanisms in neurodegenerative diseases.* Nat Rev Neurosci, 2010. **11**(3): p. 155-9.
156. Sanders, D.W., S.K. Kaufman, S.L. DeVos, A.M. Sharma, H. Mirbaha, A. Li, S.J. Barker, A.C. Foley, J.R. Thorpe, L.C. Serpell, T.M. Miller, L.T. Grinberg, W.W. Seeley, and M.I. Diamond, *Distinct tau prion strains propagate in cells and mice and define different tauopathies.* Neuron, 2014. **82**(6): p. 1271-88.
157. Rauch, J.N., G. Luna, E. Guzman, M. Audouard, C. Challis, Y.E. Sibih, C. Leshuk, I. Hernandez, S. Wegmann, B.T. Hyman, V. Gradinaru, M. Kampmann, and K.S. Kosik, *LRP1 is a master regulator of tau uptake and spread.* Nature, 2020. **580**(7803): p. 381-385.
158. Dujardin, S., C. Commins, A. Lathuiliere, P. Beerepoot, A.R. Fernandes, T.V. Kamath, B. Mark, N. Klickstein, D.L. Corjuc, and B.T. Corjuc, *Tau molecular diversity contributes to clinical heterogeneity in Alzheimer's disease.* Nature medicine, 2020. **26**(8): p. 1256-1263.
159. Walker, D.G., L.F. Lue, T.M. Tang, C.H. Adler, J.N. Caviness, M.N. Sabbagh, G.E. Serrano, L.I. Sue, and T.G. Beach, *Changes in CD200 and intercellular adhesion molecule-1 (ICAM-1) levels in brains of Lewy body disorder cases are associated with amounts of Alzheimer's pathology not α-synuclein pathology.* Neurobiol Aging, 2017. **54**: p. 175-186.
160. Laurent, C., L. Buée, and D. Blum, *Tau and neuroinflammation: What impact for Alzheimer's Disease and Tauopathies?* Biomedical journal, 2018. **41**(1): p. 21-33.
161. Eftekharzadeh, B., J.G. Daigle, L.E. Kapinos, A. Coyne, J. Schiantarelli, Y. Carlomagno, C. Cook, S.J. Miller, S. Dujardin, A.S. Amaral, J.C. Grima, R.E. Bennett, K. Tepper, M. DeTure, C.R. Vanderburg, B.T. Corjuc, S.L. DeVos, J.A. Gonzalez, J. Chew, S. Vidensky, F.H. Gage, J. Mertens, J. Troncoso, E. Mandelkow, X. Salvatella, R.Y.H. Lim, L. Petrucelli, S. Wegmann, J.D. Rothstein, and B.T. Hyman, *Tau Protein Disrupts Nucleocytoplasmic Transport in Alzheimer's Disease.* Neuron, 2018. **99**(5): p. 925-940.e7.
162. Parsons, C.G., W. Danysz, A. Dekundy, and I. Pulte, *Memantine and cholinesterase inhibitors: complementary mechanisms in the treatment of Alzheimer's disease.* Neurotox Res, 2013. **24**(3): p. 358-69.
163. Jimbo, D., Y. Kimura, M. Taniguchi, M. Inoue, and K. Urakami, *Effect of aromatherapy on patients with Alzheimer's disease.* Psychogeriatrics, 2009. **9**(4): p. 173-9.
164. Fukui, H., A. Arai, and K. Toyoshima, *Efficacy of music therapy in treatment for the patients with Alzheimer's disease.* Int J Alzheimers Dis, 2012. **2012**: p. 531646.

165. Peck, K.J., T.A. Girard, F.A. Russo, and A.J. Fiocco, *Music and Memory in Alzheimer's Disease and The Potential Underlying Mechanisms.* J Alzheimers Dis, 2016. **51**(4): p. 949-59.
166. de la Rubia Ortí, J.E., M.P. García-Pardo, C.C. Iranzo, J.J.C. Madrigal, S.S. Castillo, M.J. Rochina, and V.J.P. Gascó, *Does Music Therapy Improve Anxiety and Depression in Alzheimer's Patients?* J Altern Complement Med, 2018. **24**(1): p. 33-36.
167. Farina, N., J. Rusted, and N. Tabet, *The effect of exercise interventions on cognitive outcome in Alzheimer's disease: a systematic review.* Int Psychogeriatr, 2014. **26**(1): p. 9-18.
168. Mega, M.S., *The cholinergic deficit in Alzheimer's disease: impact on cognition, behaviour and function.* Int J Neuropsychopharmacol, 2000. **3**(7): p. 3-12.
169. Shinotoh, H., H. Namba, K. Fukushi, S. Nagatsuka, N. Tanaka, A. Aotsuka, T. Ota, S. Tanada, and T. Irie, *Progressive loss of cortical acetylcholinesterase activity in association with cognitive decline in Alzheimer's disease: a positron emission tomography study.* Ann Neurol, 2000. **48**(2): p. 194-200.
170. Meriney, S.D. and E.E. Fanselow, *Chapter 16 - Acetylcholine*, in *Synaptic Transmission*, S.D. Meriney and E.E. Fanselow, Editors. 2019, Academic Press. p. 345-367.
171. Nordberg, A., *Nicotinic receptor abnormalities of Alzheimer's disease: therapeutic implications.* Biological Psychiatry, 2001. **49**(3): p. 200-210.
172. Hynd, M.R., H.L. Scott, and P.R. Dodd, *Glutamate-mediated excitotoxicity and neurodegeneration in Alzheimer's disease.* Neurochem Int, 2004. **45**(5): p. 583-95.
173. Hardy, J. and R. Cowburn, *Glutamate neurotoxicity and Alzheimer's disease.* Trends in Neurosciences, 1987. **10**(10): p. 406.
174. Francis, P.T., *Glutamatergic systems in Alzheimer's disease.* Int J Geriatr Psychiatry, 2003. **18**(Suppl 1): p. S15-21.
175. Cacabelos, R., M. Takeda, and B. Winblad, *The glutamatergic system and neurodegeneration in dementia: preventive strategies in Alzheimer's disease.* Int J Geriatr Psychiatry, 1999. **14**(1): p. 3-47.
176. Koutsilieri, E. and P. Riederer, *Excitotoxicity and new antiglutamatergic strategies in Parkinson's disease and Alzheimer's disease.* Parkinsonism & Related Disorders, 2007. **13**: p. S329-S331.
177. Schousboe, A., B. Belhage, and A. Frandsen, *Role of Ca+2 and other second messengers in excitatory amino acid receptor mediated neurodegeneration: clinical perspectives.* Clin Neurosci, 1997. **4**(4): p. 194-8.
178. Danysz, W., C.G. Parsons, H.J. Mobius, A. Stoffler, and G. Quack, *Neuroprotective and symptomatological action of memantine relevant for Alzheimer's disease--a unified glutamatergic hypothesis on the mechanism of action.* Neurotox Res, 2000. **2**(2-3): p. 85-97.
179. Reisberg, B., R. Doody, A. Stöffler, F. Schmitt, S. Ferris, and H.J. Möbius, *Memantine in Moderate-to-Severe Alzheimer's Disease.* New England Journal of Medicine, 2003. **348**(14): p. 1333-1341.
180. Cummings, J., G. Lee, K. Zhong, J. Fonseca, and K. Taghva, *Alzheimer's disease drug development pipeline: 2021.* Alzheimer's & Dementia: Translational Research & Clinical Interventions, 2021. **7**(1): p. e12179.
181. Budd Haeberlein, S., J. O'Gorman, P. Chiao, T. Bussière, P. von Rosenstiel, Y. Tian, Y. Zhu, C. von Hehn, S. Gheuens, L. Skordos, T. Chen, and A. Sandrock, *Clinical Development of Aducanumab, an Anti-Aβ Human Monoclonal Antibody Being Investigated for the Treatment of Early Alzheimer's Disease.* J Prev Alzheimers Dis, 2017. **4**(4): p. 255-263.
182. Hooker, J.M., *FDA Approval of Aducanumab Divided the Community but Also Connected and United It.* ACS Chemical Neuroscience, 2021. **12**(15): p. 2716-2717.
183. Ribarič, S., *Peptides as Potential Therapeutics for Alzheimer's Disease.* Molecules (Basel, Switzerland), 2018. **23**(2): p. 283.

184. Devlin, J., L. Panganiban, and P. Devlin, *Random peptide libraries: a source of specific protein binding molecules.* Science, 1990. **249**(4967): p. 404-406.
185. Scott, J. and G. Smith, *Searching for peptide ligands with an epitope library.* Science, 1990. **249**(4967): p. 386-390.
186. Lien, S. and H.B. Lowman, *Therapeutic peptides.* Trends Biotechnol, 2003. **21**(12): p. 556-62.
187. Schumacher, T.N., L.M. Mayr, D.L. Minor, Jr., M.A. Milhollen, M.W. Burgess, and P.S. Kim, *Identification of D-peptide ligands through mirror-image phage display.* Science, 1996. **271**(5257): p. 1854-7.
188. Wiesehan, K., K. Buder, R.P. Linke, S. Patt, M. Stoldt, E. Unger, B. Schmitt, E. Bucci, and D. Willbold, *Selection of D-Amino-Acid Peptides That Bind to Alzheimer's Disease Amyloid Peptide Aβ1–42 by Mirror Image Phage Display.* ChemBioChem, 2003. **4**(8): p. 748-753.
189. Wiesehan, K., J. Stöhr, L. Nagel-Steger, T. van Groen, D. Riesner, and D. Willbold, *Inhibition of cytotoxicity and amyloid fibril formation by a D-amino acid peptide that specifically binds to Alzheimer's disease amyloid peptide.* Protein Eng Des Sel, 2008. **21**(4): p. 241-6.
190. Aileen Funke, S., T. van Groen, I. Kadish, D. Bartnik, L. Nagel-Steger, O. Brener, T. Sehl, R. Batra-Safferling, C. Moriscot, G. Schoehn, A.H. Horn, A. Müller-Schiffmann, C. Korth, H. Sticht, and D. Willbold, *Oral treatment with the d-enantiomeric peptide D3 improves the pathology and behavior of Alzheimer's Disease transgenic mice.* ACS Chem Neurosci, 2010. **1**(9): p. 639-48.
191. van Groen, T., I. Kadish, S.A. Funke, D. Bartnik, and D. Willbold, *Treatment with D3 removes amyloid deposits, reduces inflammation, and improves cognition in aged AβPP/PS1 double transgenic mice.* J Alzheimers Dis, 2013. **34**(3): p. 609-20.
192. Brener, O., T. Dunkelmann, L. Gremer, T. van Groen, E.A. Mirecka, I. Kadish, A. Willuweit, J. Kutzsche, D. Jürgens, S. Rudolph, M. Tusche, P. Bongen, J. Pietruszka, F. Oesterhelt, K.J. Langen, H.U. Demuth, A. Janssen, W. Hoyer, S.A. Funke, L. Nagel-Steger, and D. Willbold, *QIAD assay for quantitating a compound's efficacy in elimination of toxic Aβ oligomers.* Sci Rep, 2015. **5**: p. 13222.
193. Jiang, N., D. Frenzel, E. Schartmann, T. van Groen, I. Kadish, N.J. Shah, K.J. Langen, D. Willbold, and A. Willuweit, *Blood-brain barrier penetration of an Aβ-targeted, arginine-rich, d-enantiomeric peptide.* Biochim Biophys Acta, 2016. **1858**(11): p. 2717-2724.
194. Klein, A.N., T. Ziehm, T. van Groen, I. Kadish, A. Elfgen, M. Tusche, M. Thomaier, K. Reiss, O. Brener, L. Gremer, J. Kutzsche, and D. Willbold, *Optimization of d-Peptides for Aβ Monomer Binding Specificity Enhances Their Potential to Eliminate Toxic Aβ Oligomers.* ACS Chem Neurosci, 2017. **8**(9): p. 1889-1900.
195. Kutzsche, J., S. Schemmert, M. Tusche, J. Neddens, R. Rabl, D. Jürgens, O. Brener, A. Willuweit, B. Hutter-Paier, and D. Willbold, *Large-Scale Oral Treatment Study with the Four Most Promising D3-Derivatives for the Treatment of Alzheimer's Disease.* Molecules, 2017. **22**(10): p. 1693.
196. Schemmert, S., E. Schartmann, D. Honold, C. Zafiu, T. Ziehm, K.J. Langen, N.J. Shah, J. Kutzsche, A. Willuweit, and D. Willbold, *Deceleration of the neurodegenerative phenotype in pyroglutamate-Aβ accumulating transgenic mice by oral treatment with the Aβ oligomer eliminating compound RD2.* Neurobiol Dis, 2019. **124**: p. 36-45.
197. Schemmert, S., E. Schartmann, C. Zafiu, B. Kass, S. Hartwig, S. Lehr, O. Bannach, K.J. Langen, N.J. Shah, J. Kutzsche, A. Willuweit, and D. Willbold, *Aβ Oligomer Elimination Restores Cognition in Transgenic Alzheimer's Mice with Full-blown Pathology.* Mol Neurobiol, 2019. **56**(3): p. 2211-2223.
198. Leithold, L.H.E., N. Jiang, J. Post, N. Niemietz, E. Schartmann, T. Ziehm, J. Kutzsche, N.J. Shah, J. Breitkreutz, K.-J. Langen, A. Willuweit, and D. Willbold, *Pharmacokinetic properties of tandem d-peptides designed for treatment of Alzheimer's disease.* European Journal of Pharmaceutical Sciences, 2016. **89**: p. 31-38.

199. Kutzsche, J., D. Jürgens, A. Willuweit, K. Adermann, C. Fuchs, S. Simons, M. Windisch, M. Hümpel, W. Rossberg, M. Wolzt, and D. Willbold, *Safety and pharmacokinetics of the orally available antiprionic compound PRI-002: A single and multiple ascending dose phase I study.* Alzheimers Dement (N Y), 2020. **6**(1): p. e12001.
200. Schartmann, E., S. Schemmert, T. Ziehm, L.H.E. Leithold, N. Jiang, M. Tusche, N. Joni Shah, K.J. Langen, J. Kutzsche, D. Willbold, and A. Willuweit, *Comparison of blood-brain barrier penetration efficiencies between linear and cyclic all-d-enantiomeric peptides developed for the treatment of Alzheimer's disease.* Eur J Pharm Sci, 2018. **114**: p. 93-102.
201. Uno, H. and L.C. Walker, *The age of biosenescence and the incidence of cerebral beta-amyloidosis in aged captive rhesus monkeys.* Ann N Y Acad Sci, 1993. **695**: p. 232-5.
202. Head, E., *A canine model of human aging and Alzheimer's disease.* Biochim Biophys Acta, 2013. **1832**(9): p. 1384-9.
203. Esquerda-Canals, G., L. Montoliu-Gaya, J. Güell-Bosch, and S. Villegas, *Mouse Models of Alzheimer's Disease.* J Alzheimers Dis, 2017. **57**(4): p. 1171-1183.
204. Kaushal, A., W.Y. Wani, R. Anand, and K.D. Gill, *Spontaneous and Induced Nontransgenic Animal Models of AD: Modeling AD Using Combinatorial Approach.* American Journal of Alzheimer's Disease & Other Dementias®, 2013. **28**(4): p. 318-326.
205. Janus, C., A.Y. Flores, G. Xu, and D.R. Borchelt, *Behavioral abnormalities in APPSwe/PS1dE9 mouse model of AD-like pathology: comparative analysis across multiple behavioral domains.* Neurobiology of Aging, 2015. **36**(9): p. 2519-2532.
206. Onos, K.D., A. Uyar, K.J. Keezer, H.M. Jackson, C. Preuss, C.J. Acklin, R. O'Rourke, R. Buchanan, T.L. Cossette, S.J. Sukoff Rizzo, I. Soto, G.W. Carter, and G.R. Howell, *Enhancing face validity of mouse models of Alzheimer's disease with natural genetic variation.* PLoS genetics, 2019. **15**(5): p. e1008155-e1008155.
207. Lalonde, R., H.D. Kim, J.A. Maxwell, and K. Fukuchi, *Exploratory activity and spatial learning in 12-month-old APP(695)SWE/co+PS1/DeltaE9 mice with amyloid plaques.* Neurosci Lett, 2005. **390**(2): p. 87-92.
208. Volianskis, A., R. Køstner, M. Mølgaard, S. Hass, and M.S. Jensen, *Episodic memory deficits are not related to altered glutamatergic synaptic transmission and plasticity in the CA1 hippocampus of the APPswe/PS1δE9-deleted transgenic mice model of ß-amyloidosis.* Neurobiol Aging, 2010. **31**(7): p. 1173-87.
209. Kilgore, M., C.A. Miller, D.M. Fass, K.M. Hennig, S.J. Haggarty, J.D. Sweatt, and G. Rumbaugh, *Inhibitors of class 1 histone deacetylases reverse contextual memory deficits in a mouse model of Alzheimer's disease.* Neuropsychopharmacology, 2010. **35**(4): p. 870-80.
210. Kamphuis, W., C. Mamber, M. Moeton, L. Kooijman, J.A. Sluijs, A.H. Jansen, M. Verveer, L.R. de Groot, V.D. Smith, S. Rangarajan, J.J. Rodríguez, M. Orre, and E.M. Hol, *GFAP isoforms in adult mouse brain with a focus on neurogenic astrocytes and reactive astrogliosis in mouse models of Alzheimer disease.* PLoS One, 2012. **7**(8): p. e42823.
211. Jackson, R.J., N. Rudinskiy, A.G. Herrmann, S. Croft, J.M. Kim, V. Petrova, J.J. Ramos-Rodriguez, R. Pitstick, S. Wegmann, M. Garcia-Alloza, G.A. Carlson, B.T. Hyman, and T.L. Spires-Jones, *Human tau increases amyloid β plaque size but not amyloid β-mediated synapse loss in a novel mouse model of Alzheimer's disease.* Eur J Neurosci, 2016. **44**(12): p. 3056-3066.
212. Huang, H., S. Nie, M. Cao, C. Marshall, J. Gao, N. Xiao, G. Hu, and M. Xiao, *Characterization of AD-like phenotype in aged APPSwe/PS1dE9 mice.* Age (Dordrecht, Netherlands), 2016. **38**(4): p. 303-322.
213. Alexandru, A., W. Jagla, S. Graubner, A. Becker, C. Bäuscher, S. Kohlmann, R. Sedlmeier, K.A. Raber, H. Cynis, R. Rönicke, K.G. Reymann, E. Petrasch-Parwez, M. Hartlage-Rübsamen, A. Waniek, S. Rossner, S. Schilling, A.P. Osmand, H.-U. Demuth,

and S. von Hörsten, *Selective hippocampal neurodegeneration in transgenic mice expressing small amounts of truncated Aβ is induced by pyroglutamate-Aβ formation.* The Journal of neuroscience : the official journal of the Society for Neuroscience, 2011. **31**(36): p. 12790-12801.
214. Seifert, F., K. Schulz, B. Koch, S. Manhart, H.-U. Demuth, and S. Schilling, *Glutaminyl Cyclases Display Significant Catalytic Proficiency for Glutamyl Substrates.* Biochemistry, 2009. **48**(50): p. 11831-11833.
215. Dunkelmann, T., S. Schemmert, D. Honold, K. Teichmann, E. Butzküven, H.-U. Demuth, N.J. Shah, K.-J. Langen, J. Kutzsche, D. Willbold, and A. Willuweit, *Comprehensive Characterization of the Pyroglutamate Amyloid-β Induced Motor Neurodegenerative Phenotype of TBA2.1 Mice.* Journal of Alzheimer's Disease, 2018. **63**: p. 115-130.
216. Davis, J., F. Xu, R. Deane, G. Romanov, M.L. Previti, K. Zeigler, B.V. Zlokovic, and W.E. Van Nostrand, *Early-onset and Robust Cerebral Microvascular Accumulation of Amyloid β-Protein in Transgenic Mice Expressing Low Levels of a Vasculotropic Dutch/Iowa Mutant Form of Amyloid β-Protein Precursor*.* Journal of Biological Chemistry, 2004. **279**(19): p. 20296-20306.
217. Miao, J., F. Xu, J. Davis, I. Otte-Höller, M.M. Verbeek, and W.E. Van Nostrand, *Cerebral microvascular amyloid beta protein deposition induces vascular degeneration and neuroinflammation in transgenic mice expressing human vasculotropic mutant amyloid beta precursor protein.* The American journal of pathology, 2005. **167**(2): p. 505-515.
218. Xu, F., A.M. Grande, J.K. Robinson, M.L. Previti, M. Vasek, J. Davis, and W.E. Van Nostrand, *Early-onset subicular microvascular amyloid and neuroinflammation correlate with behavioral deficits in vasculotropic mutant amyloid beta-protein precursor transgenic mice.* Neuroscience, 2007. **146**(1): p. 98-107.
219. Choi, S., I. Singh, A.K. Singh, M. Khan, and J. Won, *Asymmetric dimethylarginine exacerbates cognitive dysfunction associated with cerebrovascular pathology.* The FASEB Journal, 2020. **34**(5): p. 6808-6823.
220. Fan, R., F. Xu, M.L. Previti, J. Davis, A.M. Grande, J.K. Robinson, and W.E. Van Nostrand, *Minocycline reduces microglial activation and improves behavioral deficits in a transgenic model of cerebral microvascular amyloid.* The Journal of neuroscience : the official journal of the Society for Neuroscience, 2007. **27**(12): p. 3057-3063.
221. Roberson, E.D., *Mouse models of frontotemporal dementia.* Annals of neurology, 2012. **72**(6): p. 837-849.
222. Kitazawa, M., R. Medeiros, and F.M. Laferla, *Transgenic mouse models of Alzheimer disease: developing a better model as a tool for therapeutic interventions.* Current pharmaceutical design, 2012. **18**(8): p. 1131-1147.
223. Terwel, D., R. Lasrado, J. Snauwaert, E. Vandeweert, C. Van Haesendonck, P. Borghgraef, and F. Van Leuven, *Changed Conformation of Mutant Tau-P301L Underlies the Moribund Tauopathy, Absent in Progressive, Nonlethal Axonopathy of Tau-4R/2N Transgenic Mice*.* Journal of Biological Chemistry, 2005. **280**(5): p. 3963-3973.
224. Maurin, H., S.A. Chong, I. Kraev, H. Davies, A. Kremer, C.M. Seymour, B. Lechat, T. Jaworski, P. Borghgraef, H. Devijver, G. Callewaert, M.G. Stewart, and F. Van Leuven, *Early structural and functional defects in synapses and myelinated axons in stratum lacunosum moleculare in two preclinical models for tauopathy.* PLoS One, 2014. **9**(2): p. e87605.
225. Boekhoorn, K., D. Terwel, B. Biemans, P. Borghgraef, O. Wiegert, G.J. Ramakers, K. de Vos, H. Krugers, T. Tomiyama, H. Mori, M. Joels, F. van Leuven, and P.J. Lucassen, *Improved long-term potentiation and memory in young tau-P301L transgenic mice before onset of hyperphosphorylation and tauopathy.* J Neurosci, 2006. **26**(13): p. 3514-23.

226. Samaey, C., A. Schreurs, S. Stroobants, and D. Balschun, *Early Cognitive and Behavioral Deficits in Mouse Models for Tauopathy and Alzheimer's Disease.* Front Aging Neurosci, 2019. **11**: p. 335.
227. Hong, S., V.F. Beja-Glasser, B.M. Nfonoyim, A. Frouin, S. Li, S. Ramakrishnan, K.M. Merry, Q. Shi, A. Rosenthal, B.A. Barres, C.A. Lemere, D.J. Selkoe, and B. Stevens, *Complement and microglia mediate early synapse loss in Alzheimer mouse models.* Science, 2016. **352**(6286): p. 712-716.
228. Oblak, A.L., S. Forner, P.R. Territo, M. Sasner, G.W. Carter, G.R. Howell, S.J. Sukoff-Rizzo, B.A. Logsdon, L.M. Mangravite, A. Mortazavi, D. Baglietto-Vargas, K.N. Green, G.R. MacGregor, M.A. Wood, A.J. Tenner, F.M. LaFerla, and B.T. Lamb, *Model organism development and evaluation for late-onset Alzheimer's disease: MODEL-AD.* Alzheimers Dement (N Y), 2020. **6**(1): p. e12110.
229. McQuail, J.A., A.R. Dunn, Y. Stern, C.A. Barnes, G. Kempermann, P.R. Rapp, C.C. Kaczorowski, and T.C. Foster, *Cognitive Reserve in Model Systems for Mechanistic Discovery: The Importance of Longitudinal Studies.* Frontiers in Aging Neuroscience, 2021. **12**(532).
230. Camargo, L.C., M. Schöneck, N. Sangarapillai, D. Honold, N.J. Shah, K.J. Langen, D. Willbold, J. Kutzsche, S. Schemmert, and A. Willuweit, *PEAβ Triggers Cognitive Decline and Amyloid Burden in a Novel Mouse Model of Alzheimer's Disease.* Int J Mol Sci, 2021. **22**(13).
231. Schemmert, S., L.C. Camargo, D. Honold, I. Gering, J. Kutzsche, A. Willuweit, and D. Willbold, *In Vitro and In Vivo Efficacies of the Linear and the Cyclic Version of an All-d-Enantiomeric Peptide Developed for the Treatment of Alzheimer's Disease.* Int J Mol Sci, 2021. **22**(12).
232. Al Dahhan, N.Z., F.G. De Felice, and D.P. Munoz, *Potentials and Pitfalls of Cross-Translational Models of Cognitive Impairment.* Front Behav Neurosci, 2019. **13**: p. 48.
233. Engler, H., A. Forsberg, O. Almkvist, G. Blomquist, E. Larsson, I. Savitcheva, A. Wall, A. Ringheim, B. Långström, and A. Nordberg, *Two-year follow-up of amyloid deposition in patients with Alzheimer's disease.* Brain, 2006. **129**(11): p. 2856-2866.
234. Brown, M.W. and J.P. Aggleton, *Recognition memory: What are the roles of the perirhinal cortex and hippocampus?* Nature Reviews Neuroscience, 2001. **2**(1): p. 51-61.
235. Chen, G., K.S. Chen, J. Knox, J. Inglis, A. Bernard, S.J. Martin, A. Justice, L. McConlogue, D. Games, S.B. Freedman, and R.G. Morris, *A learning deficit related to age and beta-amyloid plaques in a mouse model of Alzheimer's disease.* Nature, 2000. **408**(6815): p. 975-9.
236. Ennaceur, A. and J. Delacour, *A new one-trial test for neurobiological studies of memory in rats. 1: Behavioral data.* Behavioural brain research, 1988. **31**(1): p. 47-59.
237. Lueptow, L.M., *Novel object recognition test for the investigation of learning and memory in mice.* JoVE (Journal of Visualized Experiments), 2017(126): p. e55718.
238. Antunes, M. and G. Biala, *The novel object recognition memory: neurobiology, test procedure, and its modifications.* Cognitive processing, 2012. **13**(2): p. 93-110.
239. Spowart-Manning, L. and F. Van der Staay, *The T-maze continuous alternation task for assessing the effects of putative cognition enhancers in the mouse.* Behavioural brain research, 2004. **151**(1-2): p. 37-46.
240. Deacon, R.M. and J.N. Rawlins, *T-maze alternation in the rodent.* Nat Protoc, 2006. **1**(1): p. 7-12.
241. West, M.J., *Regionally specific loss of neurons in the aging human hippocampus.* Neurobiol Aging, 1993. **14**(4): p. 287-93.
242. Tanila, H., *Wading pools, fading memories—place navigation in transgenic mouse models of Alzheimer's disease.* Frontiers in Aging Neuroscience, 2012. **4**(11).
243. Zhu, H., H. Yan, N. Tang, X. Li, P. Pang, H. Li, W. Chen, Y. Guo, S. Shu, Y. Cai, L. Pei, D. Liu, M.-H. Luo, H. Man, Q. Tian, Y. Mu, L.-Q. Zhu, and Y. Lu, *Impairments of spatial*

memory in an Alzheimer's disease model via degeneration of hippocampal cholinergic synapses. Nature Communications, 2017. **8**(1): p. 1676.
244. Morris, R., *Developments of a water-maze procedure for studying spatial learning in the rat.* J Neurosci Methods, 1984. **11**(1): p. 47-60.
245. Shoji, H., K. Takao, S. Hattori, and T. Miyakawa, *Contextual and cued fear conditioning test using a video analyzing system in mice.* JoVE (Journal of Visualized Experiments), 2014(85): p. e50871.
246. Knafo, S., C. Venero, P. Merino-Serrais, I. Fernaud-Espinosa, J. Gonzalez-Soriano, I. Ferrer, G. Santpere, and J. DeFelipe, *Morphological alterations to neurons of the amygdala and impaired fear conditioning in a transgenic mouse model of Alzheimer's disease.* The Journal of Pathology, 2009. **219**(1): p. 41-51.
247. España, J., L. Giménez-Llort, J. Valero, A. Miñano, A. Rábano, J. Rodriguez-Alvarez, F.M. LaFerla, and C.A. Saura, *Intraneuronal β-Amyloid Accumulation in the Amygdala Enhances Fear and Anxiety in Alzheimer's Disease Transgenic Mice.* Biological Psychiatry, 2010. **67**(6): p. 513-521.
248. Nasrouei, S., J.A. Rattel, M. Liedlgruber, J. Marksteiner, and F.H. Wilhelm, *Fear acquisition and extinction deficits in amnestic mild cognitive impairment and early Alzheimer's disease.* Neurobiol Aging, 2020. **87**: p. 26-34.
249. Dineley, K.T., R. Kayed, V. Neugebauer, Y. Fu, W. Zhang, L.C. Reese, and G. Taglialatela, *Amyloid-beta oligomers impair fear conditioned memory in a calcineurin-dependent fashion in mice.* Journal of neuroscience research, 2010. **88**(13): p. 2923-2932.
250. Grudzien, A., P. Shaw, S. Weintraub, E. Bigio, D.C. Mash, and M.M. Mesulam, *Locus coeruleus neurofibrillary degeneration in aging, mild cognitive impairment and early Alzheimer's disease.* Neurobiol Aging, 2007. **28**(3): p. 327-35.
251. Kelly, S.C., B. He, S.E. Perez, S.D. Ginsberg, E.J. Mufson, and S.E. Counts, *Locus coeruleus cellular and molecular pathology during the progression of Alzheimer's disease.* Acta Neuropathol Commun, 2017. **5**(1): p. 8.
252. Clinton, L.K., L.M. Billings, K.N. Green, A. Caccamo, J. Ngo, S. Oddo, J.L. McGaugh, and F.M. LaFerla, *Age-dependent sexual dimorphism in cognition and stress response in the 3xTg-AD mice.* Neurobiol Dis, 2007. **28**(1): p. 76-82.
253. Deacon, R.M., D. Reisel, V.H. Perry, J. Nicholas, and P. Rawlins, *Hippocampal scrapie infection impairs operant DRL performance in mice.* Behav Brain Res, 2005. **157**(1): p. 99-105.
254. Deacon, R.M.J., *Digging and marble burying in mice: simple methods for in vivo identification of biological impacts.* Nature Protocols, 2006. **1**(1): p. 122-124.
255. Rogers, D.C., E.M. Fisher, S.D. Brown, J. Peters, A.J. Hunter, and J.E. Martin, *Behavioral and functional analysis of mouse phenotype: SHIRPA, a proposed protocol for comprehensive phenotype assessment.* Mamm Genome, 1997. **8**(10): p. 711-3.
256. Hallett, M. and S. Khoshbin, *A physiological mechanism of bradykinesia.* Brain, 1980. **103**(2): p. 301-14.
257. Desmurget, M., S.T. Grafton, P. Vindras, H. Gréa, and R.S. Turner, *Basal ganglia network mediates the control of movement amplitude.* Exp Brain Res, 2003. **153**(2): p. 197-209.
258. Matsuura, K., H. Kabuto, H. Makino, and N. Ogawa, *Pole test is a useful method for evaluating the mouse movement disorder caused by striatal dopamine depletion.* Journal of Neuroscience Methods, 1997. **73**(1): p. 45-48.
259. Hanseeuw, B.J., F. Lopera, R.A. Sperling, D.J. Norton, E. Guzman-Velez, A. Baena, E. Pardilla-Delgado, A.P. Schultz, J. Gatchel, D. Jin, K. Chen, E.M. Reiman, K.A. Johnson, and Y.T. Quiroz, *Striatal amyloid is associated with tauopathy and memory decline in familial Alzheimer's disease.* Alzheimer's research & therapy, 2019. **11**(1): p. 17-17.
260. Castelli, M., M. Federici, S. Rossi, V. De Chiara, F. Napolitano, V. Studer, C. Motta, L. Sacchetti, R. Romano, A. Musella, G. Bernardi, A. Siracusano, H.H. Gu, N.B. Mercuri,

A. Usiello, and D. Centonze, *Loss of striatal cannabinoid CB1 receptor function in attention-deficit/hyperactivity disorder mice with point-mutation of the dopamine transporter.* European Journal of Neuroscience, 2011. **34**(9): p. 1369-1377.
261. Unger, E.L., D.J. Eve, X.A. Perez, D.K. Reichenbach, Y. Xu, M.K. Lee, and A.M. Andrews, *Locomotor hyperactivity and alterations in dopamine neurotransmission are associated with overexpression of A53T mutant human α-synuclein in mice.* Neurobiology of Disease, 2006. **21**(2): p. 431-443.
262. Miyakawa, T., M. Yamada, A. Duttaroy, and J. Wess, *Hyperactivity and intact hippocampus-dependent learning in mice lacking the M1 muscarinic acetylcholine receptor.* The Journal of neuroscience : the official journal of the Society for Neuroscience, 2001. **21**(14): p. 5239-5250.
263. Brilliant, M.J., R.J. Elble, M. Ghobrial, and R.G. Struble, *The distribution of amyloid β protein deposition in the corpus striatum of patients with Alzheimer's disease.* Neuropathology and Applied Neurobiology, 1997. **23**(4): p. 322-325.
264. Gearing, M., A.I. Levey, and S.S. Mirra, *Diffuse Plaques in the Striatum in Alzheimer Disease (AD): Relationship to the Striatal Mosaic and Selected Neuropeptide Markers.* Journal of Neuropathology & Experimental Neurology, 1997. **56**(12): p. 1363-1370.
265. Braak, H. and E. Braak, *Alzheimer's Disease: Striatal Amyloid Deposits and Neurofibrillary Changes.* Journal of Neuropathology & Experimental Neurology, 1990. **49**(3): p. 215-224.
266. Bolivar, V.J., B.J. Caldarone, A.A. Reilly, and L. Flaherty, *Habituation of Activity in an Open Field: A Survey of Inbred Strains and F1 Hybrids.* Behavior Genetics, 2000. **30**(4): p. 285-293.
267. Light, K.R., H. Grossman, S. Kolata, C. Wass, and L.D. Matzel, *General learning ability regulates exploration through its influence on rate of habituation.* Behavioural Brain Research, 2011. **223**(2): p. 297-309.
268. Luna-Muñoz, J., L. Chávez-Macías, F. García-Sierra, and R. Mena, *Earliest Stages of Tau Conformational Changes are Related to the Appearance of a Sequence of Specific Phospho-Dependent Tau Epitopes in Alzheimer's Disease.* Journal of Alzheimer's Disease, 2007. **12**: p. 365-375.
269. Augustinack, J.C., A. Schneider, E.-M. Mandelkow, and B.T. Hyman, *Specific tau phosphorylation sites correlate with severity of neuronal cytopathology in Alzheimer's disease.* Acta neuropathologica, 2002. **103**(1): p. 26-35.
270. Terry, R.D., E. Masliah, D.P. Salmon, N. Butters, R. DeTeresa, R. Hill, L.A. Hansen, and R. Katzman, *Physical basis of cognitive alterations in alzheimer's disease: Synapse loss is the major correlate of cognitive impairment.* Annals of Neurology, 1991. **30**(4): p. 572-580.
271. Scheff, S.W. and D.A. Price, *Alzheimer's disease-related alterations in synaptic density: neocortex and hippocampus.* J Alzheimers Dis, 2006. **9**(3 Suppl): p. 101-15.
272. Scheff, S.W., D.A. Price, F.A. Schmitt, M.A. Scheff, and E.J. Mufson, *Synaptic loss in the inferior temporal gyrus in mild cognitive impairment and Alzheimer's disease.* J Alzheimers Dis, 2011. **24**(3): p. 547-57.
273. Mattsson, N., P.S. Insel, S. Palmqvist, E. Portelius, H. Zetterberg, M. Weiner, K. Blennow, O. Hansson, and I. Alzheimer's Disease Neuroimaging, *Cerebrospinal fluid tau, neurogranin, and neurofilament light in Alzheimer's disease.* EMBO molecular medicine, 2016. **8**(10): p. 1184-1196.
274. Brinkmalm, A., G. Brinkmalm, W.G. Honer, L. Frölich, L. Hausner, L. Minthon, O. Hansson, A. Wallin, H. Zetterberg, and K. Blennow, *SNAP-25 is a promising novel cerebrospinal fluid biomarker for synapse degeneration in Alzheimer's disease.* Molecular neurodegeneration, 2014. **9**(1): p. 1-13.
275. Sutphen, C.L., L. McCue, E.M. Herries, C. Xiong, J.H. Ladenson, D.M. Holtzman, A.M. Fagan, and Adni, *Longitudinal decreases in multiple cerebrospinal fluid biomarkers of neuronal injury in symptomatic late onset Alzheimer's disease.* Alzheimer's & dementia : the journal of the Alzheimer's Association, 2018. **14**(7): p. 869-879.

276. Nagai, J., A.K. Rajbhandari, M.R. Gangwani, A. Hachisuka, G. Coppola, S.C. Masmanidis, M.S. Fanselow, and B.S. Khakh, *Hyperactivity with Disrupted Attention by Activation of an Astrocyte Synaptogenic Cue.* Cell, 2019. **177**(5): p. 1280-1292.e20.
277. Klein, A.N., T. Ziehm, M. Tusche, J. Buitenhuis, D. Bartnik, A. Boeddrich, T. Wiglenda, E. Wanker, S.A. Funke, O. Brener, L. Gremer, J. Kutzsche, and D. Willbold, *Optimization of the All-D Peptide D3 for Aβ Oligomer Elimination.* PLoS One, 2016. **11**(4): p. e0153035.
278. Dunkelmann, T., K. Teichmann, T. Ziehm, S. Schemmert, D. Frenzel, M. Tusche, C. Dammers, D. Jürgens, K.J. Langen, H.U. Demuth, N.J. Shah, J. Kutzsche, A. Willuweit, and D. Willbold, *Aβ oligomer eliminating compounds interfere successfully with pEAβ(3-42) induced motor neurodegenerative phenotype in transgenic mice.* Neuropeptides, 2018. **67**: p. 27-35.